**School of Pharmacy**

# Pharmacokinetics and Allometric Scaling of Antimalarial Drugs

**Senarathna Mudiyanselage Dona Kalyani Ganga Senarathna**

**This thesis is presented for the Degree of**

**Doctor of Philosophy**

**of**

**Curtin University**

**March 2015**

# Declaration

**To the best of my knowledge and belief this thesis contains no material previously published by any other person except where due acknowledgement has been made. This thesis contains no material which has been accepted for an award of any other degree or diploma in any university.**

**S M D K Ganga Senarathna**

**March 2015**

# Abstract

In order to delay development of drug resistance and to obtain maximum drug efficacy, it is important to prescribe optimum drug combinations and doses, which requires clear knowledge of the pharmacokinetics of antimalarials. This study covered two main areas of pharmacokinetics of antimalarials. The first aim of this study was to carry out allometric scaling of antimalarial drugs to interpolate pharmacokinetic parameters and drug doses for children. The second principal aim was to establish drug permeability, P-glycoprotein mediated drug transport and regulation of P-glycoprotein expression by antimalarials in single and combination therapy using *in-vitro* Caco-2 cell lines.

Strong allometric relationships were found for clearance and volume of distribution with $r^2$ values $\geq 0.9$ except for volume of distribution of artesunate. Clearance exponents ranged from 0.4 for quinine to 0.96 of piperaquine. The exponents and 95 % confidences interval did not encompass fixed exponent values of 0.67 or 0.75, and exponent 1 for all drugs studied. Therefore fixed exponent allometry and linear (mg/kg adult dose) dosing are not supported by the current study. The exponents for volume of distribution ranged from 0.78 for mefloquine to 1.16 for piperaquine (artesunate was excluded). Half-life had poor allometric relationships with low $r^2$ for the majority of the drugs. The clearance predicted using simple allometry was within the threshold limits of the observed drug clearance in clinical studies. The correction factors maximum life span potential, Rule of Exponents and liver blood flow correction did not improve the simple allometric predictions. The liver weight correction performed well and had the predictive success for all drugs compared. However a clear improvement in clearance prediction compared to simple allometry was not observed.

Comparison of drug clearance in healthy human adults and malarial infected patients showed quinine clearance to be significantly lower in the former compared to the latter. The paediatric doses predicted based on exponents derived from simple allometry of healthy species for arbitrary body weights of 15 and 25 kg were 10 to 70% higher than the currently recommended mg/kg adult dosing except for artemether. The artemether doses used are higher than the mg/kg adults dosing and similar or higher than the allometrically predicted doses.

The conventional allometry where preclinical clearance data are used to extrapolate pharmacokinetics for humans did not work for all antimalarials. Addition of human pharmacokinetic data improved clearance prediction and was within threshold values at all times.

The second part of the study which consisted of bidirectional transport studies required development of a robust Caco-2 cell monolayer with sufficient P-gp expression. Three interventions [exposure of cells to a potent P-gp inducer rifampicin (Caco-2 RIF), exposure of cells to a potent P-gp substrate vinblastine at nanomolar concentration (Caco-2 VIN) and regular passaging to attain late passage Caco-2 cells] were adopted to improve P-gp expression in early passage Caco-2 cells (passage 44). Caco-2 VIN model had the highest P-gp expression with an efflux ratio of 13, however development of this model was a time consuming process. Late passage Caco-2 cells had sufficient improvement on P-gp expression with an efflux ratio of 4.7 compared to 1.4 of the early passage Caco-2 cells.

Mefloquine showed P-gp inhibitory properties, where 50% inhibition of P-gp mediated efflux transport of rhodamine123 was observed at 100 µM in late passage Caco-2 cells. Amodiaquine, artesunate, methylene blue and artemisone did not show inhibitory properties in early and late passage Caco-2 cells.

Out of the antimalarials studied, mefloquine, amodiaquine, artesunate and artemisone permeated through passive diffusion. The apical to basolateral directional apparent permeability ($P_{app}$) values for mefloquine and artesunate were 6 to $10 \times 10^{-6}$ and 7 to $10 \times 10^{-6}$ cm/sec respectively, therefore showing medium permeability and incomplete drug absorption *in-vivo*. Whereas amodiaquine and artemisone showed near complete drug absorption with apical to basolateral directional $P_{app}$ of 16 to $23 \times 10^{-6}$ and 37 to $60 \times 10^{-6}$ cm/sec, respectively. Mefloquine permeability was not altered when co-incubated with artesunate, artemisone and methylene blue and artesunate. Amodiaquine and artesunate showed some efflux with efflux ratios in the range of 1.2 to 1.5; however such small increases in efflux are unlikely to change the *in-vivo* drug absorption and systemic availability of drug.

Methylene blue showed higher basolateral to apical transport compared to apical to basolateral transport which suggested possible P-gp mediated efflux transport of

methylene blue. Efflux transport was consistently observed in all Caco-2 models. However the efflux transport of methylene blue was not completely inhibited by PSC833 with 50% inhibition observed. Therefore it is probable that methylene blue efflux transport is mediated.

A clear up-regulation of P-gp was observed for artemisone and dihydroartemisinin in combination with amodiaquine or mefloquine in both Caco-2 and LS174 T cells. This was not observed for artesunate combinations. An up-regulation of P-gp was not observed for antimalarials in single therapy for 48 hours. However up-regulation was observed for methylene blue, amodiaquine, artesunate and dihydroartemisinin when exposed for 96 hours.

Overall, simple allometric scaling is a plausible technique for dose determination in children. The correction factors were unable to show clear improvement in clearance prediction compared to simple allometry. Mefloquine exhibited P-gp inhibitory properties. Mefloquine, amodiaquine, artesunate and artemisone did not exhibit P-gp substrate activity. Methylene blue was found to have P-gp mediated efflux transport as one of the multiple mechanisms available to transport methylene blue. It also showed low permeability, while mefloquine and artesunate showed medium and amodiaquine and artemisone high permeability across Caco-2 monolayers. A clear up-regulation of P-gp expression was observed for dihydroartemisinin and artemisone in combination with amodiaquine and mefloquine in Caco-2 and LS174 T cells.

## Acknowledgment

I would like to extend my sincerer gratitude to my supervisors Dr Andrew Crowe and Prof Kevin Batty who spend their valuable time to guide me achieve my objectives.

First of all I would to like thank to Dr Andrew Crowe for agreeing to take the full responsibility of supervising my work after Prof. Kevin Batty left the University. Your through knowledge in the areas of drug transport and protein studies helped me immensely to overcome many hurdles I came across.

I am grateful to Prof Kevin Batty for introducing me to the pharmacokinetic research and your patience, critical comments and empathetic guidance was instrumental for completion of my work.

I am extremely grateful to Dr Madhu Page Sharp for teaching me all the analytical skills needed and being the pillar of strength. Without your constant support, guidance, close supervision, invaluable advices and friendship, I wouldn't have been able to complete my work.

I wish to acknowledge with gratitude my friend, Gaewyn Ellison for proof reading and Joyce Thomas for providing the thesis template.

I wish to thanks my roommates Julia Koehn, Gaewyn Ellison, Malini Visweswaran, Chee Wai Wong, Naz Huda, Aparna Warrier, Hilai Ahmadzai, Vishal Chaturvedi and Aziz Niazi for their friendship and moral support throughout my study.

I acknowledge the staff of the School of Pharmacy, Curtin University for supporting me in various ways and welcoming and making me part of the big family.

I thank Curtin University for supporting me with Curtin Strategic International Research scholarship to support my financial needs.

I admire and thank most fondly my son Manuka Wickramasuriya and daughter Gihanga Wickramasuriya for bearing with me for all the long hours spend away from them for during last 3.5 years. I thank my husband Asoka Wickramasuriya for taking all the family responsibilities and being patient with me during my PhD Journey. I most gratefully acknowledge my mother and mother in-law for looking after my

children during my study, without for them I won't be able to complete my work. I am thankful to my father, brother, sister and sister-in laws for accommodating their needs and sending our mothers away to support my work.

I also would like to thank my family friend Sisira Jayarathna and his family for housing us when we first came to Australia and my landlord James Britain for helping us in various ways.

I would like to extend my gratitude to all the Pharmacy Lecturers at the University of Sri Jayewardenepura for shouldering my teaching responsibilities while I was away. I wish to thank Professor Sherain Fernando, Professor Mohan De Silva and University of Sri Jayewardenepura, Sri Lanka for granting me study leave.

# Abbreviations

| | |
|---|---|
| DHA | Dihydroartemisinin |
| ART | Artesunate |
| MQ | Mefloquine |
| MB | Methylene blue |
| AM | Artemisone |
| Rh123 | Rhodamine123 |
| IM | Intramuscular |
| IR | Intra rectal |
| IV | Intravenous |
| IP | Intraperitoneal |
| SC | Subcutaneous |
| CL | Clearance |
| AUC | Area under the curve |
| CL/F | Apparent clearance |
| Vz | Volume of distribution |
| Vz/F | Apparent volume of distribution |
| $t_{1/2}$ | Half-life |
| $C_{max}$ | Maximum concentration |
| $t_{max}$ | Time taken to reach maximum concentration |
| Vss | Volume at steady state |

| | |
|---|---|
| WHO | World Health Organization |
| FDC | Fixed dose combination |
| CSF | Cerebrospinal fluid |
| ACT | Artemisinin combination therapy |
| P-gp | Permeability glycoprotein, P-glycoprotein |
| F | Bioavailability |
| r | Rat |
| m | Mice |
| d | Dog |
| p | Pig |
| h | Human |
| CI | Confidence interval |
| MLP | Maximum life span potential |
| $P_{oct}$ | Octanol water portioning coefficient |
| Papp | Apparent permeability |
| DMEM | Dulbecco's modified eagle medium |
| FCS | Foetal calf serum |
| HBSS | Hank balance salt solution |
| Ap-Bas | Apical to basolateral |
| Bas-Ap | Basolateral to apical |
| TEER | Transepithelial electrical resistance |

| | |
|---|---|
| TBS | Tris Buffered saline |
| TBST | Tris Buffered saline with 0.05% Tween 20 |
| DMSO | Dimethyl Sulfoxide |
| $KH_2PO_4$ | Potassium dihydrogen ortho phosphate |
| $H_3PO_4$ | Phosphoric acid |
| Caco-2 | Colorectal adenocarcinoma-2 cells |
| HPLC | High performance liquid chromatography |
| LC-MS-MS | liquid chromatography and mass spectrometry |
| SEM | Standard error of mean |
| BCS | Biopharmaceutical classification system |
| IVIV | *In-vivo* and *In-vitro* correlation |
| PXR | Pregnane X receptor |
| MDCK | Madin Darby canine kidney |
| ATCC | American Type Culture Collection |
| FDA | Food and drug administration |
| MDR | Multi drug resistance |
| LS174 T | Dukes' type B,colorectal adenocarcinoma cells |
| PBS | Phosphate buffered saline |
| P | Passage |

# Publications and Presentations

## Full research papers

Senarathna SG, Batty KT. Interspecies allometric scaling of antimalarial drugs and potential application to pediatric dosing. ***Antimicrobial Agents Chemotherapy***. 2014; 58(10):6068-78

S M D K Ganga, Senarathna, Andrew, Crowe. The influence of passage number for Caco-2 cell models when evaluating P-gp mediated drug transport. ***PHARMAZIE***. 2015;70:1-6

## Abstracts and presentations

Senarathna S.M.D.K.G, Batty Kevin T. Allometric scaling of antimalarial drugs. In Joint Australasian Society of Clinical and Experimental Pharmacologist and Toxicologist and Australasian Pharmaceutical Sciences Association 2012 conference. Sydney, Australia, 2-5 December 2012

Senarathna S.M.D.K.G, Batty Kevin T. Allometric scaling of antimalarial drugs. Mark Liveris Research Seminar, Faculty of Health Sciences, Curtin University, Australia, 11 November 2013

Senarathna S.M.D.KG. Page-Sharp Madhu, Crowe A. *In-vitro* drug transport of anti-malarials; amodiaquine, mefloquine and methylene blue. In 63$^{rd}$ Annual meeting of American Society of Tropical Medicine and Hygiene, New Orleans, USA, American Society of Tropical Medicine and Hygiene,2-6 November 2014.

Senarathna S.M.D.KG, Crowe A. Development of a robust Caco-2 cell model for drug transport studies. In Science on the Swan Inaugural Conference 2015, Perth, Australia, 21-23 April 2015.

Crowe A, Senarathna S.M.D.KG. Page-Sharp Madhu**.** The interactions of P-glycoprotein with antimalarial drugs, including substrate affinity and inhibition. In Science on the Swan Inaugural Conference 2015, Perth, Australia, 21-23 April 2015

Senarathna S.M.D.KG. Page-Sharp Madhu. Crowe A. The influence of artemisone exposure in Caco-2 cell monolayers on P-gp mediated transport and expression; Comparison with Artesunate. In 128th International conference of Sri Lanka Medical Association, Colombo, Sri Lanka, 5-8 July 2

# Table of Contents

# List of Tables

# List of Figures

# 1 Introduction

## 1.1 Malaria

The history of malaria goes back over 4000 years, and a disease with symptoms similar to malaria was described in ancient Chinese medical writing. Later this seasonal, intermittent fever was named as mal'aria and widely recognized along with its clinical symptoms in the 4th century BC (1).

Even today, malaria is a devastating fatal parasitic infection and a significant cause of morbidity and mortality in the developing world in spite of the advancement of biology and discovery of new drugs (2-4). The disease killed about 0.5 million children in 2013 (5).

Malaria is a protozoan parasitic infection of red blood cells caused by the Apicomplexan pathogen of genus *Plasmodium*. There are five *Plasmodium* species that can cause malaria in human; *Plasmodium falciparum, Plasmodium vivax, Plasmodium ovale, Plasmodium malariae* and *Plasmodium knowlesi* even though there are over 200 species of *Plasmodium*. Of these, the most deadly is *Plasmodium falciparum* which causes more than 95% of all malaria deaths (6). Inoculation of the *Plasmodium* parasite into a human host is commonly through the female Anopheles mosquito, though transmission may also occur through blood transfusions and transplacentally. The parasitic life cycle in the human has two phases (7).

Exo-erythrocytic phase

Sporozoites, the infective form of *Plasmodium,* are introduced through the skin by the *Anopheles* mosquito, commencing the human cycle. Sporozoites not destroyed by the human host immune system, travel into the liver and undergo multiplication. A number of days later, merozoites are liberated causing clinical symptoms of the primary attack (7, 8).

Erythrocytic phase

The erythrocytic phase begins when red blood cells become infected with merozoites. In the red blood cells, merozoites pass through several stages of development from early trophozoites (rings) to late schizonts. The erythrocytic cycle terminates with the rupture

of red blood cells and the release of merozoites to commence the next cycle of red blood cell invasion. Release of merozoites causes clinical symptoms of malaria and this happens 48 hourly for *Plasmodium falciparum*, every 48-72 hours for *Plasmodium vivax* and *Plasmodium ovale*, every 72 hours for *Plasmodium malariae* and every 24 hour for *Plasmodium knowlesi* (7). The figure below shows the exo-erythrocytic and erythrocytic stages of the life cycle.

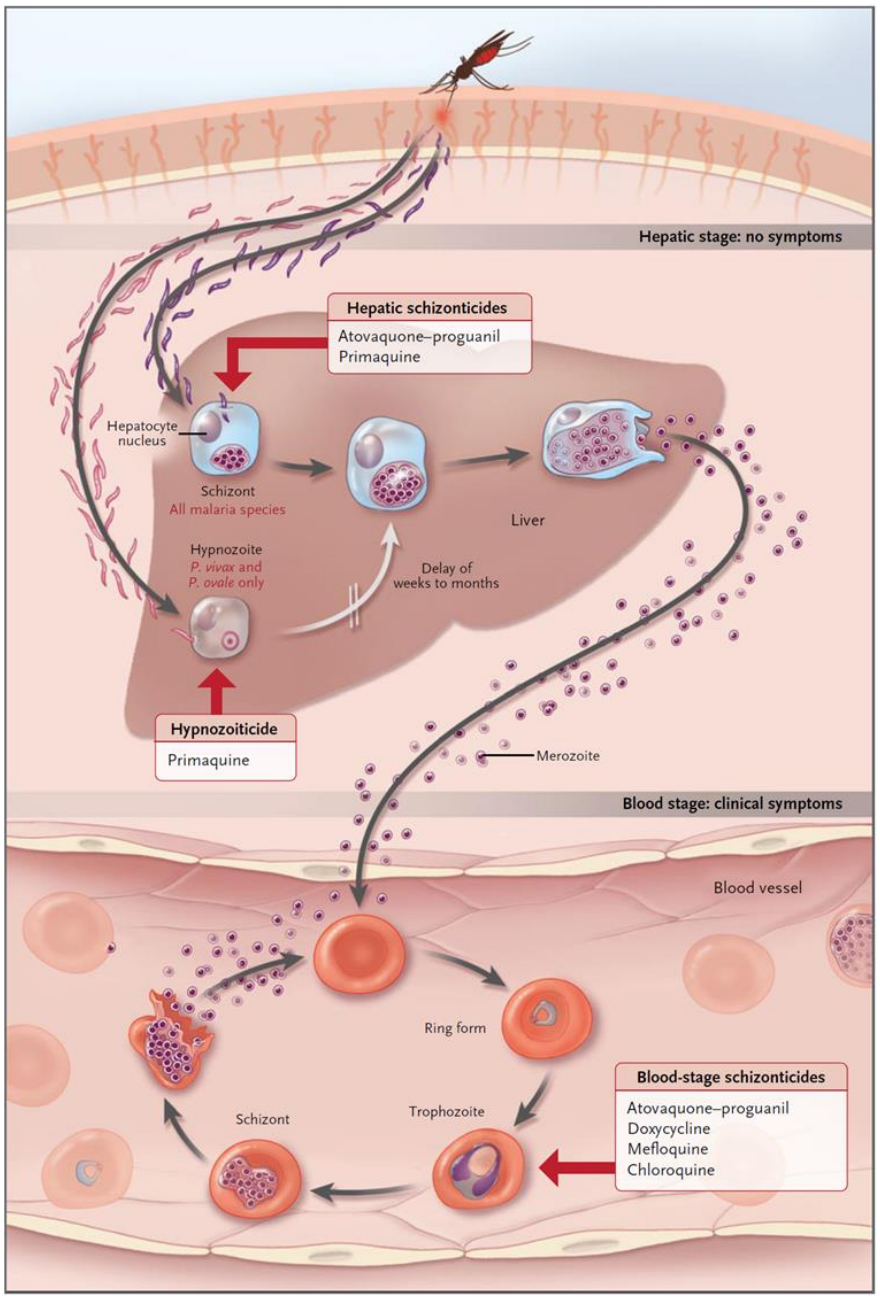


**Figure 1-1**: Exo-erythrocytic and erythrocytic phases of plasmodium parasite in human host (obtained from Baird (8))

The clinical symptoms of uncomplicated malaria consist of a cold (sensation of cold, shivering), hot (fever, headaches, vomiting; seizures in young children) and sweating (sweats, return to normal temperature, tiredness) stages (1). Whereas cerebral malaria, metabolic acidosis and severe anaemia are the three overlapping clinical symptoms of severe malaria (1, 9). Cerebral malaria and metabolic acidosis still account for 15-20% of malaria mortality (9).

The diagnosis of malaria is mostly based on clinical symptoms and microscopic detection of parasite on a blood film (10). The laboratory finding of mild anaemia, elevation of bilirubin and aminotransferases and mild decrease in blood platelets (thrombocytopaenia) are additional laboratory investigations that could help in the diagnosis of malaria (1).

Drugs used in the management of malaria target asexual blood parasitic stages and reduce the disease symptoms, parasite load and progression to severe malaria (11). Drugs used in malaria are discussed in section 1.4 of the thesis.

## 1.2 Epidemiology of malaria

Malaria is a major global health problem with an estimated 225 million cases of malaria in 2009 and 584,000 deaths reported in world in 2013 (3, 5, 12). Worldwide malaria mortality over 2000-2013 is shown in Figure 1.2 (5). There are 106 malaria endemic countries. Of these, 43 are in Africa, 23 in South America and 20 in the South East Asian and Western Pacific regions (3, 12). The highest mortality (91%) and morbidity (81%) of malaria is in Africa, with children under five years old and pregnant women most severely affected (5). Asia is recognised as a region with a high risk of malaria and 6% of total malaria deaths were reported from South-East Asia (12, 13).

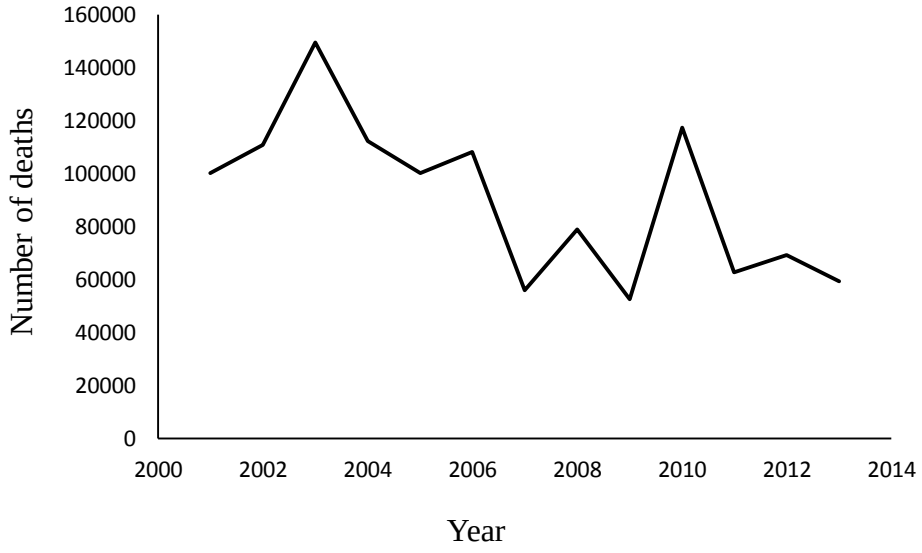


**Figure 1-2:** The reported malaria deaths over 2000 to 2013 in the world based on World Malaria report 2014 (5).

## 1.3 Drug development in malaria

Antimalarials along with antipyretics are the most commonly used and misused medications in tropical parts of the world (14). The extensive use of inexpensive, long elimination half-life medication such as chloroquine and sulphadoxine-pyrimethamine were subjected to drug resistance minimising the potential use of these medications in the treatment of malaria (14). The control of malaria is not an easy task, one of the main reasons being the gap in demand and supply of new and affordable drugs. The antimalarial drug market is one of the largest in the world requiring over half a billion treatments per year. However, the majority of patients are unable to afford their medication (15). The antimalarial drug market is not attractive to the pharmaceutical industry due to lack of financial return. Thus investment for new drug development is minimal. However with an increase in funding for new drugs and malaria control programs from philanthropic organizations (15), some control in malaria morbidity and mortality has been observed over recent years as shown in Figure 1.2 (5).

The need for development of new antimalarial drugs will continue as there is a high probability that malaria parasites will eventually develop resistance to all existing remedies. Pharmacokinetic research for optimum dosing and dosage regimens for existing and new medication is also of crucial importance as drug resistance is mostly

linked to suboptimal drug concentrations of medication with a long elimination half-life (16). Altered pharmacokinetics in malaria infection is observed for drugs such as quinine and therefore pharmacokinetics established in healthy volunteers might not be valid in malaria infection (17, 18). The presently recommended artemisinin-based combination therapy for uncomplicated Plasmodium falciparum malaria need to be replaced with non-artemisinin based combinations if resistance emerged for most potent artemisinin and its derivatives. Severe Plasmodium falciparum malaria requires intravenous medication. Hence, new drugs that can be administered intravenously and their pharmacokinetic profile need to be established to replace quinine and artesunate. Another important goal would be to develop medications that can reverse severe malaria complications and risk of long-term disability (9).

## 1.4 Drugs in malaria

There are about 10 different chemical classes of antimalarial drugs available for the management of malaria; sesquiterpene lactones, arylaminoalcohols, 4-aminoquinolines, 8-aminoquinolines, cinchona alkaloids, dihydrofolate reductase inhibitors, naphthoquinones and antibiotics. These drugs are used in single and combination therapy in the chemoprophylaxis (to prevent persistence of the parasite and chemotherapy (to suppress and clear parasitaemia) of malaria (6, 19).

Antimalarials act on various stages of the parasite life cycle to exert their pharmacological action and drugs can be classified based on the specific stage of parasite activity they target; blood schizonticide (chloroquine, quinine, mefloquine, amodiaquine, artemisinin derivatives, tetracycline and sulfadoxine-pyrimethamine), tissue schizonticides (primaquine, pyrimethamine and proguanil), gametocytocides (primaquine and artemisinin derivatives) and sporonticides (primaquine, chloroguanidine and proguanil) (6, 20).

Pharmacokinetic literature on the drugs of interest for my thesis are summarized in the below section.

The chart below classifies the antimalarials based on their chemical class.

**Chemical classification of anti-malarial drugs (19, 21)**

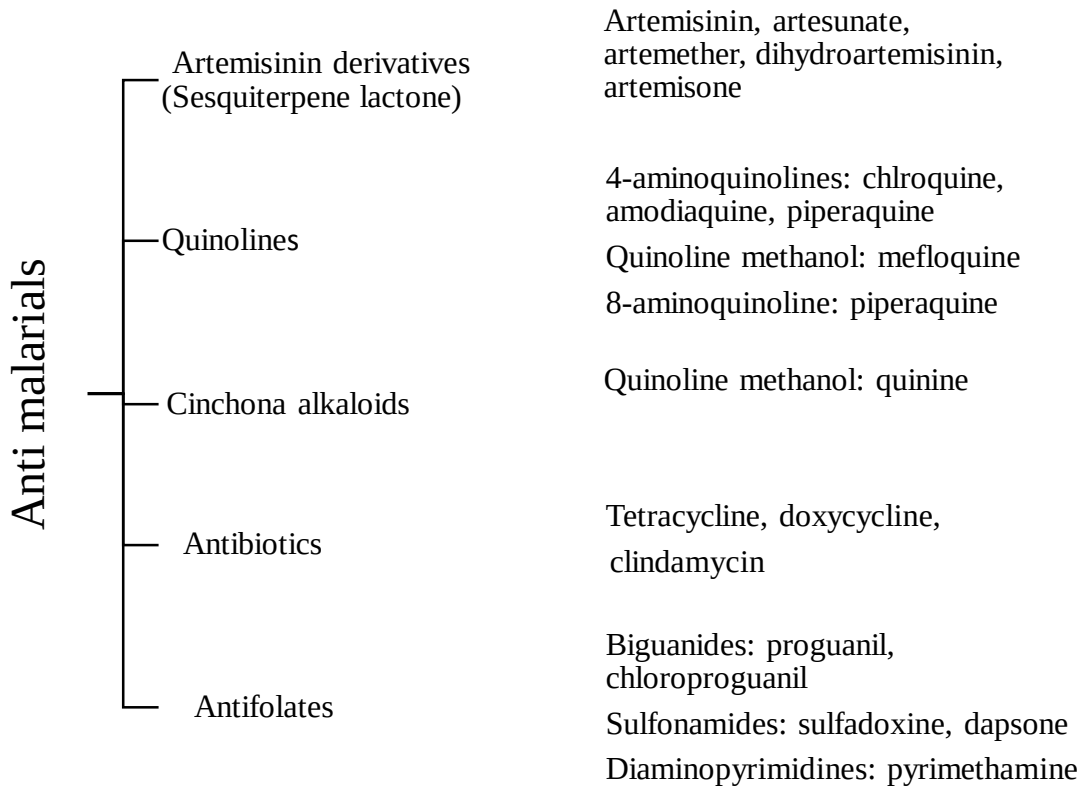

**Chemical structures of selected drugs**

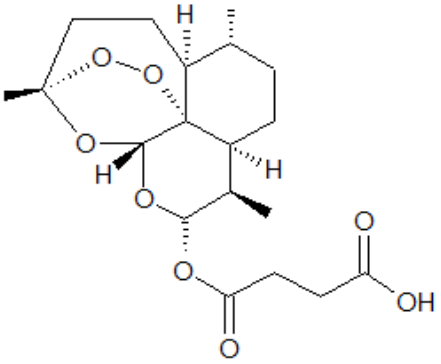


Artesunate

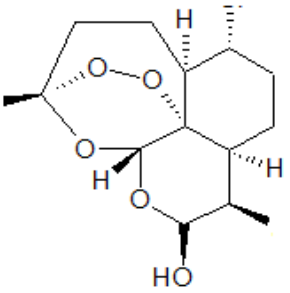


Dihydroartemisinin

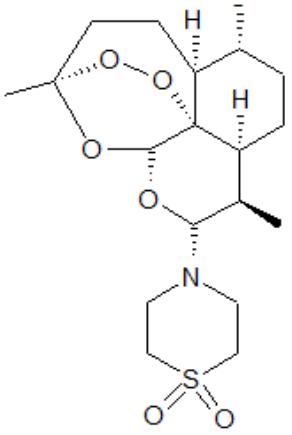


Artemisone

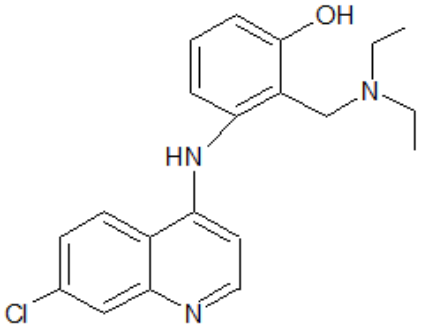


Amodiaquine

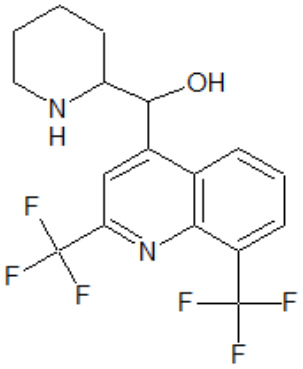


Mefloquine

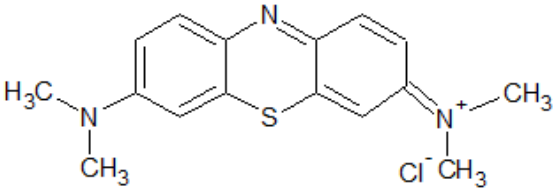


Methylene blue

**Figure 1-3**: Chemical structures of selected antimalarial drugs

***Artemisinin derivatives***

## 1.4.1 Artemisinin

Molecular formula: $C_{15}H_{22}O_5$, Molecular weight: 282.3 g, Log P: 3.14 ± 0.84 (3, 22, 23)

Artemisinin (Qinghaosu) is a natural antimalarial agent isolated from the Chinese herb sweet wormwood *Artemisia annua L*, which was used in China for the treatment of malaria (24). The clinically active isolate has a sesquiterpene lactone with an internal endoperoxide linkage, an essential component for the parasiticidal effect (25). Artemisinin has a low solubility and can only be given orally and rectally, hence artemisinin derivatives with increased solubility and efficacies were developed. The semi-synthetic artemisinin derivatives: dihydroartemisinin (DHA), artesunate (ART), artemether and arteether were later introduced into clinical practice. It is strongly discouraged for artemisinin and its derivatives to be given as single therapy due to the short duration of action, instead combinations with long acting quinolines are recommended.

**Pharmacokinetics:** The artemisinin rectal bioavailability relative to the oral route, and oral bioavailability relative to intramuscular (IM) route was found to be 30% and 32% respectively (26-28). Artemisinin has shown good *in-vitro* drug permeability with bidirectional transport values of $30 \times 10^{-6}$ in Caco-2 cell models (29). It is suggested that artemisinin could have a high liver extraction due to its high permeability, lower bioavailability and lack of correlation between oral clearance (CL) and half-life of the drug (30).

Artemisinin is metabolised in the liver mainly via CYP2B6 to its inactive metabolites (27, 31). Auto induction of enzymes/time dependent pharmacokinetic (increase in half-life with increase in doses) and inter-individual variability in pharmacokinetic were observed for artemisinin (31, 32). The fraction of unbound artemisinin in plasma was 15% and correlated weakly with alpha 1-acid glycoprotein (27).

A pharmacokinetic study of artemisinin in combination with mefloquine found a lower area under the curve (AUC) and lower apparent clearance (CL/F) in combination therapy compared to artemisinin therapy alone. This could be due to the metabolic interactions in the gut or in the liver (33).

The World Health Organisation (WHO) Guide for malaria (3) has not published artemisinin dosing recommendations for uncomplicated malaria. However the standard dosage regimen used is 250 mg two times a day for 5 days (34). There are tablets (250 mg) and suppositories (100 mg, 200 mg, 300 mg, 400 mg and 500 mg) available to deliver the current regimen.

### 1.4.2 Artesunate

Molecular formula: $C_{19}H_{28}O_8$, Molecular weight: 384.4 g, $pK_a$: 4.28±0.17, Log P: 3.291±0.883 (3, 23)

Artesunate is a salt of the hemisuccinate ester, prepared by reducing the artemisinin and adding a hemisuccinate ester component. This is the only artemisinin derivate soluble in water at physiological pH, but has a poor stability when solubilized (21, 35, 36). The drug can be administered parenterally, orally and through the rectum. There are pharmacokinetic advantages of parenteral artesunate compared to IM artemether, therefore it is preferred in severe malaria (37). There are reports of increasing rates of treatment failure and an increase in parasite clearance time for artesunate-mefloquine combination in uncomplicated *Plasmodium falciparum* malaria, hence signs of decrease in efficacy of artesunate combination therapy (38).

**Pharmacokinetics:** Artesunate is rapidly converted to the active metabolite dihydroartemisinin. The ratio of $AUC_{DHA}/AUC_{AS}$ is 5.26 and 4.3-9.7 for malarial infected rats and humans respectively and therefore is considered as a pro-drug of dihydroartemisinin (39-41).

It is claimed that a pH dependent chemical hydrolysis conversion of artesunate to dihydroartemisinin occurs in the stomach. Artesunate has better stability in plasma than in the stomach (42). The dihydroartemisinin peak concentration was achieved in 10 minutes after intravenous (IV) artesunate indicating rapid conversion of artesunate to dihydroartemisinin in the systemic circulation. The oral bioavailability for artesunate was found to be 23% for five patients on oral artesunate (40, 41).

A gradual decline in drug concentration was seen when artesunate was administered over three days to malaria infected rats. This was attributed to possible auto induction

of hepatic drug metabolising enzymes (39). In comparison, a decline in plasma concentration of dihydroartemisinin was observed in malarial infected patients following five days of oral treatment with artesunate (43). A pharmacokinetic study of artesunate and piperaquine combination in children with uncomplicated malaria suggested an auto induction of artesunate metabolism (44). However no auto induction of CYP2B6 was observed following five days of treatment with oral artesunate in healthy volunteers (45). Similar to this finding, in a pharmacokinetic study of artesunate in healthy volunteers found no decline in drug concentration over three days of treatment (46). Therefore decline in concentration in malaria infected patients could be explained by the increase in hepatic enzymes and blood flow due to disease recovery rather than auto induction of enzymes. It is possible that not all endoperoxide antimalarials are inducers of their own metabolism and the metabolic pathway of dihydroartemisinin may be different to that of artemisinin (46).

No change in pharmacokinetics of artesunate or its active metabolite dihydroartemisinin was found when combined with mefloquine for three days (47).

Artesunate is recommended in uncomplicated malaria in combination with amodiaquine or mefloquine at an oral dose of 4 mg/kg/day and the therapeutic dose range is 2-10 mg/kg/day (3). It is strongly recommended to use intravenous (IV) artesunate in the treatment of severe malaria in preference to IV quinine therapy. The dose recommended for both adults and children is 2.4 mg/kg IM or IV artesunate at 0, 12 and 24 hours, followed by once daily treatment (3). Artesunate is available in tablets (50 or 200 mg sodium artesunate), parenteral dosage forms (60 mg anhydrous artesunic acid ampoules) and fixed dose combinations (Artesunate and amodiaquine at 25/67.5, 50/135 and 100/270 mg and artesunate and mefloquine at 50/250 mg).

### 1.4.3 Artemether

Molecular formula: $C_{16}H_{26}O_5$, Molecular weight: 298.4 g, Log P: 2.82±0.86 (3, 23).

Artemether is the O-methyl ether derivative of dihydroartemisinin. This is more lipid soluble than the other artemisinin derivatives and is administered intra muscularly and orally. Artemether is recommended to be combined with long acting lumefantrine in malaria treatment (3).

**Pharmacokinetics**: Absorption of artemether following IM administration is variable and erratic (37, 48). Artemether undergoes extensive first pass metabolism in the liver following oral administration and is metabolised by CYP3A4, 2B6 and 3A5 to its active metabolite dihydroartemisinin (37). The metabolite, dihydroartemisinin predominates following oral administration and artemether predominates following IM administration (49). Artemether is 95% plasma protein bound, mainly to alpha 1-acid glycoprotein and to a lesser extent to albumin (50). Pharmacokinetic studies of artemether for five days in rats and two days in patients with *Plasmodium falciparum* malaria have shown time dependent pharmacokinetics or auto induction of enzymes (51, 52)

The relative bioavailability of oral artemether compared to oral artesunate was 58% (53). The bioavailability of IM DHA and Intrarectal (IR) DHA relative to oral artemether was 25% and 35% respectively. The relative bioavailability of oral compared to IM artemether was 43.2% (54). In rats, bioavailability of IM artemether was 54% (55).

Bioavailability and maximum concentration ($C_{max}$) of artemether increased significantly when administered with grapefruit juice and inhibitors of CYP3A4 (56).

Artemether doses are recommended for uncomplicated malaria considering body weight ranges of the patient. The WHO guide recommends 1, 2, 3 and 4 of 20 mg tablets twice a day for three days for 5-14, 15-24, 25-34 and > 34 kg body weights respectively (the therapeutic dose range 1.4 to 4 mg/kg) (3). Artemether is recommended as an alternative therapy at the dose of 2 mg/kg on admission followed by 1.6 mg/kg per day for severe malaria in situations where first line therapy IV artesunate is not available (3). Artemether is available in both oral and parenteral dosage forms; tablets (50 mg), capsules (40 mg), injectable (40 and 80 mg in 1 mL) and fixed dose combinations (FDC) (20 mg artemether and 120 mg lumefantrine).

### 1.4.4 Dihydroartemisinin

Molecular formula: $C_{15}H_{24}O_5$, Molecular weight: 284.4 g, $pK_a$: 12.61 ± 0.70, Log P: 2.19 ± 0.86 (3, 23)

Dihydroartemisinin is the main active metabolite of artemisinin derivatives; artesunate and artemether. Dihydroartemisinin is also administered orally as a drug in its own right. It has similar efficacy to that of artesunate and is therapeutically 3-5 fold more active than the parent compound artemisinin. The increased activity also makes it more toxic with increased adverse effects (57). Dihydroartemisinin needs to be prepared in suitable excipients due to its poor water solubility and stability.

**Pharmacokinetics**: Dihydroartemisinin is 93% protein bound in malaria patients and the ratio of α-DHA: β-DHA was found to be 6 and 5 for malaria patients and volunteers respectively (58). Drug metabolism is through intestinal and hepatic glucuronidation and has a high hepatic extraction ratio (59). Dihydroartemisinin has shown a higher hepatic extraction ratio in an isolated perfused rat liver model where the hepatic extraction ratio was reduced by 20-30% in rodents infected with *Plasmodium berghei* malaria (60). A mass balance study of dihydroartemisinin in rats has shown enterohepatic cycling (61).

Bioavailability of dihydroartemisinin is reported for both healthy volunteers and malaria infected patients following administration of the pro-drug artesunate and oral dihydroartemisinin. In healthy volunteers, the absolute oral bioavailability of dihydroartemisinin was 80% and 45% following artesunate and dihydroartemisinin administration. Dihydroartemisinin parenteral dosage forms are not available, therefore calculation was based on the assumption that IV artesunate was completely converted to dihydroartemisinin (62). Oral bioavailability of dihydroartemisinin (35-48%) relative to oral artesunate was twofold higher when compared to oral dihydroartemisinin (15-21%) in healthy Caucasian volunteers. It is suggested that the higher bioavailability of dihydroartemisinin following oral artesunate could be due to protection of the metabolite from pre-systemic glucuronide conjugation. Thus it is recommended that oral artesunate should be used over oral dihydroartemisinin. (59).

In malaria infected patients, absolute IM bioavailability of dihydroartemisinin was 86-88% after administration of the pro-drug (36, 63) whereas the oral bioavailability of dihydroartemisinin relative to oral artesunate was 82-88% in patients with malaria (40, 41, 62). Newton, van Vugt (64) found a higher total area under the curve, smaller $C_{max,}$ prolonged time to reach maximum concentration ($t_{max}$) and lag time for dihydroartemisinin following oral administration of dihydroartemisinin compared to

oral artesunate in malaria infected patients. The authors recommended that oral dihydroartemisinin could be a satisfactory alternative to oral artesunate given the ease of manufacture and lower cost. The bioavailability of dihydroartemisinin for IR artesunate ranged from 16-85% in patients with malaria (36, 65).

The WHO (3) recommends dihydroartemisinin oral dosage regimen for the management of uncomplicated malaria at 4 mg/kg once daily for 3 days in combination with piperaquine (therapeutic range 2-10 mg/kg). Dihydroartemisinin tablets are available in 20, 60 and 80 mg tablet strengths.

### 1.4.5 Artemisone

Molecular formula: $C_{19}H_{31}NO_6S$, Molecular weight: 401.52 g, log P = 2.49 (66).

The newly developed artemisone is a promising semi synthetic artemisinin derivative that can be synthesized from dihydroartemisinin in a one step process (67). *In-vitro* and animal studies have shown that artemisinin and its derivatives are neurotoxic (in particular dihydroartemisinin), although the mechanisms are not fully understood (68, 69). Artemisone development was based on evidence that an artemisinin derivative with better aqueous solubility and decreased lipid solubility would give increased systemic activity and decreased neurotoxicity.

Efficacy of artemisone was determined in *in-vitro* and *in-vivo* (using *Plasmodium berghei* infected rodents) studies where both studies found artemisone to be 4 to 10 time more potent than artesunate (70). The *in-vitro* study showed that artesunate and artemisone to have similar trends of interactions, a synergistic interaction with mefloquine and somewhat antagonistic interaction with amodiaquine are observed. An *in-vivo* rodent model showed synergistic interaction between artemisone and mefloquine.

**Pharmacokinetics**: Pharmacokinetic studies of artemisone in malaria infected monkeys have shown increased *in-vivo* activity of artemisone compared to artesunate Ex-vivo bioassay study was conducted by testing blood samples against *Plasmodium falciparum* K1 (67). A comparative bioavailability study of 30 mg/kg artesunate and artemisone in

healthy Saimiri monkeys found a higher bioavailability of artemisone compared to artesunate (67).

Artemisone underwent a Phase I clinical trial in 32 healthy Caucasian volunteers (66). The trial used single and multiple doses in the range of 10 to 80 mg (oral solution and 20 mg immediate release tablets were administered) and the pharmacokinetic parameters obtained were similar to other artemisinin derivatives. The drug was rapidly absorbed and peak concentration was attained at 1.5 hours. The half-life and volume of distribution were 3.1 hours and 13.7 litres (66).

The metabolism of artemisone was through CYP3A4 and produced minimum of six metabolites with three of the metabolites still having anti-malarial properties (66, 67). Unlike the other artemisinin derivatives and artemisinin, (artemether more evident and artesunate and dihydroartemisinin less evident) artemisone does not undergo auto induction of enzymes (67).

## Quinolone derivatives

### 1.4.6 Amodiaquine

Molecular formula: $C_{20}H_{22}ClN_3O$**,** Molecular weight: 355.9 g, Most acidic $pK_a$: 9.43±0.50, Most basic $pK_a$ = 5.62±0.50, log P = 2.6 (3, 23, 71)

Amodiaquine (AQ) is a 4-aminoquinoline and has similar action and efficacy to that of chloroquine. Amodiaquine (amodiaquine dihydrochloride dihydrate) is soluble in 22 parts of water and 70 parts of alcohol (21). A solution with 2% W/V amodiaquine in water has a pH of 3.6 to 4.6. Solubility of amodiaquine decreases with increasing pH (72, 73).

**Pharmacokinetics:** This drug is rapidly absorbed from the gastrointestinal tract ($t_{max}$ within 30 minutes) and rapidly converted to its active metabolite desethylamodiaquine in the liver (74). Amodiaquine is considered to be a pro-drug. Both amodiaquine and its active metabolite are more than 90% protein bound (75). The metabolite contributes to most of the antimalarial effects and is accumulated in the blood cells with 3:1 blood to plasma ratio. The active metabolite has a longer half-life than the parent drug and is detected after 96 hours of the oral dosing (74).

Pharmacokinetic interactions for concurrent administration of artesunate and amodiaquine were studied in healthy volunteers. The study found that the area under the curves for the active metabolites of the drugs, desethylamodiaquine and dihydroartemisinin were significantly lower compared to the single therapy. The clearance and the $t_{max}$ values for dihydroartemisinin were similar to the single therapy. The day 7 desethylamodiaquine plasma levels were lower in the combination therapy and no change in $V_z/F$ and $C_{max}$ was observed (76).

Concurrent administration of artesunate and amodiaquine combination therapy with antiviral efavirenz increased the AUC for amodiaquine and decreased the desethylamodiaquine exposure in two of the five healthy human volunteers. This was linked to CYP2C8 inhibition by the antiretroviral medication (77, 78).

The WHO guide for malaria recommends amodiaquine to be administered in the dose range of 7.5 to 10 mg/kg for the treatment of uncomplicated *Plasmodium falciparum* malaria. Amodiaquine is available only for oral administration and the amodiaquine base is available in dosing strengths of 153 and 200 mg in the salts of hydrochloride and chlorohydrate.

### 1.4.7 Piperaquine

Molecular formula: $C_{29}H_{32}CL_2N_6$, Molecular weight: 535.51g, Most basic $pK_a$: 8.92 ± 0.50, Log P: 6.8 ± 1.4 (3, 23)

Piperaquine is a highly lipophilic bisquinoline molecule (20). This is commercially available either as the base or as the water soluble salt, piperaquine phosphate. Piperaquine, first synthesized in 1960s, was widely used as a single therapy for chloroquine resistant malaria from the 1970s to 1980s in China, until piperaquine resistance became widespread in the 1990s (79, 80). However, use of piperaquine resurfaced as a partner drug for artemisinin combination therapy. Currently dihydroartemisinin and piperaquine combination therapy is recommended in the treatment of uncomplicated *Plasmodium falciparum* malaria (81). This combination is found to be advantageous over the other artemisinin combinations in high transmission

areas due to the longer period of post treatment prophylaxis of piperaquine with a half-life of about 28 days (20).

**Pharmacokinetics**: Piperaquine has shown multiphasic distribution with large $V_z/F$, low apparent clearance (CL/F) and long terminal half-life. The concentration time profile for piperaquine has shown multiple peaks, which is linked to entrohepatic recycling or multisector intestinal absorption (82). However studies in rats have shown that there is negligible biliary and renal clearance of piperaquine and it is assumed to be eliminated mainly through hepatic metabolism (83). In rats and humans, a carboxylic acid metabolite is found to be the major metabolite in piperaquine metabolism (83). Piperaquine is more than 99% plasma protein bound in rat, mouse, dog and human (84) and the red blood cells to plasma ratio is 1.5 (85).

It is recommended to increase weight adjusted piperaquine doses in children compared to that of adults (86). A marked increase in drug clearance in children compared to adults with *Plasmodium vivax* and *Plasmodium falciparum* malaria was observed in a pharmacokinetic study (87). Day 7 piperaquine concentration is suggested to determine the therapeutic success of such slowly cleared drugs (88). Piperaquine multiple dose pharmacokinetics were significantly different to single dose pharmacokinetics and it is suggested that this might be due to accumulation of piperaquine from the previous doses (89, 90).

The oral bioavailability of piperaquine in rats was found to be 50% (83), yet high fatty meals are reported to increase its bioavailability (90, 91).

Piperaquine is recommended to be given at the dose of 18 mg/kg/day (therapeutic dose range between 16–26 mg/kg/dose) in combination with dihydroartemisinin for the treatment of uncomplicated *Plasmodium falciparum* malaria. Fixed dose combinations (FDCs) for dihydroartemisinin and piperaquine are available at the dose of 40 and 320 mg respectively.

### 1.4.8 Mefloquine

Molecular formula: $C_{17}H_{16}F_6N_2O$, Molecular weight: 378.3g, Most acidic $pK_a$: 12.81±0.20, Most basic $pK_a$: 9.24±0.10, Log P: 2.20±1.15 (3, 23)

Mefloquine (MQ) is a 4-methanolquinoline and available as mefloquine hydrochloride. This is recommended as a chemoprophylactic for chloroquine resistant strains, even though toxicity of the drug is a concern (92). The mechanism of action of mefloquine is unclear and claimed to have a strong blood schizonticidal activity against *Plasmodium falciparum and Plasmodium vivax* malaria (20). Mefloquine is only slightly soluble in water at physiological pH (0.3mg/mL at pH 7.4) and soluble in ethanol and is sensitive to light (93, 94). The molecule has two asymmetric carbon atoms and the commercially available mefloquine is the racemic mixture of two enantiomers.

**Pharmacokinetics**: Mefloquine shows enantioselectivity after administration of racemic mixture (95). This drug can only be given orally and parenteral use is avoided due to severe local irritation (20, 96-98). Following oral administration, it undergoes little first pass metabolism and has low intrinsic clearance (96, 99).

Mefloquine is well absorbed from the gastrointestinal tract and 98.3% bound to plasma protein (3, 20, 100, 101). Blood to plasma ratio is 1.1 (102). The drug is metabolised in the liver into inactive metabolites, 2,8-bis(trifluoromethyl)-4-quinolinecarboxylic acid; a quinoline carboxylic acid derivative. Little drug is excreted in the urine. Animal studies suggest the drug is excreted in the bile and faeces and undergoes enterohepatic recycling; this could be the reason for long half-life of the drug (3, 20, 101, 103). *In-vitro* studies on mefloquine suggest that it is a substrate and an inhibitor of CYP3A4 and P-glycoprotein (104, 105). CYP3A4 mediated pharmacokinetic interactions for mefloquine are reported for cimetidine, rifampicin and ketoconazole and enterohepatic recycling related interactions for ampicillin and tetracycline (99, 106-109). The increase in the area under the curve and $C_{max}$ of mefloquine when co-administered with ketoconazole could also be due to inhibition of P-gp by ketoconazole (109). Drug absorption of mefloquine is increased when ingested with a high fatty meal (110).

It was found that oral bioavailability and $C_{max}$ of mefloquine was significantly lower when mefloquine was given 24 hours after a single dose of artemether, which could be attributed to a decrease in mefloquine absorption or an increase in CL/F in the presence of artemether (111). In the combination therapy of artesunate and mefloquine, some pharmacokinetic parameters of mefloquine changed significantly, decrease in $C_{max}$, an increase in CL/F and expansion of $V_z/F$ were observed. This antagonistic pharmacokinetic interaction has overridden the synergistic effect of the combination

therapy with a lower cure rate for combination therapy (66%) compared to the 75% cure rate for the group receiving mefloquine alone (112). The change in pharmacokinetics could be attributed to high plasma protein binding of mefloquine; which will create competition for artesunate at plasma proteins. This could increase free mefloquine resulting in increase in CL/F and $V_z$/F. The decrease in $C_{max}$ could be attributed to a decrease in oral absorption and/or reduction in oral bioavailability. It is also worth noting that the change in pharmacokinetics of mefloquine could be attributed to artesunate itself or its active metabolite dihydroartemisinin (112).

Mefloquine is recommended in combination with artesunate at either 25mg/kg split over two days (15 mg/kg on day one and 10 mg/kg on day two) or 10 mg/kg over 3 days in the treatment of uncomplicated malaria. The therapeutic dose range is 7-11 mg/kg/dose. Mefloquine hydrochloride tablets are available in 250 mg base, FDC of 25mg artesunate and 250 mg mefloquine (3)

## Cinchona alkaloids

### 1.4.9 Quinine

Molecular formula: $C_{20}H_{24}N_2O_2$, Molecular weight: 324.4 g, Most acidic $pK_a$: 12.80±0.20, Most basic $pK_a$: 9.28±0.70, Log P: 2.83±0.43 (59)

Quinine, a 4-methanol quinoline antimalarial, is an alkaloid obtained from the bark of the cinchona tree and has been used for treatment and prevention of malaria since 1820. Quinine has been used for treatment of severe malaria before clinical trials method was used to decide comparative efficacies (3).

**Pharmacokinetics**: Following oral administration, quinine is rapidly and completely absorbed and is widely distributed in the body, including into cerebrospinal fluid (CSF), breast milk and the placenta.

Quinine is extensively metabolised in the liver via CYP3A4 and polar metabolites are excreted in the urine (113, 114). The major metabolite 3-hydroxyquinine contributes to 10% of the antimalarial activity. Renal clearance accounts for 20% of the excretion (115). Quinine is a drug with a low intrinsic clearance and sensitive to malaria infection, therefore, drug clearance could change with reduced liver enzyme activity (18, 116).

The pharmacokinetics of quinine varies depending on malaria infection status and age. Quinine is a weak base and 70% and 90% bound to alpha 1-acid glycoprotein (30% bound to albumin) in healthy volunteers and during malaria infection, respectively (117, 118). The blood to plasma ratio of quinine is 0.7 (119). The $V_z/F$ of quinine (basic drug) was reduced in acute malaria infection due to an increase in α-acid glycoprotein (120-122). Mean elimination half-life is 11, 16 and18 hours in healthy subjects, uncomplicated malaria and severe malaria respectively (20).

Malaria infection induced dysfunction of the hepatic mixed function oxidase (mainly CYP3A), impairs metabolic conversion of quinine resulting in reduction in drug clearance in malaria infection compared to the healthy state (18). The liver blood flow is also reduced in patients with acute *Plasmodium falciparum* malaria. Theoretically, hepatic drug clearance is not affected by the change in liver blood flow for low extraction ratio drugs (123), however liver blood flow could still become an important determinant of quinine clearance in very severe malaria (18, 124). Quinine clearance in malaria infected children was significantly lower than in convalescent children (125)

Pre-treatment with cimetidine resulted in decreased CL/F of quinine and concurrent administration of quinine with ritonavir resulted in a 4 fold increase in area under the curve and a 4.5 fold decrease in drug clearance in healthy volunteers (126, 127). Pre-treatment with the CYP450 enzyme inducers rifampicin, cigarette smoking and nevirapine increased the drug clearance and decreased the area under the curve of quinine (128-130). No pharmacokinetic drug interaction was found when quinine and grapefruit juice were co-administered though (131).

The oral bioavailability of quinine was 76-88% in healthy volunteers (132, 133). The relative bioavailability of rectal quinine compared to oral quinine was 21% (134).

Quinine is recommended in severe malaria; loading dose of 20 mg/kg and maintenance dose of 10 mg/kg every 8 hours is administered in a rate controlled IV infusion or IM injections (3).

## Antibiotics

### 1.4.10 Clindamycin

Molecular formula: $C_{18}H_{33}ClN_2O_5$ S, Molecular weight: 424.98 g, $pK_a$: 7.45 (135, 136)

Clindamycin is available as hydrochloride or phosphate salts in capsule form or as palmitate hydrochloride in oral solutions. In children, doxycycline may be substituted with clindamycin and this is recommended as a second line therapy in combination with artesunate or quinine in the treatment of uncomplicated *Plasmodium falciparum* malaria (3).

**Pharmacokinetics**: Clindamycin hydrochloride is rapidly absorbed from the gastrointestinal tract (3, 137). Clindamycin is about 90% plasma protein bound in humans and binds mainly to alpha 1-acid glycoprotein (138). In rats, the plasma protein binding of clindamycin was found to be 67.5% and 61% of the dose was subjected to first pass elimination (139). The drug undergoes metabolism primarily through human CYP3A4 in the liver to its active metabolites N-desmethyl clindamycin and sulphadoxides as well as to inactive metabolites (140, 141). Clindamycin has a low intrinsic clearance (142). The absolute bioavailability of clindamycin was 53% and 72% in human volunteers and dogs following oral administration of clindamycin hydrochloride.

Clindamycin 10 mg/kg twice a day for 7 days is the recommended to be combined with artesunate or quinine in the management of uncomplicated *Plasmodium falciparum* malaria. Clindamycin base 75, 150 and 300 mg capsules are available in its salt form.

### 1.4.11 Methylene blue

Molecular formula: $C_{16}H_{18}N_3SCl$, Molecular weight: 319.85 g, $pK_a$ of the reduced form: 5.8, $pK_a$ oxidized form: 0 (143, 144)

Methylene blue (MB: Methylthioninium chloride) was the first synthetic drug used in the treatment of malaria more than 100 years ago and the use of this drug was abandoned with the emergence of new treatments (145). During World War II methylene blue was disliked by soldiers because of blue colouration of urine (146). Reinvestigation of the

use of methylene blue in the treatment of malaria began in 1995 with the main aim of developing an accessible, available and affordable antimalarial to treat malaria infected children in developing countries (146). Efficacy of methylene blue in malaria has been shown in several clinical studies in children (145, 147-149). *In-vitro* studies have shown methylene blue has potent antimalarial properties (150). Methylene blue and chloroquine have shown synergistic action in combination, however a small reduction in chloroquine exposure was observed in a pharmacokinetic study of combination therapy (149). A controlled Phase II trial of children (6-10 years), randomised to receive methylene blue combinations (methylene blue-artesunate, methylene blue-amodiaquine and artesunate-amodiaquine), found a statistically significant reduction in gametocyte carrier rate in methylene blue containing regimens, thus reducing transmission of *Plasmodium falciparum* malaria (145) .

Methylyene blue has redox potential and can be present in three forms, the blue colour oxidized form ($MB^+$), semi-reduced form ($MB^{\cdot}$) and the colourless reduced form or leuco-methylene blue ($LMB^{--}$). The reduced form gets readily oxidized in the presence of oxygen (143). The blue coloured oxidized (cationic) methylene blue, undergoes catalytic redox reaction under physiological conditions. The conversion of oxidized methylene blue into its reduced form, colourless leuco-methylene blue is facilitated by nicotinamide adenine dinucleotide phosphate (NADPH) (146). The colourless leuco-methylene blue has very low ionization (3%) at physiological pH.

**Pharmacokinetics**: Methylene blue demonstrated multi-compartment pharmacokinetics following IV and oral administration (151, 152). The drug achieves 53 to 97% peak concentrations after 30 to 60 minutes (153). Methylene blue and leuco-methylene blue are predominantly excreted in urine, but also in bile and faeces.

The oral bioavailability of methylene blue was found to be very low (about 1%) in fasted healthy volunteers. A higher drug concentration of methylene blue was found in brain following IV administration and higher intestinal and liver concentrations were found following oral administration in rats (151).

In contrast to this, a subsequent study found a much higher absolute bioavailability for methylene blue for the oral route of administration, being 72.3 ± 33% ( plasma as matrix) and 84 ± 20% (whole blood as the matrix). A high inter-individual variation in

methylene blue area under the curve was observed. The study also observed higher plasma concentration of methylene blue when co-administered with chloroquine, but this was not observed for whole blood (152).

The blood to plasma ratio of methylene blue was 0.98 and 1.1 for IV and oral route data respectively. Investigators explained this as possible intake of methylene blue into the cells but absence of intracelluar accumulation (152). However other studies have found that cationic methylene blue is reduced on the exofacial cell surface of human erythrocytes, which allows lipophilic reduced leuco-methylene blue to enter cells by diffusion and be sequestered within the cells followed by re-oxidation to the oxidized (blue) form (144, 154, 155) .

Methylene blue is administered orally at 12 mg/kg twice daily for 3 days in children (146).

## 1.5 Artemisinin combination therapy (ACTs) and pharmacokinetics

The World Health Organization recommends artemisinin combination therapies (ACTs) as the first line therapy in the management of uncomplicated malaria. ACTs were introduced in 2001; however the widespread adoption of ACTs has been slow due to their relative cost, lack of awareness of its advantages, lack of suitable formulation and the imbalance between supply and demand (6, 156, 157).

In ACTs, a short acting and rapid onset artemisinin derivative is combined with a partner drug with a longer half-life, which provides increased efficacy, extended prophylaxis and prevents development of resistance of artemisinin derivatives (87, 158-160). The potent artemisinin derivatives cause rapid reduction of parasite biomass and resolve clinical symptoms while the remaining parasites are removed by less active, slowly eliminated long acting drugs (81). The potential advantages of ACTs include rapid reduction in parasite biomass, delay in development of drug resistance for artemisinin derivatives, effectiveness against multidrug resistant malaria parasite, reduction of gametocyte carriage, extended drug prophylaxis and lower side effects (156, 160).

Most countries have updated their treatment guides to recommend artemisinin combination therapies when existing treatments such as chloroquine and sulfadoxine-pyrimethamine treatments are no longer effective. By the end of 2010, 84 out of the 87 countries adopted ACTs into their national policy as the first line therapy for management of uncomplicated *Plasmodium falciparum* malaria (12). There are four artemisinin combination therapies currently recommended to be used in the management of uncomplicated malaria: artemether plus lumefantrine, artesunate plus mefloquine, artesunate plus amodiaquine and dihydroartemisinin plus piperaquine (3). The treatment recommendations or choice of ACTs for malaria vary from country to country depending on the level of drug resistance, acquired protective immunity of the population and cost of the drug (12).

## 1.6 Antimalarial drugs resistance

The WHO defines resistance as the ability of the parasite strain to survive and/or multiply despite administration and absorption of drugs given in either the usual or higher than recommended dosage (3). In early resistance development, symptoms disappear and the patient appears recovered, but symptoms resurface in a few weeks' time due to the original infection (recrudescence) (3).

Antimalarial drug resistance development could be due to initial genetic change (de novo drug resistance) resulting in resistant mutants and followed by selection processes, where parasites survive in the presence of a drug leading to transmission and the spread of drug resistance (14, 16). De novo drug resistance to malaria is rare and is most likely to occur at peak infection when parasite numbers are greatest and antimalarial drug concentration is highest. Parasites surviving at this high drug concentration are likely to be highly resistant to the drug. Low-level resistance can be seen when inadequate standard treatments are received (14, 16).

Chloroquine resistance was first reported in the late 1950s in Thailand, Cambodia and Colombia and by the 1960s the resistance spread into South America and South east Asia (161, 162). In the 1980s, sulphadoxine-pyrimethamine, the first line affordable antimalarial medicines used in the management of uncomplicated malaria developed increased resistance, which lead to treatment failure (163). Today resistance

development is a major problem and resistance (or reduced sensitivity) has been observed for almost all currently available antimalarials including artemisinin derivatives (8, 164, 165).

Drug resistance in malaria can be slowed or prevented by combining drugs with different mechanisms of activity and ensuring patient compliance by adherence to correct dosage regimens.

Pharmacokinetics of drugs plays a major role in the development and spread of drug resistance. Sub optimum drug doses, pharmacokinetic interactions in drug combination therapy and presence of sub-therapeutic plasma levels in the body for long period, especially for drugs with a long half-life, increase the emergence of resistant forms of the parasite (166, 167).

## 1.7 Introduction overview

The general introduction on allometric scaling and it is application to determine paediatric drug doses are covered in the chapter 2 of the thesis whereas the general introduction on P-glycoprotein is covered in chapter 3.

## 1.8 Objectives

In order to delay development of drug resistance and for maximum drug efficacy, it is important to prescribe optimum drug combinations and doses, which require clear knowledge of pharmacokinetic parameters of antimalarials. Optimum drug doses are especially lacking in children and are mostly determined on the basis of linear scaling or mg/kg adult dosing (81, 88, 168-173). In this respect, one aim was to carry out allometric scaling of antimalarials drugs in order to consider the potential value of allometry in paediatric drug dose decisions in children. Determination of drug permeability/absorption and identification of antagonistic pharmacokinetic interactions in combination therapy further facilitates decisions about the optimum drug dosing. Hence the second principal aim was to establish drug permeability, identification of Permeability glycoprotein (P-glycoprotein, P-gp) mediated drug transport and pharmacokinetic drug interactions during drug absorption using *in-vitro* Caco-2 cell lines.

The overall aim was therefore:

> To investigate allometric scaling relationships, gastrointestinal permeability, P-gp mediated drug transport and regulation of P-gp expression of antimalarial drugs in single and combination therapy.

**Specific Objectives**

Chapter 2 of the thesis covers the allometric scaling of antimalarials and dosage consideration for children, which includes two specific objectives

- To investigate the allometric scaling relationship of anti-malarial drugs using published pharmacokinetic data of healthy and malaria infected mammalian species
- To predict paediatric antimalarial drug doses for children >2 years using an interspecies allometric scaling technique

Chapter 3 covers the development of an *in-vitro* cell model for determination of drug permeability and P-gp mediated drug transport of anti-malarial drugs.

Chapter 4 covers antimalarial permeability, P-gp mediated drug transport and regulation of P-gp transporter in the presence of antimalarials and includes the specific objectives below

- To establish analytical techniques for quantification of anti-malarial drugs (artesunate, artemisone, mefloquine, amodiaquine and methylene blue) in the laboratory
- To determine the inhibitory properties of anti-malarial drugs against P-gp mediated drug efflux in single and combination therapy.
- To determine drug permeability and the potential involvement of P-gp mediated drug efflux of antimalarials in single and combination therapy.
- To determine the role of antimalarial drugs in the regulation of P-gp transporter expression.

# 2 Allometric scaling of antimalarial drugs

## 2.1 Introduction

Allometric scaling is a pharmacokinetic tool, which can be used for extrapolation of human pharmacokinetic parameters using pre-clinical data (174-177). The technique is also used to guide drug dose decision making in children > 2 years (178-180).

### 2.1.1 Interspecies scaling

The study of the proportional body size of mammals and its consequences on biological characteristics is known as allometry. The anatomical, physiological and biochemical similarities among mammals can be generalised and expressed mathematically by an equation. Hence allometry is based on the theory that the simple power law expression given below can describe the relationship between the body size of mammals with such as organ size and blood flow (181).

$$Y = a \times W^{b} \quad \textbf{(1)}$$

Y : Parameter under study

a : Allometric coefficient

W : Body size/weight of the species

b : Allometric exponent

Allometric scaling has a more empirical approach compared to the mechanistic approach of the physiological models. This technique tends to study the relationships between the relative size of the mammals with its consequences such as physiological, biochemical and anatomical parameters without necessarily understanding the reasons/rationale for the relationship(s). The present work was based on interest in the relative relationship between body size/weight of the animal and the physiological parameters, which determine the pharmacokinetics of drugs (176, 182).

The allometric scaling technique has been available and in use for many years. Galileo, in 1637, was one of the first to apply this technique, having observed that large animals have disproportionally thicker bones than smaller animals to maintain the necessary mechanical support (182, 183). It has been recognised that all mammals have quite similar basic physiology and physiological processes, even though their outward appearance is distinctively different. Therefore allometric relationships were established to account for this biological relativity among the mammalian species. This concept was further explained by introducing the concept of "physiological time", which is defined by Boxenbaum as "a species dependent unit of chronological time required to complete a species independent physiological event" (184). The life expectancy of dogs and man is 14 and 98 years, respectively. Therefore a dog ages at the rate of 7.14% of its life per year whereas man takes 7 years to age the same amount. Therefore 1 dog year is equivalent to 7 man years, these being equal physiological times necessary to produce a species independent physiological event (184).

Out of the many examples given in the literature to support this, the relative relationship between the breath time and the heartbeat time in mammals was considered (185-187). The ratio for breath time divided by the heart beat time for any mammal will be 4. This ratio remains the same irrespective of the size of the mammal, with every breath cycle being equal to four heart beats for each mammal. This is scaled using the equation below where bodyweight is given in gram.

$$\text{Breath time (seconds)} = 0.169 \times (\text{bodyweight})^{0.28} \quad \textbf{(2)}$$

$$\text{Heartbeat time (seconds)} = 0.0428 \times (\text{bodyweight})^{0.28} \quad \textbf{(3)}$$

The power function of the equation, 0.28, is used to scale the lifetime of a mammal. Small animals breath faster and their heart beat more rapidly compared to larger animals. Therefore, a given number of breaths and heart beats comes to an end for smaller mammals more quickly than for larger mammals, hence their life time is shorter compared to a larger animal.

Allometric scaling of pharmacokinetic parameters is based on this premise that physiological parameters of mammals such as heart rate, hepatic blood flow, glomerular filtration rate, cardiac output and specific organ weights are a function of the body size/weight of the animal species. Out of the given physiological parameters, glomerular

filtration rate and hepatic blood flow are closely linked physiological parameters, and are related to pharmacokinetic parameters such as clearance and half-life. If hepatic blood flow and the glomerular filtration rates of mammalian species are plotted against species body weight on a log-log scale, a linear plot is obtained (182). Therefore it is logical to expect that clearance and half-life can be related to the body size/weight of the mammal (188). If the concept of physiological time is applied to pharmacokinetics, mammals with a shorter life expectancy such as a rat will have a faster metabolic rate and shorter drug clearance time compared to a mammal with a longer life expectancy. Therefore drug clearance in different mammals can be scaled across mammals depending on their body sizes.

Drugs excreted unchanged are eliminated mainly by the renal filtration process. Filtration of a drug depends on the renal function of a mammal, which is assessed using the creatinine clearance. Creatinine clearance is allometrically related to the body size (188).

The elimination rate of a drug with a high hepatic extraction ratio depends on the blood flow to the liver (123, 189). The drug clearance of a high extraction ratio drug correlates with the body size of the animal, as blood flow depends on the liver and the body size of the animal. The larger, longer living animals have a slower total body clearance compared to the smaller, short life-span mammals (188).

With drugs having a poor extraction ratio, elimination depends on the enzymatic activity of the relevant enzymatic system rather than the liver blood flow. The intrinsic clearance of the unbound drug should correlate with the liver weight provided that the *in-vivo* enzyme activity per unit liver mass is constant among the different species (188, 190).

The volume of distribution of a drug depends on binding to plasma and tissue proteins and permeability across biological membranes. The volume of distribution will be directly related to the body tissue mass for drugs having higher tissue protein binding. This in turn results in a direct relationship between the volume of distribution of the drug and body size (188). Similarly, clearance as described above generally correlates well with the body size of the mammal. Elimination half-life is a secondary pharmacokinetic parameter, which is dependent on two primary pharmacokinetic parameters: clearance and volume of distribution.

When hepatic blood flow or renal clearance is plotted against the body weight of the mammals, a disproportionally increasing curve against body weight is obtained. However when both axes are transformed to their log value, a linear plot is obtained, enabling direct interpolation of parameters in the Y axis. Similarly when the pharmacokinetic parameter is plotted against the species bodyweight in a log-log scale, a linear plot is obtained and the relationship between the pharmacokinetic parameter of a drug and body weight can be explained by a simple power equation (182).

### 2.1.2 Past and the present of allometry

A brief chronology of development of allometry is provided below.

1637: Galileo observed the relationship between the skeletal sizes to the body mass (184).

1838: Sarrus and Ramaeux proposed that metabolic rate would be proportional to the body mass using the power function of 2/3 (191).

1932-1937: Kleiber published that mammalian basic metabolic rate is proportional to the body mass using the power function of 3/4 (192).

1949: The quantitative relationship between body weight of mammals and their basic biological parameters was identified by Adolph (181).

1967: First example of pharmacokinetic parameter scaling of alcohol metabolic oxidation rate (193).

1969: The first use of log-log plot parameter scaling by Mellett (194).

1970: Dedrick plots were introduced where application of alternative time scale was used for superimposition of various species' plasma concentration time profiles (195).

1977: Weiss and co-workers were the first to introduce allometric equations in pharmacokinetic parameter scaling (196).

1980-1986: Allometric scaling was used for scaling of pharmacokinetic parameters of drugs; antipyrine, phenytoin, caffeine, antibiotics (190, 197, 198).

1990-1995: Allometric scaling was used for scaling of anti-HIV drugs (199, 200).

1997: Theoretical explanation (fractal geometry) for allometric 0.75 power models (201).

Current: Increasing interest in using the technique for dose determination in children (178-180).

### 2.1.3 Simple allometric power equations for pharmacokinetics

The general allometric power equation used in comparative biology given below can be used for describing size and its consequences, in this case, pharmacokinetics (185). The power function given below describes the relationship between the pharmacokinetic parameters of a drug and species body weight across mammalian species.

$$Y = a \times W^b \quad \textbf{(1)}$$

Y : Pharmacokinetic parameter under study (dependent variable)

a : Allometric coefficient (intercept)

W : Species body weight (W) (independent variable)

b : Allometric exponent (slope of the curve)

The allometric exponent and coefficient are obtained upon logarithmic transformation of the above equation.

$$\log Y = b \log(W) + \log(a) \quad \textbf{(4)}$$

### 2.1.4 Allometric scaling approaches in pharmacokinetics

Allometric scaling of key pharmacokinetic parameters clearance, volume of distribution and half-life facilitate calculation of drug doses for humans (202, 203). Out of the three pharmacokinetic parameters, clearance is the most important, as the exponent value of clearance is used to determine the maintenance or regular dosing of a drug. The exponent value obtained by scaling the volume of distribution of a drug is used for determination of the loading dose for the dosing regimen. Half-life is a secondary pharmacokinetic parameter.

The allometric scaling approach adopts two main methods in extrapolation of pharmacokinetic parameters across mammalian species.

- Fixed exponent allometric scaling method
- Variable exponent allometry, based on interspecies scaling

#### 2.1.4.1 Fixed exponent allometry

Allometry has been used in biological sciences over many years and a large number of allometric relationships have been established. In 1838, one of the earliest allometric relationship was established by Sarrus and Ramaeux between body size and basic metabolic rate [cited by Brody (204) in 1945). Authors claimed that metabolic rate would be proportional to the body mass using a power function of 2/3. This was supported by Rubner in 1883, who claimed that metabolic rate of resting dogs was independent of mass when divided by the surface area (205). The use of 2/3 power value was challenged, when Kleiber (206) in 1932 published mammalian BMR scaling, where metabolic rate is proportional to the body mass using a power function of 3/4. In his article he investigated animals weighing from 0.15 to 679 kg (rats to steer) and obtained the allometric equation, metabolic rate (calories/kg) = $73.3 \times \text{Body mass}^{0.734}$ (192). In a subsequent publication in 1961, he proposed rounding off the exponent value, 0.734 to 0.75 (3/4) for convenience. One of the notable advantages of the use of the simple fraction, 3/4 was the use of the slide rule in the past for simple calculations. This exponent value, 3/4 has been used widely ever since as a fixed exponent and applied universally for interspecies scaling. The exponent value for volume of distribution and half-life has been set at 1 and 0.25 respectively (182). The exponent value of 1 for

volume of distribution indicates that this has the most direct relationship with the body weight, whereas half-life has the most distant relationship with the body weight.

According to the general pharmacokinetic theories (182)

$$\text{Half-life} = \frac{0.693\times \text{ volume of distribution}}{\text{clearance}} \quad \textbf{(5)}$$

$$\text{Half-life} = \frac{0.693\times A\times W^{1}}{A'\times W^{0.75}} \quad \text{(Where Volume of distribution} = AW^{1}, \text{ Clearance} = A'W^{0.75}) \quad \textbf{(6)}$$

A : Coefficient for volume of distribution ($V_z$)

$W^1$ : Body weight with power function of 1 ($V_z$ exponent)

A' : Coefficient for clearance

$W^{0.75}$ : Body weight with power function of 0.75 (CL exponent)

$$\text{Half-life} \propto \text{Body weight}^{0.25}$$

Allometric scaling was first used by (196) to scale the pharmacokinetic parameters among different mammals. The fixed exponent value of 0.75 has been used in pharmacokinetics universally for prediction of drug clearance and doses for humans using drug clearance values of preclinical species (207, 208).

The theoretical basis for the basic metabolic rate exponent value of 0.75 for clearance was justified by West and co-workers (201, 209) using the concept of fractal geometry where a general model describe the transport of material through space filling fractal networks of branching tubes. It was hypothesised that this model is similar to mammalian circulatory system and terminal tubes do not vary with body size.

### 2.1.4.2 Variable exponent allometry

In variable exponent allometry, drug specific allometric exponents and coefficients are derived based on physiological function of animals. The method utilizes species specific

pharmacokinetic parameters of drugs, which are determined by the physiological function of the animal. The method commonly utilizes all available pharmacokinetic parameters of preclinical species. The pharmacokinetic parameter is plotted against the bodyweight of the mammal in a log-log scale. The slope of the regression line gives the allometric exponent, b, and the antilog of the intercept gives the allometric coefficient, a.

The closer the power function/exponent to one, the more direct the linear relationship between the pharmacokinetic parameter and body weight. The correlation coefficient of the line determines the effectiveness of the scaling, with a correlation of determination ($r^2$) value close to 1 indicative of a strong allometric relationship (188).

Allometric scaling of pharmacokinetic parameters requires a minimum of three species and typically this would include one rodent species (mouse or rat). Beagle dogs, rabbits and nonhuman primate species are commonly used (175). Inclusion of at least one large animal in the scaling procedure could improve the prediction of pharmacokinetic parameters for other species (175).

This technique assumes that pharmacodynamic differences among different species are clinically negligible.

### 2.1.5 Methods used in improving allometric drug clearance prediction

There is literature to indicate that the simple allometric power model can be insufficient for accurate prediction of human pharmacokinetic parameters (203, 210-212). The term "vertical allometry" is used to refer to prediction errors of human drug clearance, mostly the over-prediction of drug clearance by the scaling method. This could be a serious concern when determining the first-time human dosing, which could lead to drug toxicity (164, 167). Therefore various methods have been proposed over the years to improve simple allometric prediction of pharmacokinetic parameters. Several investigators developed correction factors to improve pharmacokinetic parameter prediction and some of the adopted approaches are explained below.

#### 2.1.5.1 Maximum life span potential (MLP)

Interspecies scaling of drug clearance correlates well with species' body weight, when the drug clearance is mainly through the hepatic metabolism and has a high hepatic extraction ratio (184).

For drugs with a low extraction ratio, clearance depends on the plasma protein binding (fraction unbound) and intrinsic clearance of the unbound drug according to the well stirred model described by Pang and Rowland (189). Therefore it is most likely that intrinsic clearance of these drugs correlates with the species body weight (184). Boxenbaum (184) correlated the intrinsic clearance of antipyrine, phenytoin and clonazepam with body size. However, for these drugs, predicted intrinsic clearance was found to be lower than the observed clearance and human data were found to be outliers. Hence it was proposed that unbound intrinsic clearance for drugs may correlate with the longevity in addition to the body size of the mammals and therefore maximum lifespan (MLP) correction was introduced the to improve simple allometric predictions.

The life span and aging rate of a species is genetically controlled by a biological clock (184) and the biological properties of the organism. If the animal dies due to a natural reason, then the number of years the animal lived would be the maximum life span potential of that animal. Longevity relates to the anatomical developments, sociological and metabolic processes including heart rate, basal metabolic rate, body weight, temperature, brain size, gestation length, nitrogen out-flow, biological intelligence, postnatal developmental rates, onset of specific physiological functions and age of sexual maturation (184). The authors identified the total "life capacity" of an organism as its maximum lifespan potential calorie consumption, which was defined as the product of MLP and the specific metabolic rate. Therefore the rate of energy expenditure will affect the life span of a species. The rat, having a higher metabolic rate, will have a shorter longevity compared to a larger species such as the human. Therefore in order to increase life span, the species would need to economize metabolic activity. Humans have a slower maturation, reduced mixed function oxidases and a higher brain weight per unit mass than the other mammals. These variations were considered for the development of MLP correction (188). Further Brody (204) showed that resting metabolic rate and mammalian body weight had a strong power law relationship with a correlation coefficient above 0.99 for regression analysis of log body weight and

metabolic rate. Jerison (214) discussed extensively the evolution of the mammalian brain and observed a strong correlation between the log-log relationship between the brain and body weight of 98 mammalian species.

Based on these Sacher (215) in 1959 defined MLP as the maximum documented longevity of the species. He developed an equation to determine the MLP of an animal species based on the multiple regression technique.

$$MLP = 10.839 \times BW^{0.636} \times W^{(-0.225)} \quad \textbf{(7)}$$

MLP : Maximum life span (years)

BW : Brain weight (grams)

W : Body weight (grams)

The coefficient 10.839 is replaced with 185.5 if the brain and body weights are in kg (211). Table 2.1 gives the MLP for different species calculated from the above equation.

**Table 2-1:** MLP in years for animal species and human (184)

| Species | Adult brain weight (g) | Adults body weight (g) | Brain weight as a % of body weight | Calculated MLP in years |
|---|---|---|---|---|
| Human | 1530 | 70,000 | 2.19 | 93.4 |
| Rhesus monkey | 62 | 4700 | 1.32 | 22.3 |
| Cattle | 252 | 310,000 | 0.081 | 21.2 |
| Goat | 130 | 31,00 | 0.416 | 23.3 |
| Sheep | 110 | 57,600 | 0.191 | 18.3 |
| Pig | 58.2 | 77,200 | 0.075 | 11.4 |
| Dog | 75.4 | 14,200 | 0.531 | 19.7 |
| Rabbit | 9.97 | 2,550 | 0.391 | 8.01 |
| Guinea pig | 3.42 | 270 | 1.27 | 6.72 |
| Rat | 1.88 | 250 | 0.751 | 4.68 |
| Mouse | 0.334 | 23 | 1.45 | 2.67 |

Boxenbaum (184) analysed the MLP correction using pharmacokinetic data for antipyrine. He tried several plots empirically and obtained the best fit when $CL_{Uint} \times$ MLP was plotted against the body weight in a log-log scale. Similar plots were tried for

phenytoin and clonazepam and based on these data, the MLP correction was proposed. The clearance obtained from simple allometry needs to be multiplied by the MLP of the species and the value obtained is plotted against species body weight in a log-log scale to obtain corrected allometric exponents and coefficient. The resultant corrected exponent value could be used for predicting pharmacokinetic data from one species to another (184).

$$CL_{U_{int}} \times MLP = a(W)^b \quad (8)$$

$CL_{Uint}$ : The intrinsic clearance of unbound drug (mL/min)

MLP : Maximum life span potential (years)

W : Body weight (kg)

a : Allometric coefficient

b : Allometric exponent

### 2.1.5.2 Two term power equations

This correction factor was developed considering that genetically determined characteristics of mammalians results in species specific differences.

According to this model, species specific phenotypes operating within the context of an integrated control system determines the drug disposition process (216, 217). The brain size could be an indicator of the control capacity of the species, therefore an allometric relationship could exist between the rate of drug metabolism and mammalian brain weight (215, 217).

The increase in body size/weight enables the inclusion of more functional units related to drug disposition such as drug metabolising enzymes and nephrons, hence body weight could also have an allometric relationship with the drug metabolism (217).

Two term power equation was proposed by Boxenbaum and Fertig (217) to improve clearance prediction of compounds that are excreted mainly by Phase I oxidative metabolism. The method was established using unbound intrinsic clearance data for antipyrine in 15 species. Antipyrine was selected because it mainly undergoes Phase I

oxidative metabolism and has a low extraction ratio. The authors made a mathematical assumption that the dependent variable $CL_{Uint}$ could be correlated with the independent variables body weight, brain weight and the body temperature. Body temperature did not significantly contribute to variance in $CL_{Uint}$. This resulted in an empirical correction method, two term power equation based on brain weight and body weight of species (217).

$$CL_{Uint} = 0.387 \times W^{1.32} \times BW^{(-0.619)} \quad (9)$$

$CL_{Uint}$ : The intrinsic clearance of unbound drug (mL/min)

W : Body weight (kg)

BW : Brain weight (kg)

### 2.1.5.3 Brain weight correction

This correction method was proposed by Mahmood and Balian (212). In this empirical method, brain weights (Table 2.1) of different species were used to modify the drug clearance. The product of brain weight and clearance is plotted against the body weight of the species in a log-log scale based on below given power equation. The allometric plot generates provides a corrected allometric exponent and an allometric coefficient to determine pharmacokinetic parameters in humans. Human brain weight of 1.53 kg was used to determine the human clearance (212).

$$CL \times BW = a(W)^{b} \quad (10)$$

CL : Clearance (L/hr)

BW : Brain weight (kg)

W : Body weight (kg)

a : Allometric coefficient

b : Allometric exponent

### 2.1.5.4 Rule of Exponents

This rule was proposed by Mahmood and Balian (211, 218) based on the analysis of 40 drugs. The allometric scaling relationships were established for all drugs based on simple allometry, MLP correction and brain weight correction techniques. Based on the study finding, it was suggested that out of the three methods, only one method should be used for prediction of human pharmacokinetic parameters from animal data. The authors proposed 'the Rule of Exponents' based on the exponent values obtained by the simple allometry techniques. The rule suggests that one should adopt simple allometry if the resulting simple allometry exponent lies between 0.55 and 0.70. In situations where the simple allometry exponent lies between 0.71 and 0.99, the CL × MLP method should be adopted and when the exponent is > 1, CL × BW should be adopted (211, 218) .

### 2.1.5.5 Correction using *in-vitro* metabolic data

Simple allometry predictions have been shown to be predictive for renally excreted (198, 219), and highly metabolized drugs (184, 220). Allometric predictions for low extraction ratio drugs have been less predictive (184, 203, 221). Therefore another correction factor using *in-vitro* metabolic data was proposed to improve the pharmacokinetic parameter prediction of drugs with low or intermediate hepatic extraction ratio.

In this method, it was assumed that the drug is solely metabolised by the liver and that the blood to plasma ratio of the drug in different animals is equal to one. Liver samples of animals and humans were obtained and isolation of hepatocytes was done by liver tissue perfusion. Cells were seeded with culture medium and drugs were added at different concentrations (below $K_M$ values). The unchanged compound in the media was assayed after incubation for 72 hours. Intrinsic clearance was calculated from the ratio of the initial amount of the compound in the incubation medium to the corresponding AUC value determined using the concentration obtained at six different time points (221).

When *in-vitro* metabolic rates were used as a correction factor, the *in-vivo* clearance value of each animal was normalized by the ratio of *in-vitro* clearance values as indicated in the below equation.

$$CL_{in\text{-}vivo(\text{animal})} \times \frac{in\text{-}vitro\ CL_{\text{human (hepatocytes)}}}{in\text{-}vitro\ CL_{\text{animal(hepatocytes)}}} \quad (11)$$

The normalized values were extrapolated using allometric scaling technique power equation as given below.

$$CL_{\text{in-vivo(animal)}} \times \frac{\text{in-vitro } CL_{\text{human (hepatocytes)}}}{\text{in-vitro } CL_{\text{animal(hepatocytes)}}} = a \times W^{b} \quad (12)$$

W : Body weight (kg)

a : Allometric coefficient

b : Allometric exponent

An interspecies scaling of mofarotene and bosentan (drugs metabolized by CYP450) was carried out incorporating an *in-vitro* liver model to extrapolate *in-vivo* drug clearance in humans. The study found that this method better predicted drug clearance compared to the brain weight correction method (222, 223). Similarly, human clearance prediction of tolcapone, a drug metabolized by a Phase II reactions, was found to be satisfactory using the same technique (224). Lave, Dupin (221) adopted *in-vitro* correction technique to extrapolate human clearance of 10 extensively metabolized drugs, in which a significant improvement in clearance prediction was found.

It is not certain that this method can be used for predicting human drug clearance for other drugs due to the smaller number of drugs tested and limited validation in subsequent reports.

### 2.1.5.6 Allometry using unbound clearance

Obach, Baxter (225) used unbound clearance values and MLP values to improve clearance predictions using allometry.

The free clearance was defined as below.

$$CL_{p(free)} = \frac{CL_{p(total)}}{f_u} \quad (13)$$

$f_u$ : Fraction unbound

$CL_{p(free)}$ : Unbound clearance

$CL_{p(total)}$ : Total clearance

The investigators used four scaling approaches; $CL_{p(free)}$ vs body weight, $CL_{total}$ vs body weight, $CL_{p(free)}$/MLP vs body weight and $CL_{total}$/MLP vs body weight. No improvement in clearance predictions were found by incorporation of MLP into clearance values. Clearance prediction from scaling $CL_{p(free)}$ and $CL_{total}$ were within 2 fold of the actual clearance values.

The study concluded the unbound clearance method prediction was slightly more accurate than the total clearance (225). Mahmood (174) tested scaling of unbound clearance, however claimed that unbound scaling method is no better than the total clearance prediction. He further proposed that drugs exhibiting vertical allometry can be better predicted using the unbound clearance method.

### 2.1.5.7 Glomerular filtration ratio (GFR) correction factor

This method was proposed for improving clearance prediction of the drugs mainly excreted by renal clearance, given that there could be differences in renal excretion, filtration, reabsorption and secretion among species. The study adopted (GFR × Blood Flow) / (Body weight × Kidney Weight) as given in Table 2.2 to determine the GFR correction factor for each species. The predicted clearances for different species were then divided by the GFR correction factor (210). The corrected clearance is plotted in a log-log scale based on the below given allometric power equation.

$$\frac{\text{Clearance}}{\text{GFR correction factor}} = a.W^b \quad (14)$$

GFR : Glomerular filtration rate

W : Body weight (kg)

a : Allometric coefficient

b : Allometric exponent

**Table 2-2**: Glomerular filtration factors for preclinical and human species (210)

| Species | Body weight (kg) | Kidney weight (kg) | Blood flow | GFR | [a](GFR×BF)/ (W×KW) | Factor |
|---|---|---|---|---|---|---|
| Human | 70 | 0.3 | 1240 | 125 | 7381 | 1 |
| Pig | 30 | 0.13 | 600 | 65 | 10000 | 1.4 |
| Sheep | 50 | 0.2 | 900 | 90 | 8100 | 1.1 |
| Dog | 14 | 0.05 | 216 | 45 | 13886 | 1.9 |
| Monkey | 5 | 0.025 | 138 | 10.4 | 11482 | 1.6 |
| Rabbit | 2.5 | 0.013 | 80 | 7.8 | 19200 | 2.6 |
| Guinea pig | 0.29 | 0.0024 | 12.6 | 2.2 | 39828 | 5.4 |
| Rat | 0.25 | 0.002 | 9.2 | 1.31 | 24104 | 3.3 |
| Mouse | 0.02 | 0.00032 | 1.3 | 0.28 | 56875 | 7.7 |

[a]GFR; Glomerular filtration rate, BF: Blood flow, W: Body weight, KW: Kidney weight

The authors tested this method to predict pharmacokinetic parameters of 10 renally excreted drugs. The results showed that the predicted total clearance and the renal clearance of drugs were lower than the observed clearance values. This method was unable to predict both the total and non-renal clearance of renally excreted drugs which could be due to variations in the mechanism of renal excretion of drugs in different species (218). However it is difficult to make a recommendation from this study due to the small number of drugs studied and limited subsequent research.

### 2.1.5.8 Correction for biliary excreted drugs

This correction factor was proposed to improve clearance prediction of drugs, which exhibit enterohepatic recycling. The enterohepatic recycling or biliary excretion could vary from species to species. Bile is excreted from the liver; therefore the body weight, liver weight and bile flow rate of the species were used to develop the correction factor

(mouse = 5.9, rat =11.6, rabbit = 2.0, dog = 1.9, monkey = 4.3). The bile flow rate of the species was normalised using the liver and body weight of the species. The investigators carried out simple allometry first and Rule of Exponents was applied. The clearance was corrected based on the Rule of Exponents and resultant values were divided by the biliary clearance correction factor (226).

$$\frac{\text{Clearance}}{\text{Biliary clearance correction factor}} = aW^{b} \quad (15)$$

| | | |
|---|---|---|
| Clearance | : | CL or CL × BW or CL × MLP |
| W | : | Body weight (kg) |
| a | : | Allometric coefficient |
| b | : | Allometric exponent |

The clearance of eight drugs were analysed using the method and the predicted clearance of drugs undergoing enterohepatic recycling was improved by this method (226).

Another correction method was proposed to improve clearance of biliary excreted drugs using bile flow rate and microsomal UDP glucuronosyltransferase activity and found that this method is also suitable for predicting clearance of biliary excreted drugs (227).

### 2.1.5.9 Unbound clearance corrected intercept method

Tang and Mayersohn (228) proposed this method to improve clearance prediction of drugs especially anticipated to exhibit vertical allometry. The study analysed 60 drugs using this method. Simple allometric scaling was carried out and the coefficient (a) from the regression line was obtained. The fraction unbound ($f_u$) drug for human and rat was obtained from the literature. A mathematical model was developed and the equation below was obtained to determine the human drug clearance.

$$\text{Human CL} = 33.35\ (\text{ml/min}) \times \left(\frac{a}{Rf_u}\right)^{0.77} \quad (16)$$

Human CL : Human clearance

a : Simple allometric coefficient

$Rf_u$ : Ratio of unbound fraction in rats compared to human

The $Rf_u$ in the equation was obtained from the ratio of the plasma unbound fraction ($f_u$) in rats compared to humans. The study found this method to be more predictive than the Rule of Exponents correction (228).

#### 2.1.5.10 Monkey liver blood flow method

This assumed that drug clearance is mainly hepatic and blood to plasma ratio is constant across species. The clearance of the animal was expressed as a percentage of the liver blood flow. Liver blood flow values of 85, 30, 45 and 21 mL/min/kg for rat, dog, monkey and human was used respectively (180, 181). Human clearance was predicted from the product of the animal clearance with the ratio of human liver blood flow to the animal liver blood flow (229).

$$\text{Human clearance} = \text{Animal clearance} \times \frac{\text{Human liver blood flow}}{\text{Animal liver blood flow}} \quad (17)$$

The investigators found incorporation of monkey pharmacokinetic data to provide most qualitative and quantitative estimation of human clearance, having calculated human clearance using each animal species clearance and liver blood flow. This could be due to the phylogenetic proximity of monkeys to humans compared to the other commonly studied preclinical species (182).

### 2.1.6 Criticism of correction factors

The effectiveness of the correction factors in predicting drug clearance has been debated and it is claimed that there is no rational basis for most of the empirical correction factors (221, 225, 230-232).

The Rule of Exponents is based on arbitrary cut off levels of exponent values and this method was developed looking at the allometric scaling relationship of small number of drugs. The selected drugs were not randomly selected and investigator did not adopt a scientific basis to select the cut levels. This method has been discussed in the literature more frequently; however validity of the method was mostly questioned (229, 233). Tang and co-workers (232) indicated that this rule need further testing in a variety of drugs prior recommending as a correction method. MLP correction was developed to improve clearance prediction of the low extraction ratio drugs. The correction has been tested by many investigators. However the validity of this method is also yet to be fully resolved. Correction using *in-vitro* metabolic data for drugs cleared through metabolism, unbound clearance correction for low extraction ratio drug, correction using bile flow rate of species for drug under enterohepatic recycling and correction using GFR factor for drugs renally cleared have some physiological basis. Therefore, these techniques are worth exploring further, in order to make recommendation.

In a study of 103 drugs using simple allometry with and without correction factors such as brain weight, MLP and GFR, Rule of Exponents were tested (229, 233). It was concluded that none of the correction factors substantially improved the clearance predicted beyond simple allometric technique. The brain weight correction was tested by Lave and colleagues (221) and found that predicted clearance values to be tenfold lower than the observed values. Two term power equation was tested by Mahmood and Balian (211) who reported that two term power equations do not accurately predict the drug clearance. However, the noted advantage of these correction methods is that these methods can be easily tested due to readily availability of required parameters.

Mahmood (174) tested unbound clearance intercept method for clearance prediction of renally and biliary excreted drugs and found this method to be equally useful as the Rule of Exponents for clearance predictions in humans. Both monkey liver blood flow and unbound clearance corrected intercept method belong to fixed exponent allometry as two techniques involves one species with a fixed exponent in the allometric function (232). Therefore these methods have the disadvantages of fixed exponent allometry.

There have been many studies which compared predictive performance of different methods, however the controversy of this issue has not yet settled. It is apparent that none of these correction methods have been tested in large number of drugs with

differing physicochemical characteristics and differing drug clearance or metabolic pathways in one study. Therefore it appears that some of the current studies are subjected to investigator bias.

Thus, the question of validity of correction factors and superiority of correction factors over simple allometry is yet to be answered (232).

### 2.1.7 Physiologically based models

Interspecies scaling uses animal data for determination of pharmacokinetic parameters for humans. The two methods used for this are the empirical allometric scaling approach and the mechanistic physiological based models, where both methods assume that pharmacokinetic parameters can be scaled following basic physiological principles.

Physiological based models enable extrapolation of pharmacokinetic parameters from one species to another using a mechanistic approach (scaling based on physiological function) and require considerable model development (182).

Physiologically based models describe drug movement and disposition in the body based on organ blood flow and organ spaces penetrated by the drug. This mathematical model assumes that drug movement in the body is blood flow limited (234). The model requires actual organ blood flow rates, organ size, tissue to blood partitioning, permeability of drug and metabolic chemical reaction rates to develop first order differential equations to represent concentration of drug in blood and the various organs as a function of time (182, 188). Most frequently rats are used to determine these parameters.

In order to develop concentration-time profiles in man, differential equations are numerically solved assuming tissue binding and metabolic equivalency between man and animal, along with appropriate blood flow and organ size parameters of man (182). Physiological models have been found to be in limited use due to complexity, cost and time, even though the model provides inherent understanding of drug disposition.

### 2.1.8 Dedrick plots

Drug eliminating organs such as the liver and kidney are relatively larger in smaller animals compared to larger animals, as is blood perfusion. This results in higher drug disposal capacity in smaller compared to larger animals (181, 197). In order to account for the pharmacokinetic changes occurring in mammals in relation to their relative size, Dedrick and co-workers (195) developed the Dedrick plot, where he obtained plasma levels of methotrexate from mammalian species and carried out a normalisation process before scaling. In the conventional plot, log plasma level is plotted against the chronological time. In order to normalise the X and Y axis, the plasma levels were divided by the mg/kg dose to account for differences in plasma levels caused by differences in mg/kg dosing. Smaller animals have higher drug clearance (mL/min/kg) compared to that of the larger animals owing to faster metabolic rate. Thus the drug concentration tends to decline faster in smaller animals compared to the larger animals and therefore chronological times in these species need to be decelerated relative to larger species. This was achieved by dividing the time by the body weight to the 0.25 power. By doing this the chronological time was converted to pharmacokinetic time. Pharmacokinetic time scale is derived from the concept of physiological time scale, which is the time required to complete an independent physiological event of the species (184, 188, 195).

Dedrick and co-workers (195) utilized the empirical relationship established by Adolph (181) for power transformation of physiological basis of the body weight. Boxenbaum (166) in his review stated that it is logical for authors to use 0.25 as interspecies variation in methotrexate clearance (this is primarily cleared by kidney) as it correlates with 0.31 used for interspecies creatinine clearance by Adolph (181) in 1949 (184, 235).

The ratio, plasma concentration divided by normalized dose was plotted against the pharmacokinetic time (Time/Body weight $^{(0.25)}$) in a log- linear scale and resulting plot was named as the “elementary Dedrick plot” (184, 188, 195, 235).

Dedrick plots have been developed for some drugs such as new carbapenem derivative, penem antibiotic (FCE 22101) (236, 237)

### 2.1.9 Applications of interspecies scaling

#### 2.1.9.1 Veterinary medicine

In veterinary medicine, the typical method used for extrapolating doses for non-domestic animal species was to use the mg/kg dosing of the domestic animals. This resulted in linear increase in the amount of drug administered as body weight increases. However, this tends to overdose large animals and under dose small animals. Allometric scaling of pharmacokinetic parameters of animals has been used as the final method for extrapolation of doses for new animal species (202).

#### 2.1.9.2 Pre-clinical to clinical dosing

Pharmacokinetic investigations play an important role during the lead optimization in drug discovery. The pharmaceutical industry inputs substantial resources in identifying a drug with favourable *in-vivo* pharmacokinetics in preclinical species. This information is used in future preclinical pharmacology data and safety studies which increase the clinical success and decrease possible toxic effects from inappropriately high doses.

In the US, new drugs need to be studied in at least two types of animal species prior to clinical studies in humans (238). However, the pharmacokinetics of animals could vary from humans. Therefore, in order to better utilize animal pharmacokinetic data in determining human pharmacokinetic parameters, there is a need to scale pharmacokinetic parameters, such as clearance and volume of distribution from one species to another and finally to humans (176).

Interspecies allometric scaling is used in the pharmaceutical industry to establish the first dosage in human drug investigations. The established pharmacokinetic parameters of a few animal species are used to predict both human pharmacokinetic parameters and then the first IV dose for human Phase I studies (239, 240).

#### 2.1.9.3 Population pharmacokinetic modelling

Population pharmacokinetic models utilize allometric expression to incorporate body weight/size to model the pharmacokinetic behaviour of a drug. The general practice is

to use fixed exponents, 0.75 for clearance and 1 for volume of distribution for scaling between adults and children (180, 201). However, it remains undecided whether allometric exponent used in population pharmacokinetic modelling should be fixed or variable (241). There are population pharmacokinetic studies where variable exponent allometry has been adopted where drug specific allometric exponents were used for model development (242-244).

### 2.1.10 Drug dosing in children

The need for age-based pharmacotherapy was recognized over 100 years ago. Dr. Abraham Jacobi wrote: " Pediatrics does not deal with miniature men and women, with reduced doses and the same class of disease in small bodies, but has its own independent range and horizon"(245).

Pharmacokinetic studies, however, are often restricted in paediatrics, given the vulnerability of the subgroup, and dose decisions are frequently made by extrapolation from the adult population. Over the years different approaches have been used for dose selection in children. The initial dosing is scaled from adult doses and later adjusted based on the clinical response. The current textbooks of dose recommendations such as British National Formulary and Martindale Pharmacopoeia use a mixture of recommendation guides such as mg per kg dosing, age dependent dosing and weight ranges (246). British National Formulary has also published drug doses for children based on clinical experience and off-label use rather than on randomised clinical trial findings (246). There is a growing interest in using allometric scaling techniques for dose determination in children < 2 years. Some of the common drug dosing methods are described below.

#### 2.1.10.1 Scaling by body size/weight

Body weight dependent dosage regimen for drug therapy was first proposed by Professor A.J Clark of Edinburgh, where child dose was determined by multiplying the adult dose by the ratio of child weight/150 (247).

This was later modified and improved and the equation below was proposed to determine the child dosing. However it wasn't widely quoted due to mathematical complexity (247, 248).

$$\text{Child dose} = (1.5 \times \text{weight of the child}) + 10\% \text{ of adult dose} \quad (18)$$

The most common mg/kg dosing method normalises adult dose by body weight, assuming a linear relationship between body weight and the drug dose. This method gained its popularity due to its apparent simplicity (247).

$$\text{Child dose} = \text{Adult dose} \times \frac{\text{Child body weight}}{\text{Adult body weight}} \quad (19)$$

However, this method has the least accuracy in dose prediction compared to the other methods (249, 250) can leads to over dosing (toxicity) and under dosing (sub therapeutic dosing). For example, chloramphenicol is metabolised by UDP-glucuronyl-transferase enzymes, which is immature in newborns and mg/kg dosing in infants can lead to fivefold higher dosing causing grey baby syndrome. Whereas carbamazepine is metabolized by CYP3A4 and the activity of CYP3A4 is higher in children, leading to lower therapeutic levels after mg/kg dosing (246).

### 2.1.10.2 Age based rule

Age based rule determines appropriate doses on the basis of age subgroup. Children are sub-grouped into different age groups; pre-term new born, term new born, infants, toddlers, children and adolescents and specific doses are prescribed for different age groups (246). This method fails to consider physiological and biochemical changes within each age subgroup of children. This creates a situation of absence of dose response relationship for each age group.

### 2.1.10.3 Weight ranges

In the weight range method, a dose is recommended using predetermined body weight ranges for children thus not individualised. These weight ranges and corresponding doses are determined based on clinical experience (251).

### 2.1.10.4 Body surface area

Body surface area (BSA) rule has been recognized as more accurate compared to body weight method in determining doses for children. The metabolic rate of a person reflects heat loss, which is proportional to the surface area of the body (247, 249). The concept of using body surface area was first recognized by Moore (252) in 1909. Du Bois and Du Bois (253) proposed the first multidimensional formula for the surface area by investigating the surface area of nine individuals. Surface area was calculated in $cm^2$ using height in cm and weight in kg applied to the below equation.

$$\text{Surface area}(S)(cm^2) = \text{Weight}^{0.425} \times \text{Height}^{0.725} \times 71.84 \quad (20)$$

Gehan and George (254) later proposed an improved equation to derive the surface area of an individual.

$$\text{Surface area}(S) = 0.0235 \times \text{Height}^{0.42246} \times \text{Weight}^{0.51456} \quad (21)$$

Body surface area scales allometrically with a power model using exponent value of 2/3 (0.67) (231). This assumes that metabolic rate is geometrically scaled based on body size and children and adults are geometrically similar.

$$\text{Dose} = a\,(\text{Body surface area})^{\frac{2}{3}} \quad (22)$$

a : Allometric coefficient

Limitations of this method include difficulty in measuring BSA due to the complexity of the equation and uncertainty in accuracy. Mostly, the pharmacokinetic profile across all children does not change in relation to body surface area. BSA is not a descriptor of metabolic function (247).

### 2.1.10.5 Fixed exponent allometry

Evidence from allometric scaling has shown that this technique is more reliable in determining first time dosing in children compared to the dose normalisation method,

age specific dosing, body surface area method and to dose determination based on empirical clinical experience (250).

Pharmacokinetics of children are also determined using fixed exponent allometry, where fixed exponent values of 0.75 (3/4) or 0.67 (2/3) are used for maintenance dose determination in children. However, use of fixed exponents such as 0.75 for clearance and 1 for volume of distribution are similar to a size scaling method such as dose normalization by body weight and by surface area (246).

There is conflicting evidence on the use of fixed exponents for dose determination (179, 207, 208, 232, 246, 255-258). Body size may not be a surrogate for physiological change or growth development, hence it is unable to assume a linear relationship between body size and drug response, which is contrary to the principle used in the size scaling methods described above (246).

Hence allometric scaling based on physiological function (interspecies allometric scaling) is discussed further as an improved method in dose prediction for children.

### 2.1.10.6 Variable exponent allometry

Allometric scaling of a drug based on available pharmacokinetic data allows determination of drug specific allometric exponent. Pharmacokinetic parameters such as clearance and volume of distribution of mammals are plotted against the body weights of the species in a log-log scale to obtain the drug specific allometric exponent. In here, body weights of the mammalian species are considered as a surrogate of their physiological function. Hence pharmacokinetic parameters are scaled against the physiological function of the species. The rationale for this is similar to rationale of assessing pharmacokinetic in obese patients and hepatic impairment (246).

Variable exponent allometry allows, utilization of all available pharmacokinetics of drugs in preclinical and human species to derive exponents and therefore drug doses are determined based on best available pharmacokinetic information (259). Pharmacokinetics of drugs could vary in mammals due to their different physicochemical properties and therefore it is likely that drug specific allometric exponents exist.

In the development of variable exponents, it is also important to consider apparent physiological changes, for example if there are clear changes in pharmacokinetics due to the disease state, scaling need to be done using diseased mammals. In extreme age groups such as in neonates and children less than 2 years where there are clear differences in body physiology, body weight might not be a surrogate for physiological function needing to exclude this group.

### 2.1.11 Current evidence for the need of antimalarials dose optimisation in children

The current pharmacokinetic literature proposes a need for revision of drug doses in children with malaria. The evidence recommends an increase in drug doses for most drugs.

A pharmacokinetic study of sulfadoxine-pyrimethamine in 307 malaria infected children, found that dose adjusted area under the curve of sulfadoxine and pyrimethamine in children aged 2- 5 years was half than that of adult patients. The study concluded that current dosing of sulfadoxine and pyrimethamine needs to be revised to decrease treatment failure (168). Another study of chloroquine and sulfadoxine-pyrimethamine with two dosage regimens (low and high), found a strong relationship between high blood level and the cure rate in children (169). A pharmacokinetic study of 102 malaria infected children used three times higher dose of chloroquine than the current recommendation. This regimen proved to be of improved efficacy (170). Price, Hasugian (81) in a study of dihydroartemisinin-piperaquine (2.2 and 18mg/kg) for the treatment of children with uncomplicated malaria, found 38% of the children to have below 30 ng/mL day 7 piperaquine blood levels (Day 7 piperaquine level < 30 ng/mL is used as a surrogate marker for occurrence of recurrent malaria). The authors stated that the currently recommended dose of piperaquine is suboptimal. Two subsequent studies of piperaquine have endorsed the same observations indicating the need for dose revision (88, 173).

A population pharmacokinetic study of 70 children (6 months -11 years) with severe malaria on IM artesunate (2.5mg/kg 0, 12 and 24 hours) found lower blood levels of artesunate and metabolite dihydroartemisinin suggesting the need for dose changes in

children (171). Addition of a loading dose of quinine was also recommended for children (172).

## 2.2 Rationale for allometric scaling

It has been clearly recognised that pharmacokinetic properties of a drug could vary across different age groups (neonates, children, adult and the elderly) due to the differences in body composition, liver function, maturation of enzymes, kidney function, age and gender (246, 258). Recognising the need of paediatric exclusive dosing, the first British National Formulary (BNF) for children was introduced as a joint publication of the British Medical Association, the Royal Pharmaceutical Society, the Royal College of Paediatrics and Child Health, and the Neonatal and Paediatric Pharmacists Group in 2005 (260).

However, there is paucity in dose finding studies conducted in children compared to adults. In the past such studies were not warranted and considered ethically unsound due to the need for frequent blood samples of substantial volume for accurate determination of pharmacokinetic parameters. Today with the advancement of sensitive analytical techniques and availability of non-invasive assay techniques, pharmacokinetics studies in children are more feasible. However, such studies are not given priority in the pharmaceutical industry due to little financial gain from funding dose optimization studies in children once the drug has obtained market approval for adult usage (261, 262).

Hence current dosage regimens for children are mostly based on the prior pharmacokinetic information available from the adult population (263). However, it is challenging to determine how best available pharmacokinetic information can be utilized to determine the dosage regimens for children.

The most commonly adopted method of dosing is the weight based mg/kg adult dosing considering the linear relationship between body weight and dose for adults and children. Children's formularies also recommend doses based on paediatric age groups, weight bands and body surface area (246, 249). Apart from these methods, empirically based paediatric dosing recommendations are also available based on clinical

experience and off label use (246, 251). Out of these techniques, WHO and other pharmacopoeial sources recommend mg/kg adult antimalarials drug doses/linear dosing for children. Artemether and lumefantrine are exceptions, where dosing is based on predefined weight bands (3). However linear dosing could lead to under dosing of children and sub therapeutic dosing in antimicrobial chemotherapy which could lead to treatment failure and drug resistance in the long run (246, 249, 250, 255). There are clinical reports supporting this and recommending higher drug doses for sulphadoxine and pyrimethamine, chloroquine, dihydroartemisinin and piperaquine, artesunate and quinine for adequate malarial therapy (81, 88, 168-173).Therefore, it is necessary to revised drug dosage regimens to deliver the optimum drug therapy for children.

Allometry was traditionally used for first time dose determination in humans using preclinical pharmacokinetics data and also for dose extrapolations for new animal species in veterinary science (174-177). However there is a growing interest in using allometric scaling for paediatric dose determination (178-180). The allometric scaling relationship for chloroquine has been established where increase in chloroquine doses are recommended (25 mg/kg adult doses to 30 and 35 mg/kg for 10 and 20 kg body weights) (264).

Further evaluation of allometric scaling in other antimalarial drugs would help establish the validity of the technique for antimalarial dose determination in children and could be used to determine first time doses for newly discovered antimalarial drugs. Pharmacokinetic literature for antimalarial drugs in malaria infected children are available for some drugs. This enable compare the validity of allometrically predicted pharmacokinetic parameters to that of observed pharmacokinetic parameter values in clinical studies, given that there is no difference in pharmacokinetic parameters in the malaria infected state compared to the healthy state.

In this context, it is aimed to adopt interspecies allometric scaling technique to interpolate pharmacokinetic parameters for children. Drug specific allometric exponents derived will be used to scale adult doses to determine optimum drug doses for children. Therefore the specific objectives for this part of the study are

## 2.3 Specific objectives

- To investigate an allometric scaling relationship of anti-malarial drugs using published/ available pharmacokinetic data of healthy and malaria infected mammalian species
- To predict paediatric antimalarial drug doses for children above 2 years using interspecies allometric scaling technique

## 2.4 Methods

### 2.4.1 Data collection

Antimalarials used in the treatment of malaria were identified using WHO treatment guidelines (3). The initial list comprised of artemisinin, artesunate, artemether, dihydroartemisinin, mefloquine, amodiaquine, piperaquine, chloroquine, quinine, primaquine, lumefantrine, sulfadoxine-pyrimethamine, atovaquone, proguanil, tetracycline, doxycycline and clindamycin. Of these, tetracycline, and doxycycline were excluded as they were contraindicated in children. Allometric relationship for chloroquine was already established and therefore it was not included in the present study (264).

A comprehensive literature search of pharmacokinetic parameters for other selected drugs was done using key words: pharmacokinetics, disposition, pharmacokinetic parameters, specific antimalarials and mammalian species. Data base searches were done on PubMed, OvidSP, Google Scholar and citation records. Cross referencing of the articles was done to identify missing references.

Data on species, age, sex, weight, ethnicity, assay techniques, sampling duration, sample matrix, routes of drug administration, doses administered, dosage regimen, other drugs administered, pharmacokinetic modelling techniques, healthy and malaria infected status and pharmacokinetic parameters for each drug were recorded.

After compilation, data were screened for validity of pharmacokinetic parameters and study robustness. Criteria were set for the suitability of the data when screening pharmacokinetic studies. The data were screened for uniformity of biological matrix and data from a specific matrix were used for each drug. For example, quinine data generated from plasma were selected for the study and whole blood studies were excluded. A blood/plasma sample collection period of more than 3 times the half-life was preferred. Drug administered following the IV route is preferred in allometric scaling. However some antimalarials are administered only following oral routes, therefore such routes were considered more appropriate for those drugs. In instances where bioavailability of a drug was published, true or apparent clearance of the drug was calculated as required.

The drugs with pharmacokinetic data available for less than three mammalian species (amodiaquine, lumefantrine) and Fixed Dose Combinations (FDCs): (sulfadoxine-

pyrimethamine, artemether-lumefantrine, atovaquone-proguanil) were also excluded, as data for individual drugs were not readily available.

The final list of drugs (and routes of administration) was: artesunate (IV), and the active metabolite, dihydroartemisinin (IV), artemether (IV and IM), artemisinin (IV, intraperitoneal and oral), clindamycin (IV), piperaquine (oral), mefloquine (oral), quinine (IV).

Studies that met the selection criteria were screened for extraction of pharmacokinetic parameters; CL, Vz and half-life. A summary of pharmacokinetic parameter details of artemisinin, artesunate, dihydroartemisinin, artemether, clindamycin, piperaquine, mefloquine and quinine were tabulated.

### 2.4.2 Pharmacokinetic parameters

Clearance (CL), volume of distribution ($V_z$) and half-life ($t_{½}$) data were collected or calculated from the available data using the model-independent equations given below.

$$CL = k \times V_z \quad (23)$$

$$V_z = CL \div k \quad (24)$$

k : Elimination rate constant

Pharmacokinetic parameters mean resident time and $V_{ss}$ were reported in a limited range of studies and therefore not used for scaling purposes. The scaling for volume of distribution was done using $V_z$, however in instances where $V_z$ was not available $V_{ss}$ was used for the analysis.

In human studies where body weight was not reported, 60 kg was used for Asian and African subjects, whereas 70 kg was used for Caucasian subjects. The body weight of animals was not provided in a few animal studies, hence published standard body weights of the respective species were used for the allometric scaling (175, 184, 265, 266).

In human studies where different doses were administered to the same subjects and there was no evidence of dose-dependent variability, the mean value of the pharmacokinetic parameter was used. However, if separate groups were given different doses within a study, the data were treated independently.

In animal studies where different doses were administered to different groups of animals within the same study, each group was considered independently.

### 2.4.3 Interpolation of pharmacokinetics parameters for children

Simple allometry was used as the principal method for interspecies scaling and the equation given below was used to establish the allometric relationship (182, 256, 267).

$$Y = a \times W^b \quad (1)$$

Y : Pharmacokinetic parameter, CL, $V_z$ and $t_{1/2}$
W : Body weight of the species,
a : Allometric coefficient
b : Allometric exponent

The pharmacokinetic parameter data were plotted against body weight on a log-log scale (SigmaPlot version 12.5; Systat Software, Inc., Chicago, IL) to determine the allometric coefficient and exponent by regression analysis.

Pharmacokinetic parameters generated from both pre-clinical and human species were utilized for scaling purposes. Ideally, it was aimed to scale pharmacokinetic parameters of malaria infected species. However, only a limited number of pharmacokinetic studies were available on malaria infected non-human species. Hence data from healthy control subjects were used for the allometric scaling and this was considered appropriate when malaria infection has not altered the pharmacokinetic behaviour of the drug. In order to determine this, drug clearance parameters from human (adult) studies of malaria infection were compared to the healthy control data, as a guide to the application of allometric interpolation to decisions on paediatric doses.

### 2.4.4 Application of correction factors

There are many correction factors reported in the literature to improve simple allometric scaling prediction and the physiological relevance and application of some methods was not applicable in the present study (174, 176, 182, 184, 188, 211). It was also not practical to carry out all the correction methods as some of them were unable to be implemented due to lack of required data. For example, given that selected antimalarials

are cleared mainly following hepatic metabolism, *in-vitro* metabolic data would have been a good correction factor to trial. However this information was not available for most of the study drugs. Out of the feasible methods, MLP correction was considered appropriate and was selected to evaluate allometric prediction for low extraction ratio drugs (184).

In addition, it was hypothesised that liver weight and liver blood corrections could improve clearance prediction of these drugs as selected antimalarials are cleared through the hepatic metabolism.

MLP, liver weight and liver blood flow corrections were applied to clearance prediction of the antimalarials as clearance was the most relevant pharmacokinetic parameter for maintenance dose determination.

### 2.4.5 Maximum life-span potential (MLP) correction

The MLP correction was also an essential part of the 'Rule of Exponents' approach (174, 211). Based on the Rule of Exponents, simple allometry is the best predictor for exponents in the range 0.50-0.77, whereas clearance × MLP provides the best prediction method when the exponent from simple allometry is in the range of 0.71-0.99 and clearance × brain weight provides the best prediction, when simple allometry prediction is greater than 1 (211). As the clearance exponent from simple allometry was less than 1 for all antimalarial drugs, MLP correction was adopted and the brain weight correction was not implemented.

The maximum life-span potential (MLP) was calculated from the equation given below (184):

$$MLP = 10.839 \times (BW)^{0.636} \times (W)^{-0.225} \quad (25)$$

MLP : Maximum life-span potential (years)
BW : Brain weight (grams)
W : Body weight (grams)

Brain and body weight data for mammalian species were obtained from the literature (184, 265, 268). The age-specific data for 15 kg and 25 kg children (approximately 4

and 8 years of age) were calculated based on the equation provided by Haddad and colleagues (268). The brain weights for children were determined using the average for male and female brain weights calculated based on child age (a') using the equation below (268). The calculated brain weight and body weights were used to determine the MLP values for children.

$$\text{Male BW} = 10^4[(a'+0.213)/(6.030+6.895a')] \quad (26)$$

$$\text{Female BW} = 10^4[(a'+0.226)/(6.521+7.514a')] \quad (27)$$

BW : Brain weight (grams)
a' : Age (years)

The total clearance × MLP data were plotted against body weight on a log-log scale (SigmaPlot) to determine the MLP corrected coefficient ($a^*$) and exponent ($b^*$) by regression analysis. The predicted clearance values were determined as per the equation below.

$$CL \times MLP = a^* \times W^{b^*} \quad (28)$$

CL : Clearance (L/h)
MLP : Maximum life span potential (years)
$a^*$ : MLP corrected coefficient
W : Body weight (kg)
$b^*$ : MLP corrected exponent

### 2.4.6 Liver weight and liver blood flow correction

The antimalarials used in the allometric scaling are mainly excreted following liver metabolism. Ritschel and co-workers (269) found a strong relationship between clearance of coumarin (high extraction ratio) with liver blood flow, liver weight and body weight among 6 mammalian species. Clearance of a drug with a high liver extraction ratio could relate to species liver blood flow, whereas clearance of a drug with a low hepatic extraction ratio could relate to the intrinsic clearance or *in-vivo* enzyme activity (relative abundance of microsomal enzymes), therefore to the liver size of the mammalian species (123, 188, 189). Hence liver weights and liver blood flow of different preclinical species and humans were used to correct the clearance values. The

liver weights for different species were determined as a percentage of the body weight (197). Liver weight (calculated as a percentage of the body weight) and liver blood flow of different mammals given in Table 2.3 were used for analysis.

**Table 2-3**: Liver weight and liver blood flow as a percentage of total body weight (197)

| Animal species | Liver weight (% of body weight) | Liver blood flow (L/min) |
|---|---|---|
| Mouse | 5.06 | 0.00262 |
| Rat | 4.04 | 0.0172 |
| Rabbit | 4.78 | 0.122 |
| Dog | 2.91 | 0.676 |
| Pig | 1.97 | 3.36 |
| Human | 2.42 | 1.78 |

The total clearance × liver weight and total clearance × liver blood flow values were plotted against the species body weight in a log-log scale (SigmaPlot). The corrected allometric coefficient and exponents were used for determination of the drug clearance in humans.

$$CL \times LW = a^{**} \, W^{b^{**}} \quad (29)$$

CL : Clearance (L/h)
LW : Liver weight (grams)
W : Body weight (kg)
$a^{**}$ : Liver weight corrected coefficient
$b^{**}$ : Liver weight corrected exponent

Liver weight for male and female children were calculated based on child age (a) according to the equations provided in Haddad (268).

$$\text{Male LW(g)} = 0.0072a'^{5} - 0.3975a'^{4} + 7.9052a^{3} - 65.627a'^{2} + 262.02a' + 157.52 \quad (29)$$

$$\text{Female LW(g)} = 0.0057a'^{5} - 0.3396a'^{4} + 7.0134a'^{3} - 59.539a'^{2} + 251.9a' + 139.65 \quad (30)$$

| | | |
|---|---|---|
| LW | : | Liver weight (grams) |
| a' | : | Age (years) |

The liver weights for children (as calculated above), $a^{**}$ and $b^{**}$ were used for prediction of drug clearance using liver weight correction.

Liver blood flow of the children was considered as 1.78 L/min (197) and, similarly to the liver weight method clearance × liver blood flow, was plotted to obtain the coefficient ($a^{***}$) and exponent ($b^{***}$) values. These values and liver blood flow were then used to interpolate drug clearance for children.

$$CL \times LBF = a^{***} W^{b^{***}} \quad (31)$$

| | | |
|---|---|---|
| CL | : | Clearance (L/h) |
| LBF | : | Liver blood flow (L/min) |
| W | : | Body weight (kg) |
| $a^{***}$ | : | Liver blood flow corrected coefficient |
| $b^{***}$ | : | Liver blood flow corrected exponent |

### 2.4.7 Interpolation of drug clearance

Drug clearance was interpolated using simple allometry and the three correction methods and compared with observed clearance in clinical studies of children. The average body weight provided in the clinical study was used as the body weight and allometric exponents and coefficient for the four techniques were applied to the allometric power equation described in sections 2.4.5 and 2.4.6 to obtain interpolated drug clearance.

### 2.4.8 Predictive success

The observed drug clearance in clinical studies was divided by the interpolated drug clearance to determine the predictive success of clearance for the simple allometry and correction methods. The ratio of observed drug clearance to predicted drug clearance in the range of 0.5 to 2 (2 fold) has been suggested as an acceptable difference in predicted drug clearance (233, 270-272).

### 2.4.9 Interpolation of paediatric doses

A standard allometric model for interpolation of paediatric dosing is to use the equation below:

$$Dose_{CHILD} = Dose_{ADULT} \times \left( \frac{Weight_{CHILD}}{Weight_{ADULT}} \right)^{b} \quad (32)$$

| | | |
|---|---|---|
| $Dose_{CHILD}$ | : | Total dose for a child at the specified weight |
| $Weight_{CHILD}$ | : | Weight of the child |
| $Dose_{ADULT}$ | : | Standard total dose for an adult at the specified weight |
| $Weight_{ADULT}$ | : | Weight of the adult |
| b | : | Drug specific allometric exponent |

The derived exponent (b) by allometric scaling was applied to the equation above to predict doses for children. These calculated doses were then compared to pharmacopoeial or reference doses for arbitrary weights of 15 kg and 25 kg. Dose estimates for children less than 2 years were not considered, due to the known physiological and pharmacokinetic differences between very young infants and adults (207, 208, 246).

### 2.4.10 Extrapolation of human pharmacokinetic parameters

It is argued in the literature that conventional allometry works for some, but not all drugs (230).

In order to explore that, the allometric relationship between drug clearance of preclinical species and their body weight was established. The exponents and coefficients were

used to extrapolate drug clearance for healthy adults. The extrapolated clearance values of humans were compared to observed values in clinical studies to determine how well conventional allometry works for scaled antimalarial drugs.

### 2.4.11 Statistical analyses

Data analysis was done using SigmaPlot version 12.5 (Systat Software, Inc., Chicago, IL). Data were presented as mean ± standard deviation (SD) unless otherwise indicated. The 95% confidence interval (CI) was determined for the allometric exponent (95% CI = mean ± 1.96 × standard error). The Students *t*-test was used for two-sample comparison as appropriate, with a significance level of $P < 0.05$.

## 2.5 Results

### 2.5.1 Published pharmacokinetic parameters for antimalarials

Pharmacokinetic parameters from selected studies were used for the allometric scaling of pharmacokinetic parameters of each drug. It was not possible to scale pharmacokinetics for malaria infected species due to lack of availability of pharmacokinetic studies in malaria infected mammalian species (<3 species) and therefore allometric scaling for drug clearance, volume of distribution and half-life were determined for healthy species.

Artesunate pharmacokinetics were available following IV, IM, Intra peritoneal (IP), intra gastric and oral routes of drug administration to animals and IV, IM and oral drug administration to the healthy and malaria infected humans. Pharmacokinetic parameters for allometric scaling of dihydroartemisinin were based on pharmacokinetic studies of IV artesunate (the pro-drug of dihydroartemisinin) (Figure 2.1-2.6). Similar to artesunate analysis, pharmacokinetic parameters established following extra-vascular administrations of dihydroartemisinin were not utilized for allometric scaling.

Artemether is soluble in organic solvents and available in dosage forms suitable to be administered by IM, IV and oral routes of administration. Pharmacokinetic parameters following IM, IV and oral routes of administrations were available in the published literature. Artemether scaling was done using IM pharmacokinetic data alone and incorporating IV and IM data.

It was not possible to carry out scaling for artemisinin following a single route of administration. The animal pharmacokinetic data for this drug were available following IP and IV routes and human data were available following the oral route. Artemisinin has a low solubility and lacks a suitable solvent for parenteral dose formulation; hence pharmacokinetic studies for IV administration of artemisinin were absent. The apparent oral clearance was corrected using the oral/IM relative bioavailability value of 0.32 (28) and used for allometric scaling purposes. Further analysis of artemisinin was not done due to mixed routes of administration.

Pharmacokinetic parameters for clindamycin were available following IV, IM, subcutaneous (SC) and oral routes of administration in animals and oral and IV

administration in humans. Pharmacokinetic parameters following IV administration were used for allometric scaling purposes.

Mefloquine and piperaquine are drugs administered only through the oral route, hence allometric scaling was done using CL/F and $V_z$/F data resulting from oral drug administration. The exponents derived using apparent data were considered appropriate for prediction of oral doses.

Pharmacokinetic data for quinine was available following IV, IP, intraduodenal and oral routes of administration in animals and IV, IM, IP and oral routes of administration in humans. Allometric scaling of quinine was done using pharmacokinetic parameters following IV data.

### 2.5.2 Interspecies allometric scaling for clearance, volume of distribution and half-life of antimalarials

The pharmacokinetic parameters for healthy preclinical animal species and humans used for allometric scaling were obtained from studies that met the selection criteria. Allometric relationships for clearance, volume of distribution and half-life of dihydroartemisinin using healthy species are provided in Figures 2.1, 2.3 and 2.5. Pharmacokinetic parameters of dihydroartemisinin in malaria infected children and adults were overlaid on the regression analysis established using healthy species in Figures 2.2, 2.4 and 2.6

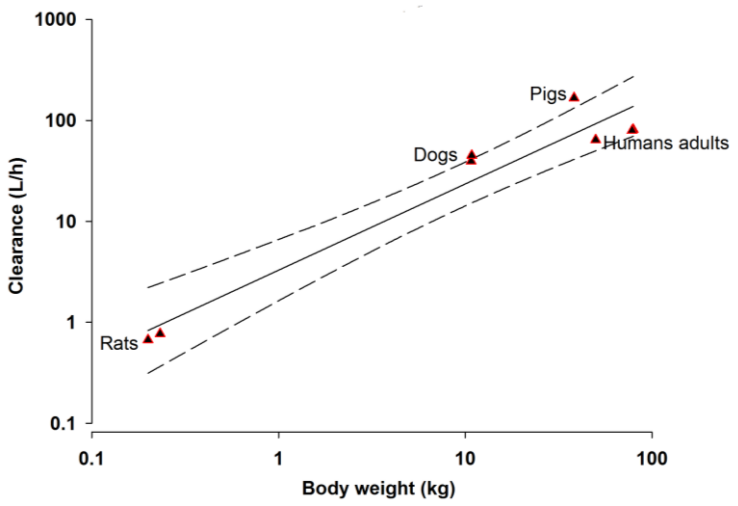


**Figure 2-1**: Dihydroartemisinin: allometric scaling relationship (regression line and 95% CI) for clearance in healthy species (from IV artesunate data)

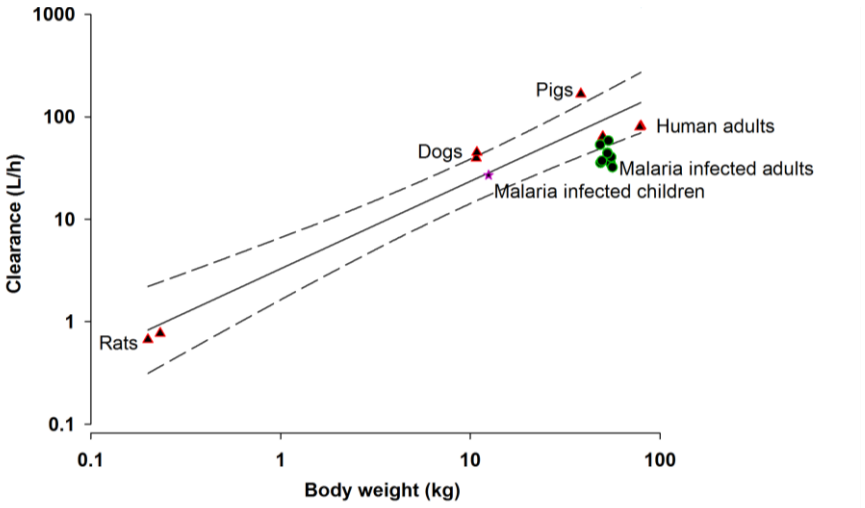


**Figure 2-2**: Dihydroartemisinin: allometric scaling relationship (regression line and 95% CI) for clearance in healthy species (▲). Drug clearance in malaria infected adult (●) and children (★) are plotted for comparison (from IV artesunate data)

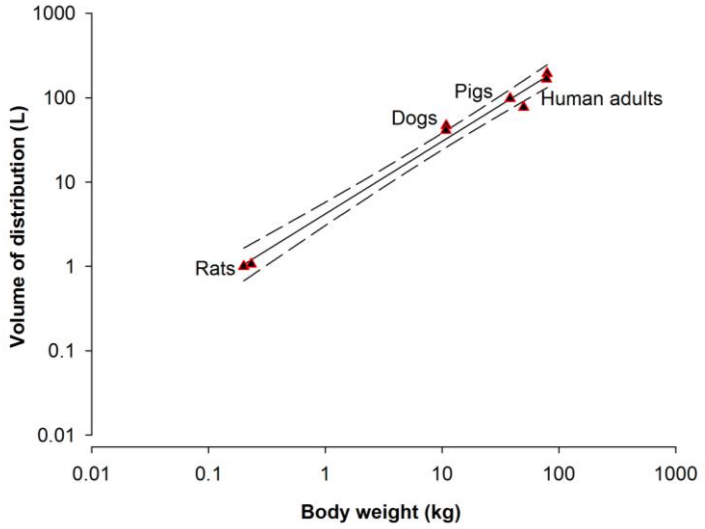


**Figure 2-3**: Dihydroartemisinin: allometric scaling relationship (regression line and 95% CI) for volume of distribution in healthy species (from IV artesunate data)

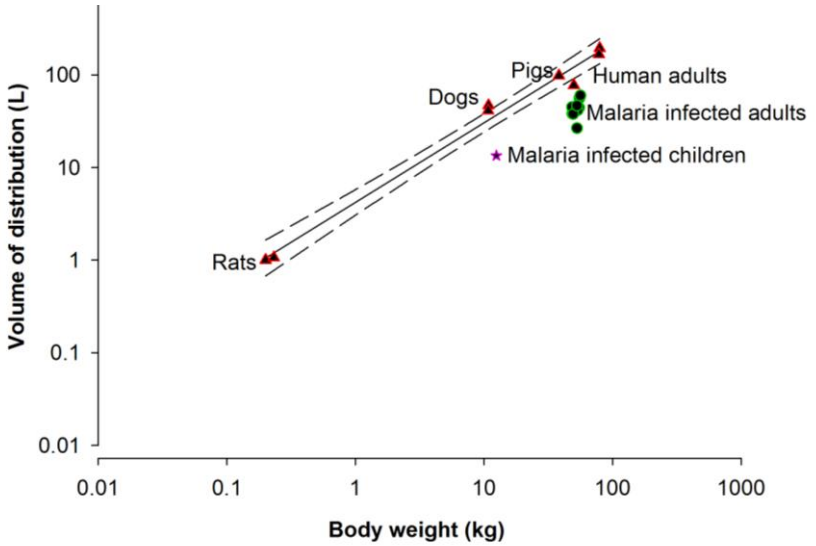


**Figure 2-4**: Dihydroartemisinin: allometric scaling relationship (regression line and 95% CI) for volume of distribution in healthy species **(▲).** Drug volume of distribution in malaria infected adult (●) and children (★) are plotted for comparison (from IV artesunate data)

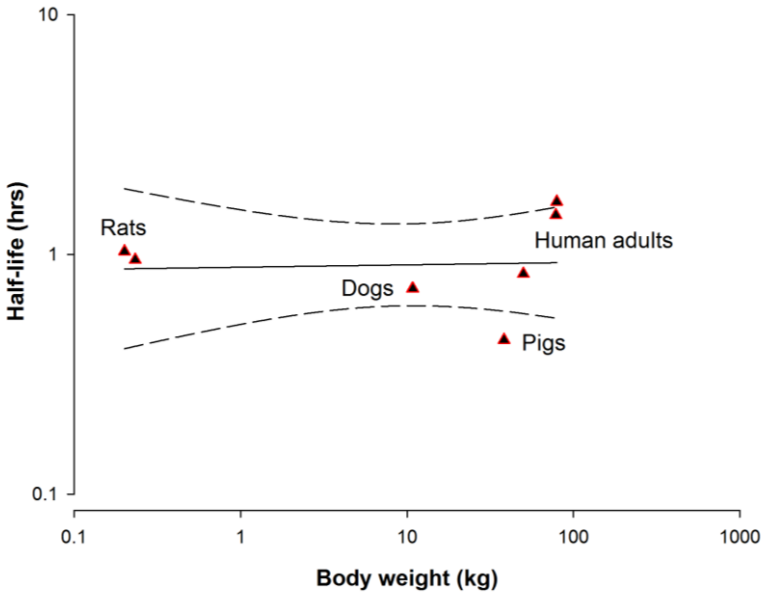


**Figure 2-5**: Dihydroartemisinin: allometric scaling relationship (the regression line and 95%CI) for half-life in healthy species (from IV artesunate data)

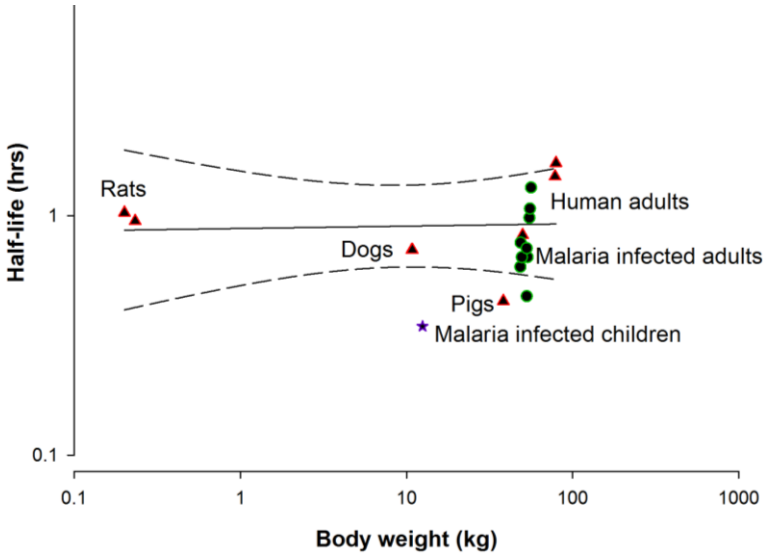


**Figure 2-6**: Dihydroartemisinin: allometric scaling relationship (regression line and 95% CI) for half-life in healthy species (▲). Drug half-life in malaria infected adult (●) and children (★) are plotted for comparison (from IV artesunate data)

### 2.5.2.1 Simple allometry for clearance of drugs

Pharmacokinetic studies in preclinical species were limited and only 2-3 pre-clinical species clearance data were available to be included in the scaling. Interestingly for all drugs, a pharmacokinetic study conducted in rats was available. Pharmacokinetic studies in large mammals were not available for any of the drugs.

The regression analysis of allometric scaling of clearance showed strong $r^2$ value for all the drugs analysed and was ≥ 0.9. The allometric exponent and coefficient values for drug clearance are given in below Table 2.4. The allometric relationships for clearance were established based on healthy species clearance data and clearance of malaria infected adults, and children were overlaid on the same graph in Figures 2-7 to 2-13 for artesunate, artemisinin, artemether, clindamycin, piperaquine, mefloquine and quinine.

**Artesunate and dihydroartemisinin**

The allometric exponent for artesunate was found to be 0.71 and was equal to the universal exponent 0.75 (3/4) (Figure 2.7). The observed clearance of artesunate in malaria infected children found to be on the line of best fit of allometric scaling relationship established using healthy species. Hence interpolated clearance using healthy species would be similar to the observed clearance in malaria infected children. Drug clearances in malaria infected adults were within the 95% confidence interval of the simple allometric exponent line except for one study.

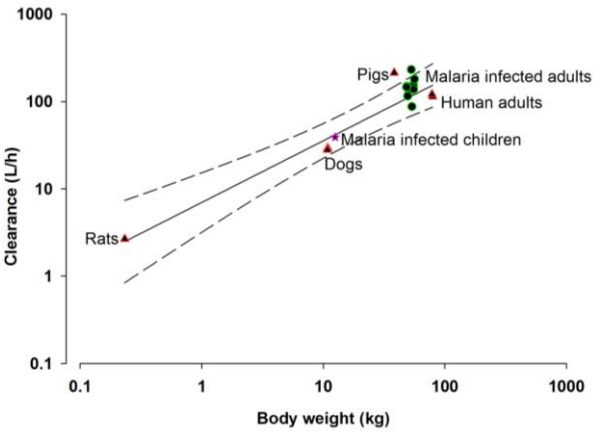


**Figure 2-7:** Artesunate: allometric scaling relationship (regression line and 95% CI) for clearance in healthy species (▲). Drug clearance in malaria infected adult (●) and children (★) are plotted for comparison (IV data)

Dihydroartemisinin exponent value was higher than artesunate and the 95% confidence interval (CI) did not encompass universal exponent of 0.67 (2/3). The observed dihydroartemisinin clearance values of malaria infected adult were found to be just below the predicted clearance and clearance reported in majority of the studies were outside the 95% CI of healthy species scaling. The dihydroartemisinin clearance observed in infected children was within the 95% CI (Figure 2.2).

**Artemisinin**

Artemisinin gave an exponent value of 0.83 when mixed clearance data following IV, IP and oral routes of administration were used (Figure 2.8). Further analysis of artemisinin was not conducted due to mixed route of administration. The observed apparent oral clearance in malaria infected children was higher than the interpolated clearance using healthy species.

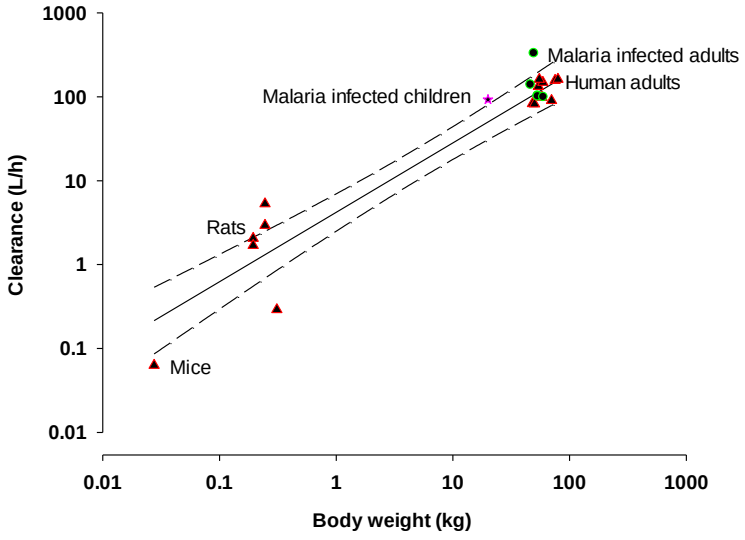


**Figure 2-8**: Artemisinin: Allometric scaling relationship (regression line and 95% CI) for clearance of in healthy species (▲). Drug clearance in malaria infected adult (●) and children (★) are plotted for comparison

## Artemether

The exponent value, 0.66, for artemether remained unchanged for scaling following IM data and IM and IV data together. Similar to artesunate and dihydroartemisinin, the interpolated drug clearance using healthy species data was similar to observed drug clearance of artemether in malaria infected children (Figure 2.9).

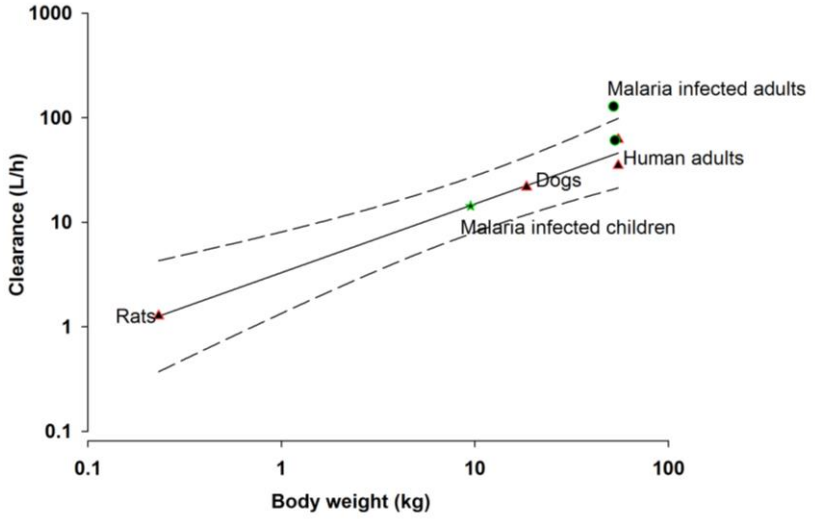


**Figure 2-9**: Artemether: allometric scaling relationship (regression line and 95% CI) for clearance in healthy species (▲). Drug clearance in malaria infected adult (●) and children (★) are plotted for comparison (IM data)

## Clindamycin

Clindamycin scaling gave an exponent value of 0.63, the narrow confidence interval did not encompass, universal exponent 0.75. The observed drug clearance of clindamycin in children (mean age of 24 weeks) was much lower compared to interpolated drug clearance, therefore was not used for the comparison of predicted verse observed drug clearance in children in Table 2.9. Clindamycin clearance in malaria infected adults were not available following IV route of drug administration for comparison (Figure 2.10).

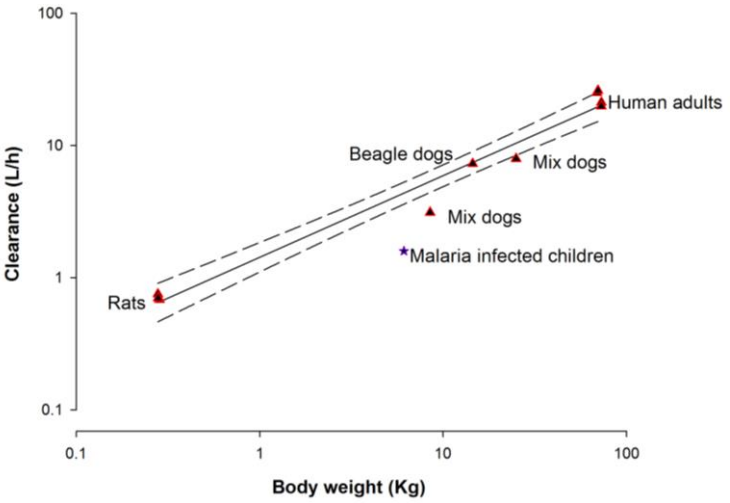


**Figure 2-10:** Clindamycin: allometric scaling relationship (regression line and 95% CI) for clearance in healthy species (▲). Drug clearance in malaria infected adult (●) and children (★) are plotted for comparison (IV data)

## Piperaquine

The piperaquine exponent value was 0.96 with a 95% CI interval encompassing 1; hence linear dosing for piperaquine could be supported. The observed drug clearance in malaria infected children and adults were within the 95% CI of the allometric relationship established using healthy species.

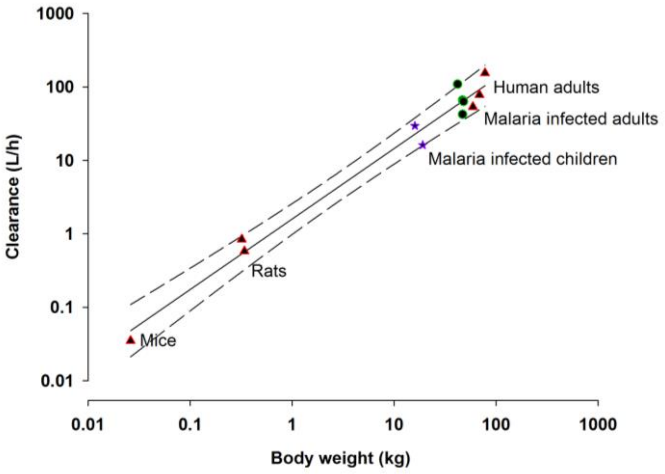


**Figure 2-11:** Piperaquine: allometric scaling relationship (regression line and 95% CI) for clearance in healthy species (▲). Drug clearance in malaria infected adult (●) and children (★) are plotted for comparison (oral data)

## Mefloquine

The exponent for mefloquine was low (0.52) and did not encompass the both universal exponent values of 0.67 and 0.75 for clearance. A small exponent value for mefloquine indicates the need of large increment in doses. The reported mefloquine clearance values in healthy human adults were wide spread. Mefloquine clearance in children were available in 5 studies, however 3 of those used whole blood as the assay matrix, hence was not included in the Figure 2.12 and Table 2.11. The observed clearance for children was below and outside the 95% CI the interpolated clearance for children, however in the 2 studies; mefloquine was administered along with sulphadoxine and pyrimethamine.

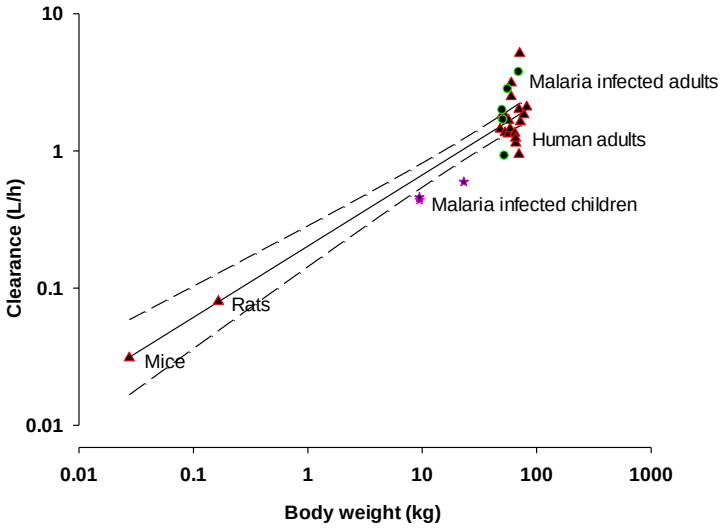


**Figure 2-12**: Mefloquine: allometric scaling relationship (regression line and 95% CI) for clearance of in healthy species (▲). Drug clearance in malaria infected adult (●) and children (★) are plotted for comparison (oral data)

## Quinine

Out of the antimalarials studies, quinine had the lowest exponent of 0.40, hence requiring large increase in doses for healthy children. Similar to mefloquine the fixed exponent allometry was not supported for quinine scaling. The 95% CI of quinine did

not encompass either of the fixed exponent values. The observed quinine clearance was clearly lower than the allometrically interpolated clearance using healthy species and this is also true for malaria infected adults (Figure 2.13).

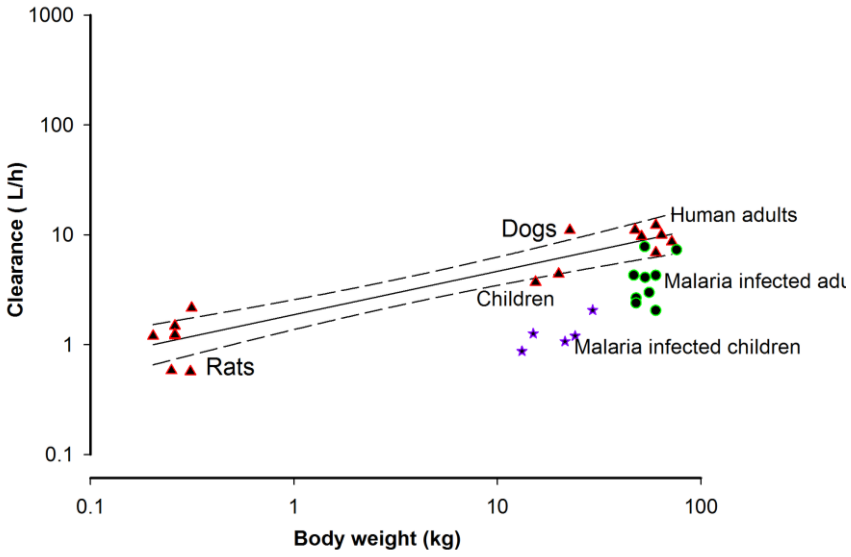


**Figure 2-13**: Quinine: allometric scaling relationship (regression line and 95% CI) for clearance of in healthy species (▲). Drug clearance in malaria infected adult (●) and children (★) are plotted for comparison (IV data)

Artesunate, artemether, artemisinin, clindamycin, mefloquine and quinine exponents indicate the absence of linear relationship between bodyweight and drug dose, therefore mg/kg dosing is not applicable fixed or universal exponent values were not supported by all the drugs.

**Table 2-4**: Simple allometric scaling data for clearance of antimalarial drugs

| Drug | Route of administration[a] | Number of species [b] | $r^2$ | Allometric exponent (95% CI) | Allometric coefficient | References |
|---|---|---|---|---|---|---|
| Artesunate | IV | 4 (r,d,p,h) | 0.92 | 0.71 (0.53-0.88) | 7.0 | (46, 55, 62, 167, 273, 274) |
| Dihydroartemisinin (from IV artesunate) | IV | 4 (r,d,p,h) | 0.94 | 0.85 (0.68-1.03) | 3.3 | (46, 55, 61, 62, 167, 273, 274) |
| Artemether | IM | 3 (r,d,h) | 0.98 | 0.66 (0.38-0.93) | 3.3 | (54, 55, 275, 276) |
| Artemether | IM or IV | 4 (r,rb,d,h) | 0.99 | 0.66 (0.56-0.75) | 3.3 | (54, 55, 275-277) |
| Artemisinin | IV, IP, Oral×F[c] | 3 (m,r,h) | 0.92 | 0.83 (0.69-0.96) | 4.2 | (28, 30, 32, 278-285) |
| Clindamycin | IV | 3 (d,r,h) | 0.98 | 0.62 (0.55-0.69) | 1.4 | (142, 286-290) |
| Piperaquine | Oral | 3 (m,r,h) | 0.99 | 0.96 (0.86-1.05) | 1.6 | (82, 83, 86, 90, 91, 291) |
| Mefloquine | Oral | 3 (m,r,h) | 0.90 | 0.52 (0.43-0.61) | 0.2 | (95, 99, 106, 109, 110, 292-304) |
| Quinine | IV | 3 (r,d,h) | 0.89 | 0.40 (0.33-0.47) | 1.9 | (116, 132, 133, 305-314) |

[a] Route of administration: IV: intravenous, IM: Intramuscular, IP: Intraperitoneal, [b] Species: m : mouse, r: rat, d: dog, p: pig, rb: rabbit, h: human [c] F: Relative bioavailability (oral/IM ) for artemisinin is 0.32 (28)

### 2.5.2.2 Simple allometry for volume of distribution of drugs

Similar to clearance data, allometric scaling of volume of distribution had a strong $r^2$ with the exception of artesunate ($r^2$ = 0.69). The $r^2$ and exponents for volume of distribution of antimalarials are given in the Table 2.5. The exponents for volume of distribution can be used for determination of loading doses of antimalarials. The allometric relationships for the volume of distribution were established based on healthy species volume of distribution data and volume of distribution of malaria infected adults, and children were overlaid on the same graph in Figures 2-14 to 2-19 for artesunate, artemether, clindamycin, piperaquine, mefloquine and quinine

**Artesunate and dihydroartemisinin**

Artesunate had comparatively lower exponent value of 0.54 volumes of distribution and wide CI (Figure 2.14). The low exponent value for artesunate could be due to the pro-drug nature of the drug. The volume of distribution of artesunate reported for malaria infected adults in the majority of the studies was lower and outside the 95% CI of the interpolated clearance using healthy species, so was for malaria infected children.

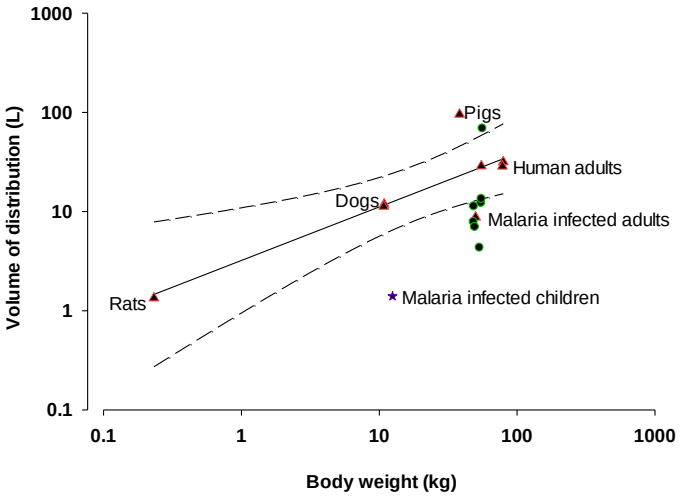


**Figure 2-14** : Artesunate: allometric scaling relationship (regression line and 95% CI) for volume of distribution in healthy species (▲). Drug volume of distribution in malaria infected adult (●) and children (★) are plotted for comparison (IV data)

Further analysis was limited to dihydroartemisinin; the active drug for artesunate. Dihydroartemisinin had an exponent value of 0.86 with a narrow confidence interval (Figure 2.4). Similar to artesunate, the observed volume of distribution values of dihydroartemisinin in malaria infected adults and children were much lower compared to the interpolated volume of distribution and not within the 95% CI of the allometric relationship established using healthy species.

**Artemether**

Artemether exponents are 0.93 (IM data) and 1.06 (IM and IV data). The narrow 95% CI includes 1, therefore linear dosing can be recommended for loading dose of artemether. The observed volume of distribution of adults were similar to the interpolated, however the infected children volume of distribution was outside the 95% CI and higher than interpolated volume of distribution (Figure 2.15).

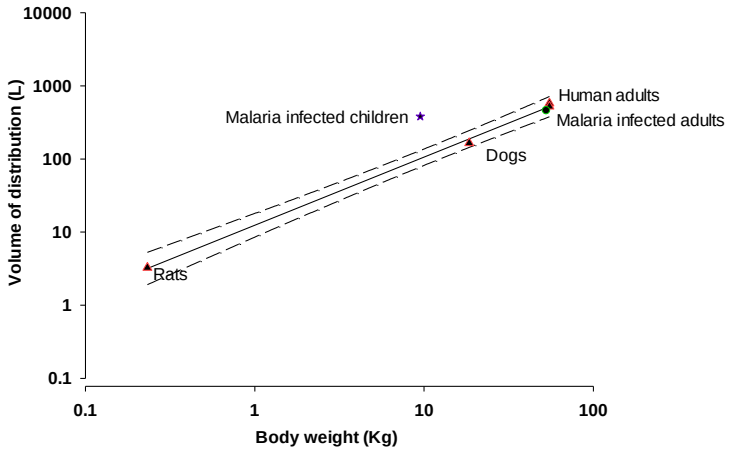


**Figure 2-15** : Artemether: Allometric scaling relationship (regression line and 95% CI) for volume of distribution in healthy species (▲). Drug volume of distribution in malaria infected adult (●) and children (★) are plotted for comparison (IM data)

**Clindamycin**

The exponent for volume of distribution is 0.81 with narrow 95% CI. Clindamycin volume of distribution in infected adults was not reported. The observed drug clearance

in malaria infected children (mean age 24 weeks) was slightly lower than the interpolated clearance and just outside the 95% CI (Figure 2.16).

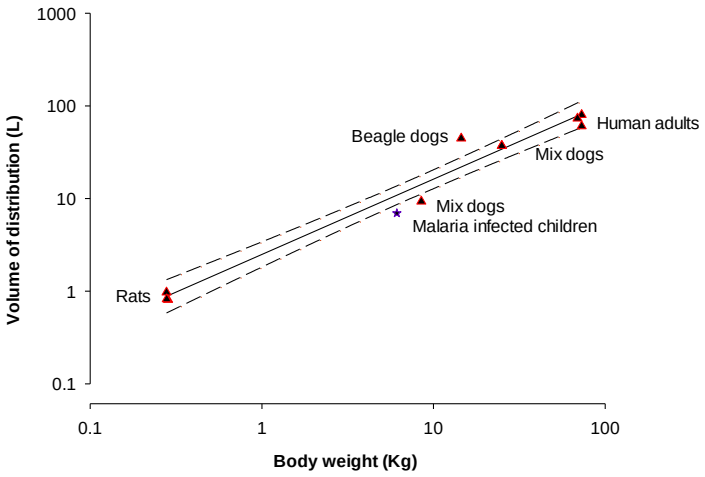


**Figure 2-16** : Clindamycin: allometric scaling relationship (regression line and 95% CI) for volume of distribution in healthy species (▲). Drug volume of distribution in malaria infected adult (●) and children (★) are plotted for comparison (IV data)

## Piperaquine

Piperaquine volume of distribution exponent was above 1 and has wide CIs. The observed volume of distribution of malaria infected adults and children were within the 95% CI of healthy species allometric relationship (Figure 2.17).

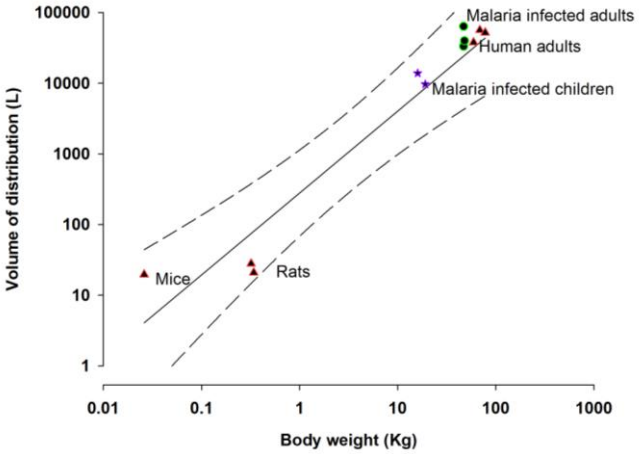


**Figure 2-17**: Piperaquine: allometric scaling relationship (regression line and 95% CI) for volume of distribution in healthy species (▲). Drug volume of distribution in malaria infected adult (●) and children (★) are plotted for comparison (oral data)

## Mefloquine

Mefloquine volume of distribution was reported in large number of heathy human adult studies narrowing the 95% CI at this end. The observed volume of distribution in infected adults and children are spread apart leaving some of the reported values outside the 95% CI of the allometric relationship established using healthy species (Figure 2.18).

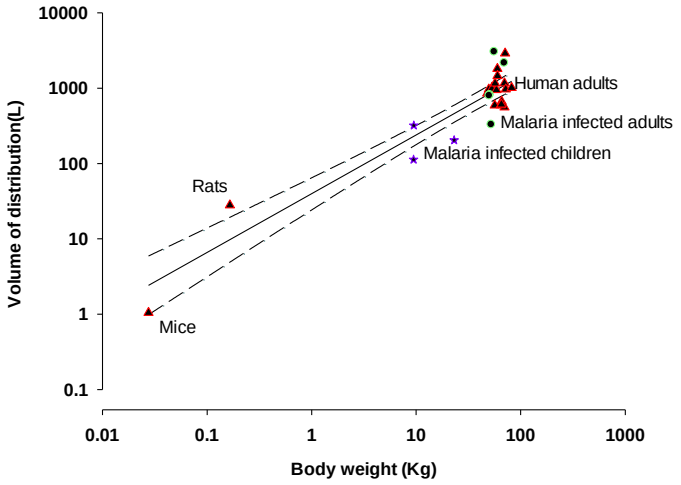


**Figure 2-18**: Mefloquine: allometric scaling relationship (regression line and 95% CI) for volume of distribution in healthy species (▲). Drug volume of distribution in malaria infected adult (●) and children (★) are plotted for comparison (oral data)

## Quinine

Quinine exponent was 0.88 and the 95 % CI enclosed 1, therefore quinine loading doses can be mg/kg adult doses for healthy humans. However the observed volume of distribution of malaria infected children and adults were much lower than the interpolated values using healthy species scaling and was outside the 95% CI, which indicate clear difference in volume of distribution of quinine in healthy species compared to malaria infected status (Figure 2.19).

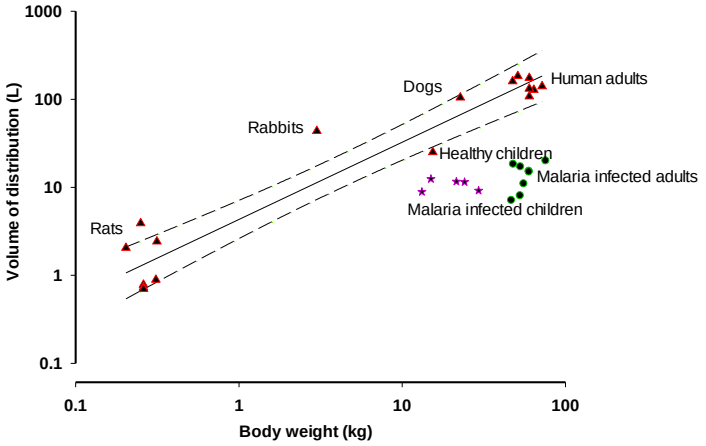


**Figure 2-19**: Quinine: allometric scaling relationship (regression line and 95% CI) for volume of distribution in healthy species (▲). Drug volume of distribution in malaria infected adult (●) and children (★) are plotted for comparison (IV data)

No further analysis of volume of distribution was done as loading doses are not recommended for adults with malaria infection for the drugs scaled, except for quinine in severe malaria (pharmacokinetic modelling studies have suggested loading dose of 20 mg/mg quinine, in a rate controlled slow infusion (twice the maintenance dose) .

**Table 2-5** : Simple allometric scaling data for volume of distribution ($V_z$) of antimalarial drugs

| Drug | Route of administration [a] | Number of species [b] | $r^2$ | Allometric exponent (95% CI) | Allometric coefficient | References |
|---|---|---|---|---|---|---|
| Artesunate | IV | 4 (r,d,p,h) | 0.69 | 0.54 (0.22-0.85) | 3.2 | (46, 55, 62, 167, 273, 274) |
| Dihydroartemisinin (from IV artesunate) | IV | 4 (r,d,p,h) | 0.99 | 0.86 (0.78-0.94) | 4.2 | (46, 55, 61, 62, 167, 273, 274) |
| Artemether | IM | 3 (r,d,h) | 0.99 | 0.93 (0.82-1.05) | 12.4 | (54, 55, 275, 315) |
| Artemether | IM or IV | 4 (r,rb,d,h) | 0.96 | 1.06 (0.75-1.38) | 6.7 | (54, 55, 275, 277, 315) |
| Clindamycin | IV | 3 (d,r,h) | 0.98 | 0.81 (0.72-0.91) | 2.5 | (139, 142, 286-290) |
| Piperaquine | Oral | 3 (m,r,h) | 0.94 | 1.16 (0.87-1.45) | 280 | (82, 91, 291) |
| Mefloquine | Oral | 3 (m,r,h) | 0.91 | 0.78 (0.66-0.90) | 39.8 | (95, 99, 106, 109, 110, 292-304) |
| Quinine | IV | 3 (r,d,h) | 0.92 | 0.88 (0.74-1.01) | 4.61 | (116, 132, 133, 305-314, 316) |

[a] Route of administration: IV: intravenous, IM: Intramuscular, [b] Species: m : mouse, r: rat, d: dog, p: pig, rb: rabbit, h: human

### 2.5.2.3 Simple allometry for half-life of drugs

Table 2.6 gives the allometric scaling relationship for half-life of antimalarials. As shown in the Table 2.6, half-life scaling did not provide strong $r^2$ for most of the drugs. The allometric relationships for half-life were established based on healthy species half-life data and half-life of malaria infected adults, and children were overlaid on the same graph in Figures 2-20 to 2-25 for artesunate, artemether, clindamycin, piperaquine, mefloquine and quinine.

**Artesunate and dihydroartemisinin**

The universal exponent value for half-life is 0.25 and artesunate and its active drug dihydroartemisinin exponent values for half-life deviated very much from the universal exponent value. The 95% CIs were wide for both artesunate and dihydroartemisinin scaling. Similar to volume of distribution, the observed artesunate half-life is below the 95% CI interval of healthy species scaling, except for one reported study (Figure 2.20). The observed half-life values of dihydroartemisinin in malaria infected adults spread widely however mostly within the 95% CI of the healthy species scaling due to the wide CI whereas observed half-life of infected children was not within the CI (Figure 2.6).

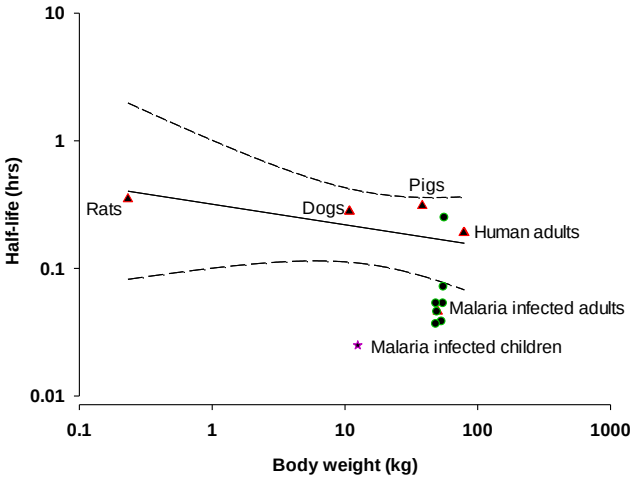


**Figure 2-20**: Artesunate: allometric scaling relationship (regression line and 95% CI) for half-life of in healthy species (▲). Drug half-life in malaria infected adult (●) and children (★) are plotted for comparison (IV data)

## Artemether

Artemether (IM dataa0 showed a good allometric relationship for half-life with an $r^2$ of 0.94. The exponent value for artemether changed slightly (0.28 to 0.35) when IV data was combined with IM data. The observed half-life for malaria infected children was outside the 95% CI of healthy species scaling (Figure 2.21).

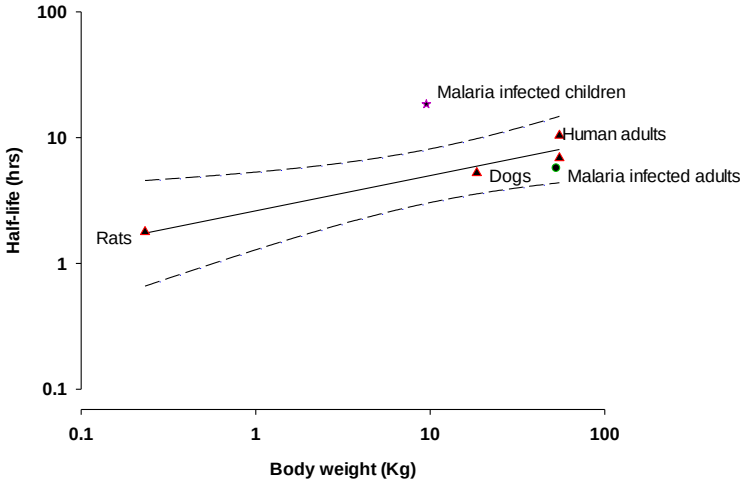


**Figure 2-21**: Artemether: allometric scaling relationship (regression line and 95% CI) for half-life of in healthy species (▲). Drug half-life in malaria infected adult (●) and children (★) are plotted for comparison (IM data)

## Clindamycin

Clindamycin half-life had a poor allometric relationship and exponent value was 0.17 with fairly wide 95% CIs. The observed half-life of the infected children (mean age 24 weeks) was outside the 95% CI of the healthy species scaling (Figure 2.22).

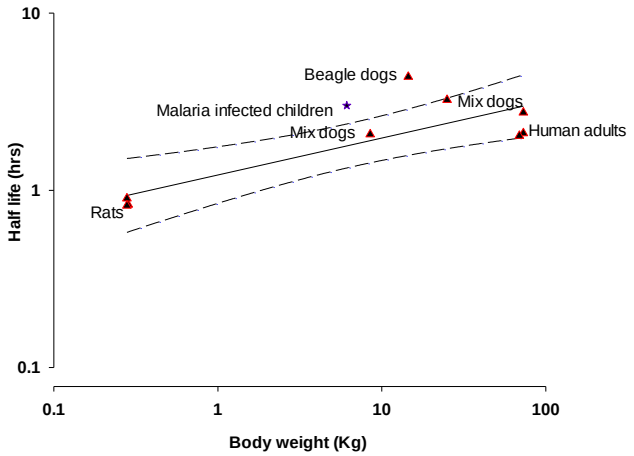


**Figure 2-22**: Clindamycin: allometric scaling relationship (regression line and 95% CI) for half-life of in healthy species (▲). Drug half-life in malaria infected adult (●) and children (★) are plotted for comparison (IV data)

## Piperaquine

Piperaquine gave a very low $r^2$ and wide 95% CI for allometric relationship of half-life. The exponent was 0.27 and close to the fixed exponent of half-life. The observed half-life of malaria infected adults and children were within the 95% CI of the healthy species (Figure 2.23).

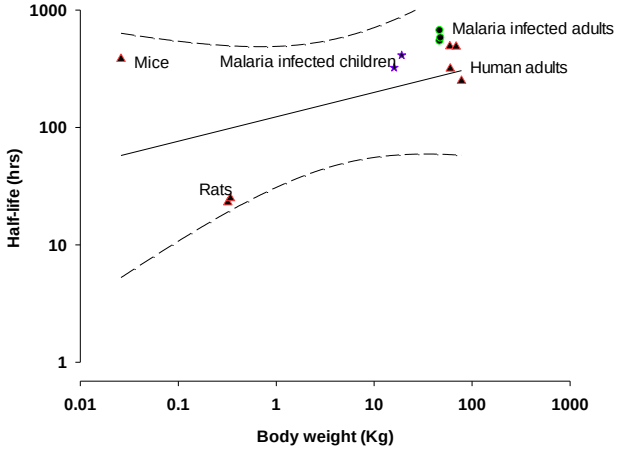


**Figure 2-23**: Piperaquine: allometric scaling relationship (regression line and 95% CI) for half-life in healthy species (▲). Drug half-life in malaria infected adult (●) and children (★) are plotted for comparison (oral data)

## Mefloquine

Mefloquine half-life exponent was similar to the fixed exponent value for half-life. The observed half-life values of the malaria infected children were much lower and outside the 95% CI of healthy species scaling (Figure 2.24).

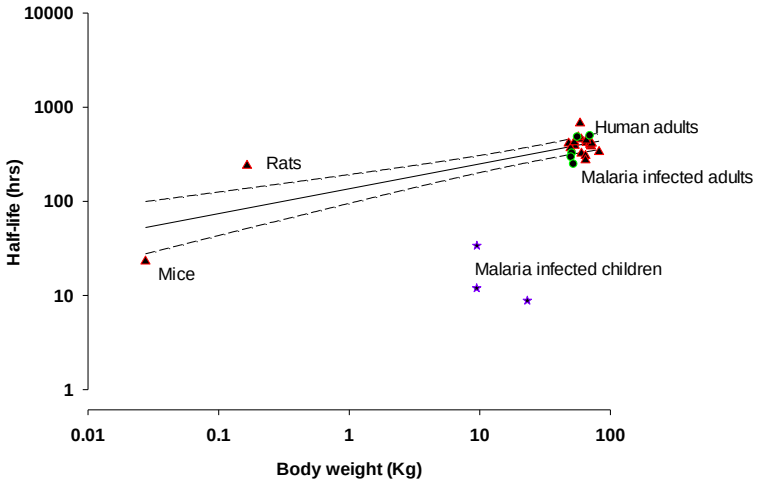


**Figure 2-24**: Mefloquine: allometric scaling relationship (regression line and 95% CI) for half-life of in healthy species (▲). Drug half-life in malaria infected adult (●) and children (★) are plotted for comparison (oral data)

## Quinine

The allometric relationship for half-life had a $r^2$ of 0.81 and the exponent was 0.35 with comparatively narrow 95% CI. The clearance and volume of distribution of quinine in malaria infected children was lower compared to the interplolated values using healthy species. The observed half life of the malarial infected children dependent on clearance and volume of distribution were higher than the interploated half-life using healthy species. Whereas observed half-life in malaria infected adults were moslty within the 95% CI of healthy species scaling (Figure 2.25).

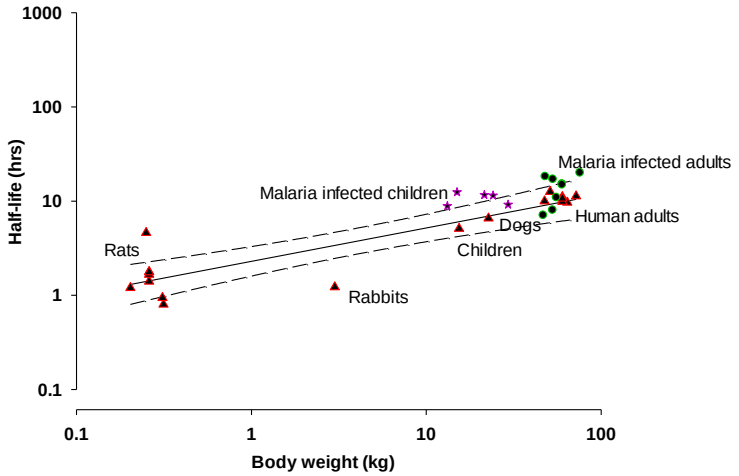


**Figure 2-25:** Quinine: allometric scaling relationship (regression line and 95% CI) for half-life of in healthy species (▲). Drug half-life in malaria infected adult (●) and children (★) are plotted for comparison (IV data)

Half-life is dependent on drug clearance and volume of distribution. Given the poor allometric relationship of half-life of most of the antimalarials studied, no further analysis of half-life was carried out.

**Table 2-6**: Simple allometric scaling data for half-life of antimalarial drugs

| Drug | Route of administration [a] | Number of species [b] | $r^2$ | Allometric exponent (95% CI) | Allometric coefficient | References |
|---|---|---|---|---|---|---|
| Artesunate | IV | 4 (r,d,p,h) | 0.23 | -0.16 (-0.50-0.18) | 0.32 | (46, 55, 62, 167, 273, 274) |
| Dihydroartemisinin (from IV artesunate) | IV | 4 (r,d,p,h) | 0.003 | 0.01 (-0.16-0.18) | 0.89 | (46, 55, 61, 62, 167, 273, 274) |
| Artemether | IM | 3 (r,d,h) | 0.94 | 0.28 (0.06-0.50) | 2.62 | (54, 55, 275, 315) |
| Artemether | IM or IV | 4 (r,rb,d,h) | 0.64 | 0.35 (-0.13-0.84) | 1.71 | (54, 55, 275, 277, 315) |
| Clindamycin | IV | 3 (d,r,h) | 0.46 | 0.17 (-0.04-0.39) | 1.38 | 121, 124, 242-244, 246, 271) |
| Piperaquine | Oral | 3 (m,r,h) | 0.27 | 0.21 (-0.19-0.60) | 123 | (82, 91, 291) |
| Mefloquine | Oral | 3 (m,r,h) | 0.70 | 0.26 (0.18-0.35) | 135 | (95, 99, 106, 109, 110, 292-304) |
| Quinine | IV | 3 (r,d,h) | 0.81 | 0.35 (0.26-0.45) | 2.31 | (116, 132, 133, 305-314, 316) |

[a] Route of administration: IV: Intravenous, IM: Intramuscular, [b] Species: m: mouse, r: rat, d: dog, p: pig, rb: rabbit, h: human

### 2.5.3 Comparison of pharmacokinetics in healthy and malaria infected adults

There is a paucity of pharmacokinetic studies in malaria infected mammals. Therefore it was not possible to establish an allometric scaling relationship for pharmacokinetic parameters using malaria infected species. In order to determine changes in pharmacokinetic profile during malaria infection, drug clearance in healthy adults and malaria infected patients were compared (Table 2.7). Quinine drug clearance in malaria infected adults was significantly lower compared to healthy adult clearance. Despite limited data, quinine showed a clear difference in drug clearance in malaria infection. Similar trends were observed for dihydroartemisinin, however the power of the test was low (0.56) and was below the desired value of 0.8, and therefore was unable to establish a definitive difference in clearance in malaria infection compared to the healthy status. Drug clearance for artesunate, artemether and mefloquine was not significantly different in malaria infection compared to healthy adults. However the power of the statistical tests was low and with high standard deviation, therefore similar to dihydroartemisinin it was difficult to be definitive.

It was not possible to determine the change in piperaquine clearance in malaria infection, due to the absence of clearance data in single therapy for malaria infected patients. No difference ($P = 0.24$) in clearance was found, following co-administration of piperaquine-dihydroartemisinin when compared with piperaquine single therapy in healthy adult (82, 90, 91, 317, 318). Therefore piperaquine studies for healthy volunteers included piperaquine single and piperaquine-dihydroartemisinin combination therapy data and piperaquine-dihydroartemisinin combination data for malaria infected adults. This comparison showed no difference in piperaquine clearance in healthy and malaria infected adults. Nevertheless allometric exponents and coefficients of healthy species were used for dose determination in malaria infection for dihydroartemisinin, artemether, mefloquine and piperaquine. It was not possible to compare clearance data for clindamycin in malaria infected and healthy status. Clindamycin clearance data were not available in infected adults. Clindamycin apparent clearance following oral administration of fosmidomycin and clindamycin was available; however it was unable to establish whether fosmidomycin would change the clearance profile of clindamycin.

**Table 2-7**: Mean clearance of antimalarial drugs in healthy adults compared to malaria infected patients

| Drug | Route of administration | CL (L/h/kg) mean ± SD [Number of groups [a]] | | Healthy Vs Malaria | | References |
|---|---|---|---|---|---|---|
| | | Healthy | Malaria infected | P value | Power | |
| Artesunate | IV | 1.9 ± 0.6 [n = 3] | 2.9 ± 0.8 [n = 8] | 0.09 | 0.4 | (36, 40, 41, 46, 62, 274, 319-321) |
| Dihydroartemisinin (from IV artesunate) | IV | 1.1 ± 0.16 [n = 3] | 0.81 ± 0.2 [n =9 ] | 0.04 | 0.56 | (36, 40, 41, 46, 62, 274, 319-321) |
| Artemether | IM | 0.88 ± 0.35 [n = 2] | 1.8 ± 0.9 [n = 2] | 0.32 | 0.13 | (48, 54, 275, 322) |
| Clindamycin | IV | 0.32 ± 0.12 [n = 3] | n/a [b] | n/a [b] | n/a [b] | (142, 288, 289) |
| Piperaquine [c] | Oral | 0.86 ± 0.65[n = 6] | 1.55 ± 0.73 [n = 4] | 0.15 | 0.28 | (82, 86, 87, 90, 91, 317, 318, 323, 324) |
| Mefloquine | Oral | 0.030 ± 0.014 [n =17] | 0.039 ± 0.014 [n = 5] | 0.24 | 0.21 | (95, 99, 106, 109, 110, 293-303) |
| Quinine | IV | 0.17 ± 0.05 [n = 6] | 0.07 ± 0.03 [n = 9] | 0.0002 | 0.99 | (18, 116, 132, 133, 311-314, 325-329) |
| Quinine (children) | IV | 0.24 [n = 1] | 0.064 ± 0.014 [n = 5] | n/a [b] | n/a [b] | (125, 311, 330) |

[a] Some studies comprised several groups, [b] Not available, [c] Piperaquine studies included piperaquine alone and piperaquine-dihydroartemisinin data for healthy volunteers, but only piperaquine-dihydroartemisinin data for patients with malaria. Our data and a previous report (89) indicate that there is no significant difference in piperaquine clearance when administered alone or in combination with dihydroartemisinin

### 2.5.4 Application of correction factor, maximum life span potential

As described in the methods sections, in order to correct the clearance value using the maximum life span potential (MLP) correction factor, the clearance values were multiplied by the MLP values. The calculated MLP values were 2.7, 4.8, 8.7, 20, 16, 93, 109 and 106 years for mice, rats, rabbits, dogs, pigs, human adults, 15 kg children and 25 kg children, respectively (268). Multiplication of clearance by these MLP values result in an increase of the product (MLP corrected clearance) by many fold; 3-5 fold for rodents, 16-20 fold for dogs and pigs, 93 fold for adult humans and >100 fold in human children. Thus MLP corrected clearance in the Y-axis (Figure 2.27) was extended by about two orders of magnitude compared to simple allometry (Figure 2.26). This lead to improvement of $r^2$ values for dihydroartemisinin, mefloquine and quinine using MLP compared to the simple allometry. However, $r^2$ values were slightly lower for artemether, clindamycin and piperaquine (Table 2.8). The exponent values obtained for MLP correction were higher than the simple allometric exponent and were above 0.9 for all drugs.

### 2.5.5 Application of liver weight and liver blood flow correction factors.

In order to correct the clearance values using liver weight and blood flow method, liver blood flow and liver weight of the mammalian species were multiplied by the total clearance values. The liver weight ranged from 0.0014 kg for mice to 1.58 kg for human adults. This resulted in decreasing the clearance value for mice by 800 fold and increasing the clearance value for humans by about 1.5 fold. Therefore, similar to the MLP correction, the Y-axis was extended by two orders of magnitude (Figure 2.29). The liver blood flow correction followed similar trends and the Y-axis was extended (Figure 2.30). The $r^2$ value for the liver weight correction method improved for all the drugs ($r^2 = 0.98$), whereas the $r^2$ value for the liver blood flow method was improved for dihydroartemisinin, clindamycin, piperaquine, mefloquine and quinine and slightly decreased for artemether and artesunate. The exponent values for both liver blood flow ($\geq$1.3) and weight corrections ($\geq$1.3) were higher compared to the simple allometry. The

$r^2$, exponent and coefficient for MLP, liver weight and liver blood flow corrections are given in Table 2.8.

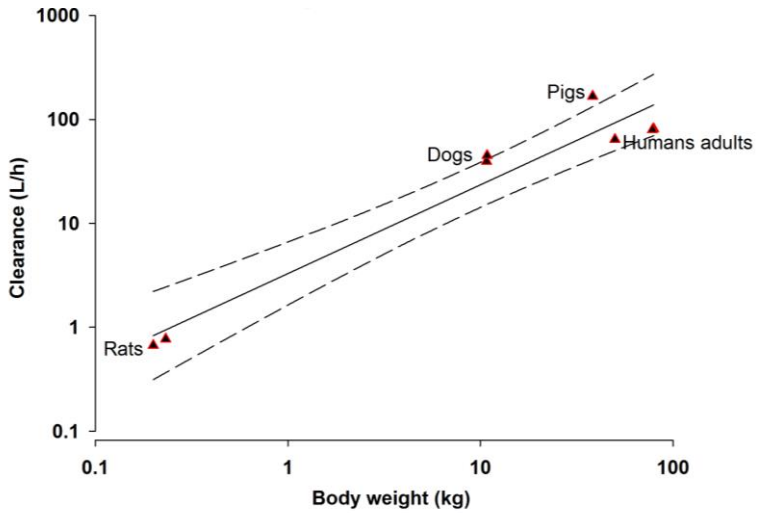


**Figure 2-26**: The regression line and 95% CI for allometric scaling relationship for dihydroartemisinin using simple allometry

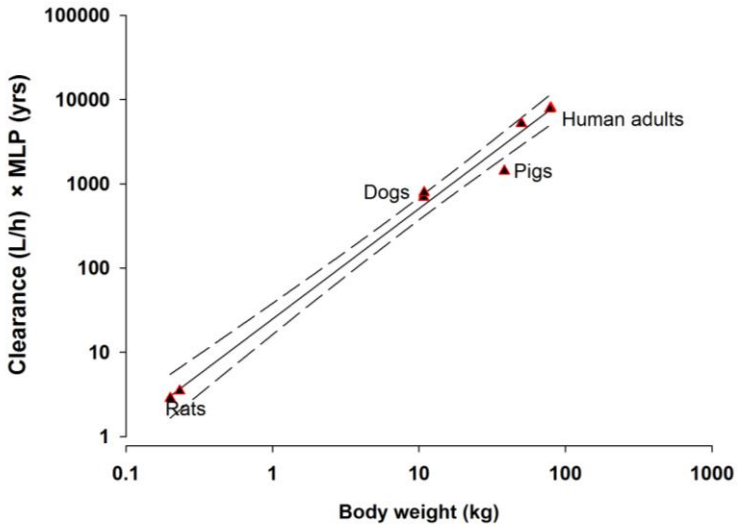


**Figure 2-27:** The regression line and 95% CI for allometric scaling relationship for dihydroartemisinin using MLP correction

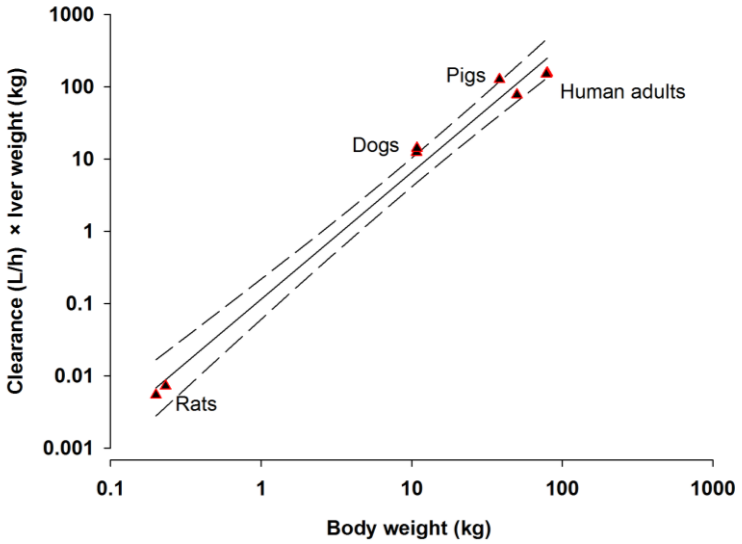


**Figure 2-28:** The regression line and 95% CI for allometric scaling relationship for dihydroartemisinin using liver weight correction

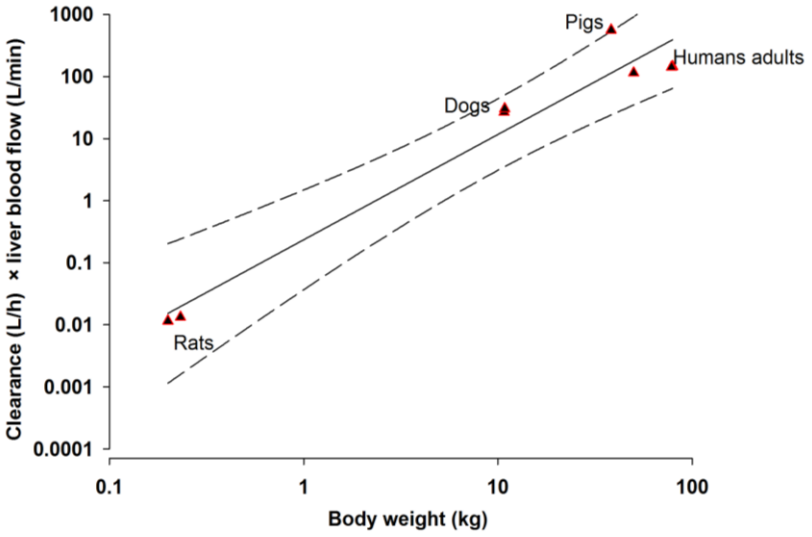


**Figure 2-29:** The regression line and 95% CI for allometric scaling relationship for dihydroartemisinin using liver blood flow correction

**Table 2-8**: The exponent, coefficient and coefficient of determination ($r^2$) values for simple allometry and MLP, liver body weight and liver blood flow corrections

| Drug | Simple allometry | | | MLP correction | | | Liver weight correction | | | Liver blood flow correction | | | References |
|---|---|---|---|---|---|---|---|---|---|---|---|---|---|
| | $r^2$ | b | a | $r^2$ | $b^*$ | $a^*$ | $r^2$ | $b^{**}$ | $a^{**}$ | $r^2$ | $b^{***}$ | $a^{***}$ | |
| Artesunate (IV) | 0.92 | 0.71 | 7 | 0.95 | 1.19 | 47.9 | 0.99 | 1.61 | 0.25 | 0.71 | 1.31 | 0.73 | (46, 55, 62, 167, 273, 274) |
| Dihydroartemisinin (from IV artesunate) | 0.94 | 0.85 | 3.3 | 0.99 | 1.31 | 25 | 0.99 | 1.76 | 0.12 | 0.95 | 1.70 | 0.23 | (46, 55, 61, 62, 167, 273, 274) |
| Artemether (IM) | 0.98 | 0.66 | 3.3 | 0.98 | 1.17 | 28.2 | 0.996 | 1.57 | 0.12 | 0.97 | 1.50 | 0.19 | (54, 55, 275, 276) |
| Clindamycin (IV) | 0.98 | 0.62 | 1.7 | 0.94 | 1.13 | 11.5 | 0.996 | 1.53 | 0.05 | 0.99 | 1.46 | 0.079 | (142, 286-290) |
| Piperaquine (oral) | 0.99 | 0.96 | 1.6 | 0.91 | 1.46 | 16.2 | 0.997 | 1.86 | 0.06 | 0.99 | 1.8 | 0.078 | (82, 83, 86, 90, 91, 291) |
| Mefloquine (oral) | 0.90 | 0.52 | 0.2 | 0.96 | 1.0 | 2.6 | 0.98 | 1.44 | 007 | 0.97 | 1.35 | 0.013 | (95, 99, 106, 109, 110, 292-304) |
| Quinine (IV) | 0.89 | 0.40 | 1.9 | 0.98 | 0.93 | 18.2 | 0.99 | 1.31 | 0.07 | 0.98 | 1.27 | 0.11 | (116, 132, 133, 305-314) |

a, b: Allometric coefficient and exponent for simple allometry, $a^*$, $b^*$: Allometric coefficient and exponent for MLP correction, $a^{**}$, $b^{**}$: Allometric coefficient and exponent for liver weight correction, $a^{***}$, $b^{***}$: coefficient and exponent for liver blood flow correction

### 2.5.6 Interpolation of drug clearance for children

Table 2.9 compares the antimalarial drug clearance in malaria infected children (except quinine) from published clinical studies with the interpolated drug clearance based on the simple allometric technique and correction methods; MLP, liver weight and liver blood flow correction. The observed drug clearance in quinine in healthy children was listed for comparison as quinine drug clearance in malarial infection was significantly different to healthy status.

Predicted clearance values obtained by simple allometry (based on preclinical and human adult clearance data) for all the drugs were within the threshold of 0.5 to 2 fold of the observed clearance in pharmacokinetic clinical studies of children. Dihydroartemisinin and artemether predicted clearance values were similar to the observed clearance with fold difference of 1. The piperaquine clearance was available from two clinical studies; however the values were different from one study to the other. The average body weight of piperaquine study participants were 16 and 19, therefore predicted clearance values were similar. Therefore observed clearance was an under prediction for one study and over prediction for the other study. Mefloquine and quinine clearance values were slightly over predicted by the simple allometric techniques.

MLP correction under predicted the drug clearance for all the drugs. The predicted clearance values for artemether and dihydroartemisinin were more than 4 fold lower. Mefloquine and quinine clearance interpolations were within 2 fold of the observed clearance.

Clearance interpolated using liver weight correction was within 0.5 to 2 fold for all drugs.

Liver blood flow corrections under-predicted the drug clearance for all the drugs. Predicted clearance for quinine was within the accepted value of 0.5 to2.

**Table 2-9**: Observed drug clearance of children in clinical studies compared to interpolated drug clearance using simple allometry and MLP, liver weight and liver blood flow corrections.

| Drug | Predicted drug CL (L/h/kg) [a] (Observed CL/Predicted CL ) | | | | Observed CL in Clinical studies [b] | | References |
|---|---|---|---|---|---|---|---|
| | Simple allometry | MLP correction | Liver weight correction | Liver blood flow correction | CL (L/h/kg) | Weight (kg) | |
| Dihydroartemisinin ( from IV artesunate) | 2.25 (1) | 0.48 (4.5) | 1.17 (1.8) | 0.78 (2.8) | 2.16 | 13 | (63) |
| Artemether (IM) | 1.52 (1) | 0.35 (4.3) | 1.79 (0.8) | 0.33 (4.5) | 1.5 | 9.5 | (331) |
| Piperaquine (oral) | 1.39 (0.6) | 0.50 (1.7) | 1.15 (1.7) | 0.46 (1.8) | 0.85 [c] | 19.1 | (87) |
| Piperaquine (oral) | 1.40 (1.3) | 0.57 (3.2) | 1.06 (1.8) | 0.40 (4.6) | 1.85 [c] | 16 | (332) |
| Mefloquine (oral) | 0.068 (0.7) | 0.023 (2) | 0.04 (1.0) | 0.02 (2.3) | 0.046 [d] | 9.5 [e] | (333) |
| Mefloquine (oral) | 0.068 (0.7) | 0.023 (2.1) | 0.04 (1.1) | 0.02 (2.4) | 0.048 [d] | 9.5 [e] | (334) |
| Mefloquine (oral) | 0.045 (0.6) | 0.024 (1.1) | 0.03 (0.8) | 0.02 (1.3) | 0.026 [d] | 23 | (335) |
| Quinine (IV) [f] | 0.37 (0.6) | 0.13 (1.8) | 0.31 (0.8) | 0.13 (1.8) | 0.24 | 15.4 | (311) |

[a] Drug clearance was interpolated using healthy control data, [b] Drug clearance of clinical studies were from malaria infected children and CL /F was reported for artemether, piperaquine and mefloquine [c] Piperaquine observed CL /F was reported from studies of dihydroartemisinin and piperaquine, [d] Mefloquine CL /F was determined from studies of mefloquine-sulfadoxine and pyrimethamine, [e] Malaria infected children were < 2 years and mean age was 1.6 years, [f] CL interpolated and observed for quinine were using healthy control data

### 2.5.7 Paediatric dose determination

Doses were predicted for children weighing 15 and 25 kg using simple allometric exponent values and adult doses. Table 2.10 compares the predicted doses with the reference doses according to the current dosing recommendation for children. Allometrically predicted doses were within 10-70% higher compared to the current dose recommendation for children weighing 15 and 25 kg except for artemether.

The predicted artemether dose was lower compared to the reference dosing recommendation. The current artemether dosing recommendations are for body weight ranges, 1, 2, 3 and 4 × 20 mg tablets for 5-14 kg, 15-24 kg, 25-34 kg and >34 kg, respectively. Therefore a dose of 40 mg is applicable for 15 to 24 kg and 60mg is applicable to 25-34 kg. The adult dose of 80 mg is applicable for 35 to 70 kg and above. The normalized reference doses for 5, 14, 15, 24, 25, 34, 35 and 70 kg are 4, 1.42, 2.67, 1.67, 2.40, 1.67, 2.28 and 1.14 mg/kg, therefore currently recommend children normalised doses are always higher than the adult doses. Allometrically predicted doses for 15 and 25 kg are 11/2(2 mg/kg) and 2 tablets (1.6 mg/kg). Hence, current practical dose recommendations are mostly higher than adults and close or higher than the allometric predictions.

Given the lower exponent values, a large increase in doses was predicted for mefloquine and were 1.6 to 2.5 fold higher compared to the reference doses. However the observed clearance for mefloquine (in combination with sulfadoxine and pyrimethamine) was slower compared to the predicted clearance (2.11).

Allometric interpolation estimated doubling the dose of quinine for healthy individuals. However quinine clearance was lower in malaria infection (Table 2.7) and the observed clearance in healthy children was lower compared to the simple allometry predictions (Table 2.9). Therefor dose increments for malaria infected children need to be done cautiously.

**Table 2-10**: Allometric interpolation of antimalarial doses in comparison to current dosage recommendations

| Drug | | Standard regimen [a] | Dose (mg) for 15 kg child | | | Dose (mg) for 25 kg child | | |
|---|---|---|---|---|---|---|---|---|
| | | | Reference [b] | Allometry [c] (Total) | (mg/kg) | Reference [b] | Allometry [c] (Total) | (mg/kg) |
| Dihydroartemisinin (as IV artesunate) | IV | Dose at 0, 12, 24 h, then once/day (2.4 mg/kg/dose) | 36 | 45 | 3 | 60 | 70 | 2.8 |
| Artemether | IM | Twice/day for 3 days (40 and 60 mg for 15 and 25 kg weights) | 40 | 30 | 2 | 60 | 40 | 1.6 |
| Clindamycin | IV | Twice/day for 7 days (10 mg/kg/dose) | 150 | 260 | 17.3 | 250 | 360 | 24 |
| Piperaquine | Oral | Once/day for 3 days (18 mg/kg/day) | 270 | 290 | 19.3 | 450 | 470 | 18.8 |
| Mefloquine | Oral | 15 mg day 1, 10mg day 2 (25 mg/kg total dose) | 375 | 790 | 52.6 | 625 | 1025 | 41 |
| Quinine | IV | Three times per day for 5-7 days (10 mg/kg/dose) | 150 | 370 | 24.6 | 250 | 460 | 18.4 |

[a] World Health Organization (3) and confirmed by reference to British National Formulary (251), [b] Based on mg/kg doses and practical recommendations
[c] Based on reference doses and equation ($Dose_{CHILD} = Dose_{ADULT} \times (Weight_{CHILD}/Weight_{ADULT})^b$, where adult dose was according to 70 kg body weight and exponent (b) from Table 2.4. Doses mostly rounded to 10 mg increment, rather than nearest practical dose.

### 2.5.8 Extrapolation of clearance for human adults using preclinical species

Finally, the exponents and coefficient for clearance of anti-malarial drugs were determined using only preclinical data. This enables determination of whether preclinical clearance data of antimalarials can be used to predict clearance for humans.

Table 2.11 provides allometric coefficient and exponent obtained from scaling clearance of preclinical species. The table also compares the observed healthy adult clearance (in healthy and malaria infected adults) and predicted clearance from scaling preclinical data and both preclinical and human data together. Figure 2.30 and 2.31 shows the regression analysis for allometric scaling of clearance of dihydroartemisinin (following IV artesunate) and artemether (IV and IM data) using preclinical species data.

A minimum number of three species were required for allometric scaling, however clindamycin, piperaquine, mefloquine and quinine had clearance data from only two pre-clinical species. Despite this, predicted clearance for mefloquine based on preclinical species was similar to the observed clearance in clinical studies and predicted clearance using both preclinical and human data.

The addition of human data did not alter the exponent values for artemether and the drug clearance predicted is very much similar to the observed clearance in clinical studies, therefore allometric scaling using preclinical data is plausible for some drugs.

The predicted values were within 0.5 to 2 fold of observed clearance for other drugs except dihydroartemisinin and piperaquine.

The predicted clearance for dihydroartemisinin and piperaquine using preclinical data was much higher compared to the observed clearance in clinical studies was 4 and 6 fold higher than the observed clearance in healthy adults. Despite the large difference in predicted clearance, a very strong $r^2$ value (0.999) was observed for dihydroartemisinin (Figure 2.30). The addition of human data substantially improved the predicted clearance for both drugs and was within the defined threshold of 0.5 to 2 fold of the observed clearance.

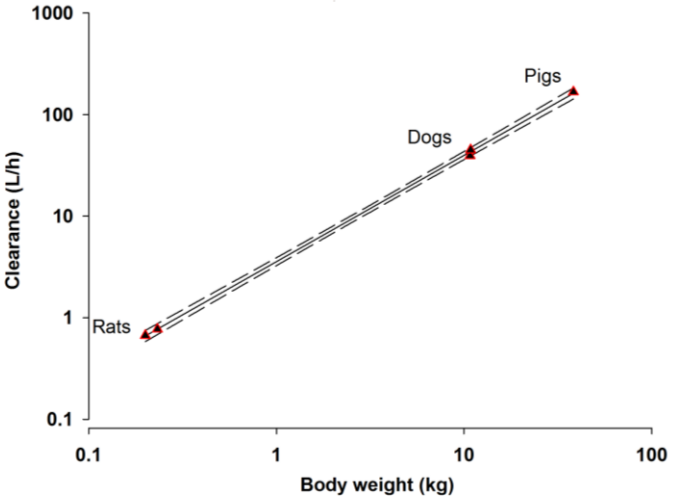


**Figure 2-30**: Regression line and 95% CI for interspecies scaling relationship for dihydroartemisinin (following IV artesunate) clearance using preclinical species

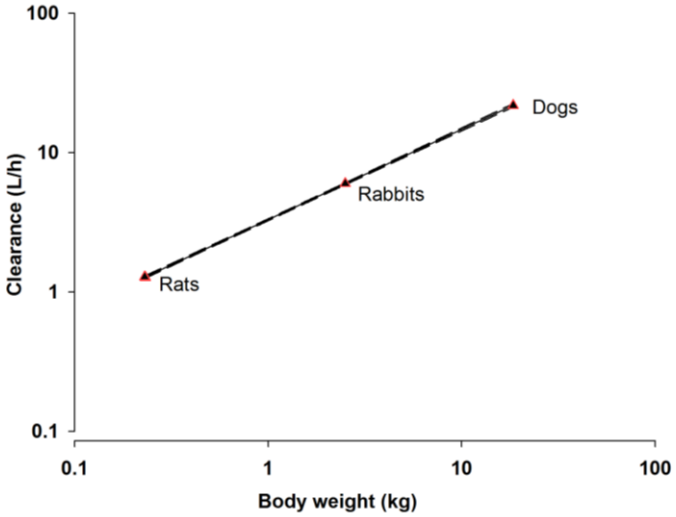


**Figure 2-31**: Regression line and 95% CI for Interspecies scaling relationship for artemether (IM and IV data) clearance using preclinical species

T**able 2-11**: Allometric prediction of drug clearance for 70 kg adult using preclinical species compared to observed clearance in human studies and clearance predicted using preclinical and humans data.

| Drugs | Allometric exponent /coefficient | | Predicted CL for 70 kg human adults (L/hr/kg) [b] | | Observed CL (Mean ± SD) (L/hr/kg) [c] | References |
|---|---|---|---|---|---|---|
| | Preclinical species [a] | Preclinical species and human | Preclinical species [d] | Preclinical species and human [d] | Healthy Adults [No of groups] | |
| Artesunate (IV) | 0.78/6.8 (r,d,p) | 0.71/7.0 | 2.65 (0.7) | 2.04 (0.9) | 1.9±0.6 [n = 3] | (36, 40, 41, 46, 62, 274, 319-321) |
| Dihydroartemisinin (from IV artesunate) | 1.05/3.6 (r,d,p) | 0.85/3.3 | 4.40 (0.2) | 1.74 (0.6) | 1.1±0.16 [n = 3] | (36, 40, 41, 46, 62, 274, 319-321) |
| Artemether (IM) | 0.65/3.3 (r,d) | 0.65/3.3 | 0.75 (1.2) | 0.75 (1.2) | 0.88±0.35 [n = 2] | (54, 55, 275, 276) |
| Artemether (IM&IV) | 0.65/3.3 (r,rb,d) | 0.66/3.3 | 0.75 (1.2) | 0.79 (1.1) | 0.88±0.35 [n = 2] | (54, 55, 275, 276) |
| Clindamycin (IV) | 0.53/1.4 (r,d) | 0.62/1.4 | 0.19 (1.7) | 0.33 (1.0) | 0.32±0.05 [n=3] | (142, 288, 289) |
| Piperaquine (oral) | 1.17/2.6 (m,r) | 0.96/1.6 | 5.35 (0.2) | 1.35(0.6) | 0.86±0.65 [n = 6] | (82, 86, 87, 90, 91, 317, 318, 323, 324) |
| Mefloquine (oral) | 0.53/0.2 (m,r) | 0.52/0.2 | 0.03 (1) | 0.03 (1) | 0.03±0.014[n =17] | (95, 99, 106, 109, 110, 293-303) |
| Quinine (IV) | 0.51/2.2 (r,d) | 0.42/1.9 | 0.27 (0.6) | 0.16 (1.1) | 0.17±0.05 [n = 6] | (18, 116, 132, 133, 311-314, 325-329) |

[a] Species: m : mouse, r : rat, d : dog, p : pig, rb : rabbit, h : human, [b] The exponent/coefficient in column 2 for preclinical species and column 3 for preclinical and human species were applied to equation ( predicted CL = $aW^b$) to determine predicted CL for 70 kg adult. [c] The observed CL for healthy were obtained from Table 2.7, [d] The ratio of observed CL /Predicted CL in heathy adults are given within the bracket

## 2.6 Discussion

Allometric scaling is based on well-established theoretical principles of a power law relationship between the biological parameters and the body size of the mammals. The present study utilized all valid published preclinical and human pharmacokinetic data to establish the allometric relationship in order to predict paediatric dosing. Thus interpolations were based on best available preclinical and human pharmacokinetic data compared to those made using conventional allometry where only preclinical species are used to extrapolate pharmacokinetic parameters for humans.

There was a paucity of pharmacokinetic literature of antimalarials in preclinical species, which limited the number of drugs studied. This was evident from the reduction in the target list of antimalarials (amodiaquine, lumefantrine, methylene blue and artemisone) due to the unavailability of pharmacokinetic studies in a minimum of three preclinical species. Combination drug therapy is recommended in the management of malaria in order to delay development of drug resistance. Therefore there is a lack of published pharmacokinetic studies following monotherapy for some antimalarials which further limited the list of antimalarials studied. The true pharmacokinetic parameters following IV administration would have provided optimum interspecies scaling results; however it was considered appropriate to scale CL/F and $V_z$/F following an oral route of administration for mefloquine and piperaquine.

The study describes the allometric relationship of the pharmacokinetic parameters clearance, volume of distribution and half-life for seven antimalarials. Drug clearance interpolations enable determination of maintenance dosing of a drug. A strong allometric relationship ($r^2 \geq 0.9$) was found for clearance of all drugs and the power relationship for each drug was found to be different from one another.

The allometric power relationship for basic metabolic rate was initially described with a fixed exponent value of 2/3 (0.67) and later a value of 3/4 (0.75) was adopted (191, 201, 232, 336). Over the many years, these fixed exponent values have been translated to be used in pharmacokinetics, where the exponents 3/4 (0.75), 1 and 1/4 (0.25) were established for scaling drug clearance, volume of distribution and half-life, respectively (123, 188, 207, 256). However, the use of fixed exponent allometry in dose

determination has been extensively debated and may not be universally applicable for all drugs (191, 201, 207, 208, 232, 256, 337).

In the present study, the clearance exponent and 95% CI for the antimalarial drugs studied did not encompass the fixed exponent 0.75 for clindamycin, piperaquine, mefloquine and quinine. Therefore current study data does not support the use of fixed exponent allometry for all drugs. Artesunate and artemether exponents and their 95 % CI included both 0.67 and 0.75 fixed exponent values; therefore there is no clear distinction or advantage between the two fixed exponent values. Linear or mg/kg maintenance dosing was not supported for all drugs although the 95 % CI for dihydroartemisinin and piperaquine encompassed 1 (Table 2.4).

Interpolation of volume of distribution enables determination of loading dose of a dosage regimen. A strong allometric relationship was observed for volume of distribution of drugs scaled ($r^2 \geq 0.91$) with the exception of artesunate. In contrast to the clearance, volume of distribution exponent and its 95 % CI encompassed 1 for artemether, piperaquine and quinine and exponent values were $\geq 0.8$ for other drugs (except artesunate). Hence linear scaling of loading dose is applicable for most of the antimalarials studied (Table 2.5).

Riviere (177) found half-life to be the most robust pharmacokinetic parameter for allometric prediction. In contrast to this finding, a poor allometric relationship was found for half-life of study drugs with the exception of artemether (Table 2.6). This is comparable with Ritschel's (269) finding that the half-life of coumarin was poorly related to physiological parameters, and therefore lacked interspecies scaling relationships. The half-life exponent values for antimalarials ranged widely (-0.16 to 0.35); however artemether, clindamycin, piperaquine and mefloquine exponents were close to the half-life fixed exponent value of 0.25, but 95% CI ranged widely.

The impact of the exponent on dose determination varies depending on the body weight. When the recommended dosing for a 70 kg adult is 10 mg/kg, the hypothetical exponents of 0.6 and 1 would lead to a predicted dose of 19.4 mg/kg and 10 mg/kg for a 10 kg child and 16.5mg/kg and 20mg/kg for a 20 kg child. The difference in dose due to change in exponent for a 10 kg child is higher and decreases with an increase in body

weight. Therefore it is important to have good quality, accurate allometric data as a small change in exponent can lead to a bigger change in doses for smaller children.

At commencement, this study aimed to predict dosing for malaria infected children, which requires scaling of pharmacokinetic parameters of malaria infected species. In the absence of sufficient pharmacokinetic data in malaria infected preclinical species, exponents derived using healthy species were adopted to predict dose for malaria infected children provided there is no alteration in pharmacokinetics due to the infection. In keeping with the published literature, a clear decrease in quinine clearance was found in malaria infected adults compared to healthy individuals (Table 2.7), therefore requiring cautious use of exponents derived from data collected in healthy species.

There is literature to show a higher area under the curve for dihydroartemisinin (hence lower clearance) in malaria infected patients compared to healthy individuals (62). In the present study, similar trends were observed when mean clearance reported from three heathy volunteer studies and nine patients studies were compared; however the power of the test was poor, hence robust conclusions were unable to be drawn as a Type 1 error cannot be excluded. Hence the dihydroartemisinin exponent derived using healthy species was used for dose predictions of children.

Similarly, there is pharmacokinetic literature which indicates significantly lower apparent drug clearance of mefloquine in severe malaria infection compared to that in healthy individuals (296, 302). However in the present study, no change in clearance was found when mean clearance reported in 17 pharmacokinetic studies of healthy adult were compared to mean clearance of 5 malaria infected patient studies.

In the absence of an exponent derived using malaria infected species, healthy species exponent was used for dose predictions of antimalarials even though power of the two tailed t test was below the required power of 0.8 except for quinine.

Improvement in clearance prediction for children was explored using different correction factors. Most techniques required more data than was available, limiting their usefulness. For example, techniques such as Dedrick plots required raw concentration time data and *in-vitro* correction methods required *in-vitro* metabolism data, neither of which were available (184, 221). As described in Chapter 1, scaled antimalarials are mostly cleared through hepatic metabolism therefore it was assumed that correction for

change in liver weight (for low extraction ratio drug) and liver blood flow (for high extraction ratio drugs) between mammalian species would improve clearance prediction by simple allometry. MLP correction is a widely adopted correction method for low extraction ratio drugs and the required data were available (184).

Simple allometry had the best predictive success compared to MLP, liver blood flow and liver weight corrections according to the observed/predicted ratio, with predicted drug clearance values within 0.5-2 fold of observed clearance for all seven drugs. Nevertheless a general trend of over prediction of clearance was observed.

While the $r^2$ values were improved for three out of seven drugs when interpolated drug clearance was based on MLP correction, the predicted clearance was not improved for all. For example, predicted clearance for dihydroartemisinin was 4.5 fold lower based on MLP correction whereas predicted clearance by simple allometry was similar to the observed clearance even though $r^2$ for dihydroartemisinin was improved by MLP correction. The MLP correction underestimated drug clearance at all times and mefloquine and quinine predicted clearance was slightly improved with improvement in $r^2$ value.

The Rule of Exponents includes MLP correction. Its use is recommended where the simple allometric exponent value is within the range of 0.71-0.99, while simple allometry is recommended for drugs with exponent in the range of 0.50 to 0.77. Thus the Rule of Exponents recommends MLP correction for dihydroartemisinin (exponent, 0.85); however as stated above the interpolated clearance by MLP correction was 4.5 fold lower than the observed clearance. Therefore the Rule of Exponents is not supported by the current study data.

Similar to MLP correction, liver blood flow correction under predicted the drug clearance for all the drugs. By contrast for liver weight correction, while the $r^2$ was improved for all drugs, the predicted clearance values were within the 0.5-2 fold of the observed clearance. The predictions using liver weight were comparable to simple allometry prediction, however a clear improvement in predictions was not observed.

Dihydroartemisinin was found to have a high hepatic extraction ratio in an isolated perfused rat liver model (60) and 93% was bound to plasma protein bound (58). Similarly artemether has shown a high hepatic extraction ratio (37) and was 95% plasma

protein bound (50). Given that both artemisinin derivatives have a high hepatic extraction ratio, simple allometric prediction should be accurate for both drugs and the study results proved the same. However, the hypothesis of incorporation of differences in liver blood flow of mammalian species, to improve clearance prediction for high extraction ratio drug was not supported. The dihydroartemisinin and artemether liver blood flow correction under predicted clearance by 2.8 and 4.5 folds, respectively. Simple allometric predictions were most accurate out of the four methods.

In rats, piperaquine has shown an absolute bioavailability of 50%, and fatty meals increased bioavailability in humans (83, 91). Piperaquine has also shown a very poor drug permeability in *in-vitro* Caco-2 cell models (338). Therefore lower bioavailability could be due to both poor absorption and high hepatic extraction ratio. Hai, Hietala (317) proposed that the low bioavailability of piperaquine is mostly due to poor drug solubility in the gastrointestinal tract rather than high hepatic extraction. The study further assumed that piperaquine is a low extraction ratio drug with less than 30 % hepatic extraction. This drug is highly protein bound (99%) in mice, rats, dogs, monkeys and human (84). Based on the literature, simple allometric prediction can be less accurate for drugs that are highly protein bound with a low extraction ratio, such as piperaquine.

The observed apparent clearance values of piperaquine in clinical studies of children were inconsistent (0.85 vs 1.85 L/h/kg). This difference could be due to clinical differences between the two populations (Table 2.9). Two recent clinical studies have reported lower apparent clearance values for piperaquine. One study reported apparent clearance of 0.57 L/h/kg, using pooled data resulting from administering piperaquine with different partner drugs; dihydroartemisinin plus piperaquine (332) and artemisinin plus piperaquine combination (44). The other study used capillary blood for the analysis and reported an apparent clearance of 0.42 L/h/kg. Authors discouraged the direct comparison of this finding with the other available data resulting from venous blood (88). Data from these two studies, therefore, cannot be directly included in the present study for comparison.

However given that piperaquine has lower observed apparent clearance in children, the predicted apparent clearance values by simple allometry and by correction methods were within 0.5-2 fold of the observed apparent clearance. However simple allometric prediction using preclinical data of piperaquine under predicted the drug clearance by 6

fold and prediction improved (1.6 fold difference) by incorporation of human data. Therefore based on piperaquine data (low extraction ratio drug) allometric dose interpolations are possible, when the exponents are derived using both preclinical and human drug clearance.

Clindamycin had shown an absolute bioavailability of 53% (289) and is 94% bound to alpha 1-acid glycoprotein (138). It is reported that clindamycin is a drug with a low hepatic extraction ratio (142, 339). Clindamycin clearance in children was not found in clinical studies. However the predicted clearance using preclinical species was 1.7 fold lower compared to the observed healthy adult clearance, therefore simple allometry could be used for dose prediction of clindamycin, even though it is identified as a low extraction ratio drug.

Mefloquine is extensively bound to plasma protein in humans (99%) and in rat (95%) and has a low intrinsic clearance (100, 101). This drug has shown enterohepatic recycling in humans and in rats and is mostly excreted in bile and faecal materials (101, 302). In a study of allometric scaling of susalimod, a highly biliary excreted drug, found predicted human clearance to be 24 times higher than the observed clearance (340). The authors concluded that biliary excreted drugs result in non-predictable human clearance by allometric scaling of preclinical data. However predicted clearance for mefloquine had predictive success and was within the 0.5 - 2 fold from the observed clearance values for simple allometry and by two correction methods; MLP and liver weights. This was also correct for simple allometric prediction using preclinical species alone. Mefloquine (low extraction ratio) clearance predictions were expected to be improved by liver weight correction and the predicted clearance by liver weight correction was closest to the observed values. It should be noted that observed clearance in the mefloquine clinical studies listed in Table 2.9 were from studies of mefloquine-sulfadoxine and pyrimethamine. Karbwang and co-workers (298) observed a slight prolongation (16.3 to 20.7 days) of $t_{1/2}$ following combination therapy compared to mefloquine alone. Therefore it is possible that mefloquine drug clearance is decreased when combined with sulfadoxine and pyrimethamine, in that case, over prediction (0.7 fold difference) of drug clearance by simple allometry can be more accurate.

Quinine is a drug with a low intrinsic clearance and is about 90% bound to alpha 1-acid glycoprotein (protein binding is not significantly altered in acute malaria infection) (18).

Both published pharmacokinetic literature and analysis from the present study have shown that clearance of quinine is further reduced in malaria infection (18). Despite this being a low extraction ratio drug, simple allometric predictions were within the threshold values and so were the predictions by the correction methods.

The dose increments recommended based on this study finding (using healthy species) ranged from no increase in dose up to doubling the currently recommended mg/kg dosing (Table 2.10). Dihydroartemisinin (available as 60 mg/ mL artesunate injectable) and clindamycin (available as 75, 150 and 300 mg clindamycin hydrochloride capsules) required modest increase in doses, which can be achieved in a clinical setting. Recent clinical studies have also recommended higher doses of IM artesunate and proposed the following doses for weight bands of children; 40 mg for 14 to 16 kg and 60 mg for 21-25 kg (171). This closely matches the allometric interpolations of this study; 3 mg/kg for 15 kg and 2.8 mg/kg for 25 kg children.

The allometric exponent for piperaquine indicates only a small increase in dose. This increase in dose is unlikely to be practical in a clinical setting and might not result in blood concentration that can cause a clinically significant difference in outcome. However, recent clinical studies have recommended higher piperaquine doses for children (81, 88, 173). Therefore allometric dose predictions are not comparable with the clinical study recommendations. The reported observed drug clearance in clinical studies ranged from 0.85 to1.85 L/h/kg for children (Table 2.9) and mean drug clearance for healthy adults and malaria infected patients were 0.86±0.65 and 1.55±0.73 L/h/kg (Table 2.7). Looking at mean piperaquine clearance values, a clear difference in drug clearance between adults and children was unable to be seen. Therefore more pharmacokinetic studies in children are needed to make clear recommendations on dose changes.

A large increase in mefloquine dose was recommended for 15 and 25 kg children; 2.1 to 1.6 fold higher doses than the reference doses. This appears large and has not been recommended in clinical studies so far. A recent study on chloroquine (another quinolone group drug) has proposed a 1.6 fold increase in dose based on the concept of allometric scaling (264). Two clinical studies have adopted 2 fold higher doses of chloroquine for children (170, 341). These increments are similar to mefloquine dose increments suggested in the present study. However the observed drug clearance for

mefloquine (children on mefloquine-sulfadoxine and pyrimethamine) was lower compared to predicted clearance using simple allometry. The observed drug clearance in children is higher compared to mean adult drugs in two of the three studies. Therefore a dose increment can be suggested, however a lower increment compared to what is suggested by allometry might be more appropriate to trial.

Based on healthy species exponents, 18-24 mg/kg quinine dosing is more appropriate than 10 mg/kg. A recent study recommended a 20 mg/kg loading dose to be used in children with malaria (171). Table 2.7 depicts the quinine clearance in healthy children is higher than the mean healthy adult clearance, however mean clearance in children with malaria was found to be lower compared to infected adults. Therefore the general observation of increased drug clearance in children is not observed for quinine clearance in malaria infected children. Allometric scaling results for quinine need to be cautiously interpreted due to complex and multifactorial effects of malaria infection on pharmacokinetics of the drug.

The allometric scaling data of the current study indicate the need for differing allometric exponent values for scaling antimalarial drugs. This could cause practical difficulties in the use of fixed-dose combination therapy. For example, the adult dose for dihydroartemisinin-piperaquine (120-960 mg) is in the ratio of 2:60 mg/kg for a 60 kg patient. In the case of linear dosing, a child weighing 15 kg can be given 30:240 mg. If allometric exponents are used, piperaquine dose would be appropriate for the child, but dihydroartemisinin dose needs to be increased by 20%. However, fixed dose combinations do not permit a disproportionate increase in doses. Hence, this would not be practically possible. Allometric finding in this study shows that artemisinin combination therapy requires a disproportionate increase in doses.

Increased availability of pediatric dosage forms such as solutions and suspensions is required and would enable accurate dispensing of doses based on drug specific allometric exponents and the child's body weight.

Nevertheless dosing recommendation based on allometric scaling cannot be used in neonates, very young children due to clear difference in physiological function and immature or altered clearance mechanisms (246).

The use of preclinical clearance data in extrapolating human clearance was explored (Table 2.11). Both piperaquine and dihydroartemisinin preclinical data scaling was not able to predict human drug clearance to an acceptable level. It should be noted that less than 3 preclinical species (below the recommended number) were included for the analysis of some drug. Incorporation human clearance data for scaling clearly improved the clearance predictions of all the drugs.

Pharmacokinetic data from young animals would have provided like for like data when allometry is used to extrapolate pharmacokinetic for children. However the evidence on the use of juvenile animals is limited and there is inadequate knowledge and no clear consensus on the species of animals to use, their appropriate age groups and organ differences at different age points (342). The European Medicines Agency and US FDA support conducting juvenile animal clinical trials only in instances where previous animal and human safety data are insufficient to support paediatric clinical trials (342). The physiological differences in mature and immature animals could result in altered metabolic profile, therefore, change in pharmacokinetic and toxicological data. Differences in maturation timing, functional differences in kidney, cardiovascular, respiratory and gastrointestinal systems and lack of robust knowledge on the different organ systems of different animal species at different time points in their maturation process pose difficulties in selection of species and their suitable ages (342, 343). Therefore, it is not easy to select appropriate animal species in their correct age group to extrapolate pharmacokinetic information to immature humans. Hence, the commonly adopted and accepted technique of allometry scaling based on adult animal species was adopted in this study.

## 2.7 Limitations

The main limitations in the study were the low number of mammalian species included for the scaling and the paucity of pharmacokinetic information in malaria infected species. The study included only two to three non-human species for the scaling, however this was consistent with previous studies (219, 264, 267). A large number of non-human species would have improved the quality of the allometric scaling findings.

It is also claimed that inclusion of large animals could improve the allometric scaling predictions (175); however pharmacokinetic studies on antimalarials in large animals were not available to be included in the analysis.

The clearance, volume of distribution and half-life of drugs for different species for allometric scaling were obtained from published studies. Therefore, pharmacokinetic parameter data points were average values for the study subjects and it was not possible to obtain pharmacokinetic parameters and weights for individual subjects. Conducting pharmacokinetic studies for drugs of interest would enable individual pharmacokinetic parameters for each study subject rather than published average values. However, these were outside the scope of the present study investigation.

The antimalarials scaled are mainly cleared by the hepatic metabolism. Therefore *in-vitro* metabolic data as a correction factor is suitable. Lack of required information precluded this from the analysis.

With the advancement in pharmacokinetic research, it has been found that there are differences in protein binding in animals and humans for certain drugs (344). The distribution and excretion of a low extraction ratio drug may be affected by drug protein binding in plasma and tissue. The difference in protein binding among species could result from differences in affinity or number of binding sites of protein (345). There could also be differences in expression of drug efflux transporters such as MDR1, MRP1, MRP2 and BCRP between different animal species and human, these variations could lead to change in drug absorption, distribution and elimination of antimalarials given that these drugs are subjected to ABC transporter mediated efflux process (346).

However possible variation in protein binding and efflux transporter protein expression were not incorporated into the current analysis due to lack of required information. It was not able to test all the published correction factors mostly due to limitation of information and time. Similarly, methods like Dedrick plots were unable to be performed as raw drug concentration time data required for these plots was not readily available in the pharmacokinetic literature.

## 2.8 Conclusion

Clearance and volume of distribution are suitable pharmacokinetic parameters for interspecies scaling of antimalarials. Half-life performed poorly for most drugs based on $r^2$ value. Drug clearance predicted for children based on simple allometry met the predictive success for all seven antimalarials irrespective of the hepatic extraction ratio. Predicted clearance based on liver weight correction was within the accepted range of the observed clearance and performed better compared to MLP and liver blood flow correction methods. No correction factor showed clear improvement in prediction compared to simple allometry. It was not possible to determine the suitability of a correction factor based on metabolism. The $r^2$ value did not indicate predictive success at all times.

Preclinical clearance data can be used for prediction of clearance for some of the study antimalarials. Incorporation of human clearance clearly improved clearance prediction for adults and children.

The linear scaling of adult to paediatric doses has been recognised as flawed (208) and interspecies simple allometric scaling (based on preclinical and humans) technique is a plausible/better method for estimation of paediatric antimalarial drug doses in children. The allometric exponents and coefficients obtained can be adopted in designing pharmacokinetic and efficacy studies and population pharmacokinetic modelling of new and current antimalarial drugs.

# 3 *In-vitro* drug permeability and P-gp mediated efflux transport studies

## 3.1 Introduction

### 3.1.1 Drug permeability

Drug transport across the gastrointestinal epithelium can be a passive or an active process. Gastrointestinal absorption of the majority of orally administered drugs in current therapeutic use is through passive permeability (passive transcellular and passive paracellular routes) (347). The physiochemical characteristics of these drugs play a large part in the permeability of drug across the lipid bilayer of gut cells from the mucosal side to the blood or serosal side.

Drugs that are smaller in molecule size and lipophilicity permeate following a passive transcellular pathway based on Fick's law in which the rate of absorption depends on the area of the absorptive surface and concentration gradient across the membrane (348).

Small, hydrophilic, ionized drugs and peptides cross through the paracellular pathway (water filled intercellular pores of the epithelium) (349). The drug absorption via this pathway is limited due to tight intercellular junctions and relatively small surface area. Small hydrophilic drugs could also be transported through passive permeability to some extent, as transcellular space in the luminal cell membrane is very large (surface area is more than 1000 times) compared to the paracellular space (348, 350).

Large (above 500 Da), hydrophilic, charged drugs often require carrier molecules for the transport process (351). This can be an active or a passive process. Active carrier mediated transport requires metabolic energy and can be transported against a concentration gradient. Some hydrophilic drugs with chemical structure similar to body chemicals or nutrients are transported partly using active transport proteins. Whereas when there is higher concentration in the gut lumen, passive carrier mediated transport (facilitated transport) can occur where a drug permeates through membranes using a carrier molecule without the use of metabolic energy. Saturation of carrier molecules

can greatly affect the extent of drug absorption, especially for drugs that have low passive permeability. For these drugs, saturation of carrier molecules results in drastic decrease in the extent of drug absorbed and systemic exposure of drugs (352). Highly permeable drugs that are absorbed following both carrier mediated transport and passive diffusion and when carrier molecules are saturated, passive transport contribute to more of drug absorption (By increase in drug dose/endogenous substrate molecules) (350).

Transcytosis/endocytosis is mostly used by highly potent hydrophilic macromolecules that cannot be transported by other transport mechanisms and is less commonly used. The transport generally occurs through membrane vehicles that contain large amount of proteolytic enzymes and these mostly get degraded in *in-vitro* cell monolayers. The reticuloendothelial system commonly uses these types of transport. Vitamin B12 and large peptides in the intestinal epithelium are also transported by endocytosis (348, 350, 353).

The ABCB1 P-gp efflux transporter protein functions differently as these carrier molecules bind to drugs/chemicals and facilitate serosal to mucosal directional transport, which is referred to as efflux transport. Drugs passing through the apical membrane of intestinal epithelium could be substrates for apical efflux transporters such as P-glycoprotein and MRP2, which push the drug back into the lumen (354-356). The efflux mechanism is an ATP-dependent process and can occur against a concentration gradient.

### 3.1.2 Physicochemical properties of drugs

The passive permeability of a drug across the gastrointestinal epithelium depends on the physicochemical properties such as molecular size, lipophilicity (octanol-water partitioning coefficient), pKa and ionization of the drug (123, 348, 350, 357).

Molecular size is a key determinant on the movement of drugs across membranes with smaller sized drug molecules capable of crossing membranes through the paracellular pathway. Atenolol (MW: 246 g) can transverse the gastrointestinal epithelium paracellularly, whereas oxytocin (MW: 1007 g) cannot cross the gastrointestinal epithelium even though it can easily pass through the loosely knit nasal membrane (123,

358). Diffusion for smaller lipophilic drugs drops sharply as molecular size increases (359).

The typical method of determining the lipophilicity of a substance is by establishing the octanol water partitioning coefficient ($P_{oct}$). The $P_{oct}$ value can be used as a predictor of drug absorption and it gives a reasonable prediction on the ability of the drug to partition into the lipid bilayer. The partitioning coefficient at pH 7.4 (the apparent distribution coefficient, $D_{oct}$) is often preferred in determining drug permeability. The permeability increases with increase in $P_{oct}$ values up to a value of 2 and drops after $P_{oct}$ value is > 4, as highly lipophilic drugs do not partition back out to the aqueous compartment and prefers to stay in the plasma membrane (360, 361). The optimum log P values for best systemic action is in the moderate log p value of 1.5 to 3 (362), with a positive correlation between drug absorption and log D up to log D of 3 (360).
The $pK_a$ of the drug and pH of the body fluid determine the ionization of drugs. Unionized drugs can readily cross membranes and vice versa. However unionized drugs don't have good solubility in aqueous solvents, thus resulting in solubility limitations for the drug.

### 3.1.3 Drug transporting ABC efflux transporters

The mammalian ABC (ATP-binding cassette) superfamily is highly diverse with about fifty different protein subfamilies and is comprised of membrane transporters, ion channels and receptors (363). Of these, the principal efflux transporter proteins are MDR1 (multidrug resistance), MRPs (multidrug resistance associated proteins) and BCRPs (breast cancer resistance proteins) as they are involved in the transport of many clinically relevant drugs. In this thesis, only MDR1 P-gp proteins will be discussed.

### 3.1.4 P-glycoprotein (MDR)

P-glycoprotein (P-gp/ABCB1/MDR1) was the first multidrug protein described and was discovered by Juliano and Liang in 1976 (364). This most commonly studied ATP-dependent efflux carrier molecule is involved in the transport of a diverse range of drugs used for different therapeutic indications. The P-gps are known as multidrug resistant

(MDR) transporters as many of the cytotoxic anticancer drugs developed cross resistance due to P-gp mediated drug efflux transport (365).

P-glycoprotein is a 170 to 180 kDa membrane glycoprotein, a polypeptide containing 2 halves, each with 6 transmembrane domains that are separated by both an extracellular loop which is highly N-glycosylated and contain two nucleotide binding domains (NDB) are located intracellularly ( Figure 3.1) (366).

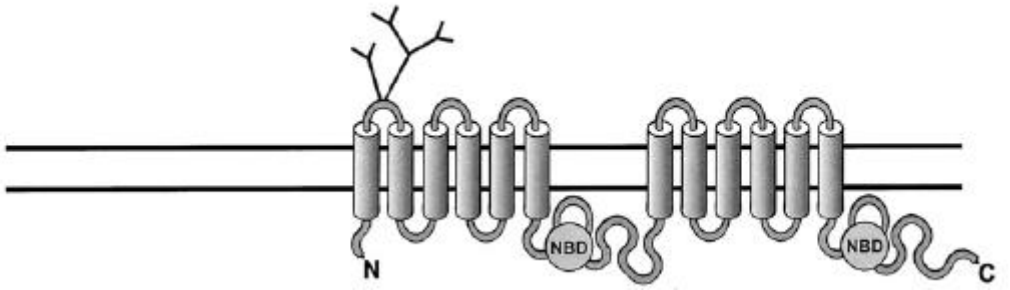


**Figure 3-1**: Molecular structure of MDR1 (P-glycoprotein) (363, 365)

In humans there are two MDR gene families; MDR1 (ABCB1) and MDR3 (ABCB4). Human MDR1 is expressed highly in the kidney and adrenal glands, with intermediate levels on the apical surface of the epithelial cells (Villus tip enterocytes) of the intestine, liver, colon and lungs and low levels in the prostate, skin, spleen, heart, ovary, stomach and skeletal muscles (367-369). P-gp transporter proteins are also found on the luminal surface of capillary endothelial cells in the brain and are highly expressed in carcinoma cells (369, 370).

Human MDR3 is expressed in liver and low levels are expressed in the normal human jejunum (371, 372). MDR3 is involved in transport of phospholipids in the liver and absence of MDR 3 protein in humans can cause type 3 progressive familial intrahepatic cholestasis (373). Digoxin, paclitaxel and vinblastine are some of the drugs with affinity for both MDR1 and MDR3 transporters in the liver (371).

### 3.1.4.1 Mechanism of action

Radio ligand binding studies have shown that there are at least four drug-binding/transport sites that can modify P-gp function (374). The drug binding sites are located in the transmembrane region, which might also function as a single binding site that can bind with more than one compound (363, 375). A model is proposed to describe P-gp substrate interaction where P-gp substrate need to interact with the lipid bilayer and partition into the lipid phase before interacting with P-gp binding sites (366, 376, 377).

P-glycoproteins' have an ability to interact with a diverse range of compounds with a higher probability of binding with lipophilic cationic compounds. It is suggested that P-gp substrates could be basic or uncharged compounds with a molecular size of 300 to 2000 Da. Some weakly acidic drugs can also get transported at a lower rate. The most common structural feature of P-gp substrates is inclusion of both hydrophilic and lipophilic segments in its structure or its amphipathic nature (363, 366, 378).

Seelig (379) proposed that recognition of whether a compound is a P-gp substrate or a modulator depends on the hydrogen bond acceptor groups and its spatial separation that interacts with the hydrogen bond donor side chains located in the transmembrane region of the P-gp. Induced fit mechanism is a hypothesis of P-gp and substrate interaction, where the shape and the size of the transmembrane segments packing of the P-gp could be altered based on the substrate (380, 381).

### 3.1.4.2 P-gp mediated drug transport studies

P-glycoprotein mediated drug efflux transport was first demonstrated using *in-vitro* Caco-2 cell lines (50). *In-vivo* efflux transport was demonstrated using MDR1 knockout mouse models. In humans, drug interactions due to P-gp mediated drug efflux can be determined by calculating the net change in area under the curve profile of a P-gp substrate when administered alone and in combination with a P-gp inhibitor. The combination therapy would result in increased systemic availability of the P-gp substrate compared to when it was given alone. However, this can be confounded by other mechanisms such as CYP 450 induction and gastrointestinal anomalies, resulting in reduced drug absorption. For this reason, inhibition studies in humans can only give a

qualitative assessment of the involvement of P-gp in drug absorption (50). Compelling evidence of P-gp mediated efflux transport in humans was demonstrated by Hoffmeyer and co-workers (382), where a good correlation between duodenal P-gp expression and plasma levels of the P-gp substrate, digoxin, was observed.

### 3.1.4.3 Role of P-gp efflux transport in the body

P-glycoprotein efflux transporters are primarily located in the plasma membrane, where drugs, metabolites, nutrients, toxins and other compounds are effluxed out of the cell. Efflux transport is a protective mechanism that limits absorption and cell accumulation of potentially toxic compounds. In humans P-gps may play an important role in drug absorption, distribution, metabolism and excretion.

The oral route is most commonly used for drug administration due to its convenience, safety, low cost and ease. However for a drug to be orally administered a reasonable gastro intestinal tract absorption ability is required. The apical membrane of the small and large intestinal epithelium contains a large number of P-gps, which pushes its substrates back into the lumen, reducing overall drug permeability. The P-gp apoprotein expression is similar in the stomach, jejunum and ileum of the human gastrointestinal tract (383). P-gp substrate with lower inherent drug permeability will have larger effect on *in-vivo* drug absorption compared to P-gp substrate with higher permeability. Other than the human physiological factors, drug absorption can be largely affected by pharmaceutical factors and the physicochemical factors of the drug itself.

Drugs need to be distributed into the site of action to deliver the desired therapeutic response. In doing so it needs to cross several bio membranes and the ability to cross the membranes depends on the physical and biochemical properties of the membrane and physiochemical properties of the drug such as lipophilicity, ionization profile and molecule size (123, 358, 384). Penetration of drug into the brain is distinct compared to other body organelles. Vascular capillaries of the brain are anatomically specialized and function as a shield separating the brain from the general blood circulation. This is referred to as the blood brain barrier and is composed of very tight cell junctions enabling penetration of only small, lipid soluble drugs into the brain. But it has been found that even some of the smaller molecular lipid soluble drugs exhibit poor

permeability into the brain. This can be explained by high P-gp expression in the apical surface of the brain capillary cells pushing drugs out of the vasculature before gaining access to the brain proper (365, 385, 386). The brain is more sensitive to toxic chemicals compared to other organs in the body; therefore P-gp has a protective function of blocking harmful chemicals reaching it.

The role of P-gp in the placenta is similar to its function in the brain and gastrointestinal tract and protects the foetus from xenobiotic (50, 365).

In the liver drugs and endogenous toxins are released from hepatocytes into the bile, which ultimately are excreted out of the body as faecal waste (365).

Other than the liver, the small intestine also contributes to the drug metabolism through CYP 450 enzymes. Metabolism in the gastrointestinal tract of a P-gp substrate could be altered by repetitive expulsion and reabsorption of drug, thus increasing the resident or exposure time to the intestinal drug metabolising enzymes (50).

The apical membrane of the proximal tubules of the kidney is another place where there are abundant amounts of P-gp (369). *In-vitro* MDCK and porcine kidney (LLC-$PK_1$) cell line studies have shown efflux transport of P-gp substrates, digoxin and vinblastine which indicate increased drug excretion in the kidney (387, 388). However this *in-vitro* study finding was not supported *in-vivo* in P-gp knock out mice and increased drug excretion in the absence of P-gp was found, rather than the expected decrease in drug clearance (50, 365, 389) This could be explained by an increased intestinal absorption or less efflux from the gut allowing more drug exposure to the kidney.

### 3.1.4.4 P-gp substrates

Drugs transported or effluxed out of the cells by the P-gp transporters are known as P-gp substrates. They have some structural similarities even though P-gp extrudes a wide variety of chemically and structurally diverse drugs.

P-gp substrates have relatively low $K_m$ values. For example, vinblastine, digoxin, cyclosporine, verapamil and indinavir have $K_m$ values of 26, 51-81, 3.8-8.4, 4.4- 31 and 140 µM, respectively (390-392). When drugs are administered at high doses, the

gastrointestinal concentration of the drug is elevated above the $K_m$ value, which results in saturation of the P-gp transporter proteins. Indinavir was given orally at a dose of 800 mg in one study, resulting in an intestinal lumen concentration in the mM range, far higher than the $K_m$ values for P-gp (50). Hence at this dose, a reduction in indinavir bioavailability will not be observed irrespective of person's P-gp expression level in the gut.

Nevertheless for P-gp substrates that have a large molecule size, lower solubility and poor dissolution will still be effluxed when given in high doses. For example cyclosporine at 100-700 mg and paclitaxel at 100-200 mg have resulted in lower bioavailability (50).

The P-gp mediated drug efflux does not always lead to poor bioavailability of all suspect drugs. There are drugs with P-gp substrate activity that have reasonable oral bioavailability. Digoxin is a good P-gp substrate but has a bioavailability between 50 to 85%. P-gp substrates can also have good passive permeability, therefore the amount of drug absorbed is equal to the net difference between the influxed amount (passive diffusion and active intake transport mechanisms) and the effluxed amount ( P-gp efflux plus the amount of drug metabolised).

Both P-gp and CYP3A4 interact with a wide range of substrates and there is much overlap between P-gp and CYP3A4/5 substrates (393). This becomes more of an issue *in-vivo* as both P-gp and CYP3A4/5 are expressed in the same organs, resulting in a greater reduction in the systemic drug concentration of common substrates (50).

Many anticancer drugs (vinblastine, paclitaxel, daunorubicin, mitoxantrone, teniposide, actinomycin D, methotrexate), anti-hypertensive (digoxin, diltiazem, verapamil), most HIV protease inhibitors, antibiotics (erythromycin, tetracycline, valinomycin, gramicidin D, sparfloxocin,), immunosuppressive agents (cyclosporine A, tacrolimus), corticosteroids, H2 receptor antagonistic (cimetidine, ranitidine), azole antifungals, some antiemetics (domperidone and ondansetron), antidiarrheal agents (loperamide), pesticides (ivermectin, abamectin), diagnostic dyes (rhodamine123, Hoechst 33342), antiarrhythmic (quinidine), anti-gout agents (colchicine), hormones (estradiol-17B-D-glucuronide, aldosterone) and analgesics (morphine) are found to have P-gp substrate activities (365, 394).

### 3.1.4.5 P-gp inhibitors

A limited number of drugs are able to inhibit P-gp mediated drug efflux transport at physiologically relevant concentrations. These agents are found to be useful in reversing multidrug resistances of cytotoxic agents. However first generation P-gp inhibitors such as verapamil and cyclosporine could not be used to reverse multidrug resistance due to their own therapeutic activities and adverse effects given at the concentrations needed to have P-gp blocking activity. Hence specific P-gp inhibitors without other systemic actions were developed. The second generation P-gp inhibitor, SDZ PSC 833 (Valspodar), a cyclosporin an analogue with no immuno suppression activity, has a high affinity to P-gp. This slowly transported substrate of P-gp acts as a very effective inhibitor because it is released from P-gp at a very slow rate (395). PSC 833 also has limited action on MRP1 an MRP2 (396). GF120918 is another such inhibitor and inhibits P-gp mediated drug transport as well has some inhibitory action on BCRP (397).

It is important to know that P-gp substrates can also function as competitive P-gp inhibitors if their concentration is high enough. In addition, the substances that were initially identified as P-gp inhibitors such as verapamil, cyclosporin A were later found to be P-gp substrates. P-gp inhibitors which do not demonstrate P-gp substrate activity such as progesterone are likely to inhibit P-gp mediated efflux by other mechanisms (365).

In order to confirm P-gp mediated drug transport, drugs can be combined with PSC 833 and GF120918 separately to determine inhibition of efflux transport. Gastrointestinal epithelium and Caco-2 cell lines have efflux transporters other than P-gp, such as MRP1, MRP2 and BCRP. Probenecid and MK571 inhibit both MRP1 and MRP2 transporters and have some action on P-gp (365). There are no compounds currently known that act as MRP2 specific inhibitor. Ko143 is a BCRP inhibitor and this can be used to determine the efflux transport of a drug through BCRP.

Atorvastatin, bromocriptine, carvedilol, cyclosporine, erythromycin, GF120918, itraconazole, ketoconazole, LY335979, meperidine, methadone, nelfinavir, pentazocine, progesterone, quinidine, ritonavir, saquinavir, tamoxifen, tariquidar, PSC 833 and verapamil have all been shown to have P-gp inhibitory properties (394).

### 3.1.4.6 P-gp mediated drug interactions

#### 3.1.4.6.1 P-gp substrate interactions

P-gp related drug-drug interactions do not follow simple kinetics but rather, follow multiple patterns and are substrate specific. It is likely that concurrent administration of P-gp substrates and inhibitors will result in drug interactions. There are three main categories of P-gp mediated drug interactions; competitive, non-competitive and cooperative stimulation.

P-gp has multiple substrate binding sites and two ATP binding domains. In competitive inhibition, two P-gp substrates would act on the same binding sites of the P-gp molecule, competing to bind to one site. Alternatively, in non-competitive inhibition, two substrates would bind to two different binding sites simultaneously and function independently (50, 398). *In-vitro* studies in multidrug resistant P388 cells have shown that P-gp mediated daunomycin uptake is competitively inhibited by verapamil, whereas vinblastine noncompetitively inhibited uptake of the drug (399).

The competition of two P-gp substrates would generally result in inhibition of P-gp mediated transport of one substrate, but in some cases activation of P-gp transport has been reported. In studies done in Chinese Hamster Ovary CH'B30 P-gp enriched cells, it was found that rhodamine123 and Hoechst 33342 simulated the P-gp mediated efflux transport of each other. Whereas daunorubicin and doxorubicin stimulated the Hoechst 33342 transport and inhibited the rhodamine123 transport (400). This indicated that P-gp can interact with two substrates allosterically.

The two ATP binding domains can also be involved in drug interactions with the blockage of ATP hydrolysis in addition to competition for drug binding sites (401, 402). For example, the common P-gp substrate verapamil, competitively binds to substrate binding sites, while sodium ortho-vanadate, interacts with the ATP binding domain and cyclosporine A interferes with the substrate binding sites and ATP hydrolysis (50).

### 3.1.4.7 P-gp inhibitor interactions

*In-vivo* mice studies have shown that co-administration of a P-gp inhibitor increased P-gp substrate concentrations in the brain more than in P-gp non-inhibited mice, and that

relation to plasma level were even higher in the plasma (403, 404). P-glycoprotein inhibition related drug interactions have also been reported in humans. Ketoconazole, a potent P-gp inhibitor, increased the CSF concentration of ritonavir and saquinavir in HIV patients, while causing minimum change in plasma concentration (405). Brain and placenta have high P-gp expression and are sensitive to P-gp inhibitors (50). Therefore P-gp inhibitors need to be used carefully to avoid risk of neurotoxicity and possible CNS related adverse effects (50).

Potent P-gp inhibitors such as PSC 833 and GF120918 can restore the anticancer drug activity increasing drug sensitivity for anticancer drugs, this also increase tissue distribution of cytotoxic drug and cytotoxicity (406, 407).

#### 3.1.4.8 P-gp regulation and induction

The expression of the ABC efflux transporter proteins is not static and is regulated at both transcriptional and non-transcriptional levels to maintain homeostasis (363).

Evidence of induction of P-gp has been demonstrated both *in-vitro* and *in-vivo* (50). P-gp induction by dexamethasone is reported in *in-vitro* mouse and rat cell lines (408, 409). Pharmacokinetic drug interactions can result from up-regulation of P-gp transporter proteins. A pharmacokinetic study of digoxin in healthy volunteers before and during administration of rifampicin found a lower area under the curve of digoxin after treatment with rifampicin. Duodenal biopsies after treatment of rifampicin had shown a 3.5 fold increase in P-gp compared to before treatment (410). These studies suggest that induction of P-gp expression can be dose, time, tissue and species dependent (50).

Co-regulation/ co-induction of P-gp and CYP3A expression has been reported in humans, rats and *in-vitro* cell lines (50). This has led to the assumption that regulation of CYP3A4 and P-gp gene expression is co-ordinated through similar mechanisms. P-gp can be induced in a similar fashion to CYP3A4 with pregnane X receptor (PXR) having a role in regulating CYP3A4 and P-gp expression (411-413). A species difference in induction of CYP3A4 was observed due to sequence differences in the (PXR) (414), however P-gp induction may be mediated by several mechanisms in

addition to PXR. The P-gp regulation process is very complex and every inducer has its own pattern of P-gp induction. Therefore it is necessary to understand the inductive process of each inducer to understand its implications and consequences.(50).

Amprenavir, clotrimazole, dexamethasone, indinavir, morphine, nelfinavir, phenothiazine, retinoic acid, rifampicin, ritonavir, saquinavir and St John's Wort have all been shown to have P-gp inducing properties (394).

### 3.1.5 *In-vitro* cell models for drug transport studies

*In-vitro* cell models are used widely to determine the drug permeability across intestinal epithelial membranes. *In-vitro* drug permeability data can be used for drug absorption screening in the early stage of drug development, which avoids further expenditure on conducting costly *in-vivo* studies on compounds with a poor absorption profile (350). *In-vitro* techniques are also used in drug industry specifically for P-gp affinity studies. Drug permeability data along with aqueous solubility and physicochemical parameters of drugs can be utilized to determine whether *in-vitro* dissolution tests can replace/waive the need for *in-vivo* bioavailability studies in establishing bioequivalence for generic drugs. The cost of establishing *in-vitro* permeability, solubility and physicochemical characterization are $1/10^{th}$ to $1/15^{th}$ of a bioequivalence study (415). *In-vitro* cell models for drug transport studies ideally should mimic transcellular and paracellular permeability of the small intestine. Similarly it should resembles the expression of carriers and enzymes within the intestine (416).

Colorectal adenocarcinoma-2 (Caco-2) cell models are the most widely used *in-vitro* cell line in establishing drug permeability of a drug.

Madin-Darby canine kidney (MDCK) cells have gained in popularity due to rapid cell growth and differentiation. These cell lines are used to determine passive permeability, active transport, and efflux transport of drugs after 3-4 days post seeding. A transfected version MDCK-MDR1 is being used to determine P-gp mediated efflux transport of drugs in many labs, although this is not commercially available at present, with no stock at the ATCC nor in the European Collection of Cell Culture (ECACC). A recent study has used MDCK-MDR1 transfected cells and Caco-2 cells to determine the drug permeability of new antimalarial compounds. The study finds MDCK-MDR1 cells to

be advantageous over Caco-2 cells in identifying P-gp mediated drug efflux and interactions (417). The main limitation of this cell line is its canine origin even though MDCK cells are transfected with human MDR, other drugs are required in the medium to maintain stable levels of human MDRI, which can impact on other cell systems.

The HT29 cell line has a useful sub clone (HT29-18-$C_1$) which differentiates in cell culture conditions to polarized absorptive cells and can also be used for drug transport studies similar to Caco-2 cells. HT29-H cells form monolayers of mucin secreting human intestinal goblet cells with 50 fold higher paracellular permeability than that of Caco-2 (418).

Shirasaka and colleges (419) developed a culture method for Caco-2 cells in vinblastine containing media as a means to increase P-gp levels of the cells to be comparable to that found in MDCK-MDR1 cell model extending the usefulness of the human Caco-2 model in active efflux research.

### 3.1.6 Caco-2 monolayers in drug transport studies

The Caco-2 cell line is a human intestinal epithelial cell line, derived from human a colorectal carcinoma (420). The cell line is preferred in transport studies due to its human origin and close correlation to *in-vivo* intestinal conditions (372, 421). Many of the efflux transporters present in the gastrointestinal tract are similar to those expressed in Caco-2 cells. A strong correlation (Figure 3.2) of gene expression of these ABC efflux transporter proteins in the human jejunum and Caco-2 cells has been established (372). Thus it is clear from Figure 3.2 that the two most important multidrug efflux proteins, P-gp and BCRP reflects normal gut proportion of activity, but BCRP is not present as widely in Caco-2 cells. This makes Caco-2 a good model for P-gp related transport studies. MRP 1 and 2 are also well represented on Caco-2 compared to the *in-vivo* gut, although their involvement in drug transport is much less reported than P-gp.

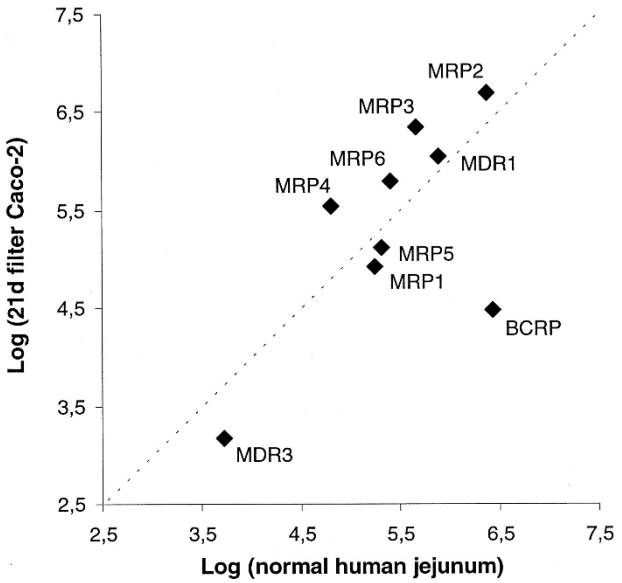


**Figure 3-2**: Correlation of gene expression of drug efflux proteins of the ATP binding cassette transporter Family in human jejunum and human epithelial Caco-2 cell monolayers (372)

Caco-2 cells have closely comparable permeability with that of *in-vivo* human jejunum, especially for drugs with high passive diffusion.

Under normal cell culture conditions Caco-2 cells spontaneously differentiate into monolayers of polarized enterocytes, expressing high levels of several brush boarder hydrolases when allowed to develop for 2-3 weeks (422). In addition, they contain intestinal transport proteins which transport large substances such as amino acids, vitamin $B_{12}$ and dipeptides (353, 423, 424) and form a tight monolayer with trans epithelial electrical resistance above 300 $\Omega cm^2$, which although higher than that of the colon (421). The tight junctions result in little or no paracellular transport which allows study of trancellular transport of a drug as drugs would inevitably pass through the cells. Caco-2 cell lines grown on permeable filter inserts for 21 to 28 days are routinely used for *in-vitro* studies on the transepithelial transport of drugs. Bidirectional drug transport studies done on Caco-2 cell monolayers can be used for determination of passive permeability of the drugs and/or active transport using carrier molecules (350). These studies help identify potential drug absorption related problems and predict likely *in-*

*vivo* drug absorption (421, 425, 426). Active transport processes involving P-gp and dipeptide carrier molecules are usually studied using a Caco-2 cell model.

The noted limitations of the Caco-2 model are its the heterogenic nature and slow growth, which can result in some differences in transport expression from lab to lab requiring analysis of transport level in batches. Caco-2 cells are also deprived of intestinal barriers such as mucus layers, which could impair drug absorption (416).

### 3.1.7 Correlation of *in-vitro* drug permeability and *in-vivo* drug absorption

Bidirectional apparent permeability ($P_{app}$) values across Caco-2 monolayers could be used to identify potential absorption related problems of drugs. The *in-vitro* Caco-2 monolayers are found to be comparable to more complex absorption models such as *in-situ* perfusion model. A study was done to establish the predictability of *in-vivo* drug absorption from *in-vitro* Caco-2 monolayers and *in-vivo* human jejunum *in-situ* using double balloon and single pass techniques. The study looked at three categories of drugs; ones that are completely and rapidly absorbed by a passive transcelluar route, those slowly and incompletely absorbed through a passive paracellular route and drugs transported by an active carrier mediated route. The study found Caco-2 monolayers to be an excellent model for predicting passive transcellular permeability with only 2-4 fold variation in *in-vitro* model prediction compared to the *in-vivo* values whereas *in-vitro* predictions for incompletely absorbed drugs were 30 to 80 fold lower compared to the *in-vivo* jejunum (350, 427, 428). Thus Caco-2 cell permeability values for low permeable drugs (peptides and peptidomimetics) do not correlate with the *in-vivo* permeability as accurately as highly permeable drugs. This difference is likely due to lower paracellular permeability resulting from greater tight junctions in Caco-2 monolayer and low permeable drugs having a long duration in the gut to slowly be absorbed. This can be factored into a mathematical model through producing a sigmoid curve to represent low, medium and high permeable drugs when estimating human drug absorption from these cells (350). Several other studies using low permeable peptidomimetics have shown that it is possible to obtain reasonable *in-vivo* prediction using in-*vitro* Caco-2 monolayer studies using this method (429, 430).

Based on $P_{app}$ values drugs are classified into low, medium and highly permeable drugs. Yee (431) used $P_{app}$ values of 1, 1-10 and greater than $10 \times 10^{-6}$ cm/sec, respectively, having studied the correlation between *in-vivo* drug absorption and *in-vitro* permeability of 36 compounds. However this study failed to consider the solubility of the drug before establishing the relationship. HT29-18-$C_1$ cell line study established a threshold value of greater than $2\times10^{-6}$ cm/sec to have more than 80 % absorption and less than $2 \times10^{-6}$ cm/sec to be poorly absorbed (426). A recent study has classified drugs into low, medium and high categories based on $P_{app}$ values of 2, 2-20 and greater than $20 \times 10^{-6}$ cm/sec (417).

The limitation of Caco-2 cell lines that they are a heterogeneous cell population of adenocarcinoma cells. It has been shown that the active transport of thyrotropin releasing hormone was present only in one Caco-2 monolayer from two populations originated from different laboratories (432). There could be also be differences in Caco-2 cells generated within the same laboratory (350, 433). It is indicated that monolayer characteristics could change within increasing passage number, duration of cell growth, media conditions and filter conditions. Nevertheless, the change in cell characteristics can be monitored by determining bidirectional transport of reference P-gp substrates such as rhodamine123. Therefore inter lab variability in drug permeability ($P_{app}$) values can be expected. But controlled bidirectional transport studies using Caco-2 monolayers still provides similar qualitative correlations of fraction absorbed irrespective of the research group or laboratory, and once controlled quantitation is possible.

### 3.1.8 Bio-pharmaceutical classification system

Aqueous solubility and permeability of a drug are the main parameters that control the rate and the extent of drug absorption across gastrointestinal epithelium (434). The pH of the gastrointestinal tract varies from pH 1.5 to 7.4 and drugs are considered highly soluble when the highest dose strength is soluble in 250 ml of aqueous media over a pH range of 1-7.5. Drug permeability values obtained using *in-vitro* Caco-2 cell line studies are considered as valid data to categorize drugs into the FDA's Biopharmaceutical classification system (415).

Amidon and co-workers (434) developed the theoretical biopharmaceutical classification system below considering the drug solubility and permeability and categorizing drugs into 4 classes. Class I and II drugs, can waive any requirement bioavailability (bio wavier) studies for establishment of bioequivalence for generic product in place of *in-vitro* dissolution test.

| **Class** | **Solubility** | **Permeability** | ***In-vivo in-vitro* (IVIV) correlation expectation (434, 435)** |
|---|---|---|---|
| I | High | High | Drug is dissolved rapidly and is well absorbed. Bioavailability problems are not expected. Dissolution test can waive *in- vivo* bioavailability & bioequivalence |
| II | Low | High | Dissolution of the drug is limited but well absorbed. Bioavailability is controlled by the dosage form and rate of release of the drug substance. Dissolution test can waive *in- vivo* bioavailability & bioequivalence |
| III | High | Low | Drug permeability is rate limited. Dissolution test cannot waive the *in-vivo* bioavailability. |
| IV | Low | Low | Drug permeability and dissolution is limited. No IVIV correlation. It is difficult to formulate a drug product that will deliver consistent drug bioavailability. An alternate route of administration may be needed. |

The solubility of a drug depends on formulation of the product factor (dissolution), gastrointestinal pH, gastrointestinal transit time, drug interaction) food and other drugs) in the intestinal tract and metabolism of drugs in the gastrointestinal tract. This classification also allows identification of class IV drugs, which has low solubility and permeability. This would allow opportunities for investigator to further improve chemical structures of drugs in order to have better solubility and permeability.

### 3.1.9 Current evidence on drug permeability, P-gp mediated efflux transport and P-gp expression regulation on antimalarials

The P-gp inhibitory properties of antimalarials have been studied more widely compared to their potential P-gp substrate activities. There are only a few studies on P-gp substrate activity of antimalarials and there is little or no information on the P-gp induction properties of antimalarials.

While there is no information on drug permeability of mefloquine and little information on its activity as a substrate for P-gp (436), there is convincing evidence for P-gp inhibitory activity (104, 436-438). However the drug transport of mefloquine in the combination therapy is lacking. The P-gp inhibitory properties and bidirectional transport of amodiaquine is reported in the current literature (439, 440). Bidirectional transport of artesunate has not been reported while the P-gp inhibitory properties for artesunate and dihydroartemisinin are available (439, 440).

Piperaquine is highly lipid soluble and drug permeability studies in a Caco-2 cell line have shown very low apical to basolateral (AP-Bas) and basolateral to apical (Bas-Ap) permeability. Ap-Bas values were below detectable and Bas-Ap was $0.1 \times 10^{-6}$ cm/sec). This drug was shown not to exhibit P-gp mediated transport (338).

*In-vitro* Caco-2 cell line studies has suggested that quinine is a potent P-glycoprotein inhibitor and it might also be a P-glycoprotein substrate (441). Quinine reversed the resistance of doxorubicin in a multidrug resistance human myeloma cell line model. In this study a synergistic inhibition of P-gp was also found when quinine was combined with verapamil (442).

Regulation of P-gp expression by artemisinin has been reported. It is reported that artemisinin induces expression of CYP2B6, CYP3A4 and P-gp in human hepatocytes and in LS174T (Dukes' type B,colorectal adenocarcinoma) cell lines through the activation of human PXR and human Constitutive Androstane receptor (CAR) (443). At 25 µM dihydroartemisinin did not activate PXR, however authors speculated that dihydroartemisinin may activate PXR when present greater than 25 µM.

## 3.2 Specific Objectives

The study of *in-vitro* drug permeability of antimalarials requires development of an robust *in-vitro* cell model. As discussed in the introduction Caco-2 cell monolayers are the most widely used human cell line for *in-vitro* drug permeability studies. However the limitation of this cell line is its possible heterogenetic nature based on cell origin and culturing condition. Therefore it was aimed to develop an *in-vitro* Caco-2 cell model for determination of drug permeability and P-gp mediated drug transport of anti-malarial drugs.

## 3.3 Methods

### 3.3.1 Materials

#### 3.3.1.1 Drugs

Artemisinin, mefloquine hydrochloride, amodiaquine dihydrochloride dihydrate, artesunate, rhodamine123 and rifampicin were purchased from Sigma Aldrich (St Louis, MO, USA). Dihydroartemisinin was supplied from DAFRA Pharma Manufacturers (Belgium). Methylene blue zinc chloride double salt was purchased from Fluka Sigma Aldrich (Steinem, Switzerland). Artemisone was kindly donated by Professor Richard Haynes, The Hong Kong University of Science and Technology, Hong Kong. Vinblastine hydrochloride was purchased from ICN biochemical (Seven hills, NSW, Australia). PSC 833, the P-gp blocking cyclosporine derivative, was donated from Novartis BioPharma (Basel, Switzerland). Mini Protease inhibitor tablets were supplied by Thermo Scientific (Rockford, USA).

#### 3.3.1.2 Chemicals

Acetonitrile, methanol and ethanol were supplied from Fisher Scientific (Fair Lawn NJ, USA). Dimethyl Sulfoxide (DMSO) was purchased from Ajax Finechem (NSW, Australia). TRIS Hydrochloride was purchased from Ultrapure bio-reagents (NJ, USA). Sodium Chloride, sodium potassium tartrate and Copper (II) sulphate were purchased Chem-Supply (Gillman, SA). Sodium Dodecyl Sulphate, Sodium Carbonate, Casein, Potassium Dihydrogen Ortho Phosphate ($KH_2PO_4$), Trifluroacetic acid, Phosphoric acid ($H_3PO_4$), Formic acid and Nonidet P40 substitute were supplied by Sigma Aldrich (MO, USA). Sodium hydroxide and Folin were supplied by BDH Merck Pvt Ltd (Victoria, Australia).All other chemicals were of analytical grade.

#### 3.3.1.3 Cells and cell culture reagents

The human colon carcinoma cell lines (Caco-2), passage 18 were obtained from American Type Culture Collection (ATCC), University Boulevard (Manassas, VA,

USA). LS174 T and Hela cells were gifted from Professor Michael Gottesman, NIH, Bethesda, USA.

High glucose Dulbecco's modified eagle medium (DMEM), Dulbecco's phosphate buffered saline (PBS), L-Glutamine, Hanks buffered salt solution (HBSS), N-2-hydroxyethylpiperazine-N'-2-ethane sulphonic acid (HEPES), Trypan blue stain (0.4%) and TrypLE Express were supplied by Gibco [Life technologies (NY, USA)]. Glucose was purchased from APS Finechemicals (NSW, Australia). Non-essential amino acid, penicillin G (10,000 u/mL) and streptomycin (10,000 µg/mL) were purchased from Trace Biosciences (Castle Hill, NSW, Australia). Foetal calf serum (FCS) was obtained from the SerANA (Bunbury, Western Australia).

NuPAGE MOPS running buffer (20X), SeeBlue Plus2 Pre-stained Standard, Bolt Sample reducing agent (10X), Bolt 4-12% Bis-Tris Plus 15 well gels, NuPage Transfer buffer (20 X), Nupage LDS Sample buffer (4X) and NuPage Antioxidant were purchased from Novex by life technologies (CA, USA).

MDR1 mouse monoclonal antibody was purchased from Santa Cruz biotechnology Inc. (Europe). Monoclonal Anti-beta-Actin antibody produced in mouse was supplied by Sigma Aldrich (MO, USA). Goat anti-mouse secondary antibodies were purchased from Jackson ImmunoResearch Laboratories Inc (West Grove, PA, USA)

Clarity Western ECL substrate was supplied by BIORAD Laboratories Inc. (USA)

## 3.3.2 Buffers, reagents and solvents

The composition of the buffers, reagents and solvents are given in Appendix 1.

### 3.3.2.1 Buffers for HPLC

Mobile phase for all assays were prepared using $KH_2PO_4$. This was prepared by dissolving 2.72 g of salt in 1 L of deionized water. The pH of 20 mM buffer was adjusted using $H_3PO_4$. The buffer was filtered through 0.45 µm filter using a vacuum pump.

#### 3.3.2.2 Solvents for LC-MS-MS sample preparation

Preconditioning solution - 1% v/v trifluroacetic acid was prepared by pipetting in 100 µL trifluroacetic acid and making up the volume to 10 mL with deionized water.

Washing solution - 0.1% v/v trifloroacetic acid was prepared by pipetting in 100 µL trifluroacetic acid and making up the volume to 100 mL.

Conditioning solution - 50 % v/v acetonitrile was prepared in deionized water.

Elution solvent - 0.1% v/v formic acid in 95% v/v of acetonitrile was prepared by mixing 11µL of 90 % formic acid, 9.5 mL of acetonitrile and 489 µL of deionized water.

### 3.3.3 Preparation of stock and working solutions

Mefloquine (MW: 378.3) 20 mM stock solution was prepared by dissolving 8.30 mg mefloquine hydrochloride (MW: 414.77) in one mL of ethanol. Concentration of mefloquine above 100 µM was not used for test conditions due to toxicity to the Caco-2 cells.

Amodiaquine (MW: 355.9) is soluble in water and sparingly soluble in ethanol and DMSO. Amodiaquine was found to be poorly soluble in pH 7.4 HBSS transport media as the solubility of amodiaquine reduces with increase in pH (72). The stock 20 mM amodiaquine was prepared in one mL of ethanol dissolving 9.30 mg of amodiaquine dihydrochloride dihydrate (MW: 464.81) and was unable to further increase the stock concentration. Maximum test concentration of amodiaquine was 300 µM (Higher concentration increases the percentage of ethanol in the working solution)

Artesunate (MW: 384.4) 20 mM and 40 mM stock solutions were prepared by dissolving 7.68 mg and 15.37 mg per 1 mL of ethanol respectively. Similar to artesunate 20 and 40 mM stock solutions for artemisone (MW: 401.52) were prepared by dissolving 8.03 mg or 16.06 mg in 1 mL of ethanol. Methylene blue (MW: 319.85) 20 mM stock solution was prepared by dissolving dissolving 7.61 mg of methylene blue zinc chloride double salt (MW: 775.98) per mL of deionized water.

Dihydroartemisinin (MW: 284.4) was sparingly soluble in ethanol and highest concentration achieved was 20 mM by dissolving 5.68 mg per 1 mL of ethanol and 0.14 mg of artemisinin was dissolved per mL of ethanol to prepare 0.5 mM artemisinin (MW: 282.33) stock solution.

Rhodamine123 (MW: 380.82) 5 mM stock solution was prepared by dissolving 1.90 mg of rhodamine123 per one mL of ethanol. The stock solutions for PSC 833 (MW: 1214.62 g), rifampicin (MW: 822.94), vinblastine (MW: 909.05) and Ko143 (MW: 469.57) were 4, 1, 0.5 and 1 mM and prepared by dissolving 4.86, 0.82, 0.45 and 0.47 mg of drugs respectively per 1mL of DMSO.

MK 571 (MW: 537.07) 10 mM stock solution in deionized water was diluted in HBSS to prepare 40 µM test solutions. Probenecid 500 µM (MW 285.36) working solution was prepared by dissolving 2.14 mg in 15 mL of HBSS.

Drug aliquots were stored at -80 $^{\circ}$C and standard series and test concentrations were prepared by using aliquots on the day of the experiment. Working/test drug solutions were prepared in HBSS and the percentage of solvent; namely ethanol and DMSO was maintained at 1% ethanol and 0.2 % DMSO. However for high concentration of amodiaquine and dihydroartemisinin (300 mM), the percentage of ethanol increased up to 1.5%.

### 3.3.4 Assay of rhodamine123

Rhodamine123 levels were quantified using Perkin Elmer Enspire multi-mode plate reader (Waltham, MA, USA) and measurement were done using fluorescence detection at excitation and emission wave length of 498 and 528 nm respectively. Enspire workstation version 4.10.3005.1440 was used for data interpretation. Figure 4.3 gives the standard curves for 70 ml (for assay of Bas-Ap sample) and 120 mL (for assay of Ap-Bas samples) of rhodamine123. Standard series (0.02 to 5 µM) were prepared in HBSS. Two standard curves were required, as samples were collected in 96 well plates in 70 (Bas-Ap sample) and 120 µL (Ap-Bas samples) volumes. The 96 well plates were directly placed in the detector to quantify the relative fluorescence (RFU) in these two

volumes. Interpretation of total fluorescence in two different volumes required the construction of two standard curves of 70 and 120 µL volumes.

A1.

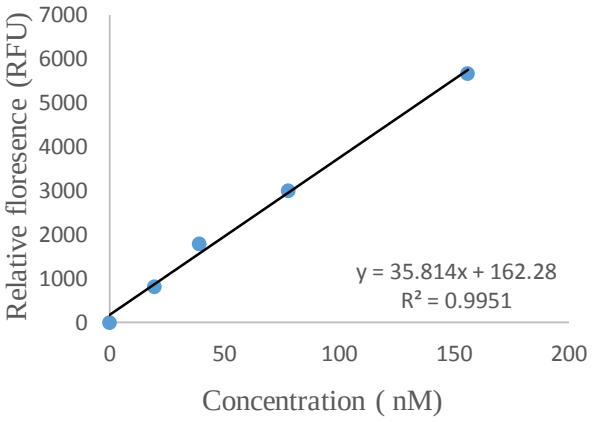


A2.

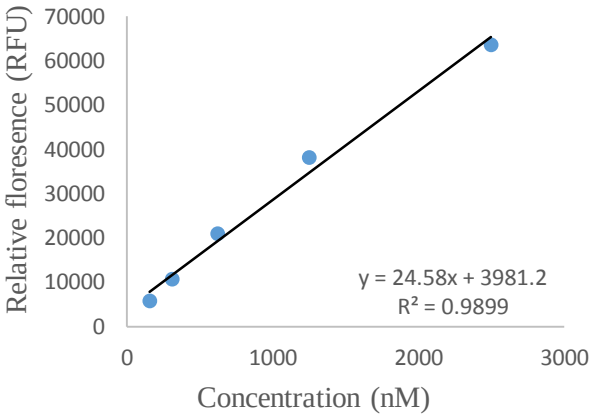


B1.

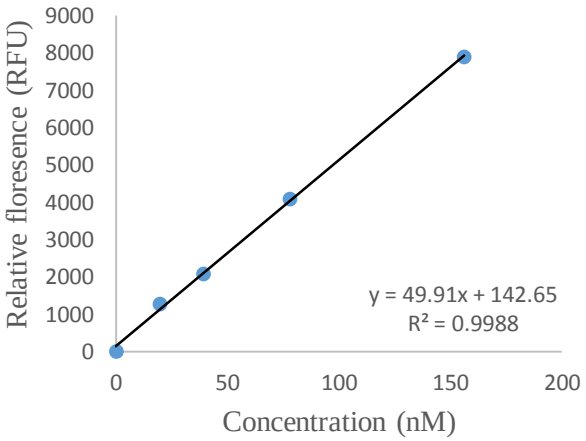


B2.

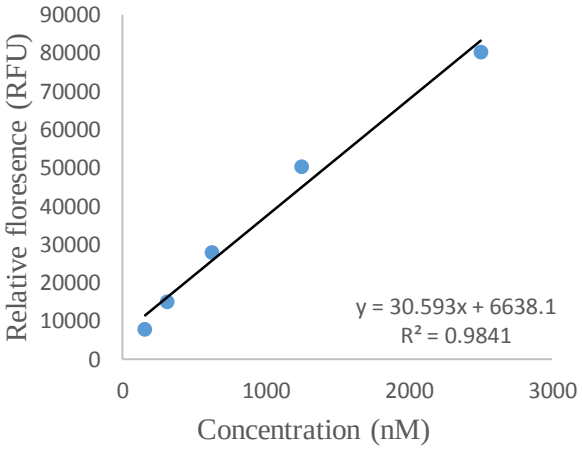


**Figure 3-3 -** Calibration curve for rhodamine 123 for concentration range A1) 0- 160 nM, A2) 160- 3000 nM for 70 µL and B1) 0- 160 nM, B2) 160- 3000 nM for 120 µL

### 3.3.5 Development of cell model for transport studies

#### 3.3.5.1 Caco-2 monolayers and maintenance

The human colon carcinoma cell line (Caco-2) passage 18 obtained from ATCC were frozen in 70 % medium, 10% DMSO and 20 % FCS in liquid nitrogen. The thawed cells were added into a falcon tube containing 11 mL of medium, centrifuged at 500 g for 7 minutes and resuspended in 3 mL of medium. Cells were seeded (10000 cells/$cm^2$) in 25 $cm^2$ flask and maintained in high glucose DMEM supplemented with 10 % FCS, glutamine, non-essential amino acid, penicillin and streptomycin incubated at 37 $^{\circ}C$, 95% humidity and 5% $CO_2$. Medium was replaced twice a week and cell splitting was done using 50:50 TrypLE Express: PBS (1.5 mL each) upon 90% confluency, in about 10 days of post seeding. The cell suspension was centrifuged at 450 g for 7 minutes in a falcon tube containing 7 mL of medium. Upon centrifugation, cell pellet was re-suspended in 3 mL of medium. Cell counting was manually carried out using haemocytometer and cell staining was done mixing 25 µL each of 0.4 % Trypan blue stain 0.4%, cell suspension and PBS. Cells were reseeded for maintenance and also to obtain late passage Caco-2 cells.

#### 3.3.5.2 Development of Caco-2 cell monolayer for transport experiments

This study was done with the aim of developing a robust Caco-2 cell monolayer with adequate level of P-gp transporter protein expression to facilitate identification of P-gp inhibitory and substrate activities for lower affinity antimalarial drugs. Three approaches were adopted to increase the P-gp transporter protein;

a). Exposure of Caco-2 monolayer to a known P-gp inducer; rifampicin

b). Exposure of Caco-2 cells to nanomolar concentrations of potent P-gp substrate, vinblastine for an extended period.

c). Regular passaging of Caco-2 cells in order to determine change in P-gp transporter protein levels.

### 3.3.5.3 Development of Caco-2 cell model using P-gp inducer rifampicin (Caco-2 RIF)

Passage 44 Caco-2 cell lines were grown on 0.6 $cm^2$ diameter 0.45 µM pore size Millipore PCF$^{TM}$ filter inserts at the cell density of 65,000 cells/$cm^2$. Cells were maintained using normal cell growth conditions as explained at 3.3.5.1. On day 24, cells were exposed to medium supplemented with 10 µM rifampicin. On day 28, cells were washed with PBS 3 times and incubated in normal medium for 4 hours. These cells were then used for transport experiments and bi-directional transport of rhodamine123 was determined. These studies were based on the protocol described in 3.3.6.1.1.

### 3.3.5.4 Development of Caco-2 cell model using increasing concentration of vinblastine (Caco-2 VIN)

Passage 41 Caco-2 cells frozen in liquid nitrogen were used for induction. Cells were seeded on to a 75 $cm^2$ flask in high glucose DMEM and incubated at 37 $^{\circ}$C with 5% $CO_2$. Normal cell growth medium was supplemented with either 10 nM vinblastine or 50 nM vinblastine to be used for cell growth. The second medium change was done with high glucose DMEM supplemented with 10 nM vinblastine. Cells were trypsinized on day 10 or upon 90% confluency using TrypLE Express. These cells were reseeded (20000 cells/ $cm^2$) back on a 75 $cm^2$ flask and maintained on medium supplemented with 10 nM vinblastine. This procedure was repeated for passage 42 and 43 cells and passage 44 Caco-2 cells were seeded onto 0.6 $cm^2$ Millipore PCF filter inserts at the cell density of 100,000 cells/$cm^2$. The remaining cells in aliquots were frozen in liquid nitrogen to be used for other studies. Cells on filter inserts were grown on high glucose DMEM supplemented with 10 nM vinblastine for 17 days and vinblastine concentration was increased on the day 17 to medium supplemented with 50 nM vinblastine. Cells were maintained on 50 nM vinblastine medium for 7 days and were ready for transport experiment on day 24. Similar to 3.3.5.3, Caco-2 VIN cells were washed with PBS 3 times and incubated in normal medium for 4 hours at 37 ºC with 5% $CO_2$ prior to adding drugs for transport experiment. The transport experiments for rhodamine123 were conducted following the protocol described in 3.3.6.1.1

#### 3.3.5.5 Development of late passage Caco-2 cell monolayers

Passage 18 Caco-2 cell lines were obtained from ATCC. These cells were grown on 25 $cm^2$ flask in high glucose DMEM and continuous culturing was done as described in 3.4.5.1. As described cell passaging was done every $10^{th}$ day upon reaching 90% confluency after post seeding until the cells above passage 80 were reached. This was achieved in a period about one and half years and the bidirectional transport for rhodamine123 was determined using late passage Caco-2 monolayers (P-80 and above) following the protocol described in 3.3.6.1.1.

### 3.3.6 Determinations of relative abundance of P-gp transporter protein in different Caco-2 models

#### 3.3.6.1 Study of bidirectional transport of a P-gp substrate

Bidirectional transport of the known P-gp substrate 5 µM rhodamine123 was done for all three cell models based on the transport study protocol described in 3.3.6.1.1. In order to confirm P-gp mediated efflux, rhodamine123 was combined with a known P-gp inhibitor, PSC 833, and change in bidirectional transport of rhodamine123 was studied. Significantly higher Bas-Ap directional transport compared to Ap-Bas transport was considered as the P-gp mediated efflux transport of rhodamine123. Inhibition of Bas-Ap directional transport of rohdamine123 in the presence of PSC 833 (known P-gp transport inhibitor) further confirmed the presence of active P-gp. The extent of the efflux or Bas-Ap direction transport was directly related to relative abundance of P-gp. Significantly higher Ap-Bas transport compared to Bas-Ap directional transport was considered as the cell uptake of the study drug.

##### 3.3.6.1.1 Transport experiments

The Caco-2 cells were seeded on 0.6 $cm^2$ 0.4 µM Millipore PCF$^{TM}$ filter inserts at the cell density of 65,000 cells/$cm^2$. The medium was replaced with high glucose DMEM medium twice a week and 300 and 600 µL were added to the apical and basolateral

chambers respectively. Cells were grown for 21-24 days for full maturation, formation of tight monolayers and P-gp (444-446).

Prior to the experiment, the medium in both apical and basolateral chambers was replaced with pre-warmed transport medium, HBSS or HBSS plus modulators and incubated for 30 minutes.

The Trans epithelial electrical resistance (TEER) was measured immediately before and after the experiment using an epithelial voltage/ohm meter (EVOM) and the ENDOHM 12 chamber (World precision instruments, Sarasota, FL). TEER values above 300 $\Omega.cm^2$ before and after the study were considered as appropriate for test condition for the study (446).

The filter inserts were placed in new 24 well plates to conduct the transport experiment (Figure 3.4). In the determination of apical to basolateral (AP-Bas) directional transport, the medium in the apical chamber (donor compartment) is replaced with 300 µL drug or drug + inhibitor dispersed in HBSS and basolateral chamber (receiver compartment) was replaced with 600 µL of fresh HBSS as shown in Figure 3.4a. At 30, 60, 90, 120 and 180 minutes transport medium (120 and 200µL for rhodamine123 and drug assays respectively) was collected from the receiver compartment (basolateral chamber) and was replaced with the same volume of fresh HBSS or HBSS+ inhibitors. At the end of the experiment, 100 µL of sample was removed from the donor, apical chamber.

a). b).

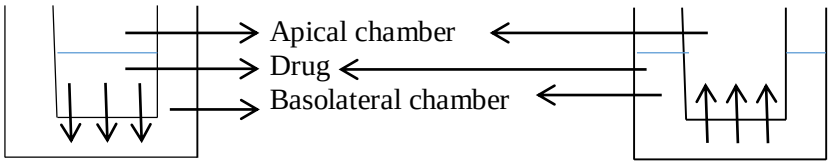


**Figure 3-4**: The diagram above shows the filter inserts placed in a 24 well plate and the arrows show the a) apical to basolateral and b) basolateral to apical directional transport of the drugs

In the determination of basolateral to apical (Bas-AP) transport, apical chamber medium was replaced with pre-warmed 300 µL HBSS and basolateral chambers were replaced

with 600 µL relevant concentration of drug or drug + inhibitor in HBSS (Figure 3.4b.). At 30, 60, 90, 120 and 180 minutes transport medium (70 and 100µL for rhodamine123 and drug assays respectively) was withdrawn from the receiver compartment (apical chamber) and replaced with blank HBSS or HBSS + inhibitor. At the end of the experiment, 100 µL of sample was removed from the donor, basolateral chamber.

The cells were kept in the incubator during the experiments and were removed from the incubator only for sample withdrawal. The plate was gently shaken soon before withdrawing the sample. The collected samples were refrigerated during the experiment. The TEER values were read at the end of the experiments to ensure monolayer tightness during the experiments. The cells were then washed with PBS three times and cell membranes were cut and placed in a microcentrifuge containing 350 µL of deionized water. Microcentrifuge tubes were sonicated for 10 minutes in a floating rack and centrifuged at 13000 RPM for 10 minutes. A sample from each supernatant was withdrawn for assay and all samples were frozen at -80 $^{\circ}$C until assayed.

The apparent permeability ($P_{app}$) value of 3 well plates were determined for each direction and mean the standard error of mean values are presented as the bidirectional transport values of the study drug.

#### 3.3.6.1.2 Determination of apparent permeability

The apparent permeability were calculated based on the below equation (421, 447, 448).

$$P_{app} = \frac{dQ}{dt} \times \frac{1}{\Delta t 60 A C_0}$$

Permeability rate = $\frac{dQ(\mu g)}{dt(min)}$

$C_0$ = Initial concentration (µg/mL)

A = Surface area ($cm^2$)

A modified version of the above equation developed by Crowe and Lemaire (447) was used to determine the permeability. This equation accounts for the amount of drug

associated with the cells (cell accumulations) at the end of the experiment. The corrected clearance volume was determined using the equation below.

$$CL.vol = A_a/\{[C_{d_0} \times V_d\text{-}[A_a+(C_a \times V_s)]\text{-}(A_c) \times n/n_{fin}\,]/V_d$$

| | | |
|---|---|---|
| CL.vol | = | Clearance volume (mL) |
| n | = | Time (min) |
| $A_a$ | = | Amount in acceptor compartment at time n (pmols) |
| $C_{d_0}$ | = | Conc. in donor compartment at time zero (nM) |
| $V_d$ | = | Volume of the donor compartment (mL) |
| $C_a$ | = | Conc. in acceptor compartment at the previous time point (nM) |
| $V_s$ | = | Sample volume of previous time point (mL) |
| $A_c$ | = | Amount of compound associated with the cells (nM) |
| $N_{fin}$ | = | Final time point (min) |

The rate of clearance was obtained by dividing the cleared volume from the time and this value was divided by the surface area of the monolayer (0.6 $cm^2$) to obtain the apparent permeability.

$$\text{Rate of clearance} = \frac{\text{CL.vol (mL)}}{\text{n (min)}}$$

$$\text{Apparent permeability (cm/sec)} = \frac{\text{Rate of clearance(mL/min)}}{\text{Surface area}(cm^2)}$$

The cleared volume for different time points were plotted against time for both Ap-Bas and Bas-Ap transport and the slope of the regression line was divided by the surface area of the monolayer to obtain the apparent permeability in cm/sec.

### 3.3.6.2 Visual confirmation of P-gp by Western blotting

Passage 44 (early) and 80s (late) Caco-2 cell lines were seeded on 9.6 $cm^2$ diameter 6 well plates at cell density of 10,000 cells/$cm^2$. Passage 44 Caco-2 cells lines exposed to 10 nM vinblastine for 3 passages (41-43) were seeded onto a 6 well plate at the cell density of 20,000 cells/$cm^2$. Similar to 3.3.5.4, cells were grown on medium supplemented with 10 and 50 nM vinblastine for 17 and 7 days respectively. Cells from early, late and Caco-2 VIN were lysed on day 21, 24 and 28 and cell lysates were prepared as described in 3.3.6.2.2. Passage 44 Caco-2 cells seeded at 10, 000 cells/$cm^2$ on 6 well plates were exposed to 10 µM rifampicin from day 24 to 28 and cells were lysed on day 28 and cell lysate was prepared. The protein content was determined based on modified micro plate Lowry protein assay as described in 3.3.6.2.1. A constant amount of protein; 60 µg of was loaded and Western blotting was done following the protocol described in 3.3.6.2.2.

#### 3.3.6.2.1 Modified micro plate Lowry protein assay

Bovine serum albumin stock solution, 2000 µg/mL was prepared in deionized water. The stock was diluted to prepare 10, 20, 50, 100, 150, 250, 500, 1000, 1500 µg/mL All samples were assayed in duplicates using the microLowry protein assay. Samples and lysis buffers were diluted at 1:6 in 96 well plates and 120 µL of Lowry reagent was added and incubated in room temperature. After 15 minutes of incubation 60 µL of 0.5 N Folin reagent was added and incubated for 30 minute in the plate shaker. The absorbance was read at 750 nm using a TECAN SUNRISE microplate absorbance reader (Austria, Europe) and protein content was determined using the standard curve.

#### 3.3.6.2.2 Western blotting

**Preparation of cell lysate**

The cells grown on 6 well plates were washed with PBS 3 times. Lysis buffer (300 µL) was added and incubated for 30 minutes. Upon lysis, cell suspension was collected into

a microcentrifuge tube and passed through a 21 gauge needle about 10 times to maximize cell lysis. Microcentrifuge tubes were centrifuged at 13000 RPM for 10 minutes and the supernatant was collected. Protein solution was frozen at -20 $^{\circ}$C.

**Western blotting**

The total protein content of the supernatant was determined using the Lowry protein assay. Protein samples/ supernantant were processed by adding 25% Nupage sample buffer, 10% reducing agent and 65% of the protein sample to a total volume of 35 µL. This was reduced by heating for 5 minutes at 95 $^{\circ}$C. Uniform amount (70 µg Caco-2 and 30 µg for LS174 indcution studies) of proteins was loaded on to 4 -12 % Bis Tris Plus 15 well plates. SeeBlue precolured molecular weight marker 10 µL was used as visual guide to electrophorosis. Gels were run at 165 V for 60 minutes using Novex Bolt Mini Gel Tank (Life Technologies, CA, USA). Immuno blot PVDF membrane were activated by soaking with methanol for 2 minutes, water for 2 minutes and finally with transfer buffer. The transfer cassette was prepared per manufacturers specification and transfer was done at 34 V for 95 minutes in a Xcell II Bolt Module (Novex, CA, USA). PVDF membrane was washed for 5 minutes using TBST. The membrane was blocked over-night at 4 $^{\circ}$C using 2% casein in TBS and washed 2 times using TBST (each was of 5 minutes duration). The primary antibody; Mdr (G-1) mouse monoclonal IgG2b 200 µg/mL in 1/225 ratio and mouse anti-beta actin (beta actin was used as the reference protein) in 1/7500 ratio was diluted in filtered blocking solution (1% casein in TBS). The membrane was incubated in the prepared primary antibody solution at room temperature in on a rocker platform for 2 hours. Upon incubation, the membrane was washed 4 times using TBST (each was of 5 minutes duration). The antibody; HRP linked 1 goat anti mouse secondary antibody was diluted in blocking solution at 1/6000 ratio and membrane was incubated in secondary antibody for 1.5 hours at room temperature. The membrane was washed 4 times in TBST and incubated in a BioRad clarity chemiluminescent substrate for 2-5 minutes. The chemiluminescent substrate was prepared by mixing 1 mL each of substrate and enhancer. The membrane sandwich was prepared for luminograph, using 2 plastic transparent sheets. The blot was read and semi quantified using the BIORAD Chemidoc mpt imager with Image Lab$^{TM}$ software.

### 3.3.7 Data analysis

The apparent permeability values were calculated based on the equation described above and Microsoft EXCEL template was used for calculations and graphing. Standard errors and two tailed t test were done using SigmaPlot version 12.5 Systat Software, Inc. (Chicago, IL).

Efflux ratios were calculated by dividing $P_{app}$ of Bas-Ap from Ap-Bas values. A higher Bas-Ap transport ($P < 0.05$) compared to Ap-Bas transport was considered as possible efflux and a higher Ap-Bas transport ($P < 0.05$) was considered as possible uptake of drug. The results are presented as the mean ± standard error of mean.

## 3.4 Results

### 3.4.1 Development of a robust Caco-2 model for bidirectional transport studies

The early and late passage Caco-2 cell monolayer showed TEER values above > 300 Ω.cm$^2$ within 21 to 24 days and hence transport studies were carried out during this period. The Caco-2 VIN model studies were done on day 24 as it took up to day 24 to achieve the TEER value above 300 Ω.cm$^2$. The Ap-Bas and Bas-Ap directional transport of rhodamine123 through passage 44 Caco-2 cells are shown in Figure 3.5.

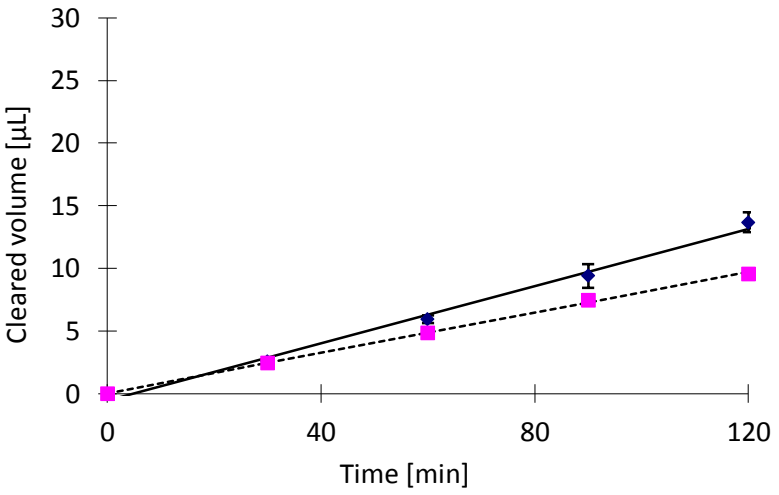


**Figure 3-5**: Ap-Bas (■) and Bas-Ap (◆) directional permeability of rhodamine123 across P-44 Caco-2 cell monolayer (N=3, Mean ± SEM)

Apparent permeability values for 5 µM rhodamine123 through 3 cell monolayer models; cells exposed to rifampicin (Caco-2 RIF), Caco-2 exposed to increasing concentrations of vinblastine (Caco-2 VIN) and late passage Caco-2 (P-80s and above) are given in the Table 3.1.

**Table 3-1:** Apparent permeability ($P_{app}$ ± SEM, N=3) for Rhodamine123 (5 µM) alone and when combined with PSC 833 (4 µM) for different Caco-2 cell monolayer models

| Caco-2 monolayer models | Drug | Ap-Bas ($10^{-6}$ $cm^2$/min) | Ap-Bas TEER[b] | Bas-Ap ($10^{-6}$ $cm^2$/min) | Bas-Ap TEER[b] | Efflux ratio | Net transport[a] (P value) |
|---|---|---|---|---|---|---|---|
| P- 44 | Rh123 | 2.2 ± 0.1 | 357 | 3.2 ± 0.2 | 387 | 1.4 | Efflux (0.02)* |
| | Rh123 + PSC | 2.3 ± 0.2 | 410 | 2.3 ± 0.1 | 390 | 1.0 | No flux (0.98) |
| Caco-2 RIF | Rh123 | 2.1 ± 0.0 | 403 | 3.1 ± 0.3 | 420 | 1.5 | Efflux (0.01)* |
| | Rh123 + PSC | 2.8 ± 0.2 | 452 | 2.6 ± 0.1 | 432 | 0.9 | No flux (0.57) |
| Caco-2 VIN | Rh123 | 0.5 ± 0.0 | 603 | 6.6 ± 0.4 | 614 | 13.2 | Efflux (0.0001)*** |
| | Rh123 + PSC | 0.7 ± 0.1 | 628 | 0.6 ± 0.0 | 599 | 0.9 | No flux (0.31) |
| P- 80 | Rh123 | 0.5 ± 0.1 | 665 | 2.4 ± 0.3 | 760 | 4.7 | Efflux (0.003)** |
| | Rh123 + PSC | 0.5 ± 0.1 | 680 | 0.5 ± 0.0 | 674 | 1.0 | No flux (0.96) |

* Significant at the level of $P < 0.05$, ** Significant at the level of $P < 0.005$, [a] The $P_{app}$ of Bas-Ap direction was divided by the Ap-Bas direction to obtain net transport, [b] The mean TEER value for 3 well plates before the test.

As shown in Table 3.1, Bas-Ap directional transport of rhodamine123 was significantly higher compared to AP-Bas directional transport in all four versions of Caco-2 cells tested. Therefore higher serosal to luminal directional transport (efflux) of rhodamine123 rather than luminal to serosal directional transport (uptake) of rhodamine123 is evident. The addition of PSC 833 inhibited the efflux transport of rhodamine123 and efflux ratio dropped to one indicating no net transport. Therefore it is evident that P-gp transporter proteins are expressed in early, Caco-2 RIF, Caco-2 VIN and late passage Caco-2 cell monolayers.

The Ap-Bas directional transport of rhodamine123 in Caco-2 VIN and late passage Caco-2 cell models was around $0.5 \times 10^{-6}$ cm/sec and the cell intake was about 4 fold lower than the early passage and Caco-2 RIF models where $P_{app}$ was in the range of 2.1-$2.2 \times 10^{-6}$ cm/sec. The serosal to mucosal directional efflux transport of rhodamine123 in the late passage Caco-2 was not higher compared to early passage Caco-2 cells. However the drop in cell uptake or Ap-Bas directional transport clearly increased the efflux ratio (1.4 to 4.74) in late passage Caco-2 cells compared to the earlier passage. Therefore later stage Caco-2 monolayers are more likely to identify moderately effluxed

P-gp substrate and thus a better model than early passage Caco-2 cells. Both early and late passage cells had cell differentiation, monolayer tightness and reached TEER > 300 $\Omega.cm^2$ by day 21-24 therefore form a good cell barrier for drug transport. But P-gp expression appeared to be higher in late passage cells and this is also illustrated in Western blotting image section (Figure 3.10).

The attempt to force a P-gp overexpression by using a continuous low level of vinblastine exposure to stress the Caco-2 cells was productive and resulted in much greater rhodamine123 efflux than that developing naturally during late passage culture. Caco-2 VIN showed the highest increase in P-gp with an efflux ratio of 13 for rhodamince123. The highest serosal to mucosal directional transport (efflux) was also observed for Caco-2 VIN model and was $6.6\times 10^{-6}$ cm/sec. However, this was rather a time consuming approach to increase P-gp expression with 3 passages of previous ongoing exposure and further exposure of vinblastine at two different concentrations. Given that late passage Caco-2 cells started to exhibit sufficient spontaneous P-gp expression, it was decided to use late passage Caco-2 cells in preference to vinblastine loading of Caco-2 cells for many studies during this thesis.

P-glycoprotein induction using rifampicin exposure did not result in notable increase of rhodamine123 Bas-Ap transport.

The presence of P-gp was further proven by complete blockage of rhodamine123 efflux transport when combined with of P-gp inhibitor, PSC 833 as shown in figures 3.6 to 3.8 for interventions (Caco-2 RIF Caco-2 VIN and late passage Caco-2 cells).

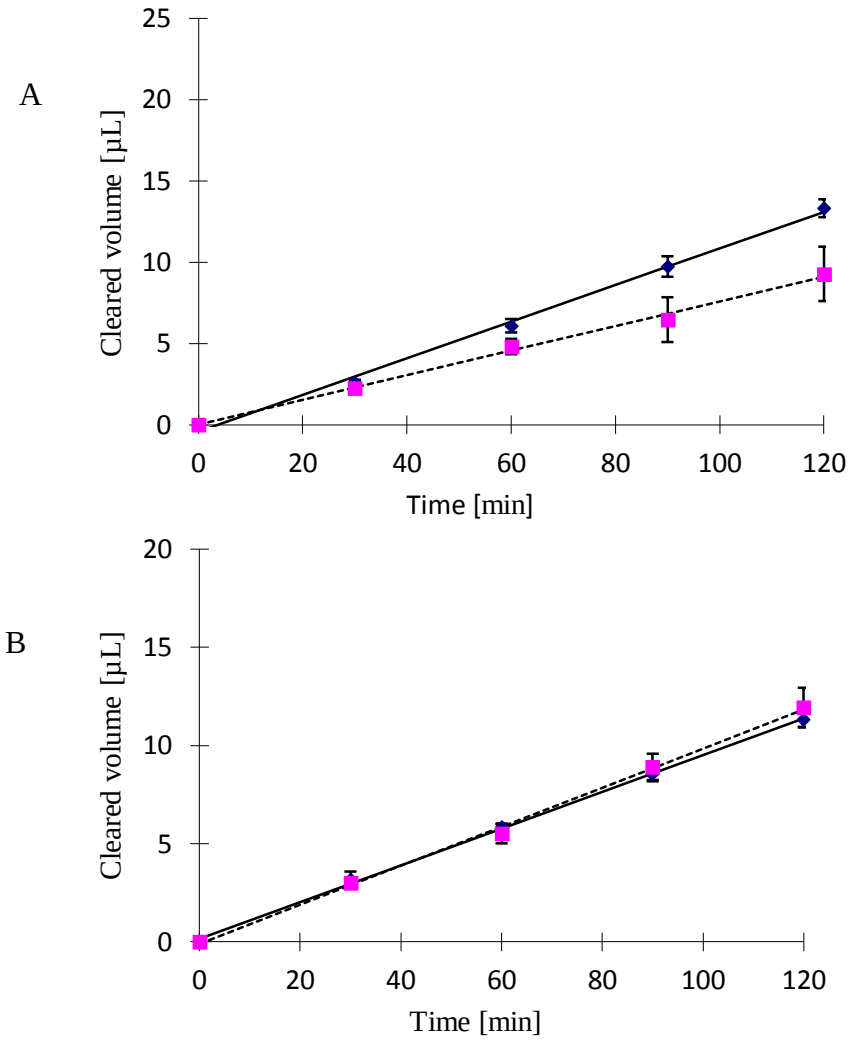


**Figure 3-6**: Ap-Bas (■) and Bas-Ap (◆) transport rhodamine123 alone (A) and combined with P-gp inhibitor PSC 833 (B) across Caco-2 RIF (N=3, Mean ± SEM)

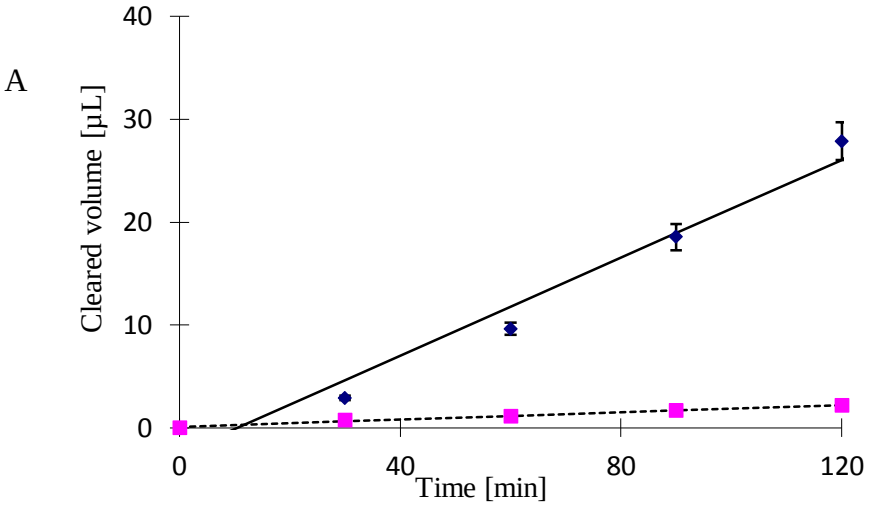

B

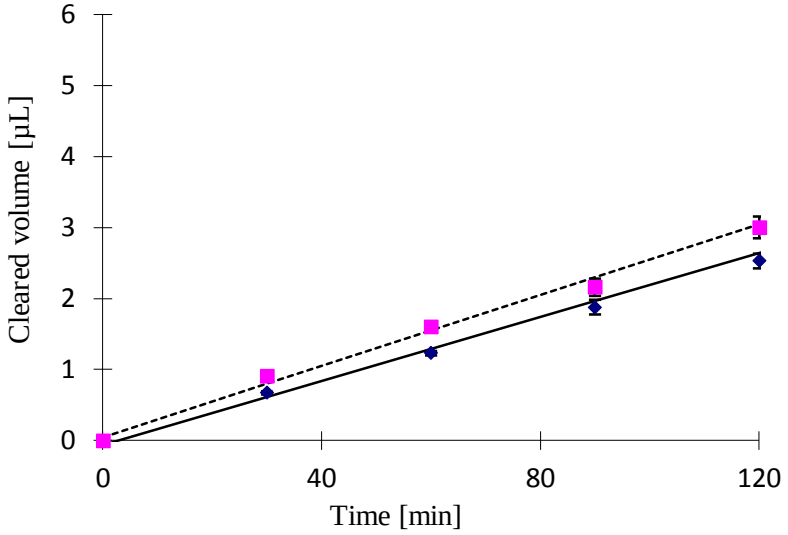


**Figure 3-7** : Ap-Bas (■) and Bas-Ap (◆) transport rhodamine123 alone (A) and combined with P-gp inhibitor PSC 833 (B) across Caco-2 VIN (N=3, Mean ± SEM)

A

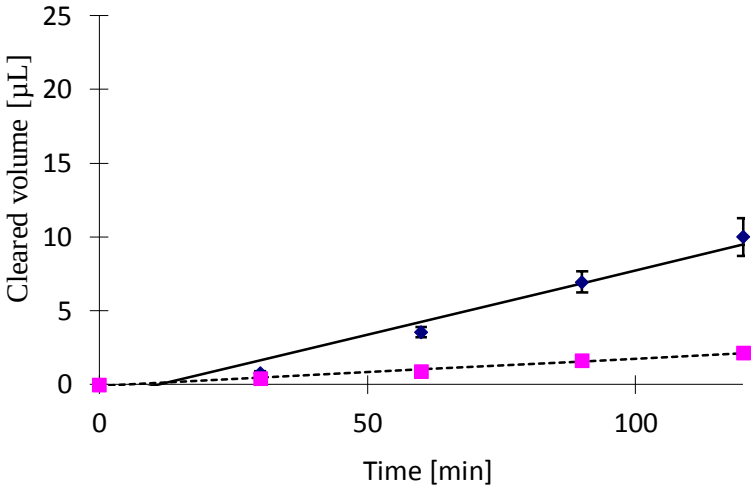


B

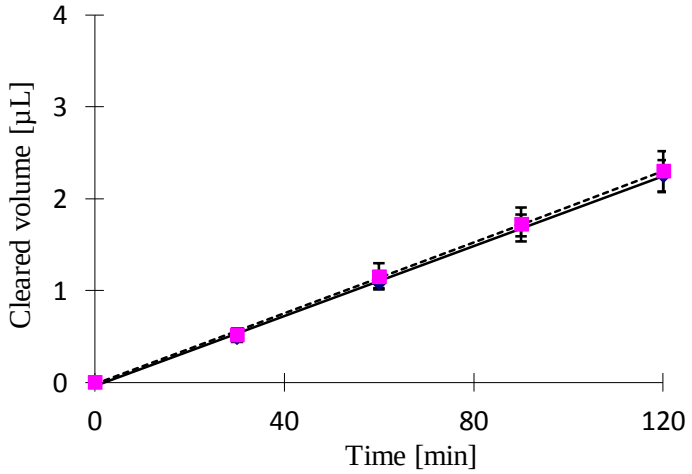


**Figure 3-8** : Ap-Bas (■) and Bas-Ap (◆) transport rhodamine123 alone (A) and combined with P-gp inhibitor PSC 833 (B) across P-80 Caco-2 cell monolayer (N=3, Mean ± SEM)

Relative abundance of P-gp transporters in different Caco-2 monolayers were determined using Western blot analysis.

Western blot images for the expression of P-gp protein are shown in Figure 3.9; Lanes 1 to 2: P-44 days 24 and 28, lane 3: P-44 Caco-2 RIF, lanes 4-6: Passage 83 day 21, 24 and 28, lane 7-9: Caco-2 VIN days 21, 24 and 28 and lanes 11 and 12 are molecular weight marker and Hela cell Positive control.

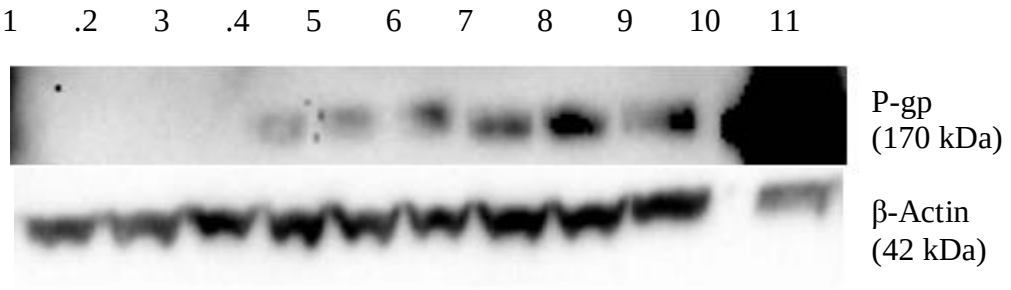


**Figure 3-9**: Western blot analysis for MDR1 P-glycoprotein (170kDa) and beta-actin (42 kDa) for 3 Caco-2 cell models. Lanes 1 to 2: P-44 days 24 and 28, lane 3: P-44 Caco-2 RIF, lanes 4-6: Passage 83 day 21, 24 and 28, lane 7-9: Caco-2 VIN days 21, 24 and 28 and lanes 10 and 11 are molecular weight marker and Hela cell Positive control respectively

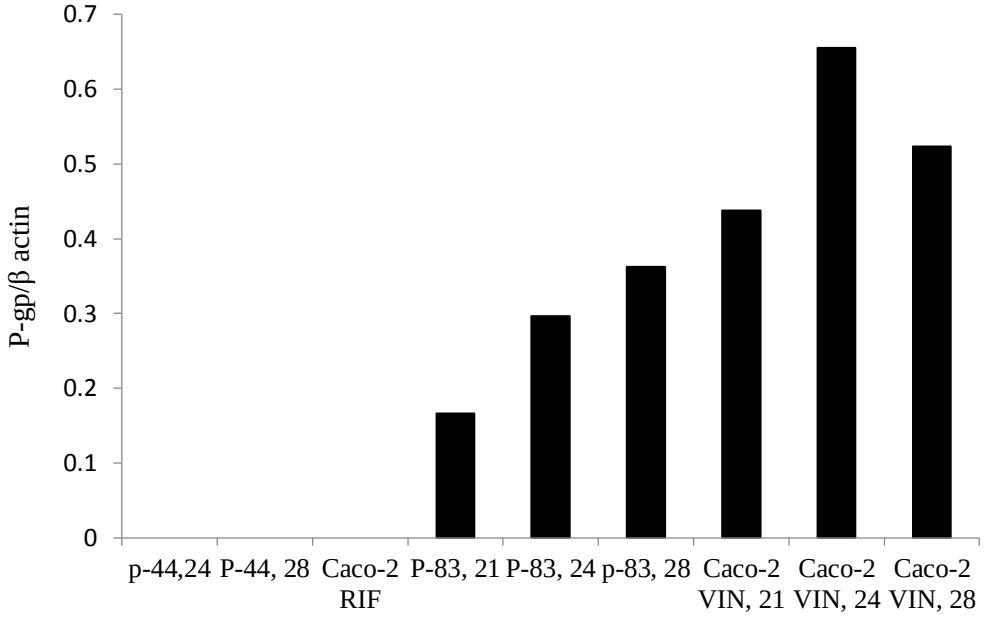


**Figure 3-10** : Expression of P-gp over day 21 to 28 for P-44 cells and 3 cell models [1-2 (P-44), 3 (Caco-2 RIF), 4-6 (P-83 caco-2), 7-9 (Caco-2 VIN)]

The highest P-gp expression was observed for day 24 Caco-2 VIN model (Lane 9) and highest P-gp expression for P-83 Caco-2 cells were observed for day 28 (Lane 7). The day 24 P-gp levels for Caco-2 VIN cells were 3 fold higher compared day 21 P-83 Caco-2 cells (Figure 3.10). This was consistent with rhodamine123 efflux ratios observed (4.7 for P-80 and 13 for Caco-2 VIN model) for 2 cell models. P-44 cells and Caco-2 RIF gave faint bands for P-gp and were unable to quantify.

Western blotting images further confirmed that the late passage Caco-2 cell lines and cells exposed to increasing concentration of vinblastine were better models to determine P-gp mediated drugs transport compared to the early passage Caco-2 cell lines.

Early passage Caco-2 cells were used for initial drug transport studies and the study was repeated using late passage Caco-2 cells.

Drug transport of antimalarials was studied using Caco-2 VIN and Caco-2 RIF models for further confirmation of results as necessary.

## 3.5 Discussion

In-vitro Caco-2 cell monolayers are the most widely used epithelial cell model for drug transport studies. Caco-2 cells have some advantages over other cell lines that form tight junctions such as the canine cell line, MDCK, which is transfected with human MDR1. Unlike the Caco-2 cells, the MDCK cell line is not of human origin and requires maintenance of high P-gp levels and tight junctions using selection pressures. Further, these transfected MDCK cell lines require a usage agreement with the laboratories that created them as they are modified cells and can also be time consuming to create de novo. Whereas Caco-2 cells are commercially available from ATCC and a good correlation is established between ABC transporter protein expression of in-vitro Caco-2 cells and in-vivo jejunum (372). Most importantly, the column shape and microvilli architecture of the Caco-2 cells allow good *in-vivo* and *in-vitro* correlation, which enables good predictions of *in-vivo* drug absorption from in-vitro apparent permeability values (372, 420, 421, 449).

The main limitation noted for use of Caco-2 cells is its heterogenic nature between labs and within each lab (416). These changes could be cell characteristics in relation to the passage number and the culturing condition within and between laboratories. Hence to minimise variability, consistent cell culture conditions were adopted in our laboratory and maintained throughout the current study. Cells were passaged upon 90% confluency to obtain maximum P-gp expression.

The passage 18 cells obtained from the ATCC for the study had little functional P-gp expression and had poorer tightness between cells. Therefore labs considering Caco-2 bidirectional efflux studies to examine P-gp substrates activity of drugs are likely to get leaky monolayers (low TEER) and low expression of P-gp at the time of test if they use low passage number Caco-2 cells.

There is some evidence in the literature supporting this. For instance, a bidirectional transport study examining peptidomimetics using passage 35-50 cells concluded that the drugs themselves were not P-gp substrates as their transport was equivalent in both directions (450). Similarly, high cell uptake for cephalosporin antibiotics were reported in passage 37 Caco-2 cells (451). While our data suggests that P-gp in early passage Caco-2s may not have been as active compared to late passages, potentially masking any real P-gp mediated efflux. Other groups that have used low passage number Caco-

2 monolayers have focused on permeability characteristics that have little to do with active efflux proteins. (452, 453), and such data would be expected to be relatively consistent irrespective of the passage used.

In this study, three interventions; Caco-2 RIF, Caco-2 VIN and continuous passaging were adopted to improve P-gp expression of early passage Caco-2 cells. Upon development of the models, cell characteristic were studied visually by Western blotting technique and functionality of the P-gp was monitored by a bidirectional transport study of a known P-gp substrate, rhodamine123. Passage 41 cells were used as the baseline cells.

The very low passage Caco-2 cells obtained from ATCC were continuously passaged. The Caco-2 cells grown for three weeks on filter inserts reached TEER values between 250 to 350 ohm.cm$^2$ for passage 20-25 and 300 to 500 ohm.cm$^2$ for passage 44s. This was one of the primary reasons for continuous passaging of Caco-2 after acquisition from ATCC. The continuous passaging enabled tighter monolayers with higher TEER (600-800 ohm.cm2) on millicell inserts for late passage Caco-2 cells (passage 80). A change in P-gp expression was also observed over 40 passages of Caco-2 cells, Ap-Bas transport of rhodamine123 was altered in late passage cells (P80+) compared to earlier passages ( < P 40s). The early passage cells had high cell uptake of rhodamine123 (2.2×10-6 cm/sec), and this dropped to 0.5×10-6 cm/sec for late passage cells. The change in rhodamine123 uptake could be attributed to increased expression of P-gp in late passage Caco-2 cell monolayer and formation of tighter monolayers. Passage number caused no significant differences in Bas-Ap transport of rhodamine123. However, the Ap-Bas changes were enough to increase the efflux ratio to 4.7 for P-80 compared to 1.4 for passage 44 cells. Western blotting imaging and quantification showed a clear increase in P-gp expression in late passage Caco-2 cells (Figure 3.9). Thus in keeping with the current literature (416), an increase in the P-gp expression over 40 passages was observed (not merely an increase in monolayer tightness) which would mostly affect the cell uptake of the potent P-gp substrate rhodamine123. Hence, it was important to study the bidirectional transport of a standard P-gp substrate (such as rhodamine123) at regular intervals with the increase in passages number (especially when the Caco-2 cells ordered from ATCC were at passage 18) (454).

A small increase in P-gp expression was also observed for P-80 cells over day 21, 24 and 28 with the highest P-gp expression on day 28. This observation is consistent with the current literature where Hosoya and co-workers (445) observed a significantly higher P-gp expression on day 27 compared to day 17.

P-gp induction properties by rifampicin have been shown before (455). However induction of P-gp expression using the P-gp inducer rifampicin did not alter the P-gp expression of P-44 cells to a notable level compared to those treated with normal media (The efflux ratio increased from 1.4 to 1.5) in the present study. The low passage Caco-2 cells with inherently low P-gp expression might not have the capacity to upregulate P-gp expression following short term co-incubation (48 hours) with an inducer such as rifampicin. It is also likely that Pregnane X receptor, the target of rifampicin is expressed in low amounts in the nuclei of these cells. In a study of P-gp induction using grapefruit juice, a much lower upregulation of P-gp expression was observed in passage 30 to 40 Caco-2 cells compared to MDCK-MDR1 cell lines. Similar to the present study, the P-gp expression of Caco-2 could be due to the inherently low P-gp in early passage Caco-2s. Hence, a short term induction model using P-gp inducer was of limited use.

However, long term exposure of P-gp inducers were successful in the current study. In the third intervention, cells were exposed to a potent P-gp substrate, vinblastine (Caco-2 VIN) at low levels for an extended period in increasing concentrations (10-50 nM) (419). The short-term culture method using differentiation medium suggested in Shirasaka and colleagues (419) was not adopted in the current study due to concerns regarding the cell monolayer tightness. This approach does not depend on Pregnane-X receptor but instead is a more chronic cell stress approach to force the cells to create more functional P-gp for their own survival. Out of the three models, Caco-2 VIN model showed the highest P-gp expression with an efflux ratio of 13. Low nanomolar concentrations of vinblastine used in the study were not found to be toxic to the cell monolayer despite the cytotoxic nature of the drug. However, use of higher cell numbers (100,000 cells/cm2 compared to 65,000 cells/cm2 for other intervention) was required when cells frozen in liquid nitrogen were seeded. The Caco-2 VIN cells reached required TEER levels which were maintained throughout the experiment. The Bas- Ap directional transport of rhodamine123 increased by about three fold. This was also visually apparent in Western blots where day 24 P-gp expression for Caco-2 VIN was three fold higher than the day 21 late passage Caco-2. Hence, the increase in efflux was

directly related to the increased P-gp expression. The Papp values for Ap-Bas directional transport of rhodamine123 was similar for both late passage Caco-2 cells and the Caco-2 VIN model, hence having similar drug absorption values, while Caco-2 VIN increased the saturation threshold for the P-gp substrate of interest. This allowed identification of low affinity P-gp substrates.

The early passage cells had comparatively lower P-gp expression; therefore this cell model is unlikely to be useful for identification of low affinity P-gp substrates. Further, extensive cell uptake could be observed for potent P-gp substrates. However, the Ap-Bas directional transport of passively permeable drugs will be minimally affected by the changes in P-gp expression in most instances. Thus, when P-gp was not likely to be involved and instead the cell monolayer only represented a physiologically relevant barrier that reflects physicochemical properties of the drugs, irrespective of early or late passages, the Caco-2 model exhibited similar results. Hence, the early and late passage Caco-2 cell models compared well to determine the passive permeability of antimalarials not shown to be P-gp substrates.

## 3.6 Limitations

The up-regulation of P-gp expression was determined by Rh123 transport and Western blotting. Molecular level confirmation based on PCR would have added increased validity and provided the molecular basis.

Further passaging of late passage (> P- 80) Caco-2 cells and Rh123 transport studies on these cells would have been helpful to further confirm the results.

The comparison of Caco-2 cell models with other *in-vitro* cell models such as MDCK MDR1 cells lines would have increased the validity, but this cell line was not commercially available.

## 3.7 Conclusion

A clear change in P-gp expression was observed over 40 passages of Caco-2 cells. A significantly higher P-gp expression was observed in the late passage Caco-2 cells and was suitable to use as a cell model for identification of the P-gp mediated drug transport of antimalarials. Exposure of Caco-2 cells to the P-gp inducer, rifampicin did not result in a notable increase in the P-gp efflux of rhodamine123. The Caco-2 VIN model had the highest P-gp expression and can function as an *in-vitro* model to identify P-gp substrates with low affinity for P-gp. Both early and late passage Caco-2 cells are suitable to determine the passive permeability of a drug.

# 4 Antimalarial transport studies

## 4.1 Rationale

The antimalarials drugs are administered orally in single and combination therapy for the management of uncomplicated *Plasmodium falciparum* malaria.

Development of drug resistance is a major problem in the management of malaria and there are reports of increased resistance for current artemisinin combination therapies. Antagonistic pharmacokinetic interactions are possible in antimalarial combination therapy and this could be drug absorption related. Hence it is important to look at the drug permeability and P-glycoprotein mediated transport of available antimalarial drugs. Clear evidence of the pharmacokinetics of antimalarials helps in the design of optimum dosage regimens which indirectly helps in combating the development of drug resistance in antimalarial therapy.

P-gp drug interactions result from concurrent administration of P-gp substrates and inhibitors. Pre-exposure to P-gp inducers could lead to decrease in absorption of a P-gp substrate. This could be a potential issue especially in antimalarial therapy as antimalarials are recommended to be administered in combinations. In Africa and South East Asia where malaria is endemic the probability of patients receiving antimalarial therapy, while being on other medications, is high. For example, many antivirals used in HIV antiretroviral therapy are identified as P-gp substrates and concurrent administration of antiviral and antimalarial drugs (77, 78, 173) with P-gp inhibitory properties can result in an unexpected increase in systemic availability of the P-gp substrate.

The literature on P-gp substrate and inhibitory actions of antimalarials is limited and no or little information of this relates to combination therapy. Artesunate and dihydroartemisinin are artemisinin derivatives used in the combination therapy of malaria. However artesunate is costly to manufacture (64) and its active metabolite dihydroartemisinin can cause neurotoxicity (68, 69). There are also reports of drug resistance developing for these derivatives (456). In order to address these issues of the currently available artemisinin derivatives, a new artemisinin derivative, artemisone,

has been introduced. The drug permeability and P-gp mediated drug transport of artemisone is not available for either single or combination therapy. It is proposed that artemisone can be given in combination with long acting quinolone derivatives such as amodiaquine and mefloquine (70). Thus it is important to determine the permeability of artemisone in single therapy in order to establish whether the permeability of artemisone would be altered in combination therapy.

Methylene blue in the treatment of malaria has been revisited and clinical trials have found superior efficacy of methylene blue plus amodiaquine therapy compared to artesunate plus amodiaquine therapy (145). Methylene blue can be administered both orally and intravenously. Similar to artemisone, permeability data and the P-gp substrate or inhibitory action of methylene blue has not been reported. It is important to determine the drug permeability and possible P-gp mediated drug interactions of methylene blue to optimize dosing in patients.

The literature on P-gp inhibitory properties of artesunate is conflicting. In two *in-vitro* studies, artesunate at 100 µM, 200 µM and 1 mM has shown P-gp inhibitory properties (440, 457). In contrast to this another study claimed lack of P-gp inhibitory properties of artesunate (439). Thus additional literature on P-gp inhibitory properties would be valuable.

Drug permeability data for mefloquine and artesunate has not been reported.

Literature on the permeability and P-gp substrate and inhibitory properties of antimalarial drugs is incomplete. There is some information on one or more of these properties for the four drugs; mefloquine, amodiaquine, artesunate and dihydroartemisinin. However, available studies discuss only the inhibitory properties of antimalarials in single therapy. There are no reports on these properties in antimalarial combination therapy to date, and this would be a valuable addition to the current literature.

Regulation of P-gp expression of antimalarials has been published for artemisinin; however this information is not available for artesunate, artemisone, amodiaquine and mefloquine. Similarly P-gp regulation in artemisinin combination therapy has not been reported in the literature to date. Up regulation of P-gp transporter protein can result in decreased systemic exposure of P-gp substrates subsequently administered, which can

lead to loss of pharmacological activity of a drug, treatment failure and eventually drug resistance.

In this context it was aimed to determine permeability and P-gp mediated drug transport of antimalarials in single and combination therapy using *in-vitro* Caco-2 based cell model.

## 4.2 Specific Objectives

To establish analytical techniques for quantification of anti- malarial drugs (artesunate, artemisone, mefloquine, amodiaquine and methylene blue) in the laboratory.

To determine the inhibitory properties of anti-malarial drugs against P-gp mediated drug efflux.

To determine drug permeability and the potential involvement of MDR1 P-gp mediated drug efflux of antimalarials.

To determine the role of antimalarial drugs in the regulation of MDR1 P-gp transporter expression.

## 4.3 Methods

### 4.3.1 P-gp inhibitory properties of antimalarials

The P-gp inhibitory properties of single and combination therapy antimalarials were studied at 100 and 300 µM concentration. Antimalarials were combined with the known P-gp substrate, 5 µM rhodamine123, and change in efflux transport of rhodamine123 was studied. As mentioned above, the maximum concentration tested was 300 µM due to solubility limitations and possible toxicity of the drugs on the cell monolayer at higher concentrations.

The early and late passage Caco-2 cell lines were used to test the inhibitory properties of the antimalarials.

Rhodamine123 levels were quantified using fluorescence detection and method described in 3.4. See Figure 3.3 for normal calibration curve for rhodamine123. However when rhodamine123 was co-incubated with methylene blue a reduction in rhodamine123 absorbance was observed at high concentrations. Therefore rhodamine123 standard curve for determination of rhodamine123 for efflux for methylene blue and rhodamine123 co-incubation study was done by serial dilution of rhodamine123 and methylene blue stock sample (10 µM each) (Figure 4.1).

#### 4.3.1.1 Assay of rhodamine123 in the presence of methylene blue

A1

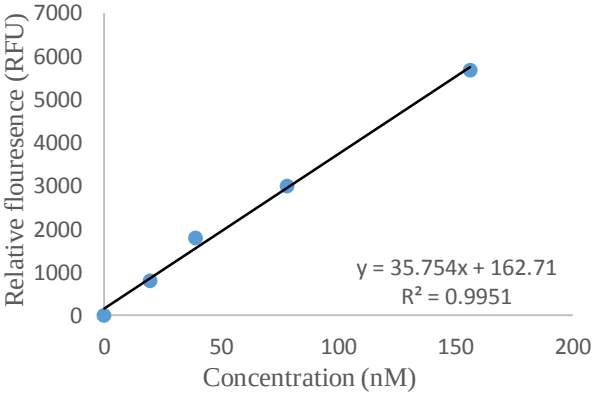


A2

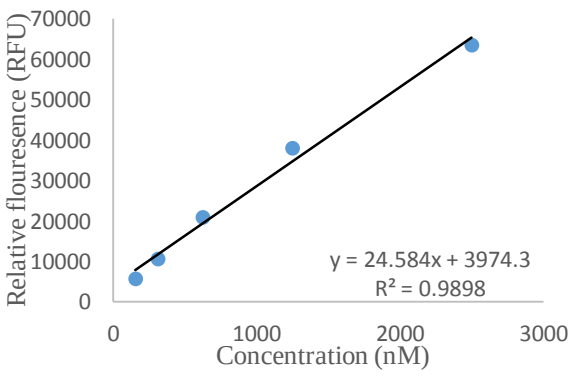

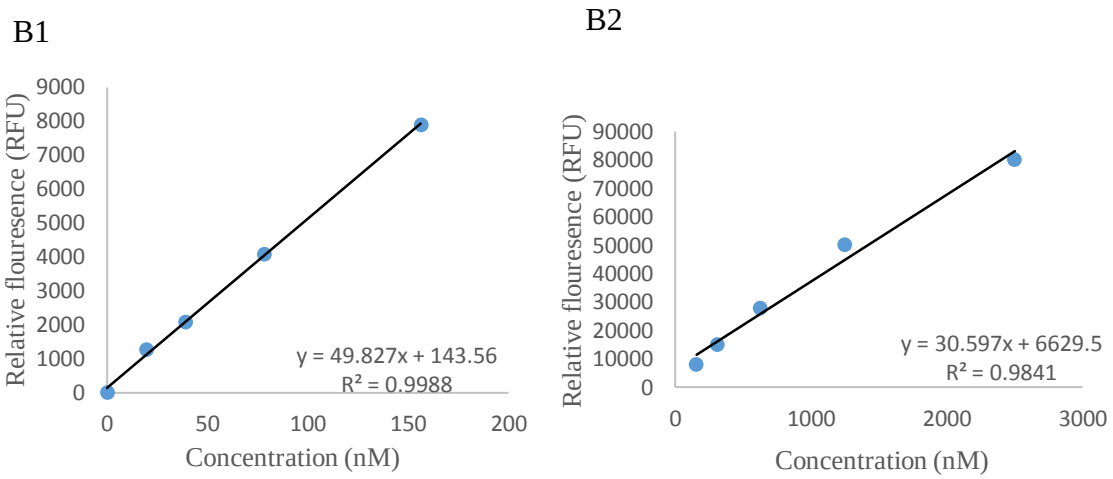


**Figure 4-1** : Calibration curve for rhodamine 123 in the presence of methylene blue for concentration range A1) 0- 160 nM, A2) 160- 3000 nM for 70 µL and B1) 0- 160 nM, B2) 160- 3000 nM for 120 µL

### 4.3.2 Drug permeability and P-gp substrate of antimalarial drugs

The permeability and P-gp substrate activity of antimalarials in single and combination therapy were studied at 10, 20 or 100 µM. Methylene blue transport was studied at 100 µM as 10 µM resulted in low recovery due to high percentage cell accumulation of methylene blue. Artesunate test dilutions were prepared at 100 µL due to drug degradation to its metabolite dihydroartemisinin. The study was initially designed to study the permeability activity of antimalarials 10 µM (low concentration) and 100 µM (high concentration). However the lower concentration of 10 µM was increased to 20 µM for later studies to increase the recovery of drugs in the system, and thus, improve reliability of the results.

The permeability and P-gp substrate activity was determined by studying the bi-directional (Ap-Bas and Bas-Ap) transport of antimalarial drugs. P-gp substrate activity or P-gp mediated efflux transport of antimalarial was confirmed by combining the drug with known P-gp inhibitor, PSC 833. Full or partial inhibition of efflux transport by PSC 833 suggested the presence of P-gp mediated drug efflux.

### 4.3.3 Drug transport studies

Bidirectional transport studies of antimalarials were conducted based on the method described in 3.3.6.1.1. The transport experiments were repeated in at least two concentrations. The permeability tests of methylene blue were performed in 10 and 100 µM (however due to lower recovery at 10 µM, the results are not shown in the thesis). Samples were collected at 30, 60, 90 and 120 minutes (triplicates, N=3 for each sample point) for both Ap-Bas and Bas-Ap directional transport. The TEER values were measured just before and at the completion of the experiment. The experimental results were considered valid only if the TEER was maintained > 300 Ω.cm2 throughout the experiment. Passive permeability and absence of paracellular permeability was based on > 300 Ω.cm2 TEER values before and throughout the experiments. The apparent permeability (Papp) value of 3 well plates (N=3) were determined for each direction and mean ± standard error of mean values are presented as the bidirectional transport values of study drugs.

Amodiaquine, mefloquine and methylene blue drug samples were assayed using HPLC techniques and artesunate, artemisone and dihydroartemisinin were assayed using LCMS-MS techniques.

### 4.3.4 Assays of mefloquine, amodiaquine and methylene blue

#### 4.3.4.1 HPLC instrumentation and chromatographic conditions

All three drugs were assayed using High Performance Liquid Chromatography (HPLC) techniques. The analysis was performed using Agilent 1200 series HPLC consisting of binary gradient pump with a degasser, auto sampler, a thermostated column oven and a duel wave length UV detector (Agilent Technology, Waldbronn, Germany). Chemstation software version, Rev. B. 03.01.SRI was used to process data (Agilent Technology, Waldbronn, Germany).

#### 4.3.4.2 Development of calibration curves for mefloquine, amodiaquine and methylene blue

All authentic standard curves were prepared at the concentration of 20 mM in ethanol, aliquots and stored at -80 °C. Working standard solutions were prepared by serial dilution in HBSS from the primary stock regularly. Standard curves were prepared in HBSS as the analytical samples were dispersed in HBSS. Two separate calibration curves were constructed for lower and higher concentration ranges of each drug.

##### 4.3.4.2.1 Assay of mefloquine

Assay of mefloquine was adopted from Davis and colleague (458) with slight modifications. Drug transport study samples obtained at different time points were collected in HPLC vials and stored at – 80 °C. Samples were in HBSS solution and did not require further extraction; therefore analysis was carried out without including an internal standard. Separations were performed using an Apollo $C_{18}$ (5 µm, 4.6x150mm) column attached to an Apollo $C_{18}$ (5 µm, 4.6x5.5 mm) guard column. The mobile phase consisted of $KH_2PO_4$ (w/v 20 mM) in deionized water (42% v/v) adjusted to pH 3.0 using $H_3PO_4$ and acetonitrile (58:42). The injection volume was 40 µL. The mobile phase was pumped at 1 mL/min and the analytes were detected at UV absorbance 222 nm. The column oven was maintained at 35 °C. Retention time for mefloquine was 5.6 minutes. Peak area was used for quantification. The limit of detection and quantifications were 10 and 20 nM respectively. Inter and intra batch coefficient of variation for mefloquine was 1.0, 2.9 and 3.6% and 12.5, 8.0 and 10.8 % for 10, 1 and 0.1 µM respectively. The calibration curves for lower (a) and higher (b) concentration range are given in Figure 4.2.

A.

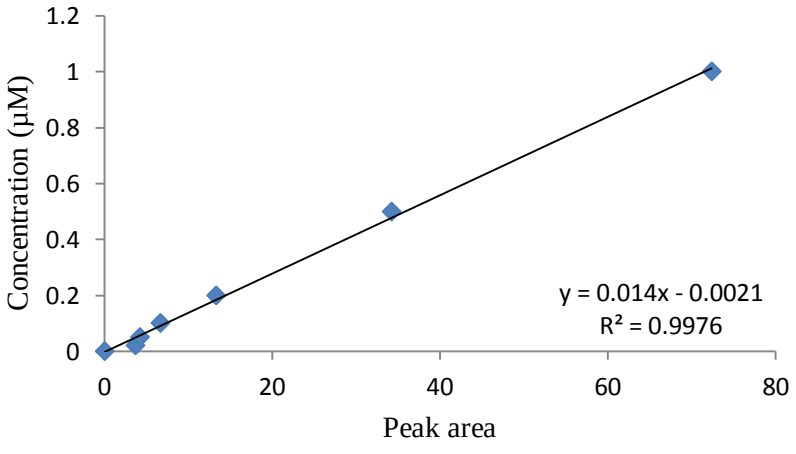

B.

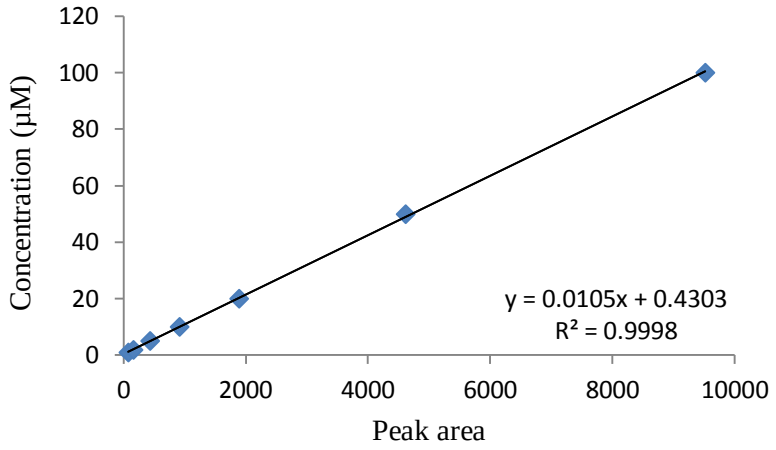


**Figure 4-2** - Calibration curve for mefloquine A) Lower concentration range (0.02- 1 µM) and B) Higher concentration range (1 -100 µM)

#### 4.3.4.2.2 Assay of amodiaquine

Assay of amodiaquine was done based on a method by Pussard and co-workers (459) and slight modifications were done to adjust laboratory conditions. Separation was done using a Prevail $C_{18}$ (3 µm, 4.6x150mm) column attached to a Direct-connect$^{TM}$ universal column prefilter. The mobile phase consisted of 20 mM (w/v) $KH_2PO_4$ in deionized water with pH adjusted 3.0 and acetonitrile (82:18) v/v. The injection volume was 40 µL and the mobile phase was pumped at 1 mL/min. The analytes were detected at UV absorbance 343 nm and column oven was maintained at 30 $^{\circ}$C. The retention time was 2.4 minutes. The limit of detection and quantifications were 2.2 and 5 nM respectively. The intra batch coefficient of variation for amodiaquine was 4.3, 3.6 and 10.9 % for 10, 1 and 0.1 µM respectively.

A.

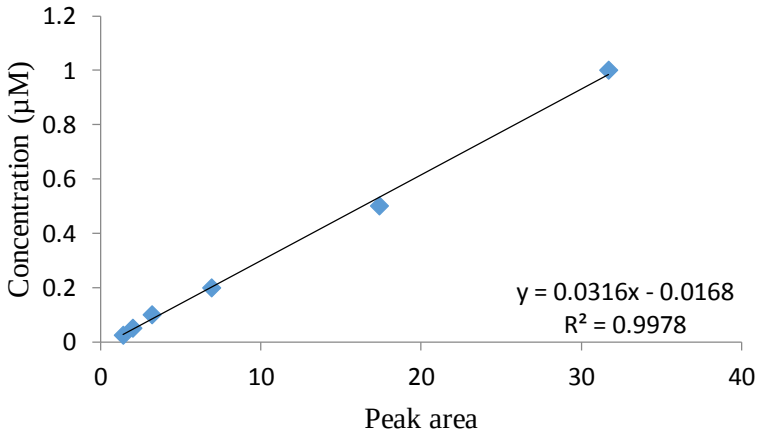

B.

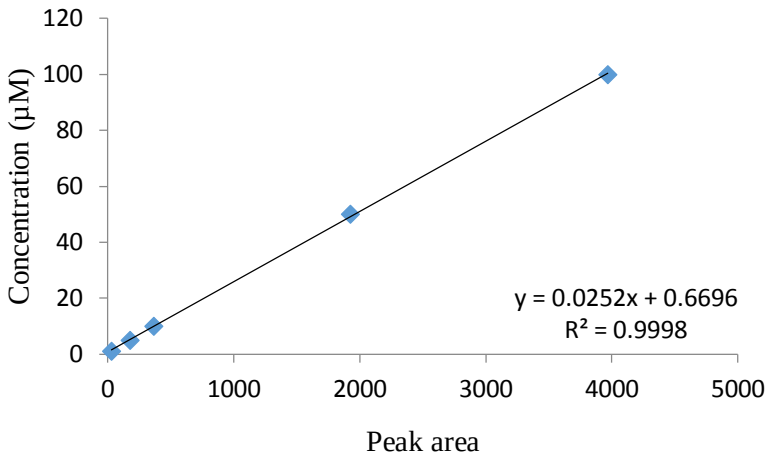


**Figure 4-3** - Calibration curve for amodaiquine A) lower concentration range 0.025 - 1 µM and B) higher concentration range (1-100 µM)

#### 4.3.4.2.3 Assay of methylene blue

Methylene blue assay was based on a method by Peter and colleagues (151) and similar to mefloquine and amodiaquine some modifications were done to suit the laboratory conditions. Drug samples in HBSS collected at different time points stored in -80 °C were thawed and centrifuged before the assay.

Separations were performed using Apollo $C_{18}$ (5 µm, 4.6x150mm) column attached to an Apollo $C_{18}$ (5 µm, 4.6x5.5mm) guard column. The mobile phase consisted of 60% 20 mM (w/v) $KH_2PO_4$ adjusted to pH 3 using $H_3PO_4$, 35% acetonitrile and 5% methanol and was pumped at 1 mL/min. The injection volume was 40 µL and the analytes were detected at 660 nm in the visual spectrum. The column oven was maintained at 30 °C. The retention time for methylene blue was 3.8 minutes and peak area was used for quantification. The limits of detection and quantification were 1.2 and 3 nM respectively. The inter and intra batch coefficient of variation was 2.1% and 4.0% for 10 µM, 0.4% and 6.9% for 1 µM and 3.3% and 12.3 % for 0.1 µM.

A.

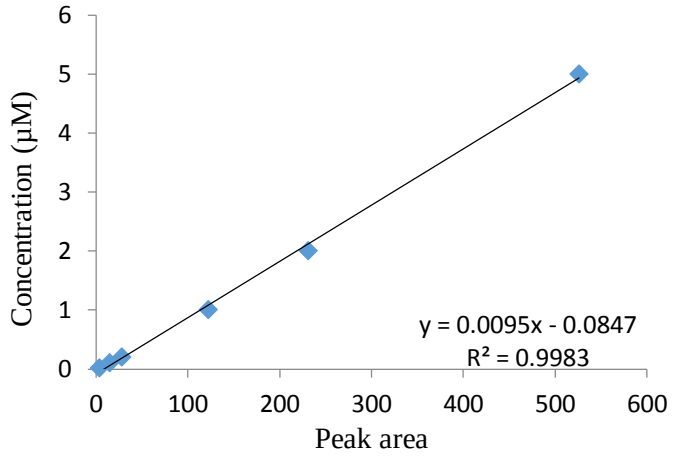


B.

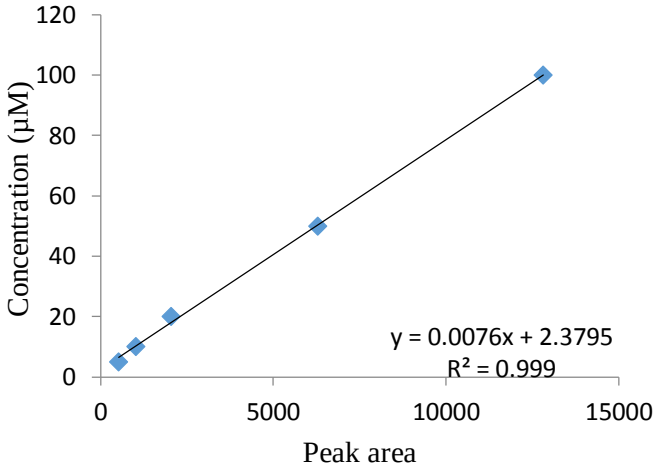


**Figure 4-4** - Calibration curve for methylene blue A) lower concentration range 0.025 - 1 µM and B). higher concentration range (1-100 µM)

#### 4.3.4.2.4 Simultaneous assay of methylene blue and mefloquine

Similar assay techniques based on Peter and colleagues (151) for methylene blue was used for simultaneous determination of mefloquine and methylene blue.

Separations were performed using an Apollo $C_{18}$ (5 µm, 4.6x150mm) column attached to an Apollo $C_{18}$ (5 µm, 4.6x5.5mm) guard column. The mobile phase consisted of 60 % 20 mM (w/v) $KH_2PO_4$, 35% acetonitrile and 5% methanol adjusted to pH 3 using $H_3PO_4$ and was pumped at 1 mL/min.. The injection volume was 40 µL and the mefloquine and methylene blue peaks were detected at 222 nM UV and 660 nm visual spectrums respectively. The column oven was maintained at 30 °C. The retention time for methylene blue and mefloquine were 3.8 and 12 minutes respectively. The peak area was used for quantification. The limit of detection and quantifications were 2.2 and 4.7 nM for methylene blue and 2.0 and 6.3 nM for mefloquine respectively.

A.

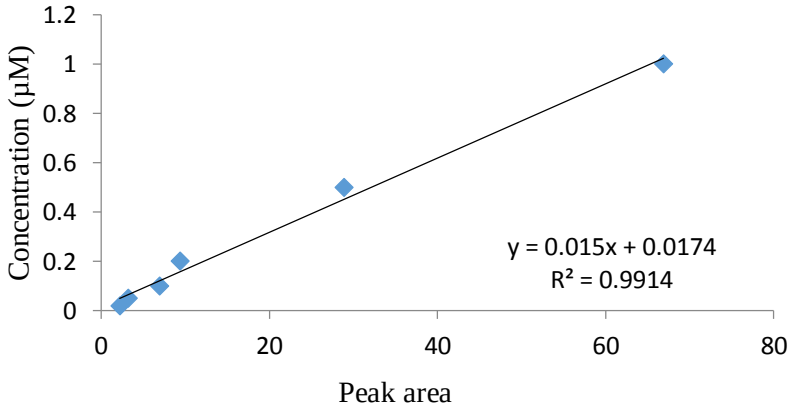


B.

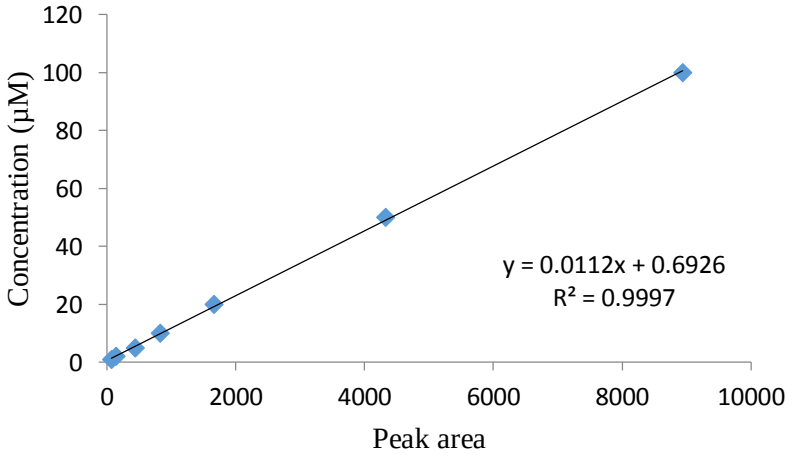


**Figure 4-5** : Calibration curve for mefloquine a) lower concentration range A). 0.02 - 1 µM and B). higher concentration range (1-100 µM)

A.

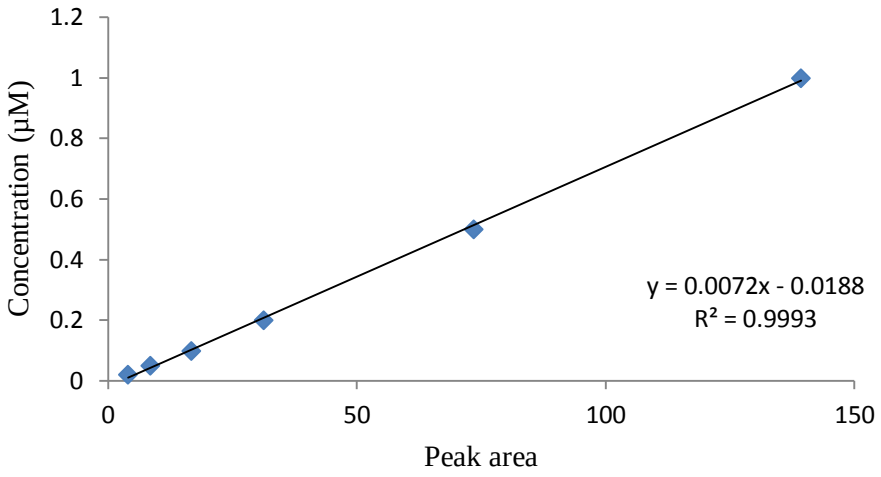


B.

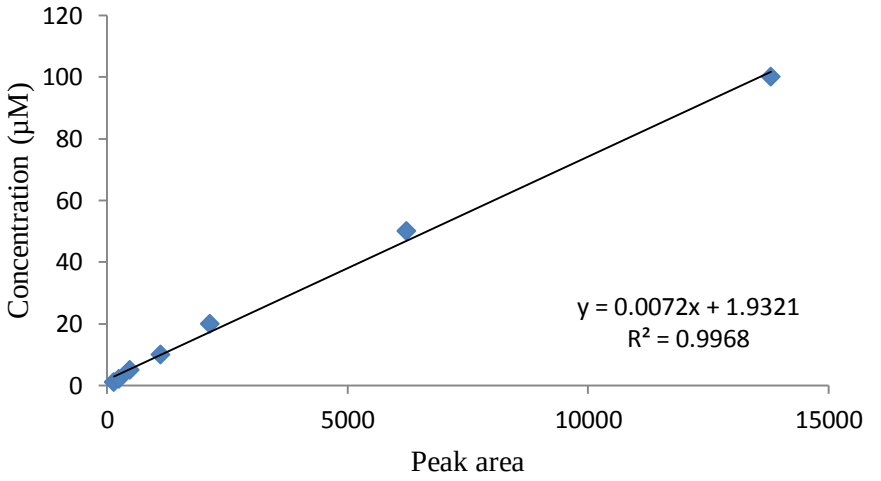


**Figure 4-6** – Calibration curve for methylene blue for A) lower concentration range 0.02 - 1 µM and B) higher concentration range (1-100 µM)

Figures 4.5 and 4.6 are the calibration curves for mefloquine and methylene blue when both drugs were detected simultaneously. The intra batch coefficient of variation was 5.9 %, 3.5% and 1.7% for methylene blue and 9%, 5% and 1.8% for mefloquine for 0.1, 1 and 10 µM respectively.

#### 4.3.4.3 Assay of artesunate, dihydroartemisinin and artemisone using liquid chromatography and mass spectrometry (LC-MS-MS) drug Assay

##### 4.3.4.3.1 Sample preparation for LC-MS-MS

Artesunate, artemisone and dihydroartemisinin sample from Caco-2 studies were collected in HBSS which contained salts; sodium chloride, potassium chloride, calcium chloride, potassium phosphate monobasic, disodium phosphate, magnesium sulphate, and sodium bicarbonate. Salt removal was necessary for assay of drugs using LC-MS-MS. Agilent Bond Elute OMIX 96 $C_4$ pipette tips contained a small bed of reversed phase or ion-exchange monolithic sorbent inserted into the pipette tip. This reversed phase resin is effective in salt removal and recommended to use prior assay using LC-MS-MS.

Therefore Agilent Bond Elute OMIX 96 $C_4$ 100 µL pipette tips were used for salt removal. A constant volume of 40 µL of sample was spiked with 5 µL internal standard from stock 0.5 mM artemisinin. The sample was pre-treated with 4 µL of 1 % trifluoroacetic solution by pipetting in and out numerous times.

The pipettor was adjusted to the maximum volume (100 µL). The tips were conditioned by aspirating and discarding a conditioning solution made up of 50 % acetonitrile and water. This step was repeated twice. Following this, an equilibration process was performed, in which washing solution (0.1% trifluoroacetic acid) was aspirated and discarded two times. These tips were used for removing salts from the pre-treated samples using the protocol as described.

Pre-treated samples were loaded into the above processed tips by gently aspirating and discarding into the same vial. The process was repeated 10 times in order to increase binding efficiency of drugs to the OMIX 96 $C_4$ matrix. The tips were washed with washing solution (0.1% TFA) by aspiration and discarding four times. The samples were then eluted in 100 µL of the elution solution (0.1% formic acid in 95% acetonitrile). 3 µL of the sample was injected into the LC-MS.

#### 4.3.4.3.2 Mass spectrometry

The UPLC-MS-MS system consisted of Nexera UPLC (LC-30A), degasser (DGU-20A5), autosampler (SIL-30A) and column oven (CTO-30A) coupled with a Shimadzu triple Quadrupole Mass Spectrometer (model 8030 Shimadzu, Kyoto, Japan). Electro Spray Ionisation (ESI) and Atmospheric Pressure Chemical Ionisation (APCI) interfaces were included in the system.

#### 4.3.4.3.3 Assay of artesunate and dihydroartemisinin

Artesunate and dihydroartemisinin were measured by previously described LC-MS method by Salman and co-workers (44) but modified to suit LC-MS-MS conditions. Chromatographic separation was performed on a Waters Acquity BEH $C_{18}$ column (1.7 µm, 2.1 x 50mm) connected with VanGuard Acquity UPLC BEH $C_{18}$ pre-column (1.7 µm, 2.1 x 5mm) (Waters Corp, Wexford, Co. Wexford, Ireland) at 40 $^{\circ}$C. Mobile phase A consisted of 0.1 % v/v formic acid and mobile phase B consisted of acetonitrile + 0.1% v/v formic acid. The analytes were eluted using the following gradient given below.

| Time (min) | Solvent A (%) | Solvent B (%) |
|---|---|---|
| 0.5 | 70 | 30 |
| 3 | 5 | 95 |
| 4 | 5 | 95 |
| 4.1 | 70 | 30 |
| 6 | Stopped | |

The retention times for α and β DHA were 2.2 and 2.4 min, respectively. The retention time for Artesunate was 2.48 min and the retention time for Artemisinin was 2.65 minute. Quantitation was performed in multiple reactions monitoring (MRM) mode, using DUIS (ESI+ and APCI+) ion sources. The Precursor-product ion pairs were as follows: DHA α and β m/z 267→249.3; Artesunate m/z 401.8→267.3 and Artemisinin m/z 283→265. The optimized mass spectra were acquired with an interface voltage of 4.5kV, a detector voltage of 1.0 kV, a heat block temperature of 500 ºC and a desolvation

temperature of 160 ºC. Nitrogen was used as the nebulizer gas at a flow rate of 3 L/min and drying gas flow was maintained at 8 L/min. Argon was used as collision gas at 230 Kpa. Dwell time for all the compound were 100 msec. Collision energy for α and β DHA was -7.2 and the collision energy for artesunate and artemisinin were -11.3 and -9.2, respectively. Limit of quantification and limit of detection for artesunate were 0.14 and 0.05 µM respectively. The intra batch variation for 0.5, 5 and 20 µM of artesunate was 3.7%, 6.7 % and 5.4 %.

A.

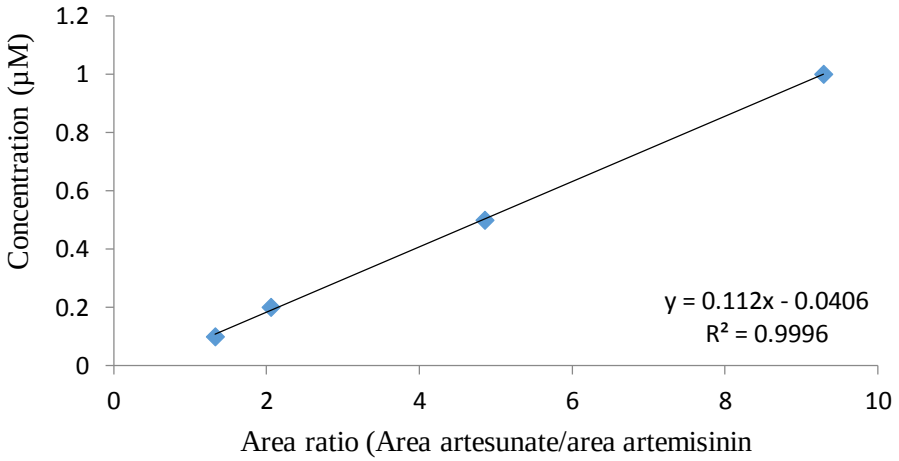


B.

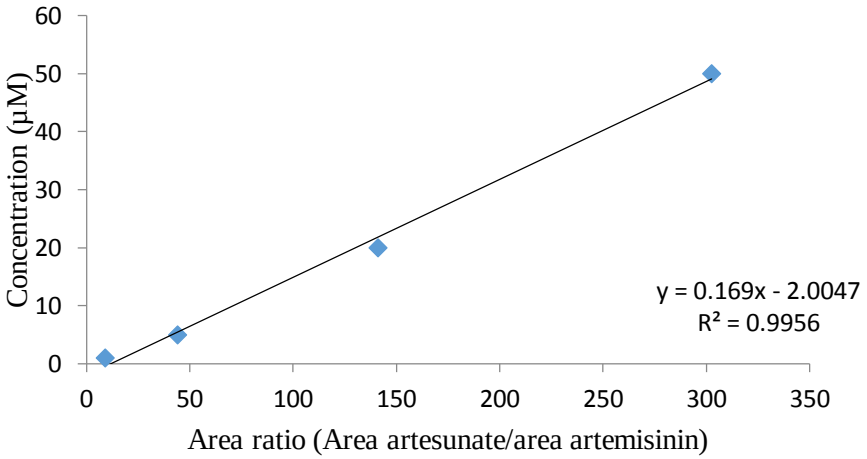


**Figure 4-7** - Calibration curve for artesunate A) lower concentration range 0.04 - 1 µM and B) higher concentration range (1-50 µM)

**Transport of dihydroartemisinin across the Caco-2 monolayer**

Transport of dihydroartemisinin across the Caco-2 cell monolayer was calculated by the percentage of the peak area of the receiver compartment divided by the peak area of the donor compartment at the last time point.

$$\text{Percentage transfer} = \frac{\text{Peak area ratio receiver compartment}}{\text{Peak area ratio donor compartment}} \times 100$$

The percentage transport of the dihydroartemisinin was compared to the percentage transfer of the prodrug, artesunate.

#### 4.3.4.3.4 Assay of artemisone

Artemisone assay was based on the LC-MS method described by Manning's group (460) and modified to suit the LC-MS-MS conditions in our laboratory. Chromatographic separation was same as described above with minor modification of gradient steps:

| Time(min) | Solvent A (%) | Solvent B (%) |
|---|---|---|
| 0.3 | 50 | 50 |
| 3 | 5 | 95 |
| 3.5 | 5 | 95 |
| 3.6 | 50 | 50 |
| 5 | stopped | |

The retention time for artemisone was 1.96 min and the retention time for the internal standard artemisinin was 1.71 min. Quantitation was performed in multiple reactions monitoring (MRM) mode, using ESI+ interface. The Precursor-product ion pairs were as follows: artemisone m/z 402.17→163.4 and artemisinin m/z 283→265. The optimized mass spectra were acquired with an interface voltage of 4.5 kV, a detector voltage of 1.0 kV, a heat block temperature of 300 ºC and a desolvation temperature of 180°C. Nitrogen was used as the nebulizer gas at a flow rate of 3 L/min and drying gas flow was maintained at 12 L/min. Argon was used as collision gas at 230 Kpa. Dwell

time for all the compound were 100 msec. Collision energy for artemisone was -21 and the collision energy for artemisinin was -9.1. Limit of quantification and limit of detection for artemisone were 0.01 µM and 0.004 µM respectively. Intra batch coefficient of variation was 1.2%, 4 % and 2.2% for 0.1, 1 and 20 µM

A.

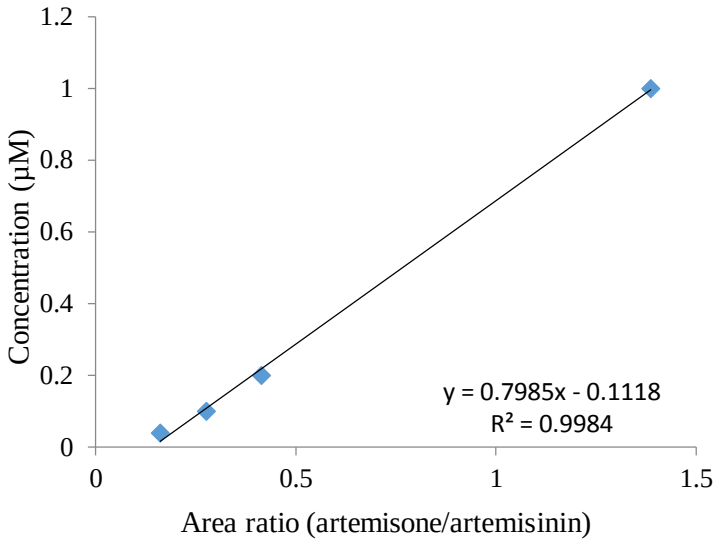


B.

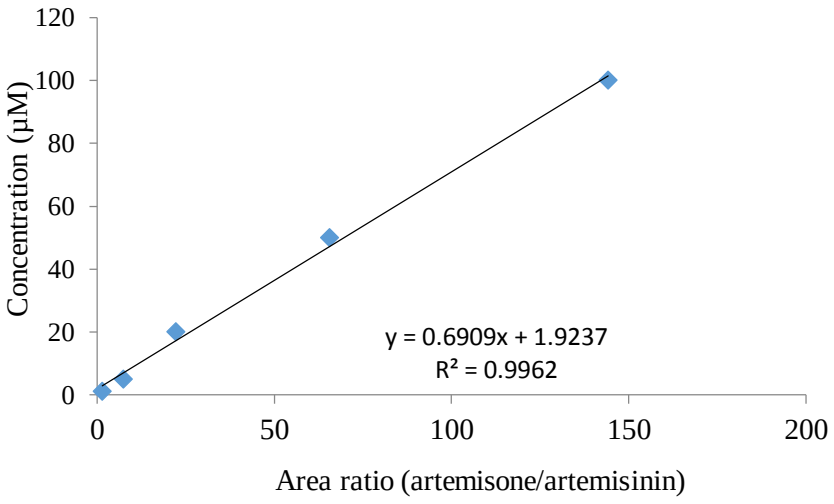


**Figure 4-8**: Calibration curve for artemisone A) lower concentration range 0.04 – 1 µM and B) higher concentration range (1-100 µM)

### 4.3.5 Determination of P-gp regulation in the presence of antimalarials

Late passage Caco-2 cells (Passage 80-83) and LS174T cells at 10,000 cells/$cm^2$ (P-66) were seeded on to 6 well plates. Cell suspension (1.5 mL) prepared (at 62,000 cells/ mL) in cell growth medium was added on to the 9.3 $cm^2$ 6 well plates and medium was replaced twice weekly.

Caco-2 cells were grown for 21 days for full maturation and formation of tight cell monolayer and LS174 T cells were grown for 6 days. Drugs and drug combinations prepared in cell growth medium were added to the cells at these times and exposed for 48 (LS174 T) or 96 (Caco-2) hours.

Caco-2 monolayers were unable to withstand 100 µM drug concentrations for 96 hours and lifted from the plate (mefloquine and amodiaquine are found to be more toxic to Caco-2 cells), therefore induction studies were done at 20 µM for 96 hours. Drugs used were artesunate, dihydroartemisinin, artemisone, mefloquine, amodiaquine and methylene blue as a single drug and drug combinations were artesunate plus amodiaquine, artesunate plus mefloquine, dihydroartemisinin plus amodiaquine, dihydroartemisinin plus mefloquine, dihydroartemisinin plus amodiaquine, dihydroartemisinin plus mefloquine, artemisone plus amodiaquine and artemisone plus mefloquine.

Artemisinin derivatives, artesunate and artemisone were found to be toxic to LS174T cells (unlike Caco-2 cells) and could not be exposed up to 96 hours. Therefore exposure was limited up to 48 hours at 20 µM.

After drug exposure, cells were washed three times using PBS and cell lysate was prepared as described in 3.3.6.2.2. The protein content was quantified using Lowry protein assay and regulation of P-gp was determined using Western blotting. Up regulation of P-gp was determined comparing Western blot images for treated and control samples.

## 4.4 Results

### 4.4.1 Inhibitory properties of anti-malarial drugs against P-gp mediated drug efflux

Bidirectional transport of rhodamine123 alone and in combination with antimalarials were studied to determine the ability of antimalarials to inhibit the P-gp activity. Relative inhibition of P-gp mediated drug efflux of rhodamine123 was determined to find the inhibitory properties of antimalarial drugs. The antimalarial drugs at 100 µM were combined with 5 µM rhodamine123 and bidirectional transport studies were done across passage 44 Caco-2 cell monolayers. Table 4.1 gives the apparent permeability values and efflux ratio for rhodamine123.

**Table 4-1**: Apparent permeability ($P_{app}$ ± SEM) for rhodamine123 (5 µM) alone and when combined with of antimalarial drugs (100 µM) across P-44 Caco-2 cell monolayers

| Drug | Ap-Bas ($10^{-6}$ cm/sec) | Ap-Bas TEER[c] | Bas-Ap ($10^{-6}$ cm/sec) | Bas-Ap TEER[c] | Efflux ratio | Ap-Bas (P value)[a] | Bas-Ap (P value)[b] |
|---|---|---|---|---|---|---|---|
| Rh123 | 2.2 ± 0.1 | 333 | 3.2 ± 0.2 | 329 | 1.4 | | |
| Rh123+ PSC | 2.3 ± 0.2 | 340 | 2.3 ± 0.1 | 399 | 1.0 | 0.83 | 0.05* |
| Rh123 + MQ | 2.1 ± 0.2 | 330 | 2.7 ± 0.1 | 358 | 1.3 | 0.55 | 0.12 |
| Rh123 + AQ | 2.5 ± 0.1 | 304 | 3.6 ± 0.1 | 310 | 1.4 | 0.14 | 0.87 |
| Rh123 + MB | 2.2 ± 0.2 | 356 | 3.8 ± 0.3 | 346 | 1.7 | 0.97 | 0.09 |
| Rh123 + AM | 2.0 ± 0.0 | 325 | 3.5 ± 0.1 | 338 | 1.7 | 0.06 | 0.29 |

[a]$P_{app}$ Ap-Bas of rhodamine123 alone was compared with Ap-Bas of rhodamine123 in combination, [b]$P_{app}$ Bas-Ap of rhodamine123 alone was compared with Bas-Ap of rhodamine123 in combination * Significant at the level of $P < 0.05$, rh123: rhodamine123, PSC: PSC833, MQ: mefloquine, AQ: amodiaquine, MB: methylene blue, AM: artemisone, [c]The mean TEER value for 3 well plates before the test.

The apparent permeability for Ap-Bas directional transport (cell uptake) was $2.24 \times 10^{-6}$ cm/sec whereas efflux transport (Bas-Ap) transport was $3.17 \times 10^{-6}$ cm/sec. Therefore only a modest P-gp substrate activity was shown for known P-gp substrate, rhodamine123 with efflux ratio of 1.4. None of the antimalarials were able to exert

inhibitory properties similar to potent PSC 833 and was not able to inhibit rhodamine123 efflux significantly when early passage Caco-2 cells were utilized for the study. As the efflux ratio was very small, it was likely that only strong inhibitors would be observable in such a weakly P-gp expressing system. This the study was repeated months later using late passage (P-80 to 83) Caco-2 cell monolayers with better native P-gp expression to observe inhibitory properties of less potent P-gp inhibitors (Table 4.2).

**Table 4-2:** Apparent permeability ($P_{app}$ ± SEM) for rhodamine123 (5 µM) alone and when combined with of antimalarial drugs (100 µM) across P-80 Caco-2 cell monolayers

| Drug | Ap-Bas ($10^{-6}$ cm/sec) | Ap-Bas TEER[c] | Bas-Ap ($10^{-6}$ cm/sec) | Bas-Ap TEER[c] | Efflux ratio | Ap-Bas[a] (P value) | Bas-Ap[b] (P value) |
|---|---|---|---|---|---|---|---|
| Rh123 (P-80) | 0.5 ± 0.1 | 624 | 2.4 ± 0.3 | 604 | 4.7 | | |
| Rh123+PSC | 0.5 ± 0.1 | 711 | 0.5 ± 0.0 | 716 | 1.0 | 0.74 | 0.003** |
| Rh123+MQ | 0.5 ± 0.0 | 643 | 1.3 ± 0.1 | 755 | 2.3 | 0.64 | 0.02* |
| Rh123+AQ | 0.4 ± 0.0 | 531 | 2.4 ± 0.3 | 557 | 5.9 | 0.14 | 0.63 |
| Rh123+MB | 0.4 ± 0.0 | 623 | 3.0 ± 0.3 | 617 | 6.7 | 0.24 | 0.21 |
| Rh123+ ART | 0.5 ± 0.0 | 523 | 2.3 ± 0.3 | 613 | 5.2 | 0.32 | 0.88 |
| Rh123+ AM | 0.5 ± 0.1 | 608 | 2.0 ± 0.1 | 610 | 4.3 | 0.54 | 0.28 |
| Rh123 + ART + MQ | 0.5 ± 0.1 | 505 | 1.3 ± 0.1 | 614 | 2.4 | 0.81 | 0.02* |
| Rh123 + AM + MQ | 0.5 ± 0.0 | 519 | 1.5 ± 0.2 | 573 | 3.3 | 0.43 | 0.05* |

[a]$P_{app}$ Ap-Bas of rhodamine123 alone was compared with Ap-Bas of rhodamine123 in combination, [b]$P_{app}$ Bas-Ap of rhodamine123 alone was compared with Bas-Ap of rhodamine123 in combination * Significant at the level of $P < 0.05$, ** Significant at the level of $P < 0.005$, rh123: rhodamine123, PSC: PSC833, MQ: mefloquine, AQ: Amodiaquine, MB: methylene blue, AM: artemisone, [c]The mean TEER value for 3 well plates before the test.

The efflux ratios for rhodamine123 found to be 4-5 when transported through late passage Caco-2 cell. Mefloquine at 100 µM, inhibited the Bas-Ap transport of rhodamine123 significantly and efflux ratio was reduced by half (Figure 4.9). The $P_{app}$ for Bas-Ap transport was reduced from 2.42 to 1.34 × $10^{-6}$ cm/sec with a significance

level of P = 0.02. Amodiaquine, artesunate, mefloquine and artemisone did not exhibit P-gp inhibitory properties at 100 µM (Table 4.2).

In addition, when mefloquine was combined with short acting artemisinin derivatives, artesunate and artemisone, the percentage of P.gp inhibition observed remained the same as when using mefloquine alone. This reaffirms the lack of inhibition by the artemisinin derivatives (Table 4.2 and Figure 4.10).

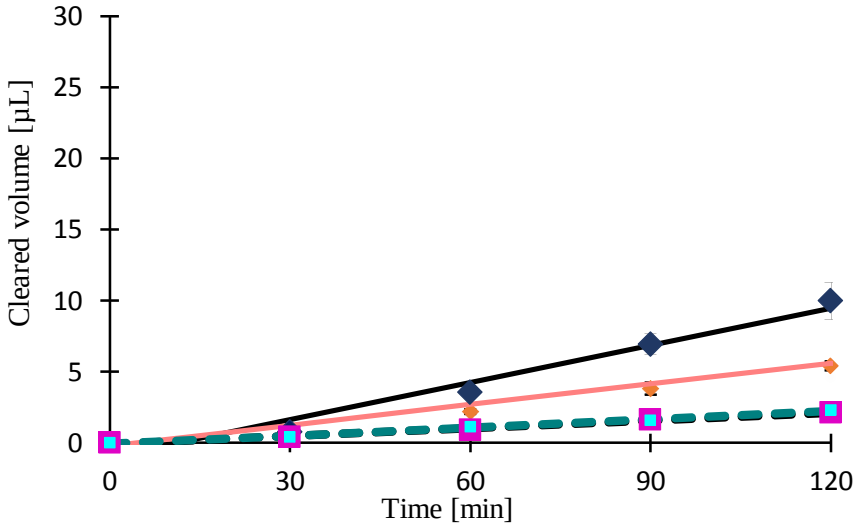


**Figure 4-9**: Ap-Bas (■) and Bas-Ap (◆) transport of rhodamine123 alone and Ap-Bas (■) and Bas-Ap (◆) transport of rhodamine123 when combined with mefloquine (N=3, Mean ±SEM)

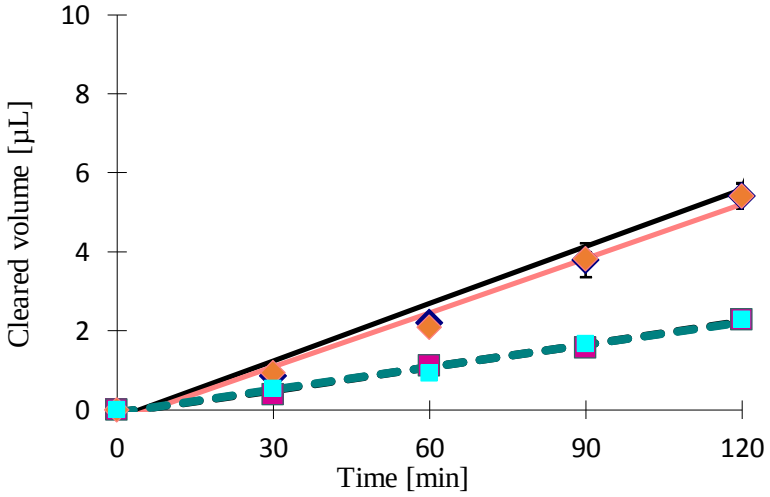


**Figure 4-10**: Ap-Bas (■) and Bas-Ap (◆) transport of rhodamine123 when combined with mefloquine and Ap-Bas (■) and Bas-Ap (◆) transport of rhodamine123 when combined with mefloquine and artesunate (N=3, Mean ±SEM)

P-gp inhibitory properties of antimalarials other than mefloquine were further tested increasing the drug concentration up to 300 µM (Table 4.3). However no change in bidirectional transport of rhodamine123 was observed, indicating no involvement of P-gp in these drug's transport.

**Table 4-3:** Apparent permeability ($P_{app}$ ± SEM) for rhodamine123 (5 µM) alone and when combined with 300 µM of antimalarials across P-82 Caco-2 cell monolayers

| Drug | Ap-Bas ($10^{-6}$ cm/sec) | Ap-Bas TEER[c] | Bas-Ap ($10^{-6}$ cm/sec) | Bas-Ap TEER[c] | Efflux ratio | Ap-Bas [a] (P value) | Bas-Ap [b] (P value) |
|---|---|---|---|---|---|---|---|
| Rh123 (P-82) | 0.5 ± 0.1 | 713 | 2.8 ± 0.6 | 798 | 5.7 | | |
| Rh123+ AQ | 0.5 ± 0.1 | 614 | 2.6 ± 0.1 | 755 | 5.0 | 0.95 | 0.09 |
| Rh123+ ART | 0.4 ± 0.0 | 608 | 2.9 ± 0.2 | 610 | 7.5 | 0.07 | 0.22 |
| Rh123+AM | 0.5 ± 0.1 | 778 | 3.0 ± 0.1 | 795 | 5.6 | 0.70 | 0.24 |
| Rh123+MB | 0.5 ± 0.0 | 665 | 2.9 ± 0.1 | 660 | 5.3 | 0.56 | 0.71 |

[a]$P_{app}$ Ap-Bas of rhodamine123 alone was compared with Ap-Bas of rhodamine123 in combination, [b]$P_{app}$ Bas-Ap of rhodamine123 alone was compared with Bas-Ap of rhodamine123 in combination, rh123: rhodamine123, PSC: PSC833, AQ: amodiaquine, MB: methylene blue, AM: artemisone, [c]The mean TEER value for 3 well plates before the test.

### 4.4.2 Determination of drug permeability and P-gp substrate activity of antimalarial drugs

If the bidirectional transport study gives equivalent $P_{app}$ in both Bas-Ap and Ap-Bas directions, this indicates equivalent transport of drug in both directions. Therefore transport ratio of efflux direction over uptake direction would give a value close to 1 indicating no net flux in either direction. Then only diffusion has taken place and it would be unlikely for P-gp to be involved in transporting the drug out of the cell.

When the $P_{app}$ value for Ap-Bas direction is higher than the Bas-Ap direction, there is influx or cell uptake of the drug. Whereas when $P_{app}$ for Bas-Ap directional transport of a drug is higher than the Ap-Bas directional transport, the serosal to mucosal directional transport is higher and there is less cell intake of drug indicating efflux transport of the drug. Incubation with a P-gp inhibitor such as PSC 833 would inhibit the efflux transport of the drug which confirms P-gp mediated drug transport.

Previous research on drug permeability studies within the our laboratory has shown that drugs with a $P_{app}$ value above 25 $\times 10^{-6}$ cm/sec to have a high permeability and would have complete drug absorption across much of the gut. Compounds with $P_{app}$ less than $1 \times 10^{-6}$ cm/sec were considered to have a low permeability and will not achieve complete drug absorption (447, 449). The threshold values 1 and $25 \times 10^{-6}$ cm/sec were used in determining the high, medium and low permeability of the drugs.

### 4.4.2.1 Bidirectional transport of mefloquine

Bidirectional transport of mefloquine was tested at the concentration of 10, 20 and 100 µM using Caco-2 cell monolayers. Ap-Bas $P_{app}$ values of mefloquine were found to be in the range of 6 to$10 \times 10^{-6}$ cm/sec and Bas-Ap directional transport ranged from 5 to $11 \times 10^{-6}$ cm/sec (Table 4.4). At 10 µM an efflux ratio of 0.7 was observed, therefore instead of efflux a potential uptake pathway was noted. At tenfold higher concentration (100 µM) of mefloquine also showed little change in efflux value, further confirming that inherent physiological chemical properties of the drug defines the bidirectional transport of mefloquine. Certainly in later passages using 20 µM mefloquine indicated similar pattern in transport, showing absence of efflux transport for mefloquine (Figure 4.11).

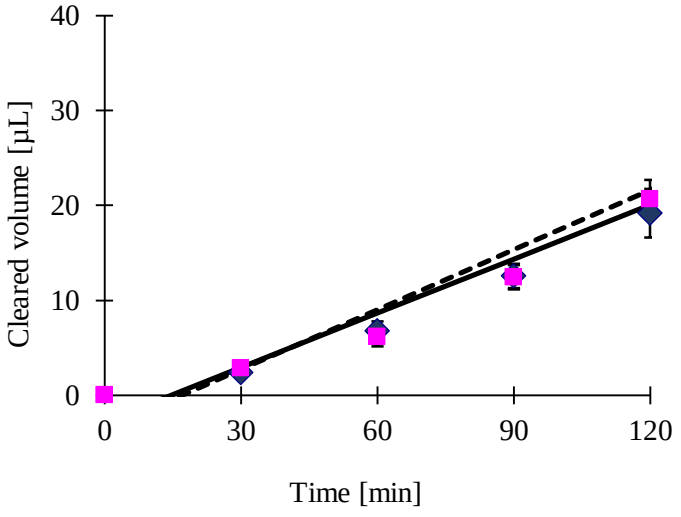


**Figure 4-11**: Ap-Bas (■) and Bas-Ap (◆) transport of mefloquine across late passage Caco-2 cells (N=3, Mean ±SEM)

When co-incubated with PSC 833, mefloquine bidirectional transport at 10 and 20 µM appeared to show very little difference from the values without co-treatment, suggesting that it was unlikely that multiple opposing mechanisms were at play when mefloquine was used alone. No net transport of mefloquine was found. Hence mefloquine is not subjected to P-gp mediated drug efflux at concentrations above10 µM.

The current WHO recommended antimalarial combinations consist of a short acting artemisinin derivative and long acting quinolone. The two quinolones studied were mefloquine and amodiaquine and combination drug studies were mostly confined to mefloquine combinations. Bidirectional transport of mefloquine in combination with short acting artemisinin derivatives and intermediate acting methylene blue were studied. A first study was done for mefloquine and artesunate combinations at 10 and 100 uM and the results are shown in Table 4.4. The transport velocity for Ap-Bas and Bas-Ap directional transport of mefloquine was not altered when combined with artesunate at low and high concentrations. Two combinations were also combined with PSC at 4 µM and this also did not alter the $P_{app}$ values of mefloquine widely.

Mefloquine was also combined with methylene blue and artemisone and two drugs in combination with mefloquine did not alter the bidirectional transport of mefloquine (Table 4.4).

No change in apparent permeability of mefloquine with the co-treatment of PSC 833, artesunate, artemisone and methylene blue shows that mefloquine passive diffusion is unlikely to be altered by the co-treatment; therefore illustrate to the absence of permeability related drug interactions.

**Table 4-4**: Apparent permeability ($P_{app}$ ± SEM) and efflux ratio for mefloquine through Caco-2 cell monolayer.

| Drug | Con: (µM) | Ap-Bas ($10^{-6}$ cm/sec) | Ap-Bas TEER[j] | Bas-Ap ($10^{-6}$ cm/sec) | Ap-Bas TEER[j] | Efflux ratio[h] | Net flow direction (P value[i]) |
|---|---|---|---|---|---|---|---|
| MQ[a] | 10 | 9.9 ± 0.7 | 328 | 6.6 ± 0.4 | 350 | 0.7 | In flux (0.02)[c] |
| MQ + PSC[a] | 10+4 | 11.0 ± 0.5 | 417 | 12.0 ± 1.0 | 429 | 1.0 | No flux(0.4) |
| MQ[a] | 100 | 8.9 ± 0.8 | 346 | 11.4 ± 0.8 | 409 | 1.2 | No flux (0.08) |
| MQ + PSC[a] | 100+4 | 11.1 ± 0.1 | 442 | 12.4 ± 0.4 | 410 | 1.1 | Efflux (0.04)[d] |
| MQ + ART[a] | 10 +10 | 14.4 ± 1.2 | 360 | 8.6 ± 0.7 | 385 | 0.6 | Influx(0.01)[e] |
| MQ + ART+ PSC[a] | 10+10 + 4 | 11.3 ± 0.1 | 390 | 9.3 ± 0.5 | 405 | 0.8 | In flux(0.02)[f] |
| MQ + ART[a] | 100 +100 | 8.4 ± 0.5 | 687 | 11.5 ± 2.1 | 706 | 1.4 | No flux(0.23) |
| MQ + ART+ PSC[a] | 100 +100 + 4 | 10.2 ± 0.4 | 674 | 14.0 ± 1.1 | 643 | 1.4 | Efflux(0.03)[g] |
| MQ[b] | 20[b] | 5.8 ± 0.7 | 728 | 5.3 ± 0.9 | 660 | 0.9 | No flux (0.66) |
| MQ + PSC[b] | 20+4 | 6.5 ± 0.4 | 671 | 7.6 ± 0.2 | 703 | 1.2 | No flux (0.44) |
| MQ+ MB[b] | 50+100 | 8.1 ± 0.3 | 617 | 9.0 ± 1.1 | 629 | 1.1 | No flux (0.79) |
| MQ + AM[b] | 50+20 | 6.7 ± 1.2 | 680 | 6.3 ± 0.6 | 720 | 0.9 | No flux (0.49) |

[a] Studies were done using passage 44 Caco-2 cell lines, [b] Studies were done using passage 80 Caco-2 cell lines [c, d,] power of the test was 0.5, [e ,f] power of the test was 0.8, [g] power of the test was 0.6, [h] Mean $P_{app}$ for Bas-Ap direction was divided by the Ap-Bas direction, [i] Mean $P_{app}$ of Ap-Bas direction and Bas-Ap direction transport was compared in a two tailed t test to determine p values (N=3), MQ: mefloquine, PSC: PSC833, ART: artesunate, MB: methylene blue, AM: artemisone, [j] The mean TEER value for 3 well plates before the test.

### 4.4.2.2 Bidirectional transport of amodiaquine

Permeability and P-gp substrate activity of amodiaquine, derivative was determined at the concentration of 10 and 100 uM. The $P_{app}$ values for both concentrations was found to be higher than mefloquine and ranged from 16 to 22 × $10^{-6}$ cm/sec in the Ap-Bas directions (Table 4.5).

At 10 µM, amodiaquine showed an efflux ratio of 1.2 with a higher Bas-Ap transport, yet the efflux ratio was low and this is unlikely to represent even a moderate affinity for P-gp. At a higher concentration (100 µM) efflux become exactly 1 showing no net efflux transport.

The high $P_{app}$ values indicates high intestinal permeability of amodiaquine, therefore any slight efflux transport at lower concentration is unlikely to affect the extent of drug absorption of amodiaquine.

**Table 4-5**: Apparent permeability ($P_{app}$ ± SEM) and efflux ratio for amodiaquine through Caco-2 cell monolayer

| Drug | Con: (µM) | Ap-Bas ($10^{-6}$ cm/sec) | Ap-Bas TEER[c] | Bas-Ap ($10^{-6}$ cm/sec) | Bas-Ap TEER[c] | Efflux ratio[a] | Net flow direction (P value[b]) |
|---|---|---|---|---|---|---|---|
| AQ [a] | 10 | 16.0 ± 1.1 | 423 | 21.5 ± 0.9 | 389 | 1.3 | Efflux (0.02)* |
| AQ [a] | 100 | 22.5 ± 2.0 | 416 | 23.3 ± 0.8 | 390 | 1.0 | No flux (0.74) |
| AQ + PSC [a] | 100 | 24.5 ± 2.0 | 418 | 26.7 ± 0.7 | 400 | 1.1 | No flux (0.36) |
| AQ + AM [a] | 10+10 | 16.7 ± 0.7 | 431 | 18.3 ± 2.6 | 434 | 1.1 | No flux (0.52) |

[a] Studies were done using Passage 44 Caco-2 cells * Significant at the level of $P < 0.05$ [a] Mean $P_{app}$ for Bas-Ap direction was divided by the Ap-Bas direction, [b] Mean $P_{app}$ of Ap-Bas direction and Bas-Ap direction transport was compared in a two tailed t test to determine p values (N=3), AQ: amodiaquine, PSC: PSC833, AM: artemisone, [c] The mean TEER value for 3 well plates before the test.

Amodiaquine permeability in combination with short acting artemisone was studied and the $P_{app}$ values for amodiaquine in the presence of artemisone were 17 and 18 × $10^{-6}$ cm/sec for Ap-Bas and Bas- Ap directions respectively. Therefore amodiaquine bidirectional transport was not significantly affected, when combined with artemisone and thus it is unlikely to cause a clinically significant alteration in absorption of amodiaquine.

Further testing of amodiaquine was not deemed necessary as high $P_{app}$ values show that major proportion of the drug is clearly absorbed following passive diffusion ensuring almost 100 % drug absorption.

### 4.4.2.3 Bidirectional transport of methylene blue

Methylene blue is an intermediate acting anti-malarial drug and clinical trials in the last few years have re-explored the use of methylene blue in anti-malarial therapy, reigniting earlier trials before the drugs of selective drug therapy in 1960s.

Methylene blue (100 µM) transport across Caco-2 cell lines were first tested using passage 44 cells and the drug exhibited increased Bas-Ap transport with the efflux ratio of 2.6. The $P_{app}$ values for Ap-Bas and Bas-Ap were 2.8 and 7.4 $\times 10^{-6}$ cm/sec as shown in Table 4.6. The low Ap-Bas transport indicate low permeability of methylene blue.

The study was repeated in Caco-2 RIF, Caco-2 VIN and on late passage Caco-2 cell monolayers in order to confirm possible P-gp mediated drug transport of methylene blue. All three studies had similar patterns with significantly higher transport in Bas-Ap direction, showing possible efflux transport of methylene blue.

**Table 4-6**: Apparent permeability ($P_{app}$ ± SEM) and efflux ratios for methylene blue transport through different Caco-2 cell models

| Drug | Cell line | Ap-Bas ($10^{-6}$ cm/sec) | Ap-Bas TEER[c] | Bas-Ap ($10^{-6}$ cm/sec) | Bas-Ap TEER[c] | Efflux ratio[a] | Net Transport (P value[b]) |
|---|---|---|---|---|---|---|---|
| MB | P-44 Caco-2 | 2.8 ± 0.1 | 438 | 7.4 ± 0.2 | 472 | 2.6 | Efflux (<0.001) |
| MB | P-80 Caco-2 | 1.8 ± 0.1 | 620 | 7.3 ± 0.5 | 634 | 4.1 | Efflux (<0.001) |
| MB+PSC | P-80 Caco-2 | 2.5 ± 0.1 | 612 | 5.5 ± 0.3 | 684 | 2.2 | Efflux (<0.001) |
| MB | Caco-2 VIN | 1.6 ± 0.1 | 720 | 8.3 ± 0.2 | 690 | 5.1 | Efflux (<0.001) |
| MB+PSC | Caco-2 VIN | 2.9 ± 0.4 | 690 | 5.3 ± 0.1 | 742 | 1.9 | Efflux (<0.01) |
| MB | Caco-2 RIF | 2.6 ± 0.1 | 534 | 6.1 ± 0.2[a] | 474 | 2.4 | Efflux (<0.001) |
| MB+PSC | Caco-2 RIF | 3.0 ± 0.1 | 556 | 4.8 ± 0.3 | 488 | 1.6 | Efflux (<0.01) |

[a] Mean $P_{app}$ for Bas-Ap direction was divided by the Ap-Bas direction, [b] Mean $P_{app}$ of Ap-Bas direction and Bas-Ap direction transport was compared in a two tailed t test to determine p values (N=3), [c] N=2, MB: methylene blue, PSC: PSC833, [c]The mean TEER value for 3 well plates before the test.

Caco-2 VIN model showed maximum efflux with an efflux ratio of 5.1 and $P_{app}$ values for Ap-Bas and Bas-Ap directions were 1.6 and 8.3 $\times 10^{-6}$ cm/sec respectively. All tests had strong statistical strength having power of 1 for all tests.

The drug was combined with a known P-gp inhibitor, PSC 833 and this resulted in increased Ap- Bas and decreased Bas-Ap transport of methylene blue for all three cell models. However PSC-833 was not able to block efflux transport of methylene blue completely suggesting involvement of gastrointestinal efflux mechanisms other the P-gp mediated efflux transport. Figures 4.12, 4.13 and 4.14 show the change in bidirectional transport of methylene blue in the presence of PSC 833 for Caco-2 cell models.

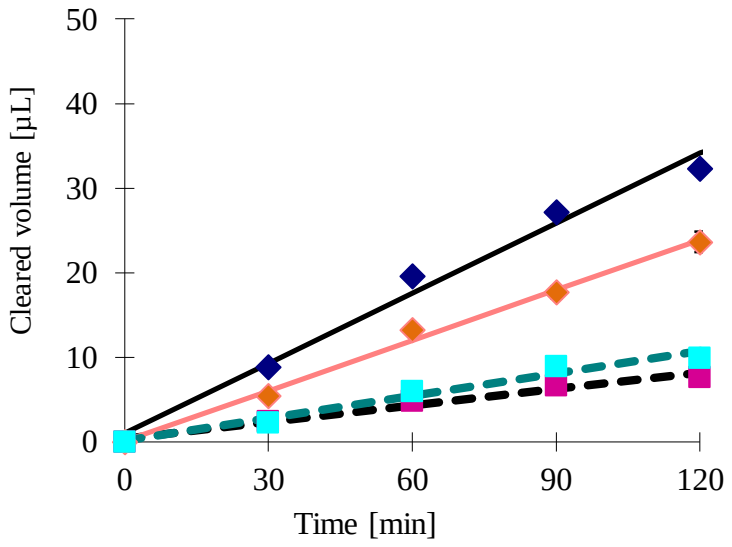


**Figure 4-12**: Ap-Bas (■) and Bas-Ap (◆) transport of methylene alone and Ap-Bas (■) and Bas-Ap (◆) of methylene blue when combined with PSC 833 across late passage Caco-2 cell monolayer (N=3, Mean ±SEM)

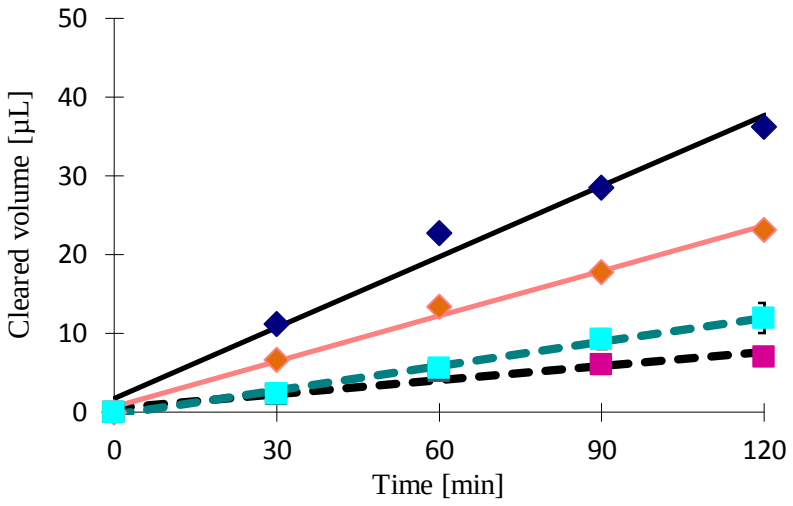


**Figure 4-13:** Ap-Bas (■) and Bas-Ap (◆) transport of methylene alone and Ap-Bas (■) and Bas-Ap (◆) of methylene blue when combined with PSC 833 across Caco-2 VIN cell monolayer (N=3, Mean ±SEM)

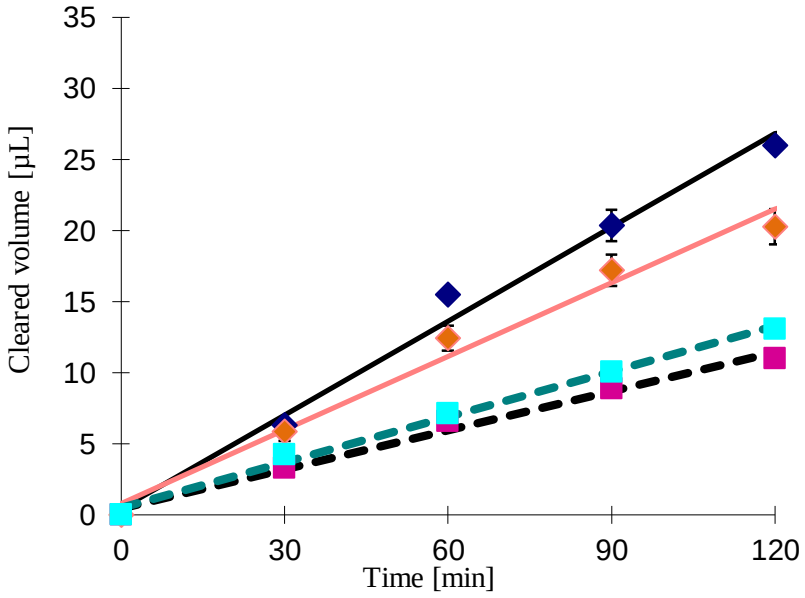


**Figure 4-14:** Ap-Bas (■) and Bas-Ap (◆) transport of methylene blue alone and Ap-Bas (■) and Bas-Ap (◆) of methylene blue when combined with PSC 833 across Caco-2 RIF cell monolayer (N=3, Mean ±SEM)

In all these figures the efflux was significantly greater than cell uptake direction. The inclusion of PSC-833 inhibited this efflux in all cases.

### 4.4.2.4 Bidirectional transport of artesunate and dihydroartemisinin

Bidirectional transport of artesunate at 100 uM was studied using test solution prepared from 20 mM stock samples frozen at -80 °C. The zero time test sample indicated that part of the artesunate has converted to its metabolite dihydroartemisinin and both α and β anomers were detected.

As shown in Table 4.8, the Bas-Ap transport of artesunate was higher compared to the Ap- Bas directional transport and the difference was significant. Efflux transport was observed again when the study was repeated. Efflux transport of artesunate was inhibited when combined with PSC 833 and mefloquine. However as indicated for amodiaquine such small increases in Bas-Ap transport or efflux will have negligible effect on systemic absorption. The $P_{app}$ values for Ap- Bas and Bas-Ap directional transport for artesunate ranged from 8-11 × $10^{-6}$ cm/sec. This permeability range of artesunate places it in a medium category suggesting passive diffusion contributes to drug absorption of artesunate, although absorption is likely to be incomplete through the gastrointestinal tract.

**Table 4-7:** Apparent permeability ($P_{app}$ ± SEM) and efflux ratios for of artesunate through Caco-2 cell lines

| Drug | Ap-Bas ($10^{-6}$ cm/sec) | Ap-Bas TEER[e] | Bas-Ap ($10^{-6}$ cm/sec) | Bas-Ap TEER[e] | Efflux ratio[c] | Net transport (P value[d]) |
|---|---|---|---|---|---|---|
| ART[a] (50 µM) | 7.2 ± 0.2 | 496 | 10.5 ± 0.5 | 477 | 1.5 | Efflux (0.003) |
| ART[a] +MQ (45 µM) | 8.5 ± 0.2 | 497 | 9.4 ± 1.5 | 513 | 1.1 | No flux (0.60) |
| ART +MQ + PSC[a] (45µM) | 9.6 ± 0.5 | 514 | 10.2 ± 0.8 | 480 | 1.1 | No flux (0.57) |
| ART[b] (55 µM) | 10.2 ± 0.3 | 705 | 12.3 ± 0.1 | 601 | 1.2 | Efflux (0.002) |
| ART + PSC[b] (60 µM) | 5.9 ± 0.1 | 697 | 9.1 ± 1.1 | 668 | 1.5 | No flux(0.05) |

[a] Stock solution was diluted to prepare 100 µM, however due to product conversion to dihydroartemisinin, the zero test concentration was in the range of 45- 50 µM and the study was done using P-44 monolayers. [b] Stock solution was diluted to prepare 100 µM, however due to product conversion to dihydroartemisinin, the test concentration was in the range of 55- 60 µM) and the study was done using P-80 monolayers, [c]Mean $P_{app}$ for Bas-Ap direction was divided by the Ap-Bas direction, [d] Mean $P_{app}$ of Ap-Bas direction and Bas-Ap direction transport was compared in a two tailed t test to determine p values (N=3), ART: artesunate, MQ: mefloquine, PSC: PSC833, [e] The mean TEER value for 3 well plates before the test

Apparent permeability of dihydroartemisinin was unable to be calculated due to absence of a separate standard curve. Therefore percentage of dihydroartemisinin and artesunate transferred across Caco-2 monolayer at the last time point were calculated and compared. The percentage of dihydroartemisinin (α and β anomers peaks were added together and peak area ratio of dihydroartemisinin to artemisinin were considered) passed across the Caco-2 monolayer at the last time point in the Ap-Bas direction ranged from 40 to 43 % and the percentage transfer in Bas-Ap directional ranged from 68 to 76%. Whereas the percentage transferred for artesunate was lower in both the directions; Ap-Bas direction 11-14 % and Bas-Ap 18-22%. Therefore dihydroartemisinin has a better permeability across the Caco-2 monolayer compared to artesunate.

#### 4.4.2.5 Bidirectional transport of artemisone

Artemisone is a newly investigated artemisinin derivative and drug permeability studies for artemisone were done at 10 and 20 µM. The net transport of artemisone was much higher than the other artemisinin derivatives tested. The Ap-Bas transport ranged from 37 to 59 × $10^{-6}$ cm/sec and Bas-Ap transport ranged from 35 to 47 × $10^{-6}$ cm/sec (Table 4.9). Therefore the new artemisinin derivative has a much higher passive diffusion than the currently used artesunate and dihydroartemisinin which ensured complete drug absorption. Addition of PSC-833 did not alter the bidirectional transport significantly; therefore artemisone is not subjected to P-gp mediated drug efflux transport.

**Table 4-8:** Apparent permeability ($P_{app}$ ± SEM) and efflux ratios for artemisone through Caco-2 cell lines

| Drug | Con: (µM) | Ap-Bas ($10^{-6}$ cm/sec) | Ap-Bas TEER[e] | Bas-Ap ($10^{-6}$ cm/sec) | Bas-Ap TEER[e] | Efflux ratio[c] | Net transport (P value[d]) |
|---|---|---|---|---|---|---|---|
| AM [a] | 10 | 59.64 ± 4.19 | 453 | 46.90 ± 8.52 | 380 | 0.79 | No flux (0.25) |
| AM [b] | 20 | 36.96 ±4.70 | 664 | 34.66 ±2.67 | 659 | 0.94 | No flux (0.69) |
| AM+ PSC [b] | 20 | 42.92±1.46 | 662 | 52.91±6.89 | 684 | 1.23 | No flux (0.23) |
| AM + MQ [b] | 20+ 50 | 57.64± 7.89 | 695 | 57.95± 8.28 | 645 | 1.00 | No flux (0.98) |

[a] Passage 44 cell were sued to determine the bidirectional transport, [b] Passage 80 cell were used to determine the bidirectional transport, [c]Mean $P_{app}$ for Bas-Ap direction was divided by the Ap-Bas direction, [d] Mean $P_{app}$ of Ap-Bas direction and Bas-Ap direction transport was compared in a two tailed t test to determine p values (N=3), AM: artemisone, PSC: PSC833, MQ: mefloquine, [e] The mean TEER value for 3 well plates before the test.

### 4.4.3 Antimalarial regulation of P-gp expression

The regulation of P-gp in the presence of antimalarials in single and combination therapies was studied. The initial exposure was planned for 100 µM for 4 days, however it was not possible as Caco-2 cell monolayers became detached from the 6 well plates after about days exposure. The similar trend was observed for 50 µM exposure. Mefloquine and amodiaquine were found to be more toxic to Caco-2 cells than artemisinin derivatives. Hence Caco-2 cell were exposed to 20 µM drug concentrations for 96 hours and protein showing Western blot images for Caco-2 cells are given in Figure 4.15. P-gp levels more than 1.5 fold of the control well was considered as the threshold level for up-regulation of the transporter protein.

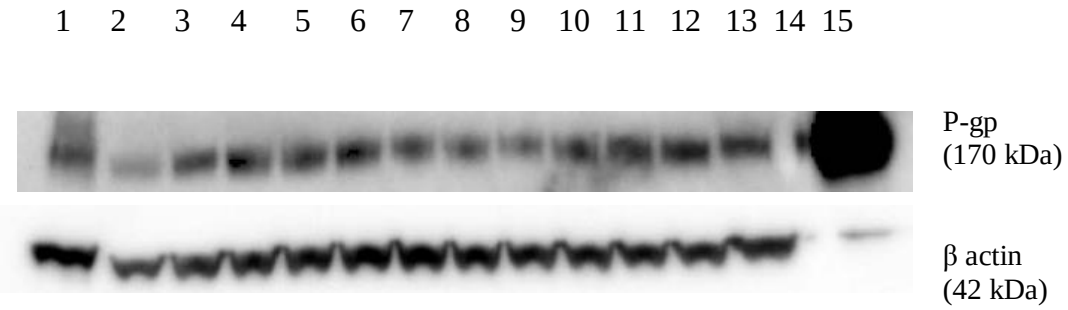


**Figure 4-15:** Western blot for 96 hours exposure of antimalarials on Caco-2 cell monolayer. Beta actin was used as the reference protein. Lanes 1-15 were loaded with cell lysates of exposure 1)methylene blue, 2)mefloquine, 3)amodiaquine, 4)artesunate, 5)dihydroartemisinin, 6)artemisone, 7)0.5% ethanol, 8)artesunate plus mefloquine, 9)artesunate plus amodiaquine, 10)artemisone plus mefloquine, 11)artemisone plus amodiaquine, 12)dihydroartemisinin plus mefloquine, and 13)dihydroartemisinin plus amodiaquine 14) molecular weight marker 15) transfected Hela MDR1 positive control respectively

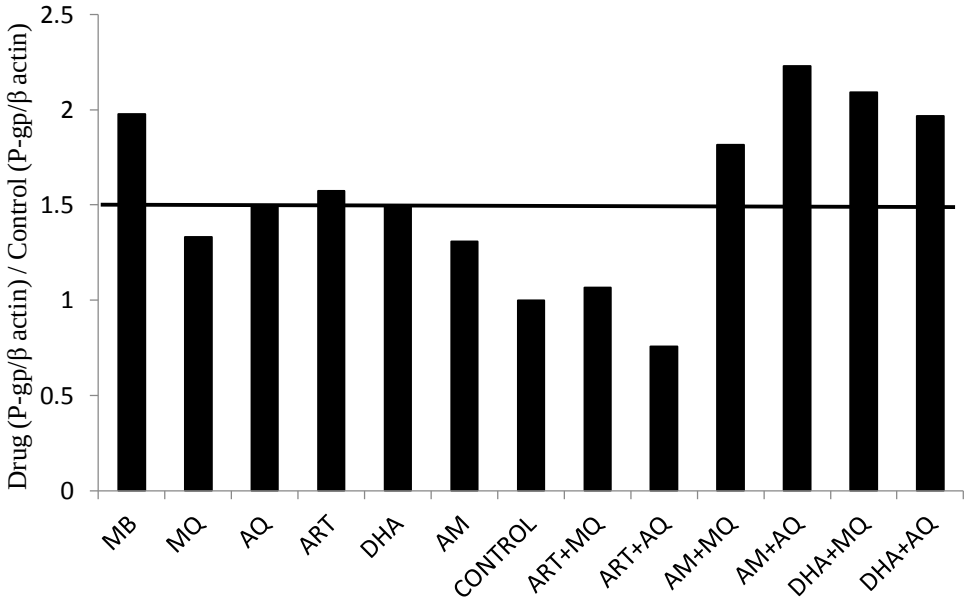


**Figure 4-16:** Regulation of P-gp transporter protein compared to control following 96 hours of antimalarials exposure on confluent Caco-2 cell monolayer.

As shown in Figure 4.16, an up regulation of transporter protein for single drugs; methylene blue, amodiaquine, artesunate and dihydroartemisinin were observed. Artemisone and dihydroartemisinin in combinations with amodiaquine and mefloquine also resulted in up regulation of P-gp. However similar trends were not observed for artesunate combinations and no up regulation was observed for artesunate in combination with mefloquine or with amodiaquine.

A similar study was done using LS174T cells and Figure 4.17 shows Western blot for cells. These cells were more sensitive to antimalarial drugs and especially artemisinin derivatives were found to be more toxic to LS174T cells compared to amodiaquine and mefloquine. The cells were exposed to drugs for 48 hours at 20 µM as longer exposure than that resulted in toxicity and cells death.

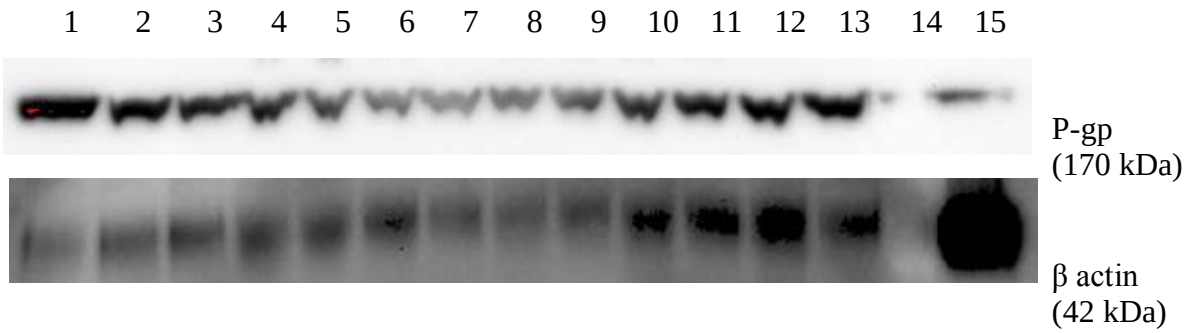


**Figure 4-17**: Western blot for 48 hours exposure of 10 µM antimalarials as single drug or combination on LS174T cells. Beta actin was used as the reference protein. Lanes 1-15 were loaded with cell lysates of exposure 1)methylene blue, 2)mefloquine, 3)amodiaquine, 4)artesunate, 5)dihydroartemisinin, 6)artemisone, 7)0.5% ethanol, 8)artesunate plus mefloquine, 9)artesunate plus amodiaquine, 10)artemisone plus mefloquine, 11)artemisone plus amodiaquine, 12)dihydroartemisinin plus mefloquine, and 13)dihydroartemisinin plus amodiaquine, 14) Molecular weight marker 15) transfected Hela MDR1 positive control respectively.

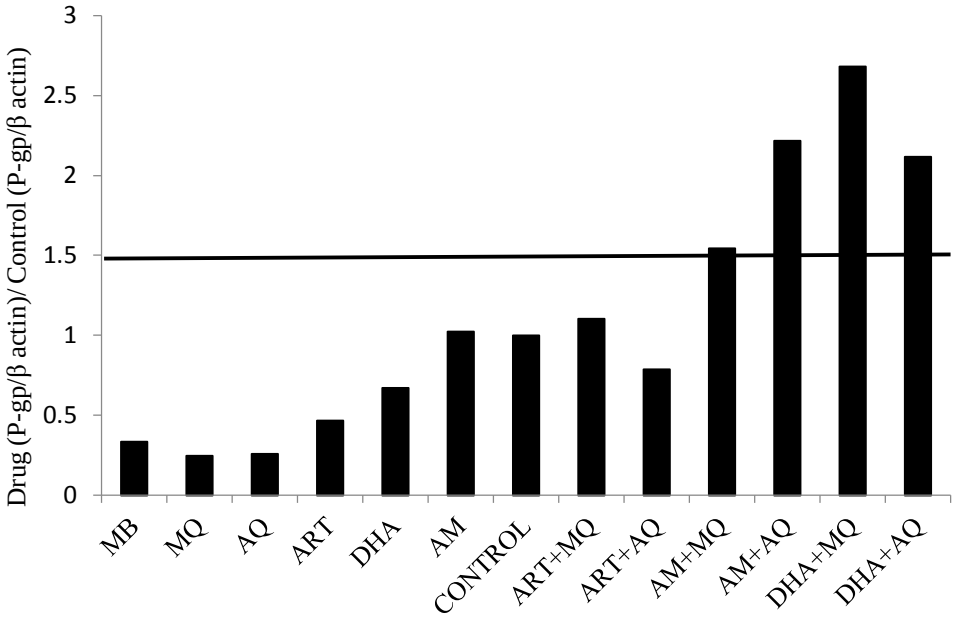


**Figure 4-18:** Regulation of P-gp transporter protein compared to control following 20 µM antimalarials exposure for 48 hours on LS174T cells.

Similar trends as of Caco-2 cells were observed for drug combinations and there was clear up regulation of P-gp for artemisone and dihydroartemisinin combinations. This trend was not observed for artesunate combination. Unlike what was observed in Caco-2 cells, no up regulation of P-gp was observed for antimalarials in single therapy (Figure 4.18).

It is clear that artemisone and dihydroartemisinin in combination therapies created greater P.gp expression than using each drug alone.

## 4.5 Discussion

### 4.5.1 Transport studies using the Caco-2 cell model

In the present study the bidirectional transport of antimalarials was studied using both early and late passage Caco-2 cells with the exception of amodiaquine where only early passage cells were used for the study. To minimise the change in P-gp expression the transport studies were confined to Passage 44 of early passage cells and 80-83 of late passage cells. Caco-2 RIF models and Caco-2 VIN were also used to study the P-gp substrate activity of methylene blue in order to confirm the P-gp substrate activity.

The threshold values 1 and $25\times10^{-6}$ cm/sec established within our laboratory were used in determining the low and high permeability of the drugs with values around $10\times10^{-6}$ cm/sec defining medium permeability (447, 449).

### 4.5.2 P-gp inhibitory action of antimalarial drugs

Low P-gp expression in early passage Caco-2 cells would enable detection of only the potent P-gp blockers. No antimalarials exhibited such potent P-gp inhibitory properties and P-gp inhibition by antimalarials was not observed in early passage Caco-2 cells utilized in the study. Thus no antimalarials tested have affinity and potency similar to the second generation P-gp inhibitor, PSC 833 in exerting P-gp inhibitory properties. Late passage Caco-2 with higher P-gp expression allowed weaker P-gp inhibitors to become evident. Hence mefloquine became detectable. Mefloquine inhibited the P-gp efflux at 100 µM and 50 % inhibition of Bas-Ap directional transport was observed and the Ap-Bas transport of rhodamine123 was not altered.

Intravenous administration of mefloquine caused local irritation at the drug administration site and hence possible toxicity of the drugs (20, 96-98). This was also exhibited in *in-vitro* cell lines where at high concentration of mefloquine cells became detached and lifted from the bottom of the flask. Therefore inhibitory properties of mefloquine were tested only at 100 µM and the general toxicity prevented the determination of the concentration at which mefloquine would bring about 100 % inhibition of P-gp efflux transport. The therapeutic dose for mefloquine at which it exerts antimalarial activity is high and would attain a high drug concentration (mM

range) in the gastrointestinal tract. The volume of the human intestinal lumen is considered to be 2.5 L (426) and at this volume, the therapeutic doses of 10 and 15 mg/kg/day would attain mefloquine concentration of between 0.75 and 1.1 mM for a 70 kg adult (homogenous distribution is unlikely but concentration in the early millimolar range is likely). This is 7 to10 fold higher than the concentration exerting 50% inhibition of the P-gp mediated efflux transport. Therefore at therapeutic dose level of mefloquine, the complete blockage of P-gp mediated efflux transport of P-gp substrate can be expected.

This finding is consistent with the published literature and P-gp inhibitory properties of mefloquine were demonstrated in four different *in-vitro* cell lines. Riffkin and co-workers (104) carried out an *in-vitro* study using the human tumour cells CEM, which had been primed with vinblastine to overexpress P-gp (CEM/VBL) and used a photo affinity labelling technique to determine the interaction of mefloquine with P-gp substrate binding sites. At a concentration of 50 µM mefloquine, verapamil and chloroquine reduced the binding of a photo-reactive analog by 89%, 75% and 20 % respectively. Therefore mefloquine has better affinity, and is thus a more potent P-gp inhibitor than verapamil. The investigators further observed that mefloquine was able to block rhodamine123 efflux efficiently. The study concluded that mefloquine at 1-10 µM serum concentration can modulate P-gp substrate function and thus should be considered for reversing multidrug resistance in cancer chemotherapy. The P-gp inhibitory properties of mefloquine were also shown in P388 leukaemia cells (P388/ADR) (437). A synergistic inhibition of P-gp was observed between the P-gp modulators mefloquine, vinblastine and tamoxifen, the interaction being non-competitive in nature. The synergistic actions allowed these drugs to be given at lower doses to inhibit P-gp (438). Stereoselectivity of mefloquine for P-gp interaction was studied using immortalised rat brain capillary endothelial cells GPNT and Caco-2 cells. P-glycoprotein inhibitory action was observed in both the cell lines for the racemic mixture and enantiomers. However, stereoselectivity was observed only in the GPNT cells. In Caco-2 cells, both stereoisomers equally inhibited the P-gp efflux (436).

Based on the present study and the previously published literature, it is evident that mefloquine clearly has P-gp inhibitory properties. The affinity of mefloquine is lower compared to PSC 833, higher compared to verapamil and has a synergistic effect in combination with vinblastine and tamoxifen. P-gp mediated drug interactions are likely

between P-gp substrates and mefloquine and could result in an unexpected increase in systemic exposure and related adverse effects of the P-gp substrate. For example, in patients with comorbidities of malaria and AIDS increased adverse effects can be expected due to increased plasma levels of antiretrovirals (P-gp substrate) if administered with mefloquine. This would also be important in antimalarial therapy itself when combination therapies are considered.

However contrary to this, in a pharmacokinetic study of ritonavir and mefloquine in humans, no change in the pharmacokinetic behaviour of ritonavir (less than 8% of AUC and $C_{max}$) was observed. The authors speculated that possible up-regulation of P-gp by mefloquine and ritonavir could have masked the P-gp inhibitory properties of mefloquine. Further these study finding was weakened by high variability of ritonavir pharmacokinetics of study participants (301). Therefore further *in-vivo* pharmacokinetic studies are needed to confirm P-gp mediated pharmacokinetic interactions of mefloquine.

Based on the current study, mefloquine exerted P-gp inhibitory properties at a 10 fold lower dose compared to the therapeutic dose for antimalarial activity whereas in a study by Riffkin and colleagues (104) inhibitory properties were observed at a 20 fold lower dose. Thus this is indicative that mefloquine has a practical role in reversing multidrug resistance in cancer chemotherapy at a much lower dose other than its role in antimalarial therapy. Further decrease in doses might be possible when combined with anticancer drugs due to P-gp synergistic effects (438). This lower dosing compared to the antimalarial dose would minimise the side effects exerted and other noted side effects such as nausea, vomiting and occasional neurotoxicity. Mefloquine has lower affinity compared to first generation P-gp inhibitors such as PSC 833 and would minimise CNS related effects resulting from penetration of the BBB.

The currently recommended artemisinin combination therapies for malaria include mefloquine and artesunate combination (3). The new artemisinin derivative artemisone has been proposed to be combined with mefloquine in the management of malaria (70). Co-incubation of mefloquine with artesunate or artemisone did not demonstrate additive P-gp inhibitory properties in Caco-2 cell lines.

Amodiaquine did not exhibit P-gp inhibitory properties at tested concentrations. In contrast to finding in the present study, P-gp inhibitory properties of amodiaquine were observed at 100 and 1000 µM concentrations in *in-vitro* Caco-2 cell lines (440). Yet other studies claimed to show P-gp mediated taxol efflux inhibited by 50% with as little as 16 µM amodiaquine (439). Amodiaquine inhibitory properties at high concentration were precluded from testing in the current study mainly due to its solubility limitations. Amodiaquine was readily soluble in water, however in pH 7.4 HBSS transport buffer it had limited solubility. Therefore amodiaquine was dissolved in a co-solvent ethanol, enabling maximum stock concentration of 20 mM. Test concentration such as 1000 µM amodiaquine would result in toxic ethanol (> 1.5%) and amodiaquine concentration to Caco-2 cells.

P-gp inhibitory properties for methylene blue are not available in the current literature and no P-gp inhibitory properties were observed for methylene blue in the present study.

The artemisinin derivatives; artesunate and artemisone did not exhibit p-gp inhibitory properties in the present study. The published literature on inhibitory properties of artesunate is inconsistent. Similar to current study findings, an *in-vitro* study of Caco-2 cell lines found no P-gp inhibitory properties of artesunate at 36 and 107 µM (439). In contrast, a study of multidrug resistance reversal by artesunate in erythromyelogenous leukemic P-gp over expressing K562/ADR cells and human small cell lung cancer observed poor inhibitory properties for artesunate (110 µM) compared to verapamil and cyclosporin (457). Similarly (440) observed P-gp inhibitory properties of artesunate at 100 and 1000 µM in *in-vitro* Caco-2 cell lines.

It is clear that mefloquine has a higher affinity and potency as a P-gp inhibitor compared to the other antimalarials tested and some of the first generation P-gp inhibitors such as verapamil. The inconsistent findings of P-gp inhibitory properties of amodiaquine, artesunate, dihydroartemisinin and artemisone of the present study and available literature show the need for further *in-vitro* and *in-vivo* studies in the area. Some studies used high concentration of the inhibitor; such concentrations however can be toxic to cell lines, in addition to P-gp inhibition complicating any interpretation regarding transporter specific functionality. However the apparent discrepancy of inhibitory properties at low concentration between studies is likely to be an anomaly P-gp related expression/activity.

### 4.5.3 Permeability and P-gp mediated drug transport of antimalarials

#### 4.5.3.1 Mefloquine drug transport

Mefloquine is a small molecule and is available as its hydrochloride salt. The n-octanol/water partition coefficient is 2.197 and is in the optimum range for maximum absorption. Mefloquine is a diprotic weak base and at physiological pH the positively charged molecular structure is more prominent, where its pyridine moiety is protonated (23, 98).

While the small molecular size and optimum log p value (within 2 to 4) facilitate passive diffusion, the ionized mefloquine at intestinal pH might slow down the process. As predicted from the physicochemical properties, the bidirectional permeability of mefloquine was found to be in the medium range and the Ap-Bas directional transport was in the range of 6 to10 $\times 10^{-6}$ cm/sec in early and late passage Caco-2 cells. Hence mefloquine is mostly likely to have medium permeability based on the threshold values set by previous studies on drug permeability within the same laboratory.

The net efflux transport of mefloquine was close to 1 and a higher Bas-Ap directional transport was not observed. Incubation with the P-gp inhibitor, PSC 833 did not alter the Bas-Ap and Ap-Bas directional transport. The equivalent transport rates in both directions, a transport ratio of efflux direction over uptake direction of 1 indicates that only diffusion has taken place. Thus mefloquine is not subjected to P-gp mediated drug efflux at concentrations above 10 µM.

Another study has shown some P-gp substrate activity of mefloquine at nanomolar concentrations, where $^{14}C$ mefloquine (160 nM) cell accumulation was decreased when incubated with 10 µM verapamil (436). However efflux transport observed at such low concentrations is unlikely to be significant when it comes to gastrointestinal drug absorption. Such low concentrations may be relevant at the blood brain barrier, which could be a significant factor in CNS toxicity of the drug. In this current study the focus was on the P-gp at the gastrointestinal tract for systemic absorption changes and the data presented in this thesis shows no significant effect. The oral dosing results in 0.74 to

1.11 mM of mefloquine concentration in the intestinal lumen. At such high concentrations of mefloquine, P-gp transporters become saturated and efflux transport observed at nanomolar concentrations becomes irrelevant to the $P_{app}$ values for passive diffusion and the extent of drug absorption.

Information on the oral bioavailability or systemic availability for mefloquine is not available in the literature and bidirectional transport of mefloquine in *in-vitro* cell lines has not been reported previously. This study suggests a medium permeability and therefore less than 100 % drug absorption of mefloquine

A pharmacokinetic study of artesunate and mefloquine in humans found changes in pharmacokinetics (increase in clearance and volume of distribution and decrease in $C_{max}$) of mefloquine when administered concurrently (112). However no change in permeability of mefloquine was found when co-incubated with artesunate in the current study, hence change in $C_{max}$ were unlikely to be permeability related. Similarly mefloquine permeability was not altered when incubated with methylene blue or artemisone. The absence of P-gp mediated efflux at test concentrations and minimum change in apparent permeability of mefloquine in the co-treatment with other drugs in the current study shows that lack of permeability related drug interactions of mefloquine.

#### 4.5.3.2 Amodiaquine drug transport

Amodiaquine is a smaller sized drug, its log D being 2.6. Similar to mefloquine, amodiaquine is a diprotic weak base and at physiological pH amodiaquine equilibrium favours the uncharged/neutral compound (23, 73), which is likely to improve passive diffusion. The Ap-Bas directional transport of amodiaquine is higher compared to mefloquine and ranged from 17 to 22 $\times 10^{-6}$ cm/sec. Hence amodiaquine appears to have high drug permeability and almost complete drug absorption. There was a small efflux transport rate (1.3) observed at 10 µM. However at higher concentration no such trend was observed and the slight efflux transport observed at 10 µM is deemed to be clinically insignificant.

Permeability data for amodiaquine is available in the literature. Hayeshi and co-workers (439) confirmed the absence of P-gp mediated drug transport of amodiaquine and bidirectional transport ranged from 44 to111 × $10^{-6}$ cm/sec between 10 and 50 µM, respectively. Cell uptake of amodiaquine was observed at all test concentrations.

The drug permeability of amodiaquine was tested while incubating the drug with artemisone and no change in permeability was found. Significant changes in amodiaquine permeability are unlikely to be seen by co-administration with other drugs due to the high passive permeability of the drug.

Suggested oral drug doses for amodiaquine ranged from 7.5 to 15 mg/kg/day resulting in gastrointestinal concentration of 0.6 to 1.2 mM (>10 µM), which would saturate P-gp carrier molecules. Based on the present study and current literature, amodiaquine has a high passive permeability, ensuring almost 100% drug absorption. Rapid absorption of amodiaquine is shown in pharmacokinetic studies where amodiaquine reaches its peak concentration within 1 hour. Amodiaquine bioavailability has not be reported in the current literature, however it is claimed that amodiaquine has a pharmacokinetic profile similar to that of chloroquine (74) and chloroquine bioavailability is found to be 78-89% (461).

#### 4.5.3.3 Methylene blue drug transport

In the drug industry, two forms of methylene blue are used: reddish brown crystal methylene blue and green golden crystal methylene blue. The reddish brown crystal methylene blue supplied by Fluka Sigma was used for drug transport studies. The blue coloured oxidized form of methylene blue which is administered as the therapeutic agent has a pKa of 0-1 and would remain oxidized in the pH range of the gut (143, 462). Cationic methylene blue has a log P value of -0.9 at pH 7 and its log D value is 0.06, hence it has poor partitioning into the lipid bilayer (462). Other than the small molecular size of methylene blue, inherent physicochemical parameters of methylene blue are not in favour of passive diffusion of this molecule.

As anticipated from the inherent physicochemical properties of cationic methylene blue, a low permeability was observed for methylene blue. The Ap-Bas directional transport

of methylene blue ranged from 1.6 to 2.8 $\times 10^{-6}$ cm/sec, therefore at the test concentration, low cell uptake of methylene blue can be expected.

The Bas-Ap transport of methylene blue was higher than the AP-Bas transport which proposes efflux transport of methylene blue in the gastrointestinal tract. The efflux transport of methylene blue was consistently observed in all four Caco-2 cell models. The highest efflux transport was observed for the Caco-2 VIN model (efflux ratio 5.1), the model with highest P-gp expression. The efflux ratio for methylene was reduced by about 50% when co-incubated with PSC 833, which still left a significant efflux ratio associated with this drug, implying other efflux transporters were functioning when P-gp was blocked. Hence efflux transport is not fully mediated by P-gp and there is possible involvement of other gastrointestinal ABC efflux transporters.

The most common structural feature of P-gp substrates is their amphipathic nature and conforming to this methylene blue has hydrophilic and hydrophobic moieties in its molecular structure.

The poor *in-vitro* cell uptake of methylene blue suggests possible low bioavailability in-*vivo*. Strikingly different bioavailability values (7% vs 72%) for methylene blue in humans are reported in two pharmacokinetics studies of humans (152, 463). The high bioavailability found in the second study was accounted for by increased sensitivity of the analytical techniques adopted in that study. Peters and Robinson (463) proposed that the earlier and low bioavailability could be due to high first pass elimination. Nevertheless, P-gp mediated drug efflux could also contribute to this large discrepancy in bioavailability. In the first pharmacokinetic study, volunteers were given 100 mg of methylene blue, which would result in gastrointestinal concentration around 125 µM, a concentration similar to the test concentration used in the present study (463). Therefore, it is likely that low *in-vivo* methylene blue bioavailability observed in the first study is related to the ABC transporters mediated efflux in the gut.

In the second study, on the other hand, a higher oral drug dose was administered resulting in a higher gastrointestinal concentration (625 µM). At this fivefold higher concentration, it is possible that saturation of efflux transporters and cell accumulation were attained. In the absence of efflux transport, a higher proportion of drug can be permeated resulting in higher bioavailability of methylene blue (152).

A high accumulation of methylene blue in the brain following IV administration was observed in rats (463). Blood brain capillaries contain a large amount of P-gp and it is unlikely for cationic methylene blue to pass through this shield unless a very high plasma concentration of methylene blue was attained. Therefore this could be due to possible exofacial conversion of cationic methylene blue into leuco-methylene blue (by NADPH) and leuco-methylene blue can easy cross through membranes (463). A high accumulation of methylene blue was found in intestinal walls of rats (463) and high accumulation of methylene blue in Caco-2 cell lines was also observed in the present study, especially at low concentrations such as 10 µM. Therefore a methylene blue dose which can saturate efflux transporters and cell accumulation is required to result in sufficient bioavailability of the drug. The currently used dose of methylene blue for children is 12 mg/kg which is 8 and 1.7 fold higher than the Peter and co-workers (463) and Walter-Sack and co-workers (152) studies, respectively. At the currently used dose efflux transporters and cell accumulation would be saturated resulting in high bioavailability of the drug. Thus 12 mg/kg methylene blue can be recommended to be used in the management of malaria to achieve adequate therapeutic concentration.

#### 4.5.3.4 Artesunate drug transport

Similar to amodiaquine and mefloquine, physiochemical parameters of artesunate are in favour of passive diffusion. However ionization of artesunate at physiological pH (pKa of 4.28) is plausible. A medium permeability was observed for artesunate with $P_{app}$ values of 7 to 10 $\times 10^{-6}$ cm/sec. A medium permeability of artesunate has been reported in previous study of Caco-2 monolayers, where $P_{app}$ value for sodium artesunate was found to be 4 $\times 10^{-6}$ cm/sec (17) Artesunate showed a higher Bas-Ap transport (efflux ratio of 1.5) therefore minimum affinity to P-gp. This is unlikely to result in difference in permeability and therefore systemic absorption.

As described in methods, the transport experiment was of 2 hours duration and during the experiment, the 24 well plated were kept in the incubator at 37 $^{\circ}$C and removed for sample collection. According to the literature, some degradation of artesunate to dihydroartemisinin is possible at incubation temperature (464). This need to be considered when *in-vitro* $P_{app}$ values of artesunate is used to predict *in-vivo* drug

absorption. However the qualitative information of artesunate is still valid which is indicative of medium permeability and less than 100% drug absorption.

The "zero" time artesunate samples also contained the active metabolite of artesunate, dihydroartemisinin. The active metabolite, dihydroartemisinin has favourable physicochemical parameters for passive diffusion with a $pK_a$ of 12.6 (unionized at the physiological pH) and log p of 2.19. The percentage of dihydroartemisinin passed across the cell monolayer was about 4 times higher than artesunate percentage passed through; therefore dihydroartemisinin is likely to have better passive diffusion compared to artesunate.

Previous work done within our own lab using an *in-vitro* Caco-2 monolayers study using radiolabelled dihydroartemisinin found Ap-Bas and Bas-Ap transport of 21 to 30 and 32 to $39\times10^{-6}$ cm/sec transport of dihydroartemisinin (338). This $P_{app}$ values are indicating almost complete drug absorption of dihydroartemisinin, which is higher than artesunate permeability observed in the current study. Similar trends were observed *in-vivo* where in healthy volunteers, the absolute oral bioavailability of dihydroartemisinin found to be 80% following oral artesunate administration (62) whereas absolute oral bioavailability of artesunate found to be 23% (40, 41).

#### 4.5.3.5 Artemisone drug transport

Artemisone has the very favourable physicochemical parameters to facilitate passive diffusion. Artemisone has a basic centre and is more likely remain unionized at the physiological pH; this has an optimum log P value and has a relatively small molecule weight for maximum drug absorption. Artemisone showed the highest $P_{app}$ value out of the drug tested for bidirectional transport confirming passive permeability and 100 % drug absorption. P-gp mediated efflux transport was not observed for artemisone, hence unlikely to observe P-gp mediated pharmacokinetic drug interactions. As anticipated, no change in $P_{app}$ of artemisone was observed when co-incubated with mefloquine. Artemisone has also shown higher bioavailability compared to artesunate in monkeys (70). P-gp mediated efflux transport was not observed for artemisone, hence unlikely to observe P-gp mediated pharmacokinetic drug interactions. As anticipated, no change in $P_{app}$ of artemisone was observed when co-incubated with mefloquine.

### 4.5.4 Biopharmaceutical classification (BCS) of antimalarials

The biopharmaceutical classification system enables establishment of *in-vivo* and *in-vitro* correlation of immediate release drugs on the basis of drug solubility and permeability. This classification can be used to determine the feasibility of using *in-vitro* dissolution data as a surrogate to establish bioequivalence of multisource generic drugs (in other words biowaiver for multisource products). This information can be useful, especially in a resource poor setting for drug regulatory bodies for registration of multisource generic products (465).

The BCS requires the solubility of the maximum dose strength of drug in 250 mL of aqueous media over the pH range of 1 to 7.5 (465). The solubility of drug in water and at pH 7.4 was obtained from the literature. Drug was considered to have a low solubility if the estimated drug concentration at the highest dose strength was higher than the reported drug solubility at physiological pH. The drug solubility, estimated gastrointestinal concentration and drug permeability obtained from the present study are listed in Table 4.10.

**Table 4-9**: Estimated gastrointestinal concentration for highest strenght dose of the drug, drug solubility and Ap-Bas directional $P_{app}$ values for antimalarials found in the present study are listed.

| Drug | Aqueous Solubility (mg/mL) | Solubility at pH 7.4 (mg/mL) | Tablet strength (mg) | GUT Con. (mg/mL) 250 mL | Ap-Bas permeability [b] ($\times 10^{-6}$ cm/s) | Reference |
|---|---|---|---|---|---|---|
| MQ | 1.8 | 0.303 | 250 | 1 | 6-10 | (3, 93, 94, 98) |
| AQ | 8 | 0.08 | 600 | 2.4 | 16-22 | (3, 73) |
| MB | 40 | n/a [a] | 200 | 0.8 | 2-3 | (143, 146, 462) |
| ART | 2 | <15 | 200 | 0.8 | 7-10 | (3, 466) |
| AM | n/a [a] | 89 | 20 | 0.1 | 37-60 | (66, 67) |

[a] Not available, [b] The *in-vitro* Ap-Bas Permeability observed in the current study for each drug is listed, MQ: mefloquine, AQ: amodiaquine, MB: methylene blue, ART: artesunate, AM: artemisone

Based on the previous work done within the our laboratory drugs with $P_{app}$ value of more than $25\times10^{-6}$ cm/s were considered to have complete drug absorption and drugs with

$P_{app}$ value less than $1\times10^{-6}$ cm/s were considered to have low permeability (447, 449). The BCS classification place drugs into highly permeable category when the extent of absorption is 90 %. Considering both solubility and the permeability, the antimalarials studied were categorized into different BCS class as given in Table 4.11.

**Table 4-10** : Biopharmaceuctical classitifiaction for antimalarials

| Drugs | Solubility | Permeability | BCS class |
|---|---|---|---|
| MQ | Low | Medium | II/IV |
| AQ | Low | High | II |
| MB | n/a[a] | Low | III/IV |
| ART | High | Medium | I/III |
| DHA | Low | Medium | II/IV |
| AM | High | High | I |

[a] Not available

Mefloquine hydrochloride showed medium permeability and less than 100 % drug absorption. The slow rate of drug absorption is evident from the clinical research where $t_{max}$ of mefloquine reported was about 20 hours (297, 298). Mefloquine has poor drug solubility at physiological pH and hence can be classified into either class II or IV of the BCS class. However given the variability in the use of excipients, formulation and manufacturing process, it would be safer to place mefloquine in class IV. Hence immediate release multisource products of mefloquine cannot be granted a biowaiver in place of *in-vitro* dissolution test. Similarly a previous study on biowaiver monograph of mefloquine hydrochloride, did not recommend a biowaiver for mefloquine (98).

In contrast, amodiaquine permeability was found to be higher than mefloquine. The Ap-Bas transport was close to the threshold value set by our laboratory and can be considered to have high permeability giving more than 90 % drug absorption. Amodiaquine has a good aqueous solubility and the solubility decreases with increase in pH. The estimated expected gastrointestinal concentration is about 30 fold higher than the solubility limitation at pH 7.4. Previously published biowaiver monograph has

placed amodiaquine in class IV due to the absence of permeability information. However considering the present study findings, other *in-vitro* literature (439) and similarity of amodiaquine pharmacokinetic data to chloroquine (461), this drug can be placed in class II of the BCS classification. Hence immediate release multisource products of amodiaquine can be granted a biowaiver in place of *in-vitro* dissolution test.

Methylene blue has a good aqueous solubility; however solubility at physiological pH has not been reported. As depicted in Table 4.11, methylene blue can be classified into class III or IV. Therefore IVIV correlation for methylene blue cannot be established for low doses (dose less than 100 mg). However based on the bioavailability data in healthy human studies, good bioavailability of methylene blue was observed in a 5 fold higher dose of methylene blue. Hence it is likely for IVIV correlation could be seen at a high dose (more than 500 g) of methylene blue. However this concentration was not tested in this present study. Further studies on drug permeability are needed to determine if methylene blue can be granted a biowaiver.

Artesunate has good drug solubility at gut pH and the estimated gut concentration is much lower than the solubility limitation of the artesunate, whereas dihydroartemisinin aqueous solubility (0.314 mg/mL) is much lower than its prodrugs and has a lower solubility threshold compared to the expected gastrointestinal concentration. This places artesunate in class I or III. Similar to mefloquine, caution is needed to place artesunate in class III of the BCS. This is also justifiable considering the limited validity of $P_{app}$ values of artesunate due to its degradation during the experiment.

The newly developed artemisinin derivative artemisone showed the highest permeability and can be placed in class I of the BCS. At the dose used for pharmacokinetic study in humans (66), the estimated gastrointestinal concentration is much lower than the solubility limitation of artemisone. Class I drugs have high permeability and when the dissolution is rapid in relation to gastric emptying, drug absorption is unlikely to be dependent on drug dissolution and gastric emptying time. IVIV correlation of artemisone can be established; hence a biowaiver for multisource products of artemisone is feasible.

### 4.5.5 Antimalarial regulation of P-gp expression

In Caco-2 cell lines, an up regulation of P-gp expression was observed for antimalarials in the single therapy yet this trend was not evident for LS174T cells. This could be due to the comparatively shorter exposure of the drugs (48 hours compared to 96 hours exposure of Caco-2). Methylene blue in Caco-2 cells up regulated the P-gp by 2 fold and this was higher than up regulation observed for other antimalarials. In the current study methylene blue was identified as a P-gp substrate; hence up regulation of P-gp expression is plausible. P-gp substrates such as vinblastine and some antiretrovirals have shown P-gp induction properties previously (365, 394).

Regulation of P-gp expression by artemisinin has been reported. It is reported that artemisinin induces expression of CYP2B6, CYP3A4 and P-gp in human hepatocytes and in LS174T cell lines through the activation of human PXR and human Constitutive Androstane receptor (CAR) (443). At 25 µM dihydroartemisinin did not activate PXR, however authors speculated that dihydroartemisinin may activate PXR at higher concentration. Up regulation of P-gp was observed in the present study when artesunate and dihydroartemisinin were exposed to Caco-2 cells for 4 days. The molecular structure of mefloquine suggests that it has the ability to induce P-glycoproteins (467). However, this was not observed in the present study. Hence further studies are required to confirm on this.

Interestingly dihydroartemisinin and artemisone in combination therapies (both in combination with mefloquine and amodiaquine) showed a clear up regulation of P-gp expression. This up regulation was seen in LS174 cells. This increases the possible drug interactions for dihydroartemisinin and artemisone combination therapies, resulting in sub-therapeutic levels of drugs with P-gp substrate activity.

Unlike the two artemisinin derivatives, incubation of artesunate with mefloquine or amodiaquine in combinations did not show up regulation of P-gp. This was evident in both the cell lines and however the possible mechanism for this is not clear.

## 4.6 Limitations

*In-vitro* study results and their implications can be of limited validity when it comes to the *in-vivo* situation. Yet *in-vitro* study data can be used to plan *in-vivo* studies for further confirmation of results.

Testing drug permeability and P-gp substrate activity of antimalarials in other *in-vitro* cells models such as MDCK MDR1 cells lines would enable further comparison. However that was not carried out due to lack of time, resources and cost involved.

During the transport study, 24 well plates were stored in the incubator at 37 ºC and withdrawn for sample removal. Some degradation of artesunate is possible at the incubation temperature. Hence small differences in $P_{app}$ values were possible. However the recovery of artesunate was measured at more than 90%.

Caco-2 cells do not have all the gut metabolising enzymes, thick mucus layer and the complex dynamic flow environment found in the human gastrointestinal epithelium. Therefore, study findings need to be interpreted considering these limitations and *in-vitro* findings need to be further tested under *in-vivo* conditions to draw final conclusions.

The very low drug concentrations expected at body organ sites (other than the gut boundary) was unable to be tested due to limitations of the sensitivity of analytical techniques for drug assays (HPLC).

.

## 4.7 Future studies

An *in-vitro* drug permeability study of methylene blue at a concentration of 500 µM needs to be done to determine the change in Ap-Bas directional transport. Co- incubation with other ABC transporter blockers such as MK571, probenecid, ko143 and with methylene blue might help in understanding other efflux transporters involved in methylene blue efflux transport. *In-vivo* bioavailability studies of methylene blue in human would be able to answer the question of dose dependent bioavailability of methylene blue.

Molecular mechanisms of up regulation of P-gp expression need to be explored. Pregnane X receptor (PXR) has shown to mediate expression of P-gp and this need to be explored in future studies. Involvement of PXR in up-regulation of P-gp expression in the artemisinin combination therapy would help understanding the molecular mechanism of up regulation of P-gp.

P-gp mediated drug interactions are multifactorial, therefore in-order to understand the *in-vivo* situation it is important to conduct *in-vivo* studies. *In-vivo* P-gp mediated pharmacokinetic drug interactions studies of P-gp inhibitors mefloquine and P-gp substrates are worth exploring.

## 4.8 Conclusion

Mefloquine exhibited P-gp inhibitory properties at 100 µM and had less affinity compared to PSC 833. Amodiaquine, methylene blue, artesunate and artemisone did not show P-gp inhibitory properties at test concentrations.

Mefloquine, amodiaquine, artesunate and artemisone did not exhibit P-gp substrate properties that can be clinically significant and permeated through passive diffusion. Amodiaquine and artemisone were found to have high permeability predicting almost 100 % drug absorption. These two drugs can be placed in class II and I of the BCS, therefore biowaiver can be granted. Mefloquine and artesunate showed medium permeability, therefore less than 100% *in-vivo* drug absorption can be expected. Methylene blue showed very low permeability, therefore drug absorption. Methylene blue found to have P-gp mediated efflux transport and however there are other efflux mechanisms involved in the process. A clear up regulation of P-gp expression was observed for dihydroartemisinin and artemisone in combination with amodiaquine and mefloquine. This trend was not observed for artesunate combination. Up regulation trends were also observed for methylene blue artesunate amodiaquine and dihydroartemisinin in Caco-2 cells.

# 5 Summary

My PhD project consists of two main areas concerning the pharmacokinetics of antimalarial drugs. The first part of the study includes allometric scaling of antimalarials for interpolation of pharmacokinetic parameters and drug doses for children.

The second part of the study includes bidirectional transport studies of antimalarial drugs in both single and combination therapy to determine drug permeability and P-gp mediated drug efflux transport of antimalarials. Finally, regulation of P-gp expression in the presence of antimalarials in single and combination therapy was determined.

Allometric scaling is a well-established pharmacokinetic technique which relates pharmacokinetic parameters of mammalian species with their body size/weight. Study antimalarials were selected using WHO guidelines for the treatment of malaria. A comprehensive literature search of pharmacokinetic parameters was conducted in main databases and by cross referencing. Pharmacokinetic parameters: clearance, volume of distribution and half-life were collected in healthy and malaria infected preclinical and human species. After data screening based on specific selection criteria, the list of drugs were limited to artesunate (IV), its active metabolite, dihydroartemisinin (IV), artemether (IV and IM), artemisinin (IV, intraperitoneal and oral), clindamycin (IV), piperaquine (oral), mefloquine (oral) and quinine (IV). Due to paucity of data it was not possible to scale pharmacokinetic parameters for malaria infected species. Instead scaling was done using healthy species. In conventional allometry pharmacokinetic parameters of pre-clinical species are used to extrapolate human pharmacokinetics whereas in the current study both preclinical species and human pharmacokinetic parameters were used for interpolation of pharmacokinetic parameters for children. The pharmacokinetic parameters were plotted in a log-log scale against the body weight of the species to obtain the allometric plot. The slope of the allometric plot was calculated to determine the allometric exponent and the antilog of the coefficient was obtained as the allometric coefficient. Allometric power relationships were established for the three pharmacokinetic parameters; clearance, volume of distribution and half-life of selected drugs,

Selected allometric correction factors were also tested to determine superiority of correction factor techniques compared to simple allometry. The correction factors maximum life span potential and Rule of Exponents were tested. In addition, two new correction factors, liver weight and liver blood flow, were also tested. It was hypothesised that liver weight correction would improve clearance prediction of low hepatic extraction ratio drugs and liver blood flow correction would improve clearance prediction of high hepatic extraction ratio drugs. The interpolated drug clearance by simple allometry and correction factors; maximum life span potential, liver weight correction and liver blood flow corrections were compared to the observed drug clearance in clinical studies in children. The predictive success was determined and the ratio of observed to predicted drug clearance in the range of 0.5 to 2 were considered acceptable.

Drug clearance in healthy and malaria infected adults was compared. Given that there is no difference in pharmacokinetics in malaria infection, the exponent derived using healthy species were used for dose determination in malaria infected children. Paediatric drug doses were determined for arbitrary body weights of 15 and 25 kg. Doses for children less than 2 years were excluded due to known physiological and pharmacokinetic differences.

Finally drug clearance values of preclinical species were used to extrapolate clearance of adults to determine the predictive success of the conventional allometry for antimalarials.

Strong allometric scaling relationships were observed for drug clearance of drugs scaled. The regression analysis for clearance had $r^2$ value above 0.9 for all drugs scaled. The allometric exponent values were 0.71, 0.85, 0.66, 0.83, 0.62, 0.96, 0.52 and 0.40 for artesunate, dihydroartemisinin (following IV artesunate), artemether, artemisinin, clindamycin, piperaquine, mefloquine and quinine, respectively. The 95% confidence interval (CI) for piperaquine, mefloquine and quinine did not encompass both universal exponent values of 0.67 and 0.75. Therefore data included in the present study does not support the use of universal exponent values for extrapolation of doses. Small exponent values indicated the need for a large increase in doses for mefloquine and quinine. The 95% CI of the exponent did not encompass one except for dihydroartemisinin and

piperaquine, therefore linear scaling or mg/kg adult dosing is not applicable for all antimalarials.

Similar to clearance, volume of distribution also showed a strong allometric relationship for all drugs ($r^2 > 0.91$) except for artesunate with an $r^2$ of 0.69. This could be due to its prodrug nature. The exponents for volume of distribution for other drugs ranged from 0.81 for clindamycin to 1.16 for piperaquine (the exponent for artesunate was 0.54). The 95% CI of the exponent for artemether, piperaquine and quinine did encompass 1, therefore linear scaling is possible. The exponent for volume of distribution is used for loading dose determination. Further analysis of volume of distribution was not done as loading doses are not recommended for adults with malaria infection except for quinine.

The regression analysis showed poor allometric relationship for half-life of antimalarials except for artemether, therefore no further analysis of half-life was carried out.

Quinine clearance in malaria infected adults was found to be lower compared to that of healthy adults. Therefore it was not suitable to use exponent data from healthy subjects for dose determination of quinine in children with malaria infection. Dihydroartemisinin showed a similar pattern, however the power of the two-tailed t test was lower. The drug clearance of artesunate, artemether, clindamycin, mefloquine and piperaquine showed no difference in malaria infection, with low power (< 0.8). The large standard deviation and low power of the test made it difficult to make definitive conclusions. Nevertheless, in the current study exponents of healthy species were used for dose interpolations of dihydroartemisinin, artemether, clindamycin, piperaquine and mefloquine for children with malaria.

In general the correction factors extended the Y axis by two orders of magnitude, which improved the $r^2$ value. The liver weight correction improved the $r^2$ value for all drugs, whereas maximum life span potential correction leads to $r^2$ improvement of dihydroartemisinin, mefloquine and quinine. The liver blood flow correction also selectively improved $r^2$ values of dihydroartemisinin, clindamycin, piperaquine, mefloquine and quinine. The exponent values for all drugs by all methods were $\geq 1$. The drug clearance predicted using simple allometry and liver body weight correction had the best predictive success. The predicted clearance based on simple allometry was within 0.5 to 2 for all the drugs scaled and mostly over-predicted the drug clearance.

The predictions using liver weight correction were also within the accepted threshold values, however no clear improvement in clearance prediction compared to simple allometry was observed. The maximum life span potential and liver blood flow corrections did not meet the predictive success in some cases and these two correction factors under-predicted the drug clearance at all times.

Of the drugs scaled, dihydroartemisinin and artemether are high extraction ratio drugs. However liver blood flow correction did not improve clearance prediction for dihydroartemisinin and artemether but simple allometry predictions were accurate. Piperaquine and mefloquine were low extraction ratio drugs. The simple allometric predictions for these drugs were found to be accurate despite literature to indicate that low extraction ratio drugs are poor predictors by simple allometry. The predicted drug clear clearance by liver weight and MLP corrections (recommended correction methods for low extraction ratio drugs) also met the predictive success for mefloquine. No correction factor performed better than simple allometric predictions.

The current recommendation for antimalarial drug dosing in children is to use mg/kg adult doses except for artemether. Artemether doses are recommended for body weight ranges. The predicted drug doses based on simple allometric exponents were 10 to 70% higher compared to the currently recommended doses with the exception of artemether. Currently recommended artemether mg/kg dosing for children is higher than the adult doses and higher than the allometric predictions in most instances. Therefore in general allometric scaling recommends an increase in doses for children compared to the mg/kg adult dosing.

The conventional allometry where preclinical clearance data are used to extrapolate pharmacokinetics for humans did not work for all antimalarials. Scaling using preclinical species alone was difficult due to insufficient data. Artemether, clindamycin, piperaquine, mefloquine and quinine scaling was done using two preclinical species. Despite this artemether and mefloquine exponents were similar to the exponent derived using both preclinical and human species. The predicted clearance for dihydroartemisinin and piperaquine were 4 and 6 fold higher than the observed clearance. Addition of human pharmacokinetic data improved clearance prediction and was within threshold values at all times.

The second part of the study required development of a robust *in-vitro* Caco-2 cell monolayer with sufficient expression of P-gp. Three interventions were adopted to improve P-gp transporter expression in early passage (P-44) Caco-2 cells; exposure of Caco-2 cells to a known P-gp inducer, rifampicin (Caco-2 RIF), exposure to Caco-2 cells to a potent P-gp substrate, vinblastine at nanomolar concentrations for an extended period (Caco-2 VIN) and lastly regular passaging of Caco-2 cells to obtain late passage Caco-2 cells.

P-gp expression was determined using the Western blotting technique and functionality of P-gp was determined by conducting bidirectional transport studies of a known P-gp substrate, rhodamine123. Rhodamine123 was quantified using fluorescence spectroscopy. Bidirectional transport studies required growth of Caco-2 cells on 0.4 micrometre filter inserts at 65,000 cells/$cm^2$ and the transport experiments were conducted on day 21 to 24 upon reaching suitable cell differentiation, monolayer tightness and transepithelial electrical resistance above 300 $\Omega/cm^2$.

Bidirectional transport studies showed efflux transport of rhodamine123 in early passage (passage 44), Caco-2 RIF, Caco-2 VIN and in late passage (passage 80s) Caco-2 cells. The efflux transport of rhodamine123 was inhibited when co-incubated with the P-gp transporter inhibitor, PSC 833. Therefore it was evident that P-gp transporter proteins are expressed in all four Caco-2 cell lines. This was also visually observed in a Western blot. Faint blots for early passage Caco-2 and Caco-2 RIF models were not quantified. The blots for late passage Caco-2 and Caco-2 VIN models showed that there was a small change in P-gp expression over days 21, 24 and 28. The highest P-gp expression for late passage Caco-2 cells and Caco-2 VIN were on day was on day 28 and 24 respectively.

There was insufficient increase in P-gp expression in the Caco-2 RIF model and the efflux ratio was 1.5 compared to 1.4 of the passage 44 Caco-2 cells. Caco-2 VIN had the highest P-gp expression with an efflux ratio of 13. However development of Caco-2 VIN model was a rather time consuming process. A clear improvement in P-gp expression was observed with the increase in passage number; the efflux ratio for passage 80 was 4.7 compared to 1.4 for passage 44 Caco-2 cells. Therefore late and early passage Caco-2 monolayers were selected for routine bidirectional transport

studies. Caco-2 VIN and Caco-2 RIF models were used only for further confirmation of P-gp substrate activity of a drug.

P-gp inhibitory properties of antimalarials were determined by assessing the change in bidirectional transport of rhodamine123, when co-incubated with antimalarials. Rhodamine123 transport alone and in combination with antimalarials was studied. The inhibition of efflux transport of rhodamine123 was used to determine the P-gp inhibitory properties of antimalarials.

P-gp inhibitory properties of antimalarials were not observed in early passage Caco-2 cells. Therefore no antimalarial in the current study had potent P-gp inhibitory properties to compare with the second generation P-gp inhibitor, PSC833. Mefloquine at 100 µM showed P-gp inhibitory properties in late passage Caco-2 cells where 50% inhibition of rhodamine123 efflux was observed. The concentration at which mefloquine exerted 100 % inhibition of efflux transport of rhodamine123 could not be determined as mefloquine was found to be toxic to cells at higher concentrations. Amodiaquine, artesunate, methylene blue and artemisone did not exhibit P-gp inhibitory properties at both 100 and 300 µM. Mefloquine in combination with artesunate or with artemisone did not attain any additive inhibition of rhodamine123 efflux compared to mefloquine incubation alone.

Bidirectional transport studies to determine the P-gp substrate activity and permeability of antimalarials require drug assays to quantify drugs at different time points in apical and basolateral compartments. Assays of mefloquine, amodiaquine and methylene blue were done using different HPLC techniques. Assay of artesunate and artemisone required an LC-MS-MS technique.

Bidirectional transport of mefloquine in early and late passage Caco-2 cells showed a $P_{app}$ value in the range of 6 to $10 \times 10^{-6}$ cm/sec in the apical to basolateral direction (cell uptake) and 5 to $11\times 10^{-6}$ cm/sec in the basolateral to apical direction (efflux to transport). The efflux ratio ranged from 0.7 to 1, therefore absence of efflux transport. Bidirectional transport was not altered in the presence of PSC 833. This further confirmed that mefloquine was not subjected to efflux transport at concentrations $\geq 10$ µM. No change in permeability of mefloquine was observed when co-incubated with artesunate, artemisone and methylene blue. Apical to basolateral $P_{app}$ values show a

medium permeability for mefloquine and this has a low solubility in the gut at physiological pH. Therefore mefloquine can be classified into Class IV of the biopharmaceutical classification system. Therefore an *in-vitro* dissolution test can't replace the requirement for *in-vivo* bioequivalence studies for bioequivalence of immediate release multisource generic products of mefloquine.

The apical to basolateral directional transport of amodiaquine ranged from 16 to 23 × $10^{-6}$ cm/sec which indicates near complete drug absorption of amodiaquine. At 10 µM, higher basolateral to apical directional transport of amodiaquine was observed with an efflux ratio of 1.3. However such small increase in serosal to mucosal directional transport will not change drug absorption and systemic availability of amodiaquine to cause a clinically significant change in outcome. At 100 µM, the efflux ratio was found to be one, indicating no net transport of amodiaquine. The $P_{app}$ value of amodiaquine indicates that amodiaquine has high permeability and drug solubility at pH 7.4 is much lower compared to the estimated drug concentration achieved from highest tablet strength. Therefore amodiaquine can be placed in class II of the bio pharmaceutical classification, which allows a biowaiver for multisource generic products of amodiaquine in place of the *in-vitro* dissolution test.

Out of the drugs studied methylene blue had the lowest bidirectional permeability and the basolateral to apical directional transport was higher than the apical to basolateral directional transport. This was consistently observed in all 4 models of the Caco-2 cell monolayers with the Caco-2 VIN model giving the highest efflux ratio of 5.1. However co-incubation with PSC833 was not able to fully block (about 50% inhibition was observed) the efflux transport of methylene blue. Therefore it is likely methylene blue efflux transport is mediated through other efflux transporters in addition to P-gp. The $P_{app}$ value apical to basolateral directional transport of methylene blue ranged from 1.6 to 2.8 × $10^{-6}$ cm/sec at 100 µM, therefore low cell uptake of methylene blue can be expected. The physicochemical parameters other than the small molecule size of methylene blue are also not in favour of passive permeability. Methylene blue has good aqueous solubility but solubility at pH 7.4 was not available in the literature. At 100 µM methylene blue has a low permeability which places methylene blue in class III or IV of the biopharmaceutical classification system, therefore *in-vivo* and *in-vitro* correlation of methylene blue cannot be established at 100µM.

Artesunate showed a medium permeability with apical to basolateral transport of 7 to $10 \times 10^{-6}$ cm/sec. Similar to amodiaquine, artesunate also showed efflux transport with an efflux ratio of 1.5 which is not large enough to cause a clinically significant difference in therapeutic outcome. Artesunate can be placed in class III of the biopharmaceutical classification system with its medium permeability and good solubility at physiological pH.

Out of the drugs studied, artemisone had the highest bidirectional permeability and this was also evident from its physicochemical parameters. The apical to basolateral and basolateral to apical transport of artemisone ranged from 37-60 to 35-47 $\times 10^{-6}$ cm/sec, respectively, indicating complete drug absorption of artemisone. Efflux transport of artemisone was not observed. Artemisone solubility at physiological pH is higher than the estimated gastrointestinal concentration from the highest dosage strength. Therefore artemisone can be placed in class I of the biopharmaceutical classification system, which allows a biowaiver for multisource generics of artemisone in place of *in-vitro* dissolution testing.

The final part of the study was to determine the regulation of P-gp expression in the presence of antimalarials in single and combination therapy. This was tested in Caco-2 and LS174 T cells. Antimalarials, especially artemisinin derivatives, were found to be toxic on LS174 T cells. Therefore exposure was limited to 48 hours at 20 µM for LS174 T cell and 96 hours for Caco-2 cells. A clear up-regulation of P-gp was observed in both cell lines for dihydroartemisinin and artemisone in combination with mefloquine or amodiaquine. This was not observed for artesunate combinations. Methylene blue upregulated the P-gp expression in Caco-2 cells when exposed for 96 hours. This could be due to P-gp substrate activity of methylene blue. However this was not observed in LS174 T cells and could be due to shorter exposure time. Some up-regulation was also observed for dihydroartemisinin, artesunate and amodiaquine in Caco-2 cells.

Overall, simple allometric scaling is a plausible technique for dose determination in children. The correction factors were unable to show clear improvement in clearance prediction compared to simple allometry. Mefloquine exhibited P-gp inhibitory properties. Mefloquine, amodiaquine, artesunate and artemisone did not exhibit P-gp substrate activity. Methylene blue was found to have P-gp mediated efflux transport as one of the multiple mechanisms available to transport methylene blue. It also showed

low permeability, while mefloquine and artesunate showed medium and amodiaquine and artemisone high permeability across Caco-2 monolayers. A clear up-regulation of P-gp expression was observed for dihydroartemisinin and artemisone in combination with amodiaquine and mefloquine in Caco-2 and LS174 T cells.

# 6 References


1. Diseases NCfZV-BaE. The history of malaria, an ancient disease: Centres for Disease Control and Prevention; 2010 [cited 2015 31 August 2015 ]. Available from: http://www.cdc.gov/malaria/about/history/index.html.
2. Phillips R. Current status of malaria and potential for control. Clin Microbiol Rev 2001;14(1):208-26.
3. Organization WH. Guidelines for the treatment of malaria. Geneva: WHO Press, World Health Organization; 2010.
4. Organization WH. Severe and complicated malaria. Trans R Soc Trop Med Hyg. 1990;84:1-65.
5. Organization WH. World malaria report 2014: World Health Organization; 2014.
6. Moore BR. Pharmacodynamic studies of antimalarial drugs in a Murine Malaria Model [PhD]: Curtin University 2011.
7. Bray R, Garnham P. The life-cycle of primate malaria parasites. Br Med Bull. 1982;38(2):117-22.
8. Baird JK. Effectiveness of antimalarial drugs. N Engl J Med.2005;352 (15) :1565-77.
9. Miller LH, Ackerman HC, Su X-z, Wellems TE. Malaria biology and disease pathogenesis: insights for new treatments. Nat Med. 2013;19(2):156-67.
10. Organization WH. Malaria diagnosis: memorandum from a WHO meeting. Bull World Health Organ. 1988;66(5):575-94.
11. Laishram DD, Sutton PL, Nanda N, Sharma VL, Sobti RC, Carlton JM, et al. The complexities of malaria disease manifestations with a focus on asymptomatic malaria. Malar J. 2012;11(1):29.
12. Organization WH. World malaria report 2012. 2012.
13. Enayati A HJ. Malaria management: past, present, and future. Annu Rev Entomol. 2010;55:569-91.

14. White N, Pongtavornpinyo W. The de novo selection of drug–resistant malaria parasites. Philos Trans R Soc London [Biol]. 2003;270(1514):545-54.

15. Craft JC. Challenges facing drug development for malaria. Curr Opin Microbiol. 2008;11(5):428-33.

16. Stepniewska K, White N. Pharmacokinetic determinants of the window of selection for antimalarial drug resistance. Antimicrob Agents Chemother. 2008;52(5):1589-96.

17. Senarathna SG, Batty KT. Interspecies allometric scaling of antimalarial drugs and potential application to pediatric dosing. Antimicrob Agents Chemother. 2014;58(10):6068-78.

18. Pukrittayakamee S, Looareesuwan S, Keeratithakul D, Davis TME, Teja-Isavadharm P, Nagachinta B, et al. A study of the factors affecting the metabolic clearance of quinine in malaria. Eur J Clin Pharmacol. 1997;52:487-93.

19. Warhurst D. Antimalarial drugs. Drugs. 1987;33(1):50-65.

20. Rosenthal P, Goldsmith R. Antiprotozoal drugs Basic and Clinical Pharmacology. 11 ed. New York, NY: Lange Medical Publications; 2009. p. 899-912.

21. Martindale W, Parfitt K, Britain RPSoG. Martindale: the complete drug reference: Pharmaceutical press London; 1999.

22. Wagner H, Hikino H, Farnsworth N. Economic and medicinal plant research: Academic Press; 2012.

23. Debrus B, Lebrun P, Kindenge JM, Lecomte F, Ceccato A, Caliaro G, et al. Innovative high-performance liquid chromatography method development for the screening of 19 antimalarial drugs based on a generic approach, using design of experiments, independent component analysis and design space. J Chromatogr A. 2011;1218(31):5205-15.

24. Luo XD, Shen CC. The chemistry, pharmacology, and clinical applications of qinghaosu (Artemisinin) and its derivatives. Med Res Rev. 1987;7(1):29-52.

25. Meshnick S, Taylor T, Kamchonwongpaisan S. Artemisinin and the antimalarial endoperoxides: from herbal remedy to targeted chemotherapy. Microbiol Rev. 1996;60(2):301-15.

26. Koopmans R, Duc DD, Kager PA, Khanh NX, Dien TK, de Vries PJ, et al. The pharmacokinetics of artemisinin suppositories in Vietnamese patients with malaria. Trans R Soc Trop Med Hyg. 1998;92(4):434-6.

27. Ashton M, Sy N, Van Huong N, Gordi T, Hai T, Huong D, et al. Artemisinin kinetics and dynamics during oral and rectal treatment of uncomplicated malaria. Clin Pharmacol Ther 1998;63(4):482-93.

28. Titulaer HAC, Zuidema J, Kager PA, Wetsteyn JCFM, Lugt CB, Merkus FWHM. The pharmacokinetics of artemisinin after oral, intramuscular and rectal administration to volunteers. J Pharm Pharmacol. 1990;42(11):810-3.

29. Augustijns P, D'Hulst A, Van Daele J, Kinget R. Transport of artemisinin and sodium artesunate in Caco-2 intestinal epithelial cells. J Pharm Sci 1996;85(6):577-9.

30. Ashton M, Gordi T, Hai TN, Van Huong N, Sy ND, Nieu NT, et al. Artemisinin pharmacokinetics in healthy adults after 250, 500 and 1000 mg single oral doses. Biopharm Drug Dispos. 1998;19(4):245-50.

31. Hassan Alin M, Ashton M, Kihamia C, Mtey G, Björkman A. Multiple dose pharmacokinetics of oral artemisinin and comparison of its efficacy with that of oral artesunate in falciparum malaria patients. Trans R Soc Trop Med Hyg. 1996;90(1):61-5.

32. Ashton M, Hai T, Sy N. Artemisinin pharmacokinetics is time-dependent during repeated oral administration in healthy male adults. Drug Metab Dispos. 1998;26:25 - 7.

33. Hassan Alin M, Ashton M, Kihamia CM, Mtey G, Björkman A. Clinical efficacy and pharmacokinetics of artemisinin monotherapy and in combination with mefloquine in patients with falciparum malaria. Br J Clin Pharmacol. 1996;41(6):587-92.

34. Gordi T, Huong DX, Hai TN, Nieu NT, Ashton M. Artemisinin pharmacokinetics and efficacy in uncomplicated-malaria patients treated with

two different dosage regimens. Antimicrob Agents Chemother. 2002;46(4):1026-31.

35. Navaratnam V, Mansor S, Sit N, Grace J, Li Q, Olliaro P. Pharmacokinetics of artemisinin-type compounds. Clin Pharmacokinet. 2000;39:255 - 70.

36. Ilett KF, Batty KT, Powell SM, Binh TQ, Thu LTA, Phuong HL, et al. The pharmacokinetic properties of intramuscular artesunate and rectal dihydroartemisinin in uncomplicated falciparum malaria. Br J Clin Pharmacol. 2002;53(1):23-30.

37. Hien TT, Davis TME, Chuong LV, Ilett KF, Sinh DXT, Phu NH, et al. Comparative Pharmacokinetics of Intramuscular Artesunate and Artemether in Patients with Severe Falciparum Malaria. Antimicrob Agents Chemother. 2004;48(11):4234-9.

38. Wongsrichanalai C, Meshnick SR. Declining artesunate-mefloquine efficacy against falciparum malaria on the Cambodia–Thailand border. Emerg Infect Dis. 2008;14(5):716.

39. Qigui Li LHX, Yuanzheng Si, ElaineWong,Ravi Upadhyay, DanielleYanez, Peter J.Weina. Toxicokinetics and hydrolysis of artelinate and artesunate in malaria infected rats. Int J Toxicol. 2005;24:241-50.

40. Batty KT, Anh Thu LT, Davis TME, Ilett KF, Xuan Mai T, Canh Hung N, et al. A pharmacokinetic and pharmacodynamic study of intravenous vs oral artesunate in uncomplicated falciparum malaria. Br J Clin Pharmacol. 1998;45(2):123-9.

41. Batty KT, AnhThu LTA, Ilett KF, Phuctien N, Powel SM, Hung NC, et al. A pharmacokinetic and pharmacodynamic study of artesunate for *Vivax* malaria. Am J Trop Med Hyg. 1998;59(5):823-7.

42. Olliaro P. Pharmacokinetics of artesunate after single oral administration to rats. BMC Pharmacol. 2001;1(1):12.

43. Khanh N, de Vries P, Ha L, van Boxtel C, Koopmans R, Kager P. Declining concentrations of dihydroartemisinin in plasma during 5-day oral treatment with artesunate for falciparum malaria. Antimicrob Agent Chemother. 1999;43:690 - 2.

44. Salman S, Page-Sharp M, Batty KT, Kose K, Griffin S, Siba PM, et al. Pharmacokinetic comparison of two piperaquine-containing artemisinin combination therapies in Papua New Guinean children with uncomplicated malaria. Antimicrob Agents Chemother. 2012;56(6):3288-97.

45. Thuy LD, Hung LN, Danh P, Na-Bangchang K. Absence of time-dependent artesunate pharmacokinetics in healthy subjects during 5-day oral administration. Eur J Clin Pharmacol. 2008;64(10):993-8.

46. Miller R, Li Q, Cantilena L, Leary K, Saviolakis G, Melendez V, et al. Pharmacokinetic profiles of artesunate following multiple intravenous doses of 2, 4, and 8mg/kg in healthy volunteers: Phase 1b study. Malar J. 2012;11(1):255.

47. Davis TM, England M, Dunlop AM, Page-Sharp M, Cambon N, Keller TG, et al. Assessment of the effect of mefloquine on artesunate pharmacokinetics in healthy male volunteers. Antimicrob Agents Chemother. 2007;51(3):1099-101.

48. Silamut K, Newton PN, Teja-Isavadharm P, Suputtamongkol Y, Siriyanonda D, Rasameesoraj M, et al. Artemether Bioavailability after Oral or Intramuscular Administration in Uncomplicated Falciparum Malaria. Antimicrob Agents Chemother. 2003;47(12):3795-8

49. Teja-Isavadharm P, Nosten F, Kyle DE, Luxemburger C, Ter Kuile F, Peggins JO, et al. Comparative bioavailability of oral, rectal, and intramuscular artemether in healthy subjects: use of simultaneous measurement by high performance liquid chromatography and bioassay. Br J Clin Pharmacol. 1996;42(5):599-604.

50. Lin JH. Drug–drug interaction mediated by inhibition and induction of P-glycoprotein. Adv Drug Deliv Rev. 2003;55(1):53-81.

51. Xing J, Bai KH, Liu T, Wang RL, Zhang LF, Zhang SQ. The multiple-dosing pharmacokinetics of artemether, artesunate, and their metabolite dihydroartemisinin in rats. Xenobiotica. 2011;41(3):252-8.

52. van Agtmael M, Shan C, Jiao X, Mull R, van Boxtel C. Multiple dose pharmacokinetics of artemether in Chinese patients treated for falciparum malaria. Int J Antimicrob Agents. 1999;12:151 - 8.

53. Suputtamongkol Y, Newton PN, Angus B, Teja-Isavadharm P, Keeratithakul D, Rasameesoraj M, et al. A comparison of oral artesunate and artemether antimalarial bioactivities in acute falciparum malaria. Br J Clin Pharmacol. 2002;52(6).

54. Karbwang J, Na-Bangchang K, Congpuong K, Molunto P, Thanavibul A. Pharmacokinetics and bioavailability of oral and intramuscular artemether. Eur J Clin Pharmacol. 1997;52(4):307-10.

55. Li QG, Peggins JO, Fleckenstein LL, Masonic K, Heiffer MH, Brewer TG. The pharmacokinetics and bioavailability of dihydroartemisinin arteether, artemether, artesunic and arteline acid in rats. J Pharm Pharmacol. 1998;50:173 - 82.

56. Van Agtmael M, Gupta V, Van Der Wösten T, Rutten J-P, Van Boxtel C. Grapefruit juice increases the bioavailability of artemether. Eur J Clin Pharmacol. 1999;55(5):405-10.

57. McLean W, Ward S. In vitro neurotoxicity of artemisinin derivatives. Med Trop (Mars). 1998;58(3 Suppl):28 - 31.

58. Batty KT, Ilett KF, Davis TM. Protein binding and α: β anomer ratio of dihydroartemisinin in vivo. Br J Clin Pharmacol. 2004;57(4):529-33.

59. Batty KT, Ilett KF, Powell SM, Martin J, Davis TME. Relative bioavailability of artesunate and dihydroartemisinin: Investigations in the isolated perfused rat liver and in healthy Caucasian volunteers. Am J Trop Med Hyg. 2002;66(2): 130- 6.

60. Batty KT, Ilett KF, Edwards G, Powell SM, Maggs JL, Park BK, et al. Assessment of the effect of malaria infection on hepatic clearance of dihydroartemisinin using rat liver perfusions and microsomes. Br J Pharmacol. 1998;125(1):159-67.

61. Xie LH. Pharmacokinetics, tissue distribution and mass balance of radiolabeled dihydroartemisinin in male rats. Malar J. 2009;8(1):112.

62. Binh TQ, Ilett KF, Batty KT, Davis TME, Hung NC, Powell SM, et al. Oral bioavailability of dihydroartemisinin in Vietnamese volunteers and in patients with falciparum malaria. Br J Clin Pharmacol 2001;51(6):541-6.

63. Nealon C, Dzeing A, Müller-Römer U, Planche T, Sinou V, Kombila M, et al. Intramuscular bioavailability and clinical efficacy of artesunate in Gabonese children with severe malaria. Antimicrob Agents Chemother. 2002;46(12):3933-9.

64. Newton PN, van Vugt M, Teja-Isavadharm P, Siriyanonda D, Rasameesoroj M, Teerapong P, et al. Comparison of oral artesunate and dihydroartemisinin antimalarial bioavailabilities in acute falciparum malaria. Antimicrob Agents Chemother. 2002;46(4):1125-7.

65. Krishna S, Planche T, Agbenyega T, Woodrow C, Agranoff D, Bedu-addo G, et al. Bioavailability and Preliminary Clinical Efficacy of Intrarectal Artesunate in Ghanaian Children with Moderate Malaria. Antimicrob Agents Chemother. 2001;45(2):509-16.

66. Nagelschmitz J, Voith B, Wensing G, Roemer A, Fugmann B, Haynes RK, et al. First assessment in humans of the safety, tolerability, pharmacokinetics, and ex vivo pharmacodynamic antimalarial activity of the new artemisinin derivative artemisone. Antimicrob Agents Chemother. 2008;52(9):3085-91.

67. Haynes RK. Artemisone—a highly active antimalarial drug of the artemisinin class. Angew Chem Int Ed 2006;118(13):2136.

68. Nontprasert A, Nosten-Bertrand M, Pukrittayakamee S, Vanijanonta S, Angus BJ, White NJ. Assessment of the neurotoxicity of parenteral artemisinin derivatives in mice. Am J Trop Med Hyg. 1998;59(4):519-22.

69. Meshnick SR. Artemisinin: mechanisms of action, resistance and toxicity. Int J Parasitol. 2002;32(13):1655-60.

70. Vivas L, Rattray L, Stewart L, Robinson B, Fugmann B, Haynes R, et al. Antimalarial efficacy and drug interactions of the novel semi-synthetic endoperoxide artemisone in vitro and in vivo. Antimicrob Agents Chemother. 2007;59(4):658-65.

71. Base BbRd. Amodiaquine BARD bioassay Research data Base Available from: https://bard.nih.gov/BARD/bardWebInterface/showCompound?cid=2165.

72. Scholtz JC. Preparation, stability and in vitro evaluation of liposomes containing amodiaquine/Jacques C. Scholtz [M.Sc. Thesis ]. Potchefstroom: North-West University; 2010.

73. Nair A, Abrahamsson B, Barends DM, Groot D, Kopp S, Polli JE, et al. Biowaiver monographs for immediate release solid oral dosage forms: Amodiaquine hydrochloride. J Pharm Sci 2012;101(12):4390-401.

74. Winstanley P, Edwards G, Orme M, Breckenridge A. The disposition of amodiaquine in man after oral administration. Br J Clin Pharmacol. 1987;23(1):1-7.

75. Pussard E, Verdier F. Antimalarial 4-aminoquinolines: mode of action and pharmacokinetics. Fundam Clin Pharmacol. 1994;8(1):1-17.

76. Orrell C. Pharmacokinetics and tolerability of artesunate and amodiaquine alone and in combination in healthy volunteers. Eur J Clin Pharmacol. 2008;64(7):683.

77. German P, Greenhouse B, Coates C, Dorsey G, Rosenthal PJ, Charlebois E, et al. Hepatotoxicity due to a drug interaction between amodiaquine plus artesunate and efavirenz. Clin Infect Dis. 2007;44(6):889-91.

78. Gasasira AF. Interactions between HIV infection and malaria in children living in sub-Saharan Africa in the era of widening access to improved interventions [Ph.D. Thesis ]: UC Berkeley; 2010.

79. Davis TM, Hung T-Y, Sim K, Karunajeewa HA, Ilett KF. Piperaquine. Drugs. 2005;65(1):75-87.

80. Hien TT, Dolecek C, Mai PP, Dung NT, Truong NT, An DTH, et al. Dihydroartemisinin-piperaquine against multidrug-resistant Plasmodium falciparum malaria in Vietnam: randomised clinical trial. Lancet. 2004;363 (9402):18-22.

81. Price RN, Hasugian AR, Ratcliff A, Siswantoro H, Purba HLE, Kenangalem E, et al. Clinical and Pharmacological Determinants of the Therapeutic Response to Dihydroartemisinin-Piperaquine for Drug-Resistant Malaria. Antimicrob Agents Chemother. 2007;51(11):4090-7.

82. Ahmed T, Sharma P, Gautam A, Varshney B, Kothari M, Ganguly S, et al. Safety, Tolerability, and Single- and Multiple-Dose Pharmacokinetics of

Piperaquine Phosphate in Healthy Subjects. J Clin Pharmacol. 2008;48(2):166-75.

83. Tarning J, Lindegardh N, Sandberg S, Day N, White N, Ashton M. Pharmacokinetics and metabolism of the antimalarial piperaquine after intravenous and oral single doses to the rat. J Pharm Sci. 2008;97(8):3400-10.

84. Gigras R, Gautam A, Paliwal JK. preclinical in vitro and in vivo diposition of an anitmalarial compound piperaquine Indian. J Pharmacol. 2008;40(2).

85. Hung T-Y, Davis TM, Ilett KF. Measurement of piperaquine in plasma by liquid chromatography with ultraviolet absorbance detection. J Chromatogr B 2003;791(1):93-101.

86. Tarning J, Ashley EA, Lindegardh N, Stepniewska K, Phaiphun L, Day NPJ, et al. Population Pharmacokinetics of Piperaquine after Two Different Treatment Regimens with Dihydroartemisinin-Piperaquine in Patients with Plasmodium falciparum Malaria in Thailand. Antimicrob Agents Chemother. 2008;52(3) :1052-61.

87. Hung T-Y, Davis TME, Ilett KF, Karunajeewa H, Hewitt S, Denis MB, et al. Population pharmacokinetics of piperaquine in adults and children with uncomplicated falciparum or vivax malaria. Br J Clin Pharmacol. 2004;57 (3):253-62.

88. Tarning J, Zongo I, Some FA, Rouamba N, Parikh S, Rosenthal PJ, et al. Population Pharmacokinetics and Pharmacodynamics of Piperaquine in Children With Uncomplicated Falciparum Malaria. Clin Pharmacol Ther. 2012;91(3):497-505.

89. Liu C, Zhang R, Hong X, Huang T, Mi S, Wang N. Pharmacokinetics of piperaquine after single and multiple oral administrations in healthy volunteers. Yakugaku Zasshi. 2007;127(10):1709-14.

90. Chinh NT, Quang NN, Thanh NX, Dai B, Travers T, Edstein MD. Short Report: Pharmacokinetics of the Antimalarial Drug Piperaquine in Healthy Vietnamese Subjects. Am J Trop Med Hyg. 2008;79(4):620-3.

91. Sim I-K, Davis TME, Ilett1 KF. Effects of a High-Fat Meal on the Relative Oral Bioavailability of Piperaquine. Antimicrob Agents Chemother. 2005;49 (6):2407-11.

92. Cook G. Malaria prophylaxis. Mefloquine toxicity should limit its use to treatment alone. Br Med J. 1995;311(6998):190.

93. European Pharmacopoeia 5.0. 2005. p. 1241.

94. U.S. Pharmacopeia. 2005; USP 29.

95. Gimenez F, Pennie RA, Koren G, Crevoisier C, Wainer IW, Farinotti R. Stereoselective pharmacokinetics of mefloquine in healthy caucasians after multiple doses. J Pharm Sci. 1994;83(6):824-7.

96. Karbwang J, White NJ. Clinical pharmacokinetics of mefloquine. Clin Pharmacokinet. 1990;19(4):264-79.

97. Desjardins RE, Pamplin CL, 3rd, von Bredow J, Barry KG, Canfield CJ. Kinetics of a new antimalarial, mefloquine. Clin Pharmacol Ther. 1979;26 (3):372-9.

98. Strauch S, Jantratid E, Dressman J, Junginger H, Kopp S, Midha K, et al. Biowaiver monographs for immediate release solid oral dosage forms: mefloquine hydrochloride. J Pharm Sci. 2011;100(1):11-21.

99. Kolawole JA, Mustapha A, Abudu-Aguye I, Ochekpe N. Mefloquine pharmacokinetics in healthy subjects and in peptic ulcer patients after cimetidine administration. Eur J Drug Metab Pharmacokinet. 2000;25(3-4):165-70.

100. Schwartz DE, Eckert G, Hartmann D, Weber B, Richard-Lenoble D, Ekue JM, et al. Single dose kinetics of mefloquine in man. Plasma levels of the unchanged drug and of one of its metabolites. Chemotherapy. 1982;28(1):70-84.

101. Mu J, Israili Z, Dayton P. Studies of disposition and metabolism of mefloquine HCl (WR 142,490), a quinolinemethanol antimalarial, in the rat Limited Studies with an Analog, WR 30,090. Drug Metab Dispos. 1975;3(3):198-210.

102. Tajerzadeh H, Cutler D. Blood to plasma ratio of mefloquine: interpretation and pharmacokinetic implications. Biopharm Drug Dispos. 1993;14(1):87-91.

103. Chung H, Jimmerson V, Rozman R, Sanders J. Disposition of the diastereoisomer of mefloquine in mice. Pharmacology. 1982;24(5):267-74.

104. Riffkin CD, Chung R, Wall DM, Zalcberg JR, Cowman AF, Foley M, et al. Modulation of the function of human MDR1 P-glycoprotein by the antimalarial drug mefloquine. Biochem Pharmacol. 1996;52(10):1545-52.

105. Håkanson A, Landberg-Lindgren A, Björkman A. Comparison of the activity in in vitro and two metabolites against Plasmodium falciparum. Trans R Soc Trop Med Hyg. 1990;84(4):503-4.

106. Ridtitid W, Wongnawa M, Mahatthanatrakul W, Chaipol P, Sunbhanich M. Effect of Rifampin on Plasma Concentrations of Mefloquine in Healthy Volunteers. J Pharm Pharmacol. 2000;52(10):1265-9.

107. Karbwang J, Na Bangchang K, Back DJ, Bunnag D. Effect of ampicillin on mefloquine pharmacokinetics in Thai males. Eur J Clin Pharmacol. 1991;40 (6):631-3.

108. Karbwang J, Na Bangchang K, Back DJ, Bunnag D, Rooney W. Effect of tetracycline on mefloquine pharmacokinetics in Thai males. Eur J Clin Pharmacol. 1992;43(5):567-9.

109. Ridtitid W, Wongnawa M, Mahatthanatrakul W, Raungsri N, Sunbhanich M. Ketoconazole increases plasma concentrations of antimalarial mefloquine in healthy human volunteers. J Clin Pharm Ther. 2005;30(3):285-90.

110. Crevoisier C, Handschin J, Barre J, Roumenov D, Kleinbloesem C. Food increases the bioavailability of mefloquine. Eur J Clin Pharmacol. 1997;53 (2):135-9.

111. Na-Bangchang K, Karbwang J, Molunto P, Banmairuroi V, Thanavibul A. Pharmacokinetics of mefloquine, when given alone and in combination with artemether, in patients with uncomplicated falciparum malaria. Fundam Clin Pharmacol 1995;9(6):576-82.

112. Karbwang J, Na Bangchang K, Thanavibul A, Back DJ, Bunnag D, Harinasuta T. Pharmacokinetics of mefloquine alone or in combination with artesunate. Bull World Health Organ. 1994;72(1):83-7.

113. Ged C, Rouillon J, Pichard L, Combalbert J, Bressot N, Bories P, et al. The increase in urinary excretion of 6 beta-hydroxycortisol as a marker of human hepatic cytochrome P450IIIA induction. Br J Clin Pharmacol. 1989;28(4):373-87.

114. Zhao X-J, Ishizaki T. The in vitro hepatic metabolism of quinine in mice, rats and dogs: comparison with human liver microsomes. J Pharmacol Exp Ther. 1997;283(3):1168-76.

115. Brodie BB, Baer JE, Craig LC. Metabolic products of the cinchona alkaloids in human urine. J Biol Chem. 1951;188(2):567-81.

116. White NJ, Chanthavanich P, Krishna S, Bunch C, Silamut K. Quinine disposition kinetics. Br J Clin Pharmacol. 1983;16(4):399-403.

117. Wanwimolruk S, Denton JR. Plasma Protein Binding of Quinine: Binding to Human Serum Albumin, α1-Acid Glycoprotein and Plasma from Patients with Malaria. J Pharm Pharmacol. 1992;44(10):806-11.

118. Roy L, Bannon P, Villeneuve JP. Quinine pharmacokinetics in chronic haemodialysis patients. Br J Clin Pharmacol. 2002;54(6):604-9.

119. Edstein MD, Prasitthipayong A, Sabchareon A, Chongsuphajaisiddhi T, Webster HK. Simultaneous measurement of quinine and quinidine in human plasma, whole blood, and erythrocytes by high-performance liquid chromatography with fluorescence detection. Ther Drug Monit,. 1990;12(5) :493-500.

120. Supanaranond W, Davis T, Pukrittayakamee S, Silamut K, Karbwang J, Molunto P, et al. Disposition of oral quinine in acute falciparum malaria. Eur J Clin Pharmacol. 1991;40(1):49-52.

121. Silamut K, Molunto P, Ho M, Davis T, White N. Alpha 1-acid glycoprotein (orosomucoid) and plasma protein binding of quinine in falciparum malaria. Br J Clin Pharmacol. 1991;32(3):311-5.

122. Silamut K, White NJ, Looareesuwan S, Warrell DA. Binding of quinine to plasma proteins in falciparum malaria. Am J Trop Med Hyg. 1985;34(4):681-6.

123. Rowland M, Tozer T. Clinical Pharmacokinetics and Pharmacodynamics: concepts and applications. 2011. Lippincott Williams & Wilkins.

124. Molyneux ME, Looareesuwan S, Menzies IS, Grainger SL, Phillips RE, Wattanagoon Y, et al. Reduced hepatic blood flow and intestinal malabsorption in severe falciparum malaria. Am J Trop Med Hyg. 1989;40(5):470-6.

125. Sabchareon A, Chongsuphajaisiddhi T, Attanath P. Serum quinine concentrations following the initial dose in children with falciparum malaria. Southeast Asian J Trop Med Public Health. 1982;13(4):556-62.

126. Wanwimolruk S, Sunbhanich M, Pongmarutai M, Patamasucon P. Effects of cimetidine and ranitidine on the pharmacokinetics of quinine. Br J Clin Pharmacol. 1986;22(3):346-50.

127. Soyinka JO, Onyeji CO, Omoruyi SI, Owolabi AR, Sarma PV, Cook JM. Pharmacokinetic interactions between ritonavir and quinine in healthy volunteers following concurrent administration. Br J Clin Pharmacol. 2010;69(3):262-70.

128. Wanwimolruk S, Kang W, Coville PF, Viriyayudhakorn S, Thitiarchakul S. Marked enhancement by rifampicin and lack of effect of isoniazid on the elimination of quinine in man. Br J Clin Pharmacol. 1995;40(1):87-91.

129. Wanwimolruk S, Wong SM, Coville PF, Viriyayudhakorn S, Thitiarchakul S. Cigarette smoking enhances the elimination of quinine. Br J Clin Pharmacol. 1993;36(6):610-4.

130. Soyinka JO, Onyeji CO, Omoruyi SI, Owolabi AR, Sarma PV, Cook JM. Effects of concurrent administration of nevirapine on the disposition of quinine in healthy volunteers. J Pharm Pharmacol. 2009;61(4):439-43.

131. Ho PC, Chalcroft SC, Coville PF, Wanwimolruk S. Grapefruit juice has no effect on quinine pharmacokinetics. Eur J Clin Pharmacol. 1999;55(5):393-8.

132. Salako LA, Sowunmi A. Disposition of quinine in plasma, red blood cells and saliva after oral and intravenous administration to healthy adult Africans. Eur J Clin Pharmacol. 1992;42(2):171-4.

133. Paintaud G, Alvan G, Ericsson O. The reproducibility of quinine bioavailability. Br J Clin Pharmacol. 1993;35(3):305-7.

134. Babalola CP, Adebayo A, Omotoso A, Ayrinde O. Comparative bioavailability study of a new quinine suppository and oral quinine in healthy volunteers. Trop J Pharm Res 2004;3(1):291-7.

135. Steen B, Rane A. Clindamycin passage into human milk. Br J Clin Pharmacol. 1982;13(5):661-4.

136. HART L, Avery G. Drug Treatment. Principles and Practice of Clinical Pharmacology and Therapeutics. Ann Intern Med. 1980;93:384-5.

137. DeHaan R, Metzler C, Schellenberg D, VandenBosch W, Masson E. Pharmacokinetic studies of clindamycin hydrochloride in humans. Int J Clin Pharmacol Ther Toxicol. 1972;6(2):105-19.

138. Gordon R, Regamey C, Kirby W. Serum protein binding of erythromycin, lincomycin, and clindamycin. J Pharm Sci. 1973;62(7):1074-7.

139. Yang SH, Lee MG. Dose-independent pharmacokinetics of clindamycin after intravenous and oral administration to rats: Contribution of gastric first-pass effect to low bioavailability. Int J Pharm. 2007;332(1–2):17-23.

140. Gatti G, Malena M, Casazza R, Borin M, Bassetti M, Cruciani M. Penetration of clindamycin and its metabolite N-demethylclindamycin into cerebrospinal fluid following intravenous infusion of clindamycin phosphate in patients with AIDS. Antimicrob Agents Chemother. 1998;42(11):3014-7.

141. Wynalda MA, Hutzler JM, Koets MD, Podoll T, Wienkers LC. In vitro metabolism of clindamycin in human liver and intestinal microsomes. Drug Metab Dispos. 2003;31(7):878-87.

142. Plaisance KI, Drusano GL, Forrest A, Townsend RJ, Standiford HC. Pharmacokinetic evaluation of two dosage regimens of clindamycin phosphate. Antimicrob Agents Chemother. 1989;33(5):618-20.

143. Impert O, Katafias A, Kita P, Mills A, Pietkiewicz-Graczyk A, Wrzeszcz G. Kinetics and mechanism of a fast leuco-Methylene Blue oxidation by copper (II)–halide species in acidic aqueous media. Dalton Trans. 2003(3):348-53.

144. Müller T. Methylene blue supravital staining: an evaluation of its applicability to the mammalian brain and pineal gland. Histol Histopathol. 1998;13(4):1019-26.

145. Coulibaly B, Zoungrana A, Mockenhaupt FP, Schirmer RH, Klose C, Mansmann U, et al. Strong gametocytocidal effect of methylene blue-based combination therapy against falciparum malaria: a randomised controlled trial. PLoS ONE. 2009;4(5).

146. Schirmer RH, Adler H, Pickhardt M, Mandelkow E. Lest we forget you—methylene blue. Neurobiol Aging. 2011;32(12):2325. e7-. e16.

147. Zoungrana A, Coulibaly B, Sié A, Walter-Sack I, Mockenhaupt FP, Kouyaté B, et al. Safety and Efficacy of Methylene Blue Combined with Artesunate or Amodiaquine for Uncomplicated Falciparum Malaria: A Randomized Controlled Trial from Burkina Faso. PLoS ONE. 2008;3(2):e1630.

148. Meissner PE, Mandi G, Witte S, Coulibaly B, Mansmann U, Rengelshausen J, et al. Safety of the methylene blue plus chloroquine combination in the treatment of uncomplicated falciparum malaria in young children of Burkina Faso [ISRCTN27290841]. Malar J. 2005;4(1):45.

149. Rengelshausen J, Burhenne J, Fröhlich M, Tayrouz Y, Singh SK, Riedel K-D, et al. Pharmacokinetic interaction of chloroquine and methylene blue combination against malaria. Eur J Clin Pharmacol. 2004;60(10):709-15.

150. Amaral L, Viveiros M, Kristiansen JE. Phenothiazines: potential alternatives for the management of antibiotic resistant infections of tuberculosis and malaria in developing countries. Trop Med Int Health. 2001;6(12):1016-22.

151. Peter C, Hongwan D, Küpfer A, Lauterburg B. Pharmacokinetics and organ distribution of intravenous and oral methylene blue. Eur J Clin Pharmacol. 2000;56(3):247-50.

152. Walter-Sack I, Rengelshausen J, Oberwittler H, Burhenne J, Mueller O, Meissner P, et al. High absolute bioavailability of methylene blue given as an aqueous oral formulation. Eur J Clin Pharmacol. 2009;65(2):179-89.

153. Disanto AR, Wagner JG. Pharmacokinetics of highly ionized drugs II: Methylene blue—absorption, metabolism, and excretion in man and dog after oral administration. J Pharm Sci. 1972;61(7):1086-90.

154. May JM, Qu Z-c, Whitesell RR. Generation of oxidant stress in cultured endothelial cells by methylene blue: protective effects of glucose and ascorbic acid. Mol Pharmacol. 2003;66(5):777-84.

155. Merker M, Bongard R, Kettenhofen N, Okamoto Y, Dawson C. Intracellular redox status affects transplasma membrane electron transport in pulmonary arterial endothelial cells. Am J Physiol Lung Cell Mol Physiol 2002;282 (1):L36-L43.

156. Mutabingwa TK. Artemisinin-based combination therapies (ACTs): Best hope for malaria treatment but inaccessible to the needy! Acta Trop. 2005;95 (3): 305-15.

157. Winstanley P. Modern chemotherapeutic options for malaria. Lancet Infect Dis 2001;1(4):242-50.

158. Basco LK, Ringwald P. In vitro activities of piperaquine and other 4-aminoquinolines against clinical isolates of Plasmodium falciparum in Cameroon. Antimicrob Agents Chemother. 2003;47(4):1391-4.

159. Nosten F, Brasseur P. Combination therapy for malaria. Drugs. 2002;62(9):1315-29.

160. Organization WH. Antimalarial drug combination therapy: Report of a WHO Technical Consultation: World Health Organization.; 2001.

161. Wellems T, Plowe C. Chloroquine-resistant malaria. J Infect Dis. 2001;184 (6):770-6.

162. Payne D. Spread of chloroquine resistance in Plasmodium falciparum. Parasitology today. 1987;3(8):241-6.

163. Watkins WM, Spencer HC, Kariuki DM, Sixsmith DG, Boriga DA, Kipingor T, et al. Effectiveness of amodiaquine as treatment for chloroquine resistant plasmodium falciparum infections in Kenya. Lancet. 1984;323(8373):357-9.

164. Boudreau E, Webster HK, Pavanand K, Thosingha L. Type II mefloquine resistance in Thailand. Lancet. 1982;320(8311):1335.

165. Dondorp AM, Nosten F, Yi P, Das D, Phyo AP, Tarning J, et al. Artemisinin resistance in Plasmodium falciparum malaria. N Engl J Med. 2009;361(5):455-67.

166. Plowe CV, Roper C, Barnwell JW, Happi CT, Joshi HH, Mbacham W, et al. World Antimalarial Resistance Network (WARN) III: molecular markers for drug resistant malaria. Malar J 2007;6(1):121.

167. Sinou V, Taudon N, Mosnier J, Aglioni C, Bressolle FM, Parzy D. Pharmacokinetics of artesunate in the domestic pig. J Antimicrob Chemother. 2008;62(3):566-74.

168. Barnes KI, Little F, Smith PJ, Evans A, Watkins WM, White NJ. Sulfadoxine-pyrimethamine pharmacokinetics in malaria: Pediatric dosing implications. Clin Pharmacol Ther. 2006;80(6):582-96.

169. Obua C, Hellgren U, Ntale M, Gustafsson LL, Ogwal-Okeng JW, Gordi T, et al. Population pharmacokinetics of chloroquine and sulfadoxine and treatment response in children with malaria: suggestions for an improved dose regimen. Br J Clin Pharmacol. 2008;65(4):493-501.

170. Ursing J, Kofoed P-E, Rodrigues A, Bergqvist Y, Rombo L. Chloroquine is grossly overdosed and overused but well tolerated in Guinea-bissau. Antimicrob Agents Chemother. 2009;53(1):180-5.

171. Hendriksen ICE, Mtove G, Kent A, Gesase S, Reyburn H, Lemnge MM, et al. Population Pharmacokinetics of Intramuscular Artesunate in African Children With Severe Malaria: Implications for a Practical Dosing Regimen. Clin Pharmacol Ther. 2013;93(5):443-50.

172. Krishna S, Nagaraja NV, Planche T, Agbenyega T, Bedo-Addo G, Ansong D, et al. Population pharmacokinetics of intramuscular quinine in children with severe malaria. Antimicrob Agents Chemother. 2001;45(6):1803-9.

173. Creek DJ, Bigira V, McCormack S, Arinaitwe E, Wanzira H, Kakuru A, et al. Pharmacokinetic predictors for recurrent malaria after dihydroartemisinin-piperaquine treatment of uncomplicated malaria in Ugandan infants. J Infect Dis. 2013;207 (11):1646-54.

174. Mahmood I. Application of allometric principles for the prediction of pharmacokinetics in human and veterinary drug development. Adv Drug Deliv Rev. 2007;59(11):1177-92.

175. Mahmood I, Martinez M, Hunter RP. Interspecies allometric scaling. Part I: prediction of clearance in large animals. J Vet Pharmacol Ther. 2006;29(5):415-23.

176. Mordenti J. Man versus beast: Pharmacokinetic scaling in mammals. J Pharm Sci. 1986;75(11):1028-40.

177. Riviere JE, Martin-Jimenez T, Sundlof SF, Craigmill AL. Interspecies allometric analysis of the comparative pharmacokinetics of 44 drugs across veterinary and laboratory animal species. J Vet Pharmacol Ther 1997;20(6):453-63.

178. Knibbe CAJ, Zuideveld KP, Aarts LPHJ, Kuks PFM, Danhof M. Allometric relationships between the pharmacokinetics of propofol in rats, children and adults. Br J Clin Pharmacol 2005;59(6):705-11.

179. Mahmood I. Interspecies Scaling for the Prediction of Drug Clearance in Children. Clin Pharmacokinet. 2010;49(7):479-92.

180. Peeters MY, Allegaert K, van Oud-Alblas HJB, Cella M, Tibboel D, Danhof M, et al. Prediction of propofol clearance in children from an allometric model developed in rats, children and adults versus a 0.75 fixed-exponent allometric model. Clin Pharmacokinet. 2010;49(4):269-75.

181. Adolph EF. Quantitative relations in the physiological constitutions of mammals. Science. 1949;109(2841):579.

182. Ings RMJ. Interspecies scaling and comparisons in drug development and toxicokinetics. Xenobiotica 1990;20(11):1201-31.

183. Boxenbaum H, D'Souza R. Interspecies pharmacokinetic scaling: Reductionist and allometric paradigms. Topics in Pharmaceutical Sciences. 1987:49-62.

184. Boxenbaum H. Interspecies scaling, allometry, physiological time, and the ground plan of pharmacokinetics. J Pharmacokinet Biopharm. 1982;10(2):201.

185. Gould SJ. Allometry and size in ontogeny and phylogeny. Biol Rev. 1966;41(4):587-638.

186. Günther B, León dlBB. On the space-time continuum in biology. Acta physiol lat am 1965;16(3):221-31.

187. Stahl WR. The analysis of biological similarity. Adv Biol Med Phys. 1962;9: 355-464.

188. Ritschel WA, Vachharajani NN, Johnson RD, Hussain AS. The allometric approach for interspecies scaling of pharmacokinetic parameters. Comp Biochem Physiol C Toxicol Pharmacol 1992;103(2):249-53.

189. Pang KS, Rowland M. Hepatic clearance of drugs. I. Theoretical considerations of a "well-stirred" model and a "parallel tube" model. Influence of hepatic blood flow, plasma and blood cell binding, and the hepatocellular enzymatic activity on hepatic drug clearance. J Pharmacokinet Biopharm. 1977;5(6):625-53.

190. Boxenbaum H. Interspecies pharmacokinetic scaling and the evolutionary-comparative paradigm. Drug Metab Rev. 1984;15(5-6):1071-121.

191. White CR, Seymour RS. Allometric scaling of mammalian metabolism. J Exp Biol 2005;208(9):1611-9.

192. Kleiber M. Body size and metabolism. ENE. 1932;1:E9.

193. Lester D, Keokosky WZ. Alcohol metabolism in the horse. Life Sci.1967;6(21) :2313-9.

194. Mellett LB. Comparative drug metabolism. Progress in Drug Research/ Fortschritte der Arzneimittelforschung/Progrès des recherches pharmaceutiques: Springer; 1969. p. 136-69.

195. Dedrick R, Bischoff K, Zaharko D. Interspecies correlation of plasma concentration history of methotrexate (NSC-740). Cancer Chemother Rep 1970;54(2):95-101.

196. Weiss M, Sziegoleit W, Förster W. Dependence of pharmacokinetic parameters on the body weight. Int J Clin Pharmacol Biopharm 1977;15(12):572-5.

197. Boxenbaum H. Interspecies variation in liver weight, hepatic blood flow, and antipyrine intrinsic clearance: extrapolation of data to benzodiazepines and phenytoin. J Pharmacokinet Biopharm. 1980;8(2):165-76.

198. Mordenti J. Forecasting cephalosporin and monobactam antibiotic half-lives in humans from data collected in laboratory animals. Antimicrob Agents Chemother. 1985;27(6):887-91.

199. Ibrahim SS, Boudinot FD. Pharmacokinetics of 2′, 3′-Dideoxycytidine in Rats: Application to Interspecies Scale-up. J Pharm Pharmacol. 1989;41(12):829-34.

200. Paxton J. The allometric approach for interspecies scaling of pharmacokinetics and toxicity of anti-cancer drugs. Clin Exp Pharmacol Physiol 1995;22(11) :851-4.

201. West GB, Brown JH, Enquist BJ. A general model for the origin of allometric scaling laws in biology. Science. 1997;276(5309):122-6.

202. Hunter RP. Interspecies allometric scaling. Handb Exp Pharmacol. 2010(199) :139-57.

203. McNamara P. Interspecies scaling in pharmacokinetics. Drugs Pharm Sci 1991;48:267-300.

204. Brody S. Bioenergetics and Growth. New York: Reinhold; 1945.

205. Hoppeler H, Weibel ER. Scaling functions to body size: theories and facts. J Exp Biol. 2005;208(9):1573-4.

206. Kleiber M. The fire of life. An introduction to animal energetics1961.

207. Anderson BJ, Holford NHG. Mechanism-Based Concepts of Size and Maturity in Pharmacokinetics. Annu Rev Pharmacol Toxicol. 2008;48(1):303-32.

208. Holford N, Heo Y-A, Anderson B. A pharmacokinetic standard for babies and adults. J Pharm Sci. 2013:n/a-n/a.

209. West GB, Brown JH, Enquist BJ. The fourth dimension of life: fractal geometry and allometric scaling of organisms. science. 1999;284(5420):1677-9.

210. Mahmood I. Interspecies scaling of renally secreted drugs. Life Sci. 1998;63(26):2365-71.

211. Mahmood I, Balian JD. Interspecies scaling: predicting clearance of drugs in humans. Three different approaches. Xenobiotica. 1996;26(9):887-95.

212. Mahmood I, Balian JD. Interspecies scaling: predicting pharmacokinetic parameters of antiepileptic drugs in humans from animals with special emphasis on clearance. J Pharm Sci. 1996;85(4):411-4.

213. The Lifespan of Animals (Colloquia on Ageing), Volume 5. In: - CFS, editor.: J & A Churchill Ltd 1959.

214. Jerison H. Evolution of the Brain and Intelligence New York: Academic Press; 1973.

215. Sacher GA. On longevity regarded as an organized behavior: The role of brain structure. Contributions to the Psychobiology of Aging: Springer; 1965. p. 99-110.

216. Boxenbaum H. Evolutionary Biology, Animal Behavior, Fourth-Dimensional Space, and the Raison d'Etre of Drug Metabolism and Pharmacokinetics. Drug Metab Rev. 1983;14(5):1057-97.

217. Boxenbaum H, Fertig JB. Scaling of antipyrine intrinsic clearance of unbound drug in 15 mammalian species. Eur J Drug Metab Pharmacokinet. 1984;9(2): 177-83.

218. Mahmood I. Interspecies pharmacokinetic scaling: Principles and Application of Allometric scaling. Rockville: Pine House Publishers; 2005.

219. Brocks DR, Freed MI, Martin DE, Sellers TS, Mehdi N, Citerone DR, et al. Interspecies pharmacokinetics of a novel hematoregulatory peptide (SK&F 107647) in rats, dogs, and oncologic patients. Pharm Res. 1996;13(5):794-7.

220. Boxenbaum H, D'souza R. Interspecies pharmacokinetic scaling, biological esign and neoteny. J adv drug res. 1990;19:139-96.

221. Lave T, Dupin S, Schmitt C, Chou R, Jaeck D, Coassolo P. Integration of in vitro data into allometric scaling to predict hepatic metabolic clearance in man: application to 10 extensively metabolized drugs. J Pharm Sci. 1997;86(5):584-90.

222. Lave T, Schmitt-Hoffmann A, Coassolo P, Valles B, Ubeaud G, Ba B, et al. A new extrapolation method from animals to man: application to a metabolized compound, mofarotene. Life Sci. 1995;56(26):473-8.

223. Lave T, Coassolo P, Ubeaud G, Brandt R, Schmitt C, Dupin S, et al. Interspecies scaling of bosentan, a new endothelin receptor antagonist and integration of in vitro data into allometric scaling. Pharm Res. 1996;13(1):97-101.

224. Lave T, Dupin S, Schmitt M, Kapps M, Meyer J, Morgenroth B, et al. Interspecies scaling of tolcapone, a new inhibitor of catechol-O-methyltransferase (COMT). Use of in vitro data from hepatocytes to predict metabolic clearance in animals and humans. Xenobiotica. 1996;26(8):839-51.

225. Obach RS, Baxter JG, Liston TE, Silber BM, Jones BC, Macintyre F, et al. The prediction of human pharmacokinetic parameters from preclinical and in vitro metabolism data. J Pharmacol Exp Ther. 1997;283(1):46-58.

226. Mahmood I, Sahajwalla C. Interspecies scaling of biliary excreted drugs. J Pharma Sci. 2002;91(8):1908-14.

227. Ward KW, Azzarano LM, Bondinell WE, Cousins RD, Huffman WF, Jakas DR, et al. Preclinical pharmacokinetics and interspecies scaling of a novel vitronectin receptor antagonist. Drug Metab Dispos. 1999;27(11):1232-41.

228. Tang H, Mayersohn M. A novel model for prediction of human drug clearance by allometric scaling. . Drug Metab Dispos. 2005;33(9):1297-303.

229. Ward KW, Smith BR. A comprehensive quantitative and qualitative evaluation of extrapolation of intravenous pharmacokinetic parameters from rat, dog and monkey to humans. I. clearance. Drug Metab Dispos. 2004;32(6):603-11.

230. Bonate PL, Howard D. Critique of prospective allometric scaling: Does the emperor have clothes? J Clin Pharmacol. 2000;40(4):335-40.

231. Boxenbaum H, DiLea C. First-Time-in-Human Dose Selection: Allometric Thoughts and Perspectives. J Clin Pharmacol. 1995;35(10):957-66.

232. Tang H, Mayersohn M. Controversies in Allometric Scaling for Predicting Human Drug Clearance: An Historical Problem and Reflections on What Works and What Does Not. Curr Top Med Chem. 2011;11(4):340-50.

233. Nagilla R, Ward KW. A comprehensive analysis of the role of correction factors in the allometric predictivity of clearance from rat, dog, and monkey to humans. J Pharma Sci. 2004;93(10):2522-34.

234. Shargel S, Wu-Pong S, Yu ABC. Applied Biopharmaceutics & Pharmacokinetics. 5 ed. United States of America McGrowe-Hill; 2005.

235. Boxenbaum H, Ronfeld R. Interspecies pharmacokinetic scaling and the Dedrick plots. Am J Physiol. 1983;245(6):R768-75.

236. Kim SH, Kim WB, Lee MG. Interspecies pharmacokinetic scaling of a new carbapenem, DA-1131, in mice, rats, rabbits and dogs, and prediction of human pharmacokinetics. Biopharm Drug Dispos 1998;19(4):231-5.

237. Efthymiopoulos C, Battaglia R, Benedetti MS. Animal phannacokinetics and interspecies scaling of FCE 22101, a penem antibiotic. J Antimicrob Chemother. 1991;27(4):517-26.

238. Gogerty J. Preclinical research evaluation. New Drug Approval Processes New York: Marcel Dekker. 1987:25-54.

239. Mahmood I, Balian JD. The pharmacokinetic principles behind scaling from preclinical results to phase I protocols. Clin Pharmacokinet. 1999;36(1):1-11.

240. Mahmood I, Green MD, Fisher JE. Selection of the First-Time Dose in Humans:Comparison of Different Approaches Based on Interspecies Scaling of Clearance. J Clin Pharmacol. 2003;43:692-7.

241. Staschen C-M, Mahmood I. A population pharmacokinetic model of remifentanil in pediatric patients using body-weight-dependent allometric exponents. Drug Metabol Drug Interact. 2013;28(4):231-7.

242. Habtemariam B, Sallas W, Sunkara G, Kern S, Jarugula V, Pillai G. Population pharmacokinetics of valsartan in pediatrics. Drug Metab Pharmacokinet 2009;24(2):145-52.

243. Trenque T, Simon N, Villena I, Chemla C, Quereux C, Leroux B, et al. Population pharmacokinetics of pyrimethamine and sulfadoxine in children with congenital toxoplasmosis. Br J Clin Pharmacol. 2004;57(6):735-41.

244. Läer S, Elshoff J-P, Meibohm B, Weil J, Mir TS, Zhang W, et al. Development of a safe and effective pediatric dosing regimen for sotalol based on population pharmacokinetics and pharmacodynamics in children with supraventricular tachycardia. J Am Coll Cardiol. 2005;46(7):1322-30.

245. Halpern SA. American pediatrics: the social dynamic of professionalism, 1880 -1980. Berkeley University of California Press; 1988.

246. Cella M, Knibbe C, Danhof M, Della Pasqua O. What is the right dose for children? Br J Clin Pharmacol 2010;70(4):597-603.

247. Lack JA, Stuart-Taylor ME. Calculation of drug dosage and body surface area of children. Br J Anaesth. 1997;78:601-5.

248. Augsberger A. Old and new rules for dosage determination in paediatrics. Triangle (Sandoz). 1962;5:200-7.

249. Johnson TN. The problems in scaling adult drug doses to children. Arch Dis Child 2008;93(3):207-11.

250. Holford NHG. A size standard for pharmacokinetics. Clin Pharmacokinet. 1996;30(5):329-32.

251. Committee PF. BNF for Children: Pharmaceutical Press; 2013.

252. Moore B. The relationship of dosage of a drug to the size of the animal treated, especially in regard to the cause of the failures to cure trypanosomiasis, and other protozoan diseases in man and in large animals. Biochem J. 1909;4(5-7):323.

253. Du Bois D, Du Bois EF. Clinical calorimetry: tenth paper a formula to estimate the approximate surface area if height and weight be known. Arch Intern Med. 1916;17(6_2):863-71.

254. Gehan EA, George SL. Estimation of human body surface area from height and weight. Cancer Chemoth Rep 1. 1970;54(4):225-35.

255. Mahmood I. Prediction of drug clearance in children from adults: a comparison of several allometric methods. Br J Clin Pharmacol. 2006;61(5):545-57.

256. Mahmood I. Theoretical versus empirical allometry: Facts behind theories and application to pharmacokinetics. J Pharm Sci. 2010;99(7):2927-33.

257. Tod M, Jullien V, Pons G. Facilitation of Drug Evaluation in Children by Population Methods and Modelling. Clin Pharmacokinet 2008;47(4):231-43.

258. Mahmood I. Prediction of drug clearance in children: impact of allometric exponents, body weight, and age. Ther Drug Monit. 2007;29(3):271-8.

259. Abernethy DR, Burckart G.J. Pediatric dose selection. Clin Pharmacol Ther. 2010;87(3):270-1.

260. British Medical Association RCopach, Royal Pharmaceutical Society of Great Britain BNF for children London: BMJ publishing group, RPS Publishing, RCPCH publications, 2006. ; 2006.

261. Meakin G. Role of propofol in paediatric anaesthetic practice. Paediatr Anaesth. 1995;5(3):147-9.

262. Anderson BJ, McKee AD, Holford NH. Size, myths and the clinical pharmacokinetics of analgesia in paediatric patients. Clin Pharmacokinet. 1997;33(5):313-27.

263. FDA U. Guidance for Industry. E11 Clinical Investigation of Medicinal Products in the Pediatric Population. 2000.

264. Moore BR. Pharmacokinetics, Pharmacodynamics and Allometric Scaling of Chloroquine in a Murine Malaria Model. Antimicrob Agents Chemother. 2011;55(8):3899.

265. Davies B, Morris T. Physiological parameters in laboratory animals and humans. Pharm Res. 1993;10(7):1093-5.

266. Cox S. Allometric scaling of marbofloxacin, moxifloxacin, danofloxacin and difloxacin pharmacokinetics: a retrospective analysis. J Vet Pharmacol Ther. 2007;30(5):381-6.

267. Hu T-M, Hayton WL. Allometric scaling of xenobiotic clearance: uncertainty versus universality. Aaps Pharmsci. 2001;3(4):30-43.

268. Haddad S, Restieri C, Krishnan K. Characterization of age-related changes in body weight and organ weights from birth to adolescence in humans. J Toxicol Env Heal B. 2001;64(6):453-64.

269. Ritschel W, Vachharajani N, Johnson R, Hussain A. Interspecies scaling of the pharmacokinetic parameters of coumarin among six different mammalian species. Methods Find Exp Clin Pharmacol. 1991;13(10):697-702.

270. Wilkinson G. Clearance approaches in pharmacology. Pharmacol Rev. 1987;39(1):1.

271. Feng MR, Lou X, Brown RR, Hutchaleelaha A. Allometric pharmacokinetic scaling: towards the prediction of human oral pharmacokinetics. Pharm Res. 2000;17(4):410-8.

272. Yamazaki S, Toth LN, Black ML, Duncan JN. Comparison of prediction methods for in vivo clearance of (S, S)-3-[3-(methylsulfonyl) phenyl]-1-propylpiperidine hydrochloride, a dopamine D2 receptor antagonist, in humans. Drug Metab Dispos. 2004;32(4):398-404.

273. Bennett K, Si Y, Steinbach T, Zhang J, Li Q. Pharmacokinetic and pharmacodynamic evaluation of intramuscular artesunate in healthy beagle dogs. Am J Trop Med Hyg. 2008;79(1):36-41.

274. Li Q, Cantilena L, Leary K, Saviolakis G, Miller R, Melendez V, et al. Pharmacokinetic profiles of artesunate after single intravenous doses at 0.5, 1, 2, 4, and 8 mg/kg in healthy volunteers: a phase I study. Am J Trop Med Hyg. 2009;81:615 - 21.

275. Zhao K-C, Chen Z-X, Lin B-L, Guo X-B, LI G-Q, Zong Z-Y. Studies on the phase 1 clinical pharmacokinetics of Artesunate and Artemether Chin J Clin Pharmacol. 1988;4(2):76-81.

276. Zhao Kai-Cun, CHEN Q-M, Zong Z-Y. Studies on the pharmacokinetics of qinghaosu and two of its active derivatives in dogs Acta Pharm Sin 1986;21:736-9.

277. Zeng Y-l, Zhang Y-d, Xu G-y, Wang C-g, Jiang J-r. The pharmacokinetics and bioavailability of omethyldihydroartemesinine in the rabbit Acta Pharmaceutica Sinica. 1984;19(2):82-3.

278. Ashton M, Johansson L, Thornqvist AS, Svensson USH. Quantitative in vivo and in vitro sex differences in artemisinin metabolism in rat. Xenobiotica. 1999;29(2):195-204.

279. Benakis A, Paris M, Loutan L, Plessas CT, Plessas ST. Pharmacokinetics of Artemisinin and Artesunate after Oral Administration in Healthy Volunteers Am J Trop Med Hyg 1997 56:17-23.

280. Duc DD, De Vries PJ, Nguyen XK, Le Nguyen B, Kager PA, Van Boxtel CJ. The pharmacokinetics of a single dose of artemisinin in healthy Vietnamese subjects. Am J Trop Med Hyg. 1994;51(6):785-90.

281. Hien TT, Hanpithakpong W, Truong NT, Dung NT, Toi PV, Farrar J, et al. Orally Formulated Artemisinin in Healthy Fasting Vietnamese Male Subjects: A Randomized, Four-Sequence, Open-Label, Pharmacokinetic Crossover Study. Clin Ther. 2011;33(5):644-54.

282. Isacchi B, Arrigucci S, Marca G, Bergonzi1 MC, Vannucchi MG, Novelli A, et al. Conventional and long-circulating liposomes of artemisinin: preparation, characterization, and pharmacokinetic profile in mice. J Liposome ResJ Liposome Res. 2011;21(3):237-44.

283. Rath K, Taxis K, Walz G, Gleiteer CH, Li SM, Heide L. Pharmacokinetic study of artemisinin after oral intake of a traditional preparation of Artemisia annua. L( annual wormwood). Am J Trop Med Hyg. 2004;70:128-32.

284. Li L, Pabbisetty D, Carvalho P, Avery MA, Williamson JS, Avery BA. Ultra-performance liquid chromatography–tandem mass spectrometric method for the determination of Artemisinin in rat serum and its application in pharmacokinetics. J Chromatogr B. 2008;867(1):131-7.

285. Zhang S-Q, Hai TN, Ilett KF, Huong DX, Davis TME, Ashton M. Multiple dose study of interactions between artesunate and artemisinin in healthy volunteers. Br J of ClinPharmacol. 2001;52(4):377-85.

286. Batzias GC, Delis GA, Athanasiou LV. Clindamycin bioavailability and pharmacokinetics following oral administration of clindamycin hydrochloride capsules in dogs. Vet J. 2005;170(3):339-45.

287. Budsberg SC, Kemp DT, Wolski N. Pharmacokinetics of clindamycin phosphate in dogs after single intravenous and intramuscular administrations. Am J Vet Res. 1992;53(12):2333-6.

288. Flaherty JF, Rodondi LC, Guglielmo BJ, Fleishaker JC, Townsend RJ, Gambertoglio JG. Comparative pharmacokinetics and serum inhibitory activity of clindamycin in different dosing regimens. Antimicrob Agents Chemother. 1988;32(12):1825-9.

289. Gatti G, Flaherty J, Bubp J, White J, Borin M, Gambertoglio J. Comparative study of bioavailabilities and pharmacokinetics of clindamycin in healthy volunteers and patients with AIDS. Antimicrob Agents Chemother. 1993;37(5):1137-43.

290. Lavy, Ziv, Shem T, Glickman, Dey. Pharmacokinetics of clindamycin HCl administered intravenously, intramuscularly and subcutaneously to dogs. J Vet Pharmacol Ther 1999;22(4):261-5.

291. Batty KT, Moore BR, Stirling V, Ilett KF, Page-Sharp M, Shilkin KB, et al. Toxicology and pharmacokinetics of piperaquine in mice. Toxicology. 2008;249(1):55-61.

292. Baudry S, Pham YT, Baune B, Vidrequin S, Crevoisier C, Gimenez F, et al. Stereoselective passage of mefloquine through the blood-brain barrier in the rat. J Pharm Pharmacol. 1997;49(11):1086-90.

293. Boudreau EF, Fleckenstein L, Pang LW, Childs GE, Schroeder AC, Ratnaratorn B, et al. Mefloquine kinetics in cured and recrudescent patients with acute falciparum malaria and in healthy volunteers. Clin Pharm Ther. 1990;48(4):399-409.

294. Charles BG, Blomgren A, Nasveld PE, Kitchener SJ, Jensen A, Gregory RM, et al. Population pharmacokinetics of mefloquine in military personnel for prophylaxis against malaria infection during field deployment. Eur J Clin Pharmacol. 2007;63(3):271-8.

295. Franssen G, Rouveix B, Lebras J, Bauchet J, Verdier F, Michon C, et al. Divided-dose kinetics of mefloquine in man. Br J Clin Pharmacol. 1989;28(2):179-84.

296. Juma FD, Ogeto JO. Mefloquine disposition in normals and in patients with severePlasmodium falciparum malaria. Eur J Drug Metab Pharmacokinet 1989;14(1):15-7.

297. Karbwang J, Back DJ, Bunnag D, Breckenridge AM. A comparison of the pharmacokinetics of mefloquine in healthy Thai volunteers and in Thai patients with falciparum malaria. Eur J Clin Pharmacol. 1988;35(6):677-80.

298. Karbwang J, Bunnag D, Breckenridge AM, Back DJ. The pharmacokinetics of mefloquine when given alone or in combination with sulphadoxine and pyrimethamine in Thai male and female subjects. Eur J Clin Pharmacol. 1987;32(2):173-7.

299. Karbwang J, Looareesuwan S, Back DJ, Migasana S, Bunnag D, Breckenridge AM. Effect of oral contraceptive steroids on the clinical course of malaria infection and on the pharmacokinetics of mefloquine in Thai women. Bull WHO. 1988;66(6):763-7.

300. Karbwang J, Looareesuwan S, Phillips RE, Wattanagoon Y, Molyneux ME, Nagachinta B, et al. Plasma and whole blood mefloquine concentrations during treatment of chloroquine-resistant falciparum malaria with the combination mefloquine-sulphadoxine-pyrimethamine. Br J of Clin Pharmacol. 1987;23(4):477-81.

301. Khaliq Y, Gallicano K, Tisdale C, Carignan G, Cooper C, McCarthy A. Pharmacokinetic interaction between mefloquine and ritonavir in healthy volunteers. Br J Clin Pharmacol. 2001;51(6):591-600.

302. Looareesuwan S, White NJ, Warrell DA, Forgo I, Dubach UG, Ranalder UB, et al. Studies of mefloquine bioavailability and kinetics using a stable isotope technique: a comparison of Thai patients with falciparum malaria and healthy Caucasian volunteers. Br J Clin Pharmacol. 1987;24(1):37-42.

303. Pennie RA, Koren G, Crevoisier C. Steady state pharmacokinetics of mefloquine in long-term travellers. Trans R Soc Trop Med Hyg. 1993;87(4):459-62.

304. Rozman RS, Molek NA, Koby R. The absorption, distribution, and excretion in mice of the antimalarial mefloquine, erythro-2,8-bis(trifluoromethyl)-alpha-(2-piperidyl)-4-quinolinemethanol hydrochloride. Drug Metab Dispos. 1978;6(6):654-8.

305. Watari N, Wakamatsu A, Kaneniwa N. Comparison of disposition parameters of quinidine and quinine in the rat. J Pharmacobiodyn. 1989;12(10):608-15.

306. Wanwimolruk S, Nyika S, Kepple M, Ferry DG, Clark CR. Effects of capsaicin on the pharmacokinetics of antipyrine, theophylline and quinine in rats. J Pharm Pharmacol 1993;45(7):618-21.

307. Zhang HU, Ramsay N, Coville PF, Wanwimolruk S. Effect of Erythromycin, Rifampicin and Isoniazid on the Pharmacokinetics of Quinine in Rats. J Pharm Pharmacol. 1999;5(7):467-72.

308. Zhang H, Wong CW, Coville PF, Wanwimolruk S. Effect of grapefruit flavonoid naringin on pharmacokinetics of quinine in rats Drug Metabol Drug Interact. 2000;17:351-63.

309. Clohisy DR, Gibson TP. Comparison of pharmacokinetic parameters of intravenous quinidine and quinine in dogs. J Cardiovasc Pharmacol. 1982;4(1):107-10.

310. Brum Jr L, Leal MG, De Toni Uchoa F, Kaiser M, Guterres SS, Dalla Costa T. Determination of quinine and doxycycline in rat plasma by LC-MS-MS: Application to a pharmacokinetic study. Chromatographia. 2011;73(11-12):1081-8.

311. Pussard E, Barennes H, Daouda H, Clavier F, Sani AM, Osse M, et al. Quinine disposition in globally malnourished children with cerebral malaria. Clin Pharmacol Ther. 1999;65(5):500-10.

312. Claessen FA, van Boxtel CJ, Perenboom RM, Tange RA, Wetsteijn JC, Kager PA. Quinine pharmacokinetics: ototoxic and cardiotoxic effects in healthy Caucasian subjects and in patients with falciparum malaria. Trop Med Int Health. 1998;3(6):482-9.

313. Karbwang J, Davis TM, Looareesuwan S, Molunto P, Bunnag D, White NJ. A comparison of the pharmacokinetic and pharmacodynamic properties of quinine and quinidine in healthy Thai males. Br J Clin Pharmacol. 1993;35(3):265-71.

314. Karbwang J, Thanavibul A, Molunto P, Na Bangchang K. The pharmacokinetics of quinine in patients with hepatitis. Br J Clin Pharmacol. 1993;35(4):444-6.

315. Zhao K-C, Chen Q-M, Song Z-Y. Studies on the pharmacokinetics of qinghaosu and two of its active derivatives in dogs Acta Pharm Sin 1986;21:736-9.

316. Hasan MM, Hassan MA, Rawashdeh NM. Effect of oral activated charcoal on the pharmacokinetics of quinidine and quinine administered intravenously to rabbits. Pharmacol Toxicol. 1990;67(1):73-6.

317. Hai TN, Hietala SF, Van Huong N, Ashton M. The influence of food on the pharmacokinetics of piperaquine in healthy Vietnamese volunteers. Acta tropica. 2008;107(2):145-9.

318. Röshammar D, Hai TN, Hietala SF, Van Huong N, Ashton M. Pharmacokinetics of piperaquine after repeated oral administration of the antimalarial combination CV8 in 12 healthy male subjects. Eur J Clin Pharmacol. 2006;62(5):335-41.

319. Byakika-Kibwika P, Lamorde M, Mayito J, Nabukeera L, Mayanja-Kizza H, Katabira E, et al. Pharmacokinetics and pharmacodynamics of intravenous artesunate during severe malaria treatment in Ugandan adults. Malar J. 2012;11:132.

320. Davis TME. Pharmacokinetics and pharmacodynamics of intravenous artesunate in severe falciparum malaria. Antimicrob Agents Chemother. 2001;45(1):181.

321. Newton P, Suputtamongkol Y, Teja-Isavadharm P, Pukrittayakamee S, Navaratnam V, Bates I, et al. Antimalarial Bioavailability and Disposition of Artesunate in Acute Falciparum Malaria. Antimicrob Agents Chemother. 2000;44(4): 972-7.

322. Karbwang J, Na-Bangchang K, Tin T, Sukontason K, Rimchala W, Harinasuta T. Pharmacokinetics of intramuscular artemether in patients with severe falciparum malaria with or without acute renal failure. Br J Clin Pharmacol. 1998;45(6):597-600.

323. Hodel EMS, Guidi M, Zanolari B, Mercier T, Duong S, Kabanywanyi AM, et al. Population pharmacokinetics of mefloquine, piperaquine and artemether-lumefantrine in Cambodian and Tanzanian malaria patients. Malar J. 2013;12(1):235.

324. Tarning J, Rijken MJ, McGready R, Phyo AP, Hanpithakpong W, Day NP, et al. Population pharmacokinetics of dihydroartemisinin and piperaquine in pregnant and non-pregnant women with uncomplicated malaria. Antimicrob Agents Chemother. 2012:AAC. 05756-11.

325. Abdelrahim I, Adam I, Elghazali G, Gustafsson L, Elbashir M, Mirghani R. Pharmacokinetics of quinine and its metabolites in pregnant Sudanese women

with uncomplicated Plasmodium falciparum malaria. J Clin Pharm Ther. 2007;32(1):15-9.

326. Couet W, Laroche R, Floch J-J, Istin B, Fourtillan J-B, Sauniere J-F. Pharmacokinetics of Quinine and Doxycycline in Patients with Acute Falciparum Malaria: A Study in Africa. Ther Drug Monit. 1991;13(6):496-501.

327. Davis TME, Supanaranond W, Sasithon P, Karbwang J, Molunto P, Sopon M, et al. A Safe and Effective Consecutive-Infusion Regimen for Rapid Quinine Loading in Severe Falciparum Malaria. J Infect Dis. 1990;161(6):1305-8.

328. Davis TME, White NJ, Looareesuwan S, Silamut K, Warrell DA. Quinine pharmacokinetics in cerebral malaria: predicted plasma concentrations after rapid intravenous loading using a two-compartment model. Trans R Soc Trop Med Hyg. 1988;82(4):542-7.

329. White NJ, Looareesuwan S, Warrell DA, Warrell MJ, Bunnag D, Harinasuta T. Quinine pharmacokinetics and toxicity in cerebral and uncomplicated falciparum malaria. Am J Med 1982;73(4):564-72.

330. Shann F, Stace J, Edstein M. Pharmacokinetics of quinine in children. J Pediatr. 1985;106(3):506-10.

331. Mithwani S, Aarons L, Kokwaro GO, Majid O, Muchohi S, Edwards G, et al. Population pharmacokinetics of artemether and dihydroartemisinin following single intramuscular dosing of artemether in African children with severe falciparum malaria. Br J Clin Pharmacol. 2004;57(2):146-52.

332. Karunajeewa HA, Ilett KF, Mueller I, Siba P, Law I, Page-Sharp M, et al. Pharmacokinetics and efficacy of piperaquine and chloroquine in Melanesian children with uncomplicated malaria. Antimicrob Agents Chemother. 2008;52(1):237-43.

333. Bourahla A, Martin C, Gimenez F, Singhasivanon V, Attanath P, Sabchearon A, et al. Stereoselective pharmacokinetics of mefloquine in young children. Eur J Clin Pharmacol. 1996;50(3):241-4.

334. Singhasivanon V, Chongsuphajaisiddhi T, Sabcharoen A, Attanath P, Webster H, Wernsdorfer W, et al. Pharmacokinetics of mefloquine in children aged 6 to 24 months. Eur J Drug Metab Pharmacokinet. 1992;17(4):275-9.

335. Singhasivanon V, Chongsuphajaisiddhi T, Sabchareon A, Attanath P, Webster H, Edstein M, et al. Pharmacokinetic study of mefloquine in Thai children aged 5–12 years suffering from uncomplicated falciparum malaria treated with MSP or MSP plus primaquine. Eur J Drug Metab Pharmacokinet. 1994;19(1):27-32.

336. West GB. The importance of quantitative systemic thinking in medicine. Lancet. 2012;379(9825):1551-9.

337. McLeay SC, Morrish GA, Kirkpatrick CM, Green B. The relationship between drug clearance and body size. Clin Pharmacokinet. 2012;51(5):319-30.

338. Crowe A, Ilett KF, Karunajeewa HA, Batty KT, Davis TM. Role of P glycoprotein in absorption of novel antimalarial drugs. Antimicrob Agents Chemother. 2006;50(10):3504-6.

339. Townsend RJ, Baker RP. Pharmacokinetic comparison of three clindamycin phosphate dosing schedules. Drug Intell Clin Pharm. 1987;21(3):279-81.

340. Palhlman I, Edholm M, Kankaaneanta S, Odell M. Pharmacokinetics of Susalimod, a Highly Biliary-excreted Sulphasalazine Analogue, in Various Species. Nonpredictable Human Clearance by Allometric Scaling. Pharm Pharmacol Commun 1998;4(10):493-8.

341. Ursing J, Kofoed P-E, Rodrigues A, Blessborn D, Thoft-Nielsen R, Björkman A, et al. Similar efficacy and tolerability of double-dose chloroquine and artemether-lumefantrine for treatment of Plasmodium falciparum infection in Guinea-Bissau: a randomized trial. J Infect Dis. 2011;203(1):109-16.

342. Baldrick P. Juvenile animal testing in drug development–Is it useful? Regul Toxicol Pharmacol. 2010;57(2):291-9.

343. Baldrick P. Developing drugs for pediatric use: a role for juvenile animal studies? Regul Toxicol Pharmacol. 2004;39(3):381-9.

344. Lin JH. Applications and limitations of interspecies scaling and in vitro extrapolation in pharmacokinetics. Drug Metab Dispos. 1998;26(12):1202-12.

345. Callan W, Sunderman Jr F. Species variations in binding of 63 NI (II) by serum albumin. Res Commun Chem Pathol Pharmacol. 1973;5(2):459.

346. Chu X, Bleasby K, Evers R. Species differences in drug transporters and implications for translating preclinical findings to humans. Expert Opin Drug Metab Toxicol 2013;9(3):237-52.

347. Hunter J, Hirst BH. Intestinal secretion of drugs. The role of P-glycoprotein and related drug efflux systems in limiting oral drug absorption. Adv Drug Deliv Rev. 1997;25(2):129-57.

348. Barthe L, Woodley J, Houin G. Gastrointestinal absorption of drugs: methods and studies. Fundam Clin Pharmacol. 1999;13(2):154-68.

349. Hayashi M, Tomita M, Awazu S. Transcellular and paracellular contribution to transport processes in the colorectal route. Adv Drug Deliv Rev. 1997;28(2):191-204.

350. Artursson P, Palm K, Luthman K. Caco-2 monolayers in experimental and theoretical predictions of drug transport. Adv Drug Deliv Rev. 1996;46(1):27-43.

351. Sinko PJ, Hu M, Amidon GL. Carrier mediated transport of amino acids, small peptides, and their drug analogs. J Controlled Release. 1987;6(1):115-21.

352. Lennernas H, Nilsson D, Aquilonius S, Ahrenstedt O, Knutson L, Paalzow L. The effect of L-leucine on the absorption of levodopa, studied by regional jejunal perfusion in man. Br J Clin Pharmacol. 1993;35(3):243-50.

353. Dix C, Hassan I, Obray H, Shah R, Wilson G. The transport of vitamin B12 through polarized monolayers of Caco-2 cells. Gastroenterology. 1990;98(5 Pt 1):1272-9.

354. Evers R, Kool M, van Deemter L, Janssen H, Calafat J, Oomen L, et al. Drug export activity of the human canalicular multispecific organic anion transporter in polarized kidney MDCK cells expressing cMOAT (MRP2) cDNA. J Clin Invest. 1998;101(7):1310.

355. Hunter J, Jepson M, Tsuruo T, Simmons N, Hirst B. Functional expression of P-glycoprotein in apical membranes of human intestinal Caco-2 cells. Kinetics of vinblastine secretion and interaction with modulators. J Biol Chem. 1993; 268(20):14991-7.

356. Hunter J, Hirst BH, Simmons NL. Drug absorption limited by P-glycoprotein-mediated secretory drug transport in human intestinal epithelial Caco-2 cell layers. Pharma Res. 1993;10(5):743-9.

357. Potts RO, Guy RH. A predictive algorithm for skin permeability: the effects of molecular size and hydrogen bond activity. Pharma Res. 1995;12(11):1628-33.

358. Levin VA. Relationship of octanol/water partition coefficient and molecular weight to rat brain capillary permeability. J Med Chem. 1980;23(6):682-4.

359. Potts RO, Guy RH. Predicting skin permeability. Pharma Res. 1992;9(5):663-9.

360. Martin YC. A practitioner's perspective of the role of quantitative structure-activity analysis in medicinal chemistry. J Med Chem. 1981;24(3):229-37.

361. Wils P, Warnery A, Phung-Ba V, Legrain S, Scherman D. High lipophilicity decreases drug transport across intestinal epithelial cells. J Pharmacol Exp Ther. 1994;269(2):654-8.

362. Ramu K, Baker JK. Synthesis, characterization, and antimalarial activity of the glucuronides of the hydroxylated metabolites of arteether. J Med Chem. 1995;38(11):1911-21.

363. Chan LM, Lowes S, Hirst BH. The ABCs of drug transport in intestine and liver: efflux proteins limiting drug absorption and bioavailability. Eur J Pharma Sci. 2004;21(1):25-51.

364. Juliano RL, Ling V. A surface glycoprotein modulating drug permeability in Chinese hamster ovary cell mutants. Biochim Biophys Acta. 1976;455(1):152-62.

365. Schinkel AH, Jonker JW. Mammalian drug efflux transporters of the ATP binding cassette (ABC) family: an overview. Adv Drug Deliv Rev. 2003;55(1):3-29.

366. Gottesman MM, Pastan I. Biochemistry of multidrug resistance mediated by the multidrug transporter. Annu Rev Biochem. 1993;62(1):385-427.

367. Gatmaitan ZC, Arias IM. Structure and function of P-glycoprotein in normal liver and small intestine. Adv Pharmacol 1993;24:77-97.

368. Fojo AT, Shen D, Mickley L, Pastan I, Gottesman M. Intrinsic drug resistance in human kidney cancer is associated with expression of a human multidrug-resistance gene. J Clin Oncol 1987;5(12):1922-7.

369. Thiebaut F, Tsuruo T, Hamada H, Gottesman MM, Pastan I, Willingham MC. Cellular localization of the multidrug-resistance gene product P-glycoprotein in normal human tissues. Proc Natl Acad Sci. 1987;84(21):7735-8.

370. Cordon-Cardo C, O'brien J, Boccia J, Casals D, Bertino J, Melamed M. Expression of the multidrug resistance gene product (P-glycoprotein) in human normal and tumor tissues. J Histochem Cytochem. 1990;38(9):1277-87.

371. Smith AJ, van Helvoort A, van Meer G, Szabó K, Welker E, Szakács G, et al. MDR3 P-glycoprotein, a phosphatidylcholine translocase, transports several cytotoxic drugs and directly interacts with drugs as judged by interference with nucleotide trapping. J Biol Chem. 2000;275(31):23530-9.

372. Taipalensuu J, Törnblom H, Lindberg G, Einarsson C, Sjöqvist F, Melhus H, et al. Correlation of gene expression of ten drug efflux proteins of the ATP-binding cassette transporter family in normal human jejunum and in human intestinal epithelial Caco-2 cell monolayers. J Pharmacol Exp Ther. 2001;299(1):164-70.

373. De Vree JML, Jacquemin E, Sturm E, Cresteil D, Bosma PJ, Aten J, et al. Mutations in the MDR3 gene cause progressive familial intrahepatic cholestasis. P Natl Acady Sci. 1998;95(1):282-7.

374. Martin C, Berridge G, Higgins CF, Mistry P, Charlton P, Callaghan R. Communication between multiple drug binding sites on P-glycoprotein. Mol Pharmacol. 2000;58(3):624-32.

375. Sharom F, LU P, LIU R, YU X. Linear and cyclic peptides as substrates and modulators of P-glycoprotein: peptide binding and effects on drug transport and accumulation. Biochem J. 1998;333:621-30.

376. Higgins CF, Gottesman MM. Is the multidrug transporter a flippase? Trends Biochem Sci 1992;17(1):18-21.

377. Bellamy WT. P-glycoproteins and multidrug resistance. Annu Rev Pharmacol Toxicol. 1996;36(1):161-83.

378. Ueda K, Taguchi Y, Morishima M, editors. How does P-glycoprotein recognize its substrates? Semin Cancer Biol; 1997: Elsevier.

379. Seelig A. A general pattern for substrate recognition by P-glycoprotein. Eur J Biochem. 1998;251(1-2):252-61.

380. Loo TW, Clarke DM. Identification of residues in the drug-binding site of human P-glycoprotein using a thiol-reactive substrate. J Biol Chem. 1997;272(51):31945-8.

381. Loo TW, Clarke DM. Identification of residues in the drug-binding domain of human P-glycoprotein Analysis of transmembrane segment 11 by cysteine-scanning mutagenesis and inhibition by dibromobimane. J Biol Chem. 1999;274(50):35388-92.

382. Hoffmeyer S, Burk O, Von Richter O, Arnold H, Brockmöller J, Johne A, et al. Functional polymorphisms of the human multidrug-resistance gene: multiple sequence variations and correlation of one allele with P-glycoprotein expression and activity in vivo. P Natl Acad Sci. 2000;97(7):3473-8.

383. Canaparo R, Finnström N, Serpe L, Nordmark A, Muntoni E, Eandi M, et al. Expression of CYP4A isoformes and P-glycoprotein in human stomach, jejunum, ilium. Clin Exp Pharmacol Physiol 2007;34(11):1138-44.

384. Chikhale EG, Ng K-Y, Burton PS, Borchardt RT. Hydrogen bonding potential as a determinant of the in vitro and in situ blood–brain barrier permeability of peptides. Pharm Res. 1994;11(3):412-9.

385. Cordon-Cardo C, O'Brien JP, Casals D, Rittman-Grauer L, Biedler JL, Melamed MR, et al. Multidrug-resistance gene (P-glycoprotein) is expressed by endothelial cells at blood-brain barrier sites. P Natl Acad Sci. 1989;86(2):695-8.

386. Thiebaut F, Tsuruo T, Hamada H, Gottesman M, Pastan I, Willingham M. Immunohistochemical localization in normal tissues of different epitopes in the multidrug transport protein P170: evidence for localization in brain capillaries and crossreactivity of one antibody with a muscle protein. J Histochem Cytochem 1989;37(2):159-64.

387. Tanigawara Y, Okamura N, Hirai M, Yasuhara M, Ueda K, Kioka N, et al. Transport of digoxin by human P-glycoprotein expressed in a porcine kidney epithelial cell line (LLC-PK1). J Pharmacol Exp Ther. 1992;263(2):840-5.

388. Horio M, Chin K-V, Currier S, Goldenberg S, Williams C, Pastan I, et al. Transepithelial transport of drugs by the multidrug transporter in cultured Madin-Darby canine kidney cell epithelia. J Biol Chem. 1989;264(25):14880-4.

389. Smit JW, Schinkel AH, Weert B, Meijer DK. Hepatobiliary and intestinal clearance of amphiphilic cationic drugs in mice in which both mdr1a and mdr1b genes have been disrupted. Br J Pharmacol. 1998;124(2):416-24.

390. Stephens R, O'neill C, Warhurst A, Carlson G, Rowland M, Warhurst G. Kinetic profiling of P-glycoprotein-mediated drug efflux in rat and human intestinal epithelia. J Pharmacol Exp Ther. 2001;296(2):584-91.

391. Fricker G, Drewe J, Huwyler J, Gutmann H, Beglinger C. Relevance of p-glycoprotein for the enteral absorption of cyclosporin A: in vitro-in vivo correlation. Br J Pharmacol. 1996;118(7):1841-7.

392. Saeki T, Ueda K, Tanigawara Y, Hori R, Komano T. Human P-glycoprotein transports cyclosporin A and FK506. J Biol Chem. 1993;268(9):6077-80.

393. Kirn RB, Wandel C, Leake B, Cvetkovic M, Fromm MF, Dempsey PJ, et al. Interrelationship between substrates and inhibitors of human CYP3A and P-glycoprotein. Pharma Res. 1999;16(3):408-14.

394. Kim RB. Drugs as P-glycoprotein substrates, inhibitors, and inducers. Drug metab Rev 2002;34(1-2):47-54.

395. Smith AJ, Mayer U, Schinkel AH, Borst P. Availability of PSC833, a substrate and inhibitor of P-glycoproteins, in various concentrations of serum. J Natl Cancer Inst. 1998;90(15):1611-166.

396. Fischer V, Rodríguez-Gascón A, Heitz F, Tynes R, Hauck C, Cohen D, et al. The Multidrug Resistance Modulator Valspodar (PSC 833) Is Metabolized by Human Cytochrome P450 3A Implications for Drug-Drug Interactions and Pharmacological Activity of the Main Metabolite. Drug Metab Dispos. 1998;26(8):802-11.

397. Hyafil F, Vergely C, Du Vignaud P, Grand-Perret T. In vitro and in vivo reversal of multidrug resistance by GF120918, an acridonecarboxamide derivative. Cancer Res. 1993;53(19):4595-602.

398. Ford J. Experimental reversal of P-glycoprotein-mediated multidrug resistance by pharmacological chemosensitisers. Eur J Cancer. 1996;32(6):991-1001.

399. Ayesh S, Shao Y-M, Stein WD. Co-operative, competitive and non-competitive interactions between modulators of P-glycoprotein. BBA-Mol Basis Dis. 1996;1316(1):8-18.

400. Shapiro AB, Ling V. Positively cooperative sites for drug transport by P-glycoprotein with distinct drug specificities. Eur J Biochem. 1997;250(1):130-7.

401. Ramachandra M, Ambudkar SV, Chen D, Hrycyna CA, Dey S, Gottesman MM, et al. Human P-glycoprotein exhibits reduced affinity for substrates during a catalytic transition state. Biochemistry. 1998;37(14):5010-9.

402. Senior AE, Al-Shawi MK, Urbatsch IL. The catalytic cycle of P-glycoprotein. FEBS letters. 1995;377(3):285-9.

403. Choo EF, Leake B, Wandel C, Imamura H, Wood AJ, Wilkinson GR, et al. Pharmacological inhibition of P-glycoprotein transport enhances the distribution of HIV-1 protease inhibitors into brain and testes. Drug Metab Dispos. 2000;28(6):655-60.

404. Polli JW, Jarrett JL, Studenberg SD, Humphreys JE, Dennis SW, Brouwer KR, et al. Role of P-glycoprotein on the CNS disposition of amprenavir (141W94), an HIV protease inhibitor. Pharma Res. 1999;16(8):1206-12.

405. Khaliq Y, Gallicano K, Venance S, Kravcik S, Cameron DW. Effect of ketoconazole on ritonavir and saquinavir concentrations in plasma and cerebrospinal fluid from patients infected with human immunodeficiency virus*. Clin Pharmacol Ther. 2000;68(6):637-46.

406. Minami H, Ohtsu T, Fujii H, Igarashi T, Itoh K, Uchiyama-Kokubu N, et al. Phase I Study of Intravenous PSC-833 and Doxorubicin: Reversal of Multidrug Resistance. Cancer Sci. 2001;92(2):220-30.

407. Giaccone G, Linn SC, Welink J, Catimel G, Stieltjes H, Van der Vijgh W, et al. A dose-finding and pharmacokinetic study of reversal of multidrug resistance with SDZ PSC 833 in combination with doxorubicin in patients with solid tumors. Clin Cancer Res. 1997;3(11):2005-15.

408. Fardel O, Lecureur V, Guillouzo A. Regulation by dexamethasone of P-glycoprotein expression in cultured rat hepatocytes. FEBS letters. 1993;327(2):189-93.

409. Zhao J, Ikeguchi M, Eckersberg T, Kuo M. Modulation of multidrug resistance gene expression by dexamethasone in cultured hepatoma cells. Endocrinology. 1993;133(2):521-8.

410. Greiner B, Eichelbaum M, Fritz P, Kreichgauer H-P, von Richter O, Zundler J, et al. The role of intestinal P-glycoprotein in the interaction of digoxin and rifampin. J Clin Invest 1999;104(2):147-53.

411. Quattrochi LC, Guzelian PS. CYP3A regulation: from pharmacology to nuclear receptors. Drug Metab Dispos. 2001;29(5):615-22.

412. Synold TW, Dussault I, Forman BM. The orphan nuclear receptor SXR coordinately regulates drug metabolism and efflux. Nat Med. 2001;7(5):584-90.

413. Geick A, Eichelbaum M, Burk O. Nuclear receptor response elements mediate induction of intestinal MDR1 by rifampin. J Biol Chem. 2001;276(18):14581-7.

414. LeCluyse EL. Pregnane X receptor: molecular basis for species differences in CYP3A induction by xenobiotics. Chem Biol Interact. 2001;134(3):283-9.

415. Bock U, Kottke T, Gindorf C, Haltner E. Validation of the Caco-2 cell monolayer system for determining the permeability of drug substances according to the Biopharmaceutics Classification System (BCS). Saarbrucken: Across Barriers. 2003:1-7.

416. Artursson P, Borchardt RT. Intestinal drug absorption and metabolism in cell cultures: Caco-2 and beyond. Pharm Res. 1997;14(12):1655-8.

417. Jin X, Luong T-L, Reese N, Gaona H, Collazo-Velez V, Vuong C, et al. Comparison of MDCK-MDR1 and Caco-2 cell based permeability assays for anti-malarial drug screening and drug investigations. J Pharmacol Toxicol Methods. 2014;70(2):188-94.

418. Wikman A, Karlsson J, Carlstedt I, Artursson P. A drug absorption model based on the mucus layer producing human intestinal goblet cell line HT29-H. Pharma Res. 1993;10(6):843-52.

419. Shirasaka Y, Kawasaki M, Sakane T, Omatsu H, Moriya Y, Nakamura T, et al. Induction of human p-glycoprotein in Caco-2 cells: development of a highly sensitive assay system for p-glycoprotein-mediated drug transport. Drug Metab Pharmacokinet 2006;21(5):414-23.

420. Fogh J, Fogh JM, Orfeo T. One hundred and twenty-seven cultured human tumor cell lines producing tumors in nude mice. J Natl Cancer Inst 1977;59(1):221-6.

421. Artursson P, Karlsson J. Correlation between oral drug absorption in humans and apparent drug permeability coefficients in human intestinal epithelial (CACO-2) cells. Biochem Biophys Res Commun. 1991;175(3):880-5.

422. Cell B. Enterocyte-like differentiation and polarization of the human colon carcinoma cell line Caco-2 in culture. Biol Cell. 1983;47.

423. Hidalgo IJ, Borchardt RT. Transport of a large neutral amino acid (phenylalanine) in a human intestinal epithelial cell line: Caco-2. BBA-Biomembranes. 1990;1028(1):25-30.

424. Dantzig AH, Bergin L. Uptake of the cephalosporin, cephalexin, by a dipeptide transport carrier in the human intestinal cell line, Caco-2. BBA-Biomembranes. 1990;1027(3):211-7.

425. Wilson G, Hassan I, Dix C, Williamson I, Shah R, Mackay M, et al. Transport and permeability properties of human Caco-2 cells: an in vitro model of the intestinal epithelial cell barrier. J Control Release. 1990;11(1):25-40.

426. Wils P, Warnery A, Phung-Ba V, Scherman D. Differentiated intestinal epithelial cell lines asin vitro models for predicting the intestinal absorption of drugs. Cell Biol Toxicol. 1994;10(5-6):393-7.

427. Lennernäs H, Palm K, Fagerholm U, Artursson P. Correlation between paracellular and transcellular drug permeability in the human jejunum and Caco-2 monolayers. Int J Pharm. 1996;127:103-7.

428. Lennernäs H, Ahrenstedt Ö, Hällgren R, Knutson L, Ryde M, Paalzow LK. Regional jejunal perfusion, a new in vivo approach to study oral drug absorption in man. Pharma Res. 1992;9(10):1243-51.

429. Kirn D-C, Burton PS, Borchardt RT. A correlation between the permeability characteristics of a series of peptides using an in vitro cell culture model (Caco-2) and those using an in situ perfused rat ileum model of the intestinal mucosa. Pharma Res. 1993;10(12):1710-4.

430. Conradi RA, Wilkinson KF, Rush BD, Hilgers AR, Ruwart MJ, Burton PS. In vitro/in vivo models for peptide oral absorption: Comparison of Caco-2 cell permeability with rat intestinal absorption of renin inhibitory peptides. Pharm Res. 1993;10(12):1790-2.

431. Yee S. In vitro permeability across Caco-2 cells (colonic) can predict in vivo (small intestinal) absorption in man—fact or myth. Pharm Res. 1997;14(6): 763-6.

432. Walter E, Kissel T. Transepithelial transport and metabolism of thyrotropin-releasing hormone (TRH) in monolayers of a human intestinal cell line (Caco-2): evidence for an active transport component? Pharma Res. 1994;11(11) :1575-80.

433. Anderle P, Niederer E, Rubas W, Hilgendorf C, Spahn-Langguth H, Wunderli-Allenspach H, et al. P-glycoprotein (P-gp) mediated efflux in Caco-2 cell monolayers: The influence of culturing conditions and drug exposure on P-gp expression levels. J Pharma Sci. 1998;87(6):757-62.

434. Amidon GL, Lennernäs H, Shah VP, Crison JR. A theoretical basis for a biopharmaceutic drug classification: the correlation of in vitro drug product dissolution and in vivo bioavailability. Pharm Res. 1995;12(3):413-20.

435. Katzung BG, Masters SB, Trevor AJ. Basic & Clinical Pharmacology McGraw-Hill LANGE; 2009.

436. Pham Y-T, Régina A, Farinotti R, Couraud P-O, Wainer IW, Roux F, et al. Interactions of racemic mefloquine and its enantiomers with P-glycoprotein in an immortalised rat brain capillary endothelial cell line, GPNT. BBA-Gen Subjects 2000;1524(2):212-9.

437. Lan L-B, Ayesh S, Lyubimov E, Pashinsky I, Stein WD. Kinetic parameters for reversal of the multidrug pump as measured for drug accumulation and cell killing. Cancer Chemother Pharmacol. 1996;38(2):181-90.

438. Shao Y-m, Ayesh S, Stein WD. Mutually co-operative interactions between modulators of P-glycoprotein. Biochimica et Biophysica Acta (BBA) - Molecular Basis of Disease. 1997;1360(1):30-8.

439. Hayeshi R, Masimirembwa C, Mukanganyama S, Ungell AL. The potential inhibitory effect of antiparasitic drugs and natural products on P-glycoprotein mediated efflux. Eur J Pharm Sci. 2006;29(1):70-81.

440. Oga E, Sekine S, Shitara Y, T. H. Potential P-glycoprotein-mediated drug-drug interactions of antimalarial agents in Caco-2 cells. Am J Trop Med Hyg 2012;87(1):64-9.

441. Ambudkar SV, Kimchi-Sarfaty C, Sauna ZE, Gottesman MM. P-glycoprotein: from genomics to mechanism. Oncogene. 2003;22(47):7468-85.

442. Lehnert M, Dalton W, Roe D, Emerson S, Salmon SE. Synergistic inhibition by verapamil and quinine of P-glycoprotein-mediated multidrug resistance in a human myeloma cell line model. Blood. 1991;77(2):348-54.

443. Burk O, Arnold KA, Nussler AK, Schaeffeler E, Efimova E, Avery BA, et al. Antimalarial artemisinin drugs induce cytochrome P450 and MDR1 expression by activation of xenosensors pregnane X receptor and constitutive androstane receptor. Mol pharmacol. 2005;67(6):1954-65.

444. Bailey CA, Bryla P, Malick AW. The use of the intestinal epithelial cell culture model, Caco-2, in pharmaceutical development. Adv Drug Deliv Rev. 1996;22(1):85-103.

445. Hosoya K-i, Kim K-J, Lee VH. Age-dependent expression of P-glycoprotein gp17O in Caco-2 cell monolayers. Pharm Res. 1996;13(6):885-90.

446. Crowe A, Wong P. pH dependent uptake of loperamide across the gastrointestinal tract: an in vitro study. Drug Dev Ind Pharm. 2004;30(5):449-59.

447. Crowe A, Lemaire M. In vitro and in situ absorption of SDZ-RAD using a human intestinal cell line (Caco-2) and a single pass perfusion model in rats: comparison with rapamycin. Pharma Res. 1998;15(11):1666-72.

448. Artursson P. Epithelial transport of drugs in cell culture. I: A model for studying the passive diffusion of drugs over intestinal absorptive (Caco-2) cells. J Pharm Sci 1990;79(6):476-82.

449. Crowe A, Teoh YK. Limited P-glycoprotein mediated efflux for anti-epileptic drugs. J Drug Target. 2006;14(5):291-300.

450. Camenisch GP, Wang W, Wang B, Borchardt RT. A comparison of the bioconversion rates and the Caco-2 cell permeation characteristics of Coumarin-based cyclic prodrugs and methylester-based linear prodrugs of RGD peptidomimetics. Pharma Res. 1998;15(8):1174-81.

451. Wenzel U, Gebert I, Weintraut H, Weber W-M, Clauss W, Daniel H. Transport characteristics of differently charged cephalosporin antibiotics in oocytes expressing the cloned intestinal peptide transporter PepT1 and in human intestinal Caco-2 cells. J Pharmacol Exp Ther. 1996;277(2):831-9.

452. Faust RA, Albers JJ. Regulated vectorial secretion of cholesteryl ester transfer protein (LTP-I) by the CaCo-2 model of human enterocyte epithelium. J Biol Chem. 1988;263(18):8786-9.

453. Dulfer WJ, Groten JP, Govers H. Effect of fatty acids and the aqueous diffusion barrier on the uptake and transport of polychlorinated biphenyls in Caco-2 cells. J Lipid Res. 1996;37(5):950-61.

454. Artursson P, Karlsson J, Ocklind G, Schipper N. Models of absorptive epithelia for studying transport processes. In: Shaw E, editor. Cell models of epithelial tissues-A practical approach: Oxford; 1996. p. 111-33.

455. Westphal K, Weinbrenner A, Zschiesche M, Franke G, Knoke M, Oertel R, et al. Induction of P-glycoprotein by rifampin increases intestinal secretion of talinolol in human beings: A new type of drug/drug interaction. J Pharmacol Exp Ther. 2000;68(4):345-55.

456. Rogers WO, Sem R, Tero T, Chim P, Lim P, Muth S, et al. Failure of artesunate-mefloquine combination therapy for uncomplicated Plasmodium falciparum malaria in southern Cambodia. Malar J. 2009;8(1):10.

457. Reungpatthanaphong P, Mankhetkorn S. Modulation of multidrug resistance by artemisinin, artesunate and dihydroartemisinin in K562/adr and GLC4/adr resistant cell lines. Biol Pharm Bull. 2002;25(12):1555-61.

458. Davis TM, England M, Dunlop A-M, Page-Sharp M, Cambon N, Keller TG, et al. Assessment of the effect of mefloquine on artesunate pharmacokinetics in healthy male volunteers. Antimicrob Agents Chemother. 2007;51(3):1099-101.

459. Pussard E, Verdier F, Blayo M-C. Simultaneous determination of chloroquine, amodiaquine and their metabolites in human plasma, red blood cells, whole blood and urine by column liquid chromatography. J Chromatogr B Biomed Sci Appl. 1986;374:111-8.

460. Manning L, Laman M, Page-Sharp M, Salman S, Hwaiwhanje I, Morep N, et al. Meningeal inflammation increases artemether concentrations in cerebrospinal fluid in Papua New Guinean children treated with intramuscular artemether. Antimicrob Agents Chemother. 2011;55(11):5027-33.

461. Gustafsson L, Walker O, Alvan G, Beermann B, Estevez F, Gleisner L, et al. Disposition of chloroquine in man after single intravenous and oral doses. Br J Clin Pharmacol. 1983;15(4):471-9.

462. Agency EM. Assessment report Methylthioninium chloride Proveblue [02.12.2014]. Available from: http://www.ema.europa.eu/docs/en_GB/document_library/EPAR_-_Public_assessment_report/human/002108/WC500107131.pdf.

463. Peters W, Robinson PJ. Handbook of Animal Models of Infection. In: In: SANDE MA ZO, editor. Malaria. London: Academic Press; 1975.

464. Batty KT, Ilett KF, Davis M. Chemical stability of artesunate injection and proposal for its administration by intravenous infusion. J Pharm Pharmacol. 1996;48(1):22-6.

465. Food, Administration D. Guidance for industry: waiver of in vivo bioavailability and bioequivalence studies for immediate-release solid oral dosage forms based

on a biopharmaceutics classification system. Food and Drug Administration, Rockville, MD. 2000.

466. Agnihotri J, Singh S, Bigonia P. Formal chemical stability analysis and solubility analysis of artesunate and hydroxychloroquinine for development of parenteral dosage form. J Pharm Res. 2013;6(1):117-22.

467. Österberg T, Norinder U. Theoretical calculation and prediction of P-glycoprotein-interacting drugs using MolSurf parametrization and PLS statistics. Eur J Pharm Sci. 2000;10(4):295-303.

# 7 Appendix

## 7.1 Buffers, reagents and solvents

**Transport media; Hank Balanced Salt Solution**

| **HBSS 25 mM transport medium ( pH 7.4)** | **250 mL** |
|---|---|
| HBSS 10 X | 25 mL |
| 25 mM glucose (MW 180.16 ) | 0.87 g |
| 10 mM HEPES (MW 283.3 ) | 0.58 g |
| Deionized water to | 250 mL |

1M NaOH was used to adjust pH to 7.

**Cell growth medium**

| **Ingredient** | **Quantity** |
|---|---|
| DMEM | 500 mL |
| 2 mM glutamine | 5 mL of 200 mM |
| 1 mM non-essential amino acid | 5 mL of 100 mM |
| 1,000 u/mL penicillin and streptomycin | 5 mL of 100,000 units/mL |
| 10% foetal calf serum (FCS) | 50 mL of 100% FCS |

**Cell lysis buffer**

| **Ingredient** | **Amount for 100 mL** |
|---|---|
| 20 mM Tris HCl (MW 157.6) | 0.315 g |
| 120 mM NaCl (MW 58.55) | 0.701 g |
| 0.1% Sodium dodecyl sulphate | 100 mg |
| Nonidet p40 substitute | 1 mL |

Mini protease inhibitor tablet was added to 10 mL aliquot of lysis buffer and sonicated for 10 minutes in a floating rack.

**CTC reagent**

| Ingredient | Quantity |
|---|---|
| $CuSO_4.H2O$ | 0.1 g |
| Na-K-Tartrate | 0.2 g |
| $Na_2CO_3$ | 10.0 g |
| Deionized water to | 100 mL |

The CTC reagent was warmed to room temperature prior use and stirred to dissolve crystals formed during refrigeration.

**Lowry Reagent for protein assay**

| Ingredient | Quantity in parts |
|---|---|
| CTC reagent | 1 |
| 0.8 M NaOH | 1 |
| Deionized water | 2 |

**Folin reagent (0.5 N)**

| Ingredient | Quantity |
|---|---|
| Folin stock ( 2N) | Part 1 |
| Deionized water | Part 4 |

**Tris Buffered saline (TBS)**

| Ingredient | Quantity |
|---|---|
| Tris HCL | 3.14 mg |
| NaCl | 9 g |
| Deionized water to | 1000mL |

5 M NaOH was used to adjust pH to 7.4

**Tris Buffered saline with 0.05% Tween 20 (TBST)**

| Ingredient | Quantity |
|---|---|
| Tris HCL | 3.14 mg |
| NaCl | 9 g |
| Tween 20 | 0.5 mL |
| Deionized water to | 1000mL |

5 M NaOH was used to adjust pH to 7.4

**Transfer Buffer**

| Ingredient | Quantity |
|---|---|
| Methanol | 200mL |
| Nupage sample anti-oxidant | 1mL |
| Transfer buffer (20X conc) | 50mL |
| Deionized water | 749mL |

**MOPs Running Buffer 1X**

| Ingredient | Quantity |
|---|---|
| 20 X BoltTM MOPS SDS running buffer | 20 mL |
| deionized water | 380 mL |

**Blocking buffer**

| Ingredient | Quantity |
|---|---|
| Casein | 4 g |
| TBS | 200 mL |